University of Glasgow

Osuagwu, Bethel Chikadibia A. (2015) *Neurorehabilitation of hand functions using brain computer interface.* PhD thesis.

http://theses.gla.ac.uk/7245/

Copyright and moral rights for this work are retained by the author

A copy can be downloaded for personal non-commercial research or study, without prior permission or charge

This work cannot be reproduced or quoted extensively from without first obtaining permission in writing from the author

The content must not be changed in any way or sold commercially in any format or medium without the formal permission of the author

When referring to this work, full bibliographic details including the author, title, awarding institution and date of the thesis must be given

Glasgow Theses Service
http://theses.gla.ac.uk/
theses@gla.ac.uk

NEUROREHABILITATION OF HAND FUNCTIONS USING BRAIN COMPUTER INTERFACE

BETHEL CHIKADIBIA A. OSUAGWU

SUBMITTED IN FULFILMENT OF THE REQUIREMENTS FOR THE DEGREE OF
Doctor of Philosophy

DEPARTMENT OF BIOMEDICAL ENGINEERING

COLLEGE OF SCIENCE AND ENGINEERING
UNIVERSITY OF GLASGOW

SEPTEMBER 2015

© BETHEL CHIKADIBIA A. OSUAGWU

Abstract

Introduction

Brain computer interface (BCI) is a promising new technology with possible application in neurorehabilitation after spinal cord injury. Movement imagination or attempted movement-based BCI coupled with functional electrical stimulation (FES) enables the simultaneous activation of the motor cortices and the muscles they control. When using the BCI- coupled with FES (known as BCI-FES), the subject activates the motor cortex using attempted movement or movement imagination of a limb. The BCI system detects the motor cortex activation and activates the FES attached to the muscles of the limb the subject is attempting or imaging to move. In this way the afferent and the efferent pathways of the nervous system are simultaneously activated. This simultaneous activation encourages Hebbian type learning which could be beneficial in functional rehabilitation after spinal cord injury (SCI). The FES is already in use in several SCI rehabilitation units but there is currently not enough clinical evidence to support the use of BCI-FES for rehabilitation.

Aims

The main aim of this thesis is to assess outcomes in sub-acute tetraplegic patients using BCI-FES for functional hand rehabilitation. In addition, the thesis explores different methods for assessing neurological rehabilitation especially after BCI-FES therapy. The thesis also investigated mental rotation as a possible rehabilitation method in SCI.

Methods

Following investigation into applicable methods that can be used to implement rehabilitative BCI, a BCI based on attempted movement was built. Further, the BCI was used to build a BCI-FES system. The BCI-FES system was used to deliver therapy to seven sub-acute tetraplegic patients who were scheduled to receive the therapy over a total period of 20 working days. These seven patients are in a 'BCI-FES' group. Five more patients were also recruited and offered equivalent FES quantity without the BCI. These further five patients

are in a 'FES-only' group. Neurological and functional measures were investigated and used to assess both patient groups before and after therapy.

Results

The results of the two groups of patients were compared. The patients in the BCI-FES group had better improvements. These improvements were found with outcome measures assessing neurological changes. The neurological changes following the use of the BCI-FES showed that during movement attempt, the activation of the motor cortex areas of the SCI patients became closer to the activation found in healthy individuals. The intensity of the activation and its spatial localisation both improved suggesting desirable cortical reorganisation. Furthermore, the responses of the somatosensory cortex during sensory stimulation were of clear evidence of better improvement in patients who used the BCI-FES. Missing somatosensory evoked potential peaks returned more for the BCI-FES group while there was no overall change in the FES-only group. Although the BCI-FES group had better neurological improvement, they did not show better functional improvement than the FES-only group. This was attributed mainly to the short duration of the study where therapies were only delivered for 20 working days.

Conclusions

The results obtained from this study have shown that BCI-FES may induce cortical changes in the desired direction at least faster than FES alone. The observation of better improvement in the patients who used the BCI-FES is a good result in neurorehabilitation and it shows the potential of thought-controlled FES as a neurorehabilitation tool. These results back other studies that have shown the potential of BCI-FES in rehabilitation following neurological injuries that lead to movement impairment. Although the results are promising, further studies are necessary given the small number of subjects in the current study.

Acknowledgements

I have had support from several people while working on this project. The list is inexhaustible but here are the people who made the most significant contribution.

My sincere gratitude goes to Dr. Aleksandra Vuckovic who deserves enormous thanks for her supervision of my thesis. I appreciate all the time she spent supporting and caring for me over the years. So I would like to say, Хвала вам.

My second supervisor, Dr. Henrik Gollee, helped me in several aspects of this project. He was always there when I needed him and I would like to say, danke.

I would like to express my gratitude to Dr. Sylvie Coupaud for the help she offered me especially for organising and leading her writing club that helped me a lot. I would like to say, thank you.

I owe so much to my many colleagues who have been there for me throughout this project. I could not have achieved anything without their intellectual and social support. I still owe Margaret and Lin for all the dinners they cooked for me. I am truly grateful to have such kind people and I would like to say to Margaret Armentano, grazie; Lin Meng, 谢谢; Adamantia Mamma, ευχαριστώ; Euan McCaughey, thenk ye; Muhammad Abul Hasan, آپ کا شکریہ; Mohammed Jarjees, شکرا; Jose Alberto Alvarez Martin, gracias; Anna Zulauf, dziękuję; Sarah Comincioli, merci; Gemma Wheeler, thank you; Aso Fatih Muhamed Muhamed, سوپاس; Manaf Kadum Hussein Al-taleb, شکرا; Salim Mohammed Hussein Alwasity, شکرا; Anna Sosnowska, dziękuję; Ruslinda Binti Ruslee, terima kasih; Xinyi Zhao, 谢谢; Ana Sofia Miranda de Castro Resende Assis, obrigado; Simão Pedro Marques Pinto de Faria, obrigado.

This project depended on many patients and able-bodied volunteers. They sacrificed their time to help finish this project. For the contribution to my project and to science, thank you.

I will not forget the Engineering and Physical Sciences Research Council (EPSRC) for funding my PhD, thank you.

I extend my gratitude to the doctors and nurses from the Southern General Hospital who immensely helped with patient recruitment and therapy delivery. I appreciate all the help I

got from the therapists at the hospital including the assistance from those in the gym and Leslie Wallace. Thank you.

I would not have got this far without my parents and guidance. They have been there supporting me in every step of the way. To my mother, Eucharia Anyanwu, ị mela, and to Remi Kukoyi, e dupe.

Dedication.

To one and only Mom, Eucharia Anyanwu and her man, Remi Kukoyi.

Declaration

I, Osuagwu A. B. C., hereby declare that except where explicit reference is made to the contribution of others, this dissertation is the result of the work of the named and has not been submitted for any other degree at the University of Glasgow or any other institution

Publications

Journal paper

Osuagwu, BA. and Vuckovic A (2014). Similarities between explicit and implicit motor imagery in mental rotation of hands: An EEG study. Neuropsychologia, 65, 197-210.

Vuckovic A, Hasan MA, Osuagwu BA, Fraser M, Allan DB, Conway BA and Nasseroleslami, B (2015). The influence of central neuropathic pain in paraplegic patients on performance of a motor imagery based Brain Computer Interface. Clinical Neurophysiology.

Reynolds C, Osuagwu, BA and Vuckovic, A (2014). Influence of motor imagination on cortical activation during functional electrical stimulation. Clinical Neurophysiology.

Vuckovic A and Osuagwu BA (2013). Using a motor imagery questionnaire to estimate the performance of a Brain–Computer Interface based on object oriented motor imagery. Clinical Neurophysiology, 124, 1586-1595.

Conference and Proceeding

Osuagwu BA and Vuckovic A. Feasibility of using time doman parameters as online therapeutic BCI features. In Proceedings of the 6th International Brain-Computer Interface Conference, Graz, Austria, 2014.

Osuagwu BA and Vuckovic A. Time-frequency activity of electroencephalogram is different for left and right hand mental rotation. In Proceedings of the 8th IEEE EMBS UK & Republic of Ireland Postgraduate Conference on Biomedical Engineering and Medical Physics, Warwick, UK, 2014.

Osuagwu BA, Vuckovic A, Fraser M, Wallace L, and Allan DB. BCI-FES hand therapy for patients with sub-acute tetraplegia. In Proceedings of the 6th International Brain-Computer Interface Conference, Graz, Austria, 2014.

Abbreviations

ACC Accuracy.

AM Attempted Movement.

ASIA American Spinal Injury Association.

BA Brodmann area.

BCI Brain computer interface.

CR Conditioned response.

CS Conditioned stimulus.

CSP common spatial pattern.

ECoG Electrocorticogram.

EEG Electroencephalogram.

EMG Electromayogram.

EOG Electrooculogram.

ERD Event related desynchronisation.

ERS Event related synchronisation.

FES Functional electrical stimulation.

fMRI Functional MRI.

HLT Hand laterality test.

ICA Independent component analysis.

IPI inter pulse interval.

LDA Linear discriminant analysis.

LI Laterality index.

MEP Motor evoked potential.

MI Motor imagery.

MMT Manual muscle test.

MNI Montreal Neurological Institute and Hospital.

MRCP Movement related cortical potential.

MRI Magnetic resonance imaging.

PCA Principle component analysis.

PET Positron emission tomography.

ROI region of interest.

ROM Range of movement.

SCI Spinal cord injury.

sLORETA Standardized low resolution electromagnetic tomography.

SSEP Somatosensory evoked potential.

SSEPLI Somatosensory evoked potential lateralisation index.

TDP Time domain parameter.

UC Update coefficient.

UR Unconditioned response.

US Unconditioned stimulus.

wLI Weighted LI.

Nomenclature

Σ Scatter/covariance matrix.

λ Eigenvalue.

μ mean/Mu EEG rhythm/micro.

β Beta frequency band.

α Alpha frequency band.

θ Theta frequency band.

σ^2 Variance.

p_w Pulse width.

a Amplitude.

A Transformation/coefficient matrix.

b Bias/sub-buffer length.

B/U Eigenvector or Buffer length.

c Class of data.

C matrix entry.

d Derivative operator/BCI-difficulty.

e Noise/error.

E Expectation value.

f Feature/ Buffer filling.

F/v Frequency/voxel/others.

G Normal distribution.

h Function.

I Current/Identity matrix.

i/k/j/m Iterators.

J Objective function.

l Left.

L Number of trials.

N/M Number of channels/feature dimension.

p Model/derivative order.

P Filter.

Q Charge.

r Right.

R Covariance matrix.

S scatter/covariance matrix.

T Transpose operator.

t/q Time and/or sample point and/or number of observations.

w Weighting.

W Transform/whitening transform.

X EEG time series.

xyz 3D coordinate.

Y Output.

Table of Contents

List of Tables

List of Figures

Chapter 1

Introduction

"The hand has several advantages over the eyes: 'it can see in the dark and it can see around corners..." John Napier

1.1 Summary

In this first chapter of the thesis, the basic concepts and terms used throughout the thesis are defined. The chapter introduces the nervous system and the hand. It highlights the nature and consequences of an injury to the spinal cord. It also states the methods of rehabilitation of hand functions following spinal cord injury. Furthermore, the chapter introduces brain computer interface and functional electrical stimulation. The chapter concludes with the aims and objectives of the thesis.

1.2 The nervous system

The nervous system consists of the peripheral nervous system and the central nervous system. The central nervous system consists of the brain and the spinal cord. The brain is the centre for cognition and decision making. For example a decision to grasp a cup of tea originates in the brain and the required *motor commands* to accomplish the *grasp function* is generated and transmitted mainly through the spinal cord. The spinal cord transmits the commands to the peripheral nerves of the peripheral nervous system. The commands are then transmitted to the nerves that innervate muscles. The sensory feedback from the activation of the muscles is sent back to the brain.

1.2.1 Central nervous system

The brain

The brain is divided into two hemispheres namely, the left and the right hemispheres. Generally, the left hemisphere controls the right side of the body while the right hemisphere controls the left side of the body [1]. The left (right) hemisphere is *contralateral* to the right (left) side of the body. The left (right) hemisphere is *ipsilateral* to the left (right) side of the body. A hemisphere may dominate the processing of a certain cognitive function and the degree of such dominance is sometimes referred to as lateralisation (see Sections 3.3.2 and 7.3.4 for indexes of lateralisation). In each hemisphere, different structures are known to specialise in different functions. Fig. 1.1a shows different brain structures of one hemisphere of the brain. Brodmann's nomenclature assigns numbers to different areas of the brain based on their cytoarchitectural organisation [2]. The *Brodmann area (BA)* is widely used. Fig. 1.1a shows some of the BAs relevant in this thesis. Fig. 1.1b shows the representation of body parts on the motor cortex [1]. Similar representation exists for the sensory cortex.

The supplementary motor areas (BA 6) are involved in coordination and direct motor control. The premotor cortex (BA 6) is involved in the planning of motor tasks. The primary motor cortex (BA 4) is involved in motor execution. The BA 4 and 6 are also called the precentral gyrus. The primary sensory cortex or the somatosensory cortex or the postcentral gyrus (mainly BA 3 but also includes BA 1 and 2) is the area that receives sensory input. The motor and the sensory areas are called the *sensorimotor* cortex and this term is used often in this thesis.

Spinal cord

The spinal cord is a tubular structure packed with nervous tissues and support cells. It is an important part of the central nervous system that provides routs of communication between the brain and the peripheral nervous system [3, 4]. The spinal cord is shown in Fig. 1.2. The spinal cord is encased in a vertebral column which has a segmented structure. The spinal cord runs along the column and pairs of nerves exit it at certain levels or segments. The sections and the pairs of spinal nerves are named according to the vertebral level/segments about which they exit. The vertebral levels/segments consist of eight cervical (C1 to C8), 12 thoracic (Th1 to Th12), five lumbar (L1 to L5), five sacral (S1 to S5) and one coccygeal, adding up to 31 segments.

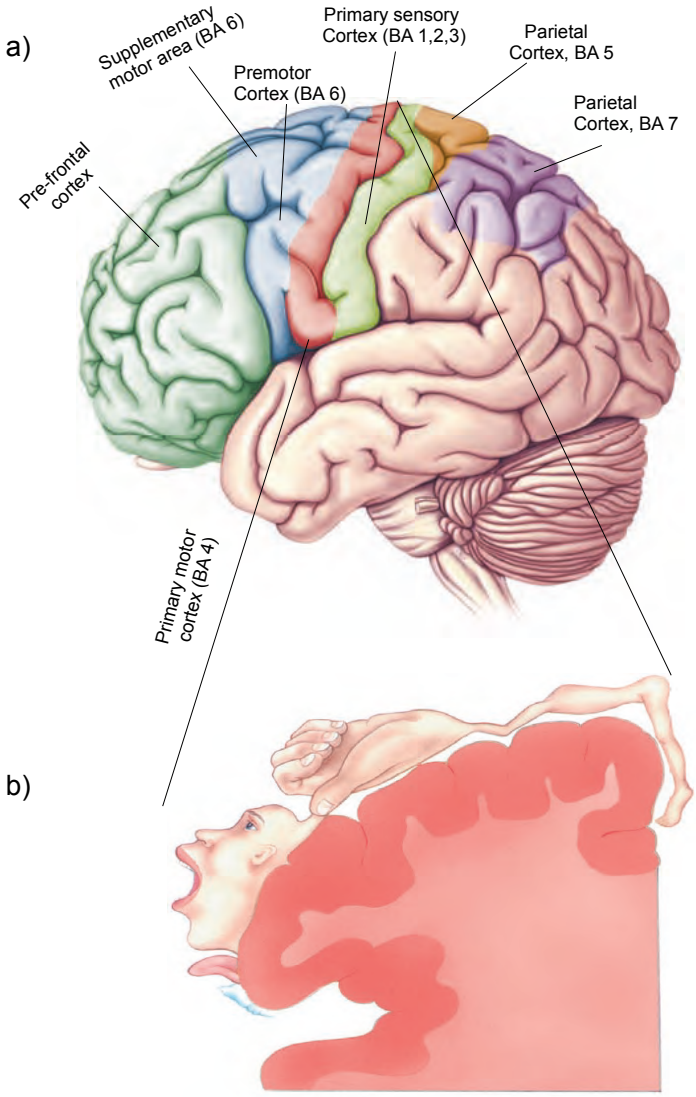

Figure 1.1: Structures on a brain hemisphere (a) and the representation of body parts in the primary motor cortex (b). (Reproduced from [1].)

1.2.2 Peripheral nervous system

The peripheral nervous system consists of the somatic and the visceral nervous system. The somatic peripheral nervous system consists of neurons that innervate muscles, skin and the joints. The visceral peripheral nervous system on the other hand comprises the neurons that innervate the internal organs, blood vessels, and glands [1]. The terms *afferent* and *efferent* axons are used to describe axons of the peripheral nervous system that carry information towards and away respectively from a point [1]

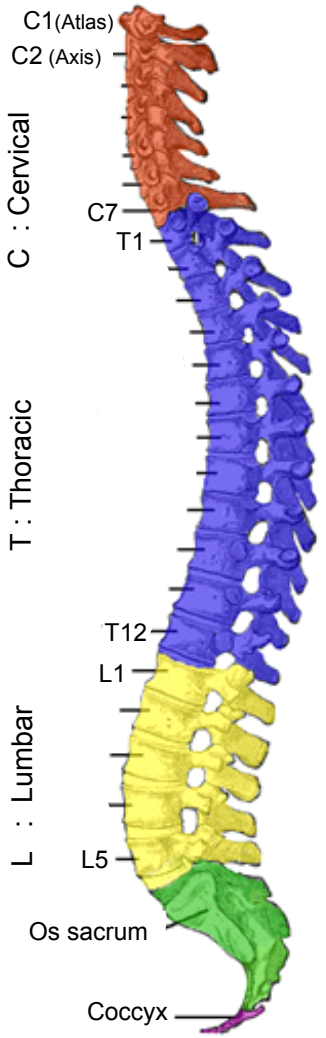

Figure 1.2: Structure of the spinal cord (Reproduced from Wikipedia commons.)

1.3 The hand

"The hand has several advantages over the eyes: 'it can see in the dark and it can see around corners; most important of all, it can interact with the environment rather than just observe it' " John Napier (1980) cited in [5]

The hand has a dense population of motor nerves that support the intricate movements that it performs. The nerves supplying the hand and the forearm include the *median*, *ulnar* and the radial nerves. These nerves have their origins at the levels C5 to T1 of the spinal segments [6]. The muscles the nerves innervate include intrinsic and extrinsic muscles. The intrinsic muscles includes those located inside the hand while the extrinsic muscles includes those located outside of the hand. The muscles of the hand and forearm are shown in Fig. 1.3[1]. The functions and the nerve supply to the main muscles are given in Table 1.1. For a com-

[1]Adapted from:`http://anatomy4fitness.blogspot.co.uk/2012/11/give-yourself-hand.html`. Accessed: 8/05/2015.

plete description of the hand muscles, see `http://www.innerbody.com/anatomy/muscular/arm-hand`.

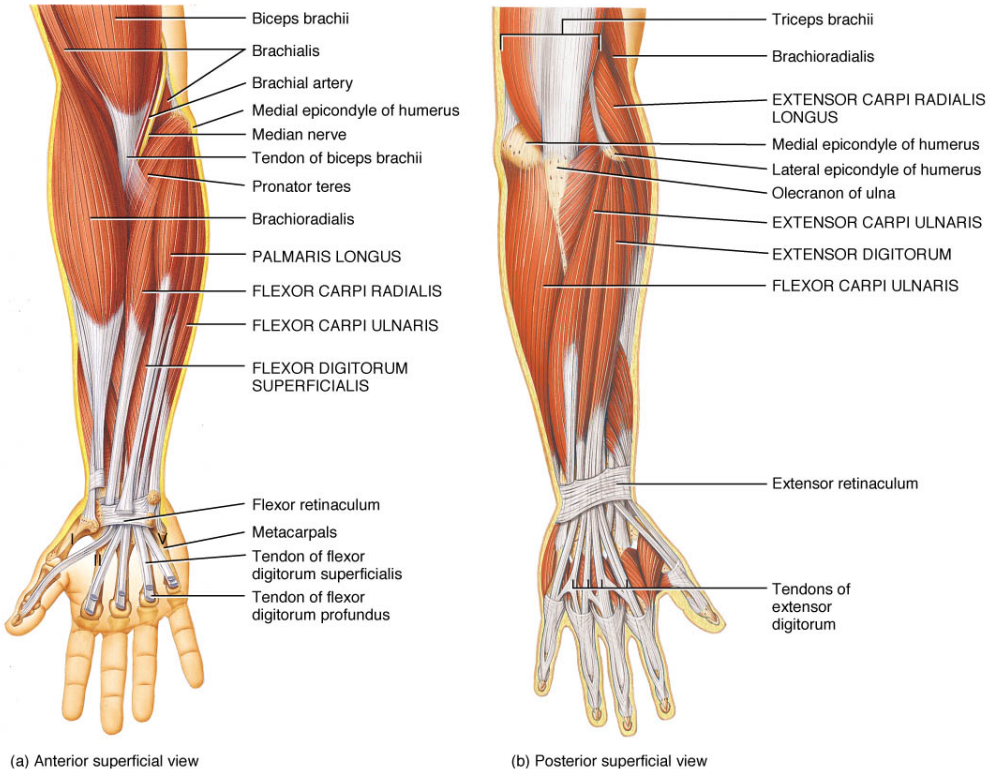

Figure 1.3: The hand and forearm muscles.

1.4 Motor control

1.4.1 Motor control in physical movement

Motor control processes are complex and involves different parts of the brain working at different stages of the process. Fig. 1.4 shows the components of the motor system. There are three hierarchical stages associated with movement control [1]. At the top of the hierarchy are the association areas of the neocortex and the basal ganglia both in the forebrain. This top level is concerned with devising the strategy that best achieve the goal of a movement. At the middle of the hierarchy are the motor cortex and the cerebellum. This middle level is concerned with devising the movement tactics which involves the succession of spatio-temporal muscle contraction needed to precisely achieve the strategic gaol. At the bottom level of the hierarchy are the brain stem and the spinal cord. This bottom level is concerned with the execution of the movement which involves the activation of motor neurons and interneuron pools and subsequently the lower motor neurones to produce the strategic goal directed movement.

Table 1.1: Main hand muscles: Functions and nerve supplies [6].

Muscles	Function	Nerve
Extensor digitorum communis	Extends the fingers at the metacarpophalangeal joint and also extends the wrist	Radial nerve, C7, 8
Extensor carpi radialis	Helps in the extension and abduction of the wrist	Radial nerve, C6, 7
Extensor pollicis longus	Extends the joints of the thumb and helps in the abduction and extension of the wrist.	Radial nerve, C7, 8
Flexor carpi radialis	Helps in the flexion and abduction of the wrist	Median nerve, C6, 7
Flexor digitorum profundus	Flexes the distal interphalangeal joint, indirectly flexes the proximal interphalangeal, metacarpophalangeal joints and the wrist joints	Median nerve,T1; Ulnar nerve, T1
Flexor digitorum supperficialis	Flexes the fingers by flexion of the metacarpophalangeal and the proximal interphalangeal joints. Indirectly flexes the wrist.	Median nerve, C7, 8, T1

The activated motor neurons carrying instruction for the goal directed movement descend from the brain via two major routs namely: the ventromedial and the lateral pathways [1]. The ventromedial pathways are under the control of the brain stem and are involved in the control of posture, balance, locomotion and certain reflex movements. They control proximal and axial muscles. The lateral pathways are under direct cortical control and are involved in the voluntary movement of distal musculatures. The ventral pathways includes the corticospinal tract which is one part of the *pyramidal tract*s.

As shown in Fig. 1.4, voluntary motor command originates from the motor cortex and projects to other parts of the central nervous system including the brain stem and the spinal cord [7]. The projection from the motor cortex to the spinal cord is the corticospinal tract and it contains the upper motor neurones with cell bodies in the motor areas of the cerebral cortex. The upper motor neurones carry motor commands down to the lower motor neurones also known as the *alpha motor neurones (α-MN)*. The axons of the α-MN innervate skeletal muscle fibres.

Following movement command generation by the motor cortex, an *efferent copy*/corollary discharge of the command is sent to be stored in an internal monitoring system [8, 9]. The command travels down the upper motor neurons in the form of *action potential* which is a neuronal electrical discharge. At the appropriate spinal segment the axons of the upper motor

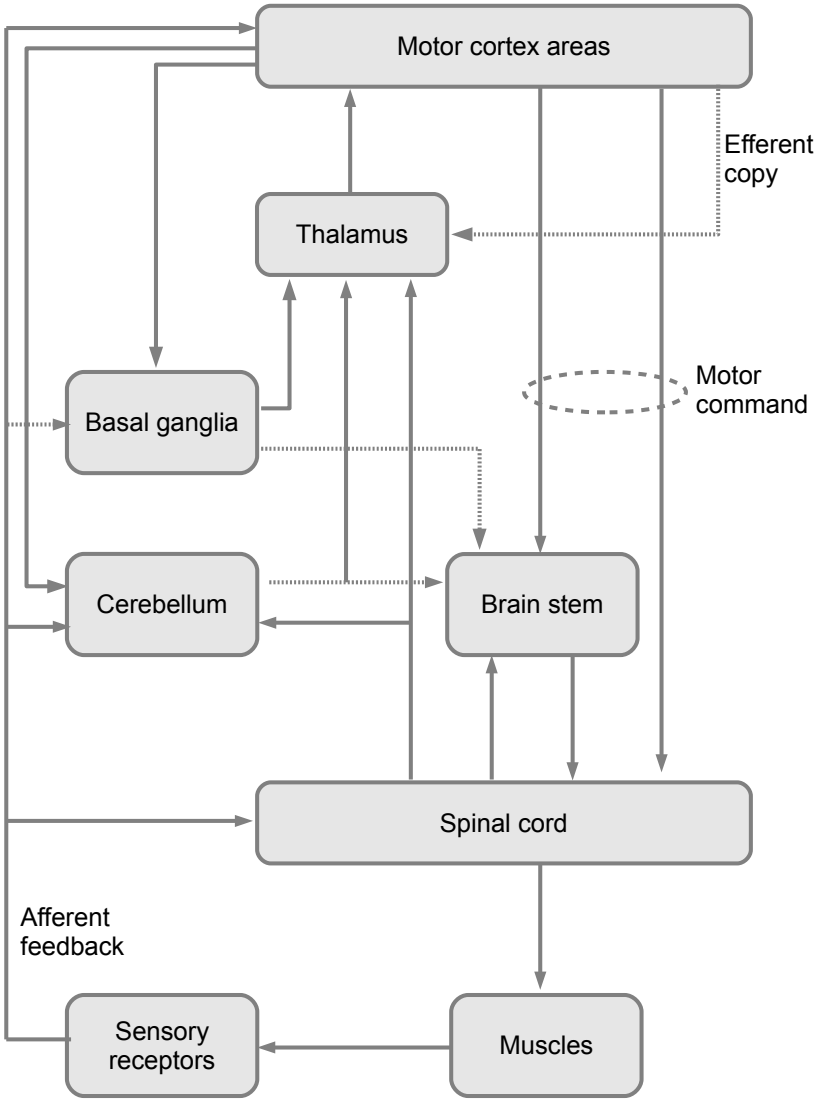

Figure 1.4: The main constituents of the motor system. (Reproduced from [7].)

neurons make synapses with the cell bodies/dendrites of the α-MN in the anterior horn of the spinal cord. The action potential so travels down the α-MNs to activate skeletal muscle fibres they innervate. In this manner a motor command originating in the brain in the form of action potential initiate the contraction of muscles. Sensory feedbacks as consequences of the executed action is received in the sensory system. The proprioceptive feedback resulting from the activated muscles is received in the somatosensory cortex. Using the efferent copy, the internal monitoring system compares the received feedback with the expected feedback and notifies the motor cortex of any error in the movement as shown on Fig. 1.5 [8, 9].

1.4.2 Internal models

In motor control theory there is a concept of *internal models* which are models in the central nervous system responsible for internal simulation of motor actions and their consequences

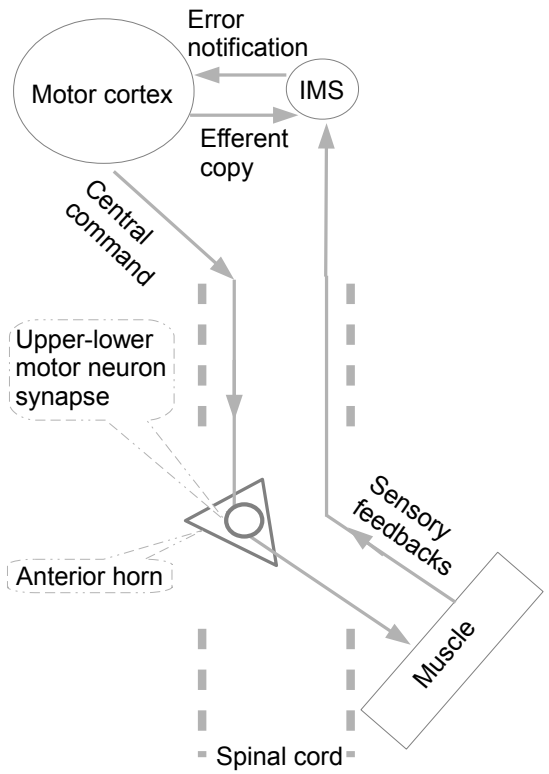

Figure 1.5: The schematic diagram showing the propagation of motor command originating from the motor cortex during an intentional movement. IMS, internal monitoring system.

[10, 11, 12, 13]. Although the internal models are theoretical, they could be used to explain processes in the central nervous system. The models could be acquired during infancy and undergo transformation during early life [14]. There are two main classes of the models, the forward models and the inverse models. The forward models are responsible for predicting the consequences of actions. They include the forward dynamic model which predicts the physical dynamics of a system given a motor action and the forward sensory model which predicts the sensory consequences of the actions given the predicted dynamics. The inverse model is responsible for the opposite transformation (i.e. from consequences to action) [10]. The sensorimotor loop in Fig 1.6 shows the interactions of the internal models.

In the sensorimotor loop in Fig 1.6, when an agent intends to perform an action like grasping an empty tea cup, the inverse model generates the required motor command considering the current state of the hand, the grasping task and the tea cup. The forward dynamic model estimates a new state of the hand given the current state of the hand, the efferent copy of the newly generated motor command and the tea cup. Then the forward sensory model predicts the sensory feedback as a result of moving from the current state to the new state of the hand given the efferent copy of the newly generated motor command and the tea cup. Following actual physical execution of the motor command the actual sensory feedback generated is compared with that predicted by the forward sensory model. The discrepancy or

error arising from this comparison is used to update the internal models in order to produce a more fine tuned motor command for use in properly performing or repeating the task if needed. The repetition of an action, especially a novel one, would generate a distribution of errors corresponding to the discrepancies between the expected (i.e. the prediction of the sensory forward model) and the actual sensory feedback. The internal models optimises the properties e.g. minimizes the variance of the error distribution to narrow the discrepancy. In this way the internal model learns to produce a more accurate motor command.

This concept of internal models points out the importance of actual sensory feedback and repetition of an action while learning a motor task. The discrepancy between the actual and predicted feedback gives a way of knowing how well the generated motor command suited the intended action. It can also be used to differentiate a self generated from externally generated action since the later will cause large discrepancy because of the lack of internally generated counterpart. It would not be possible to obtain the discrepancy or differentiate self from externally generated action if either the actual or the predicted sensory feedback is not available. There should also be issues if either the actual or the predicted sensory feedback is disrupted or altered. The actual feedback may be altered in the case of an injury to the spinal cord where a patient might experience loss of sensation/proprioception. The predicted feedback might be missing in the case of brain lesion affecting the parietal cortex including the intraparietal sulcus [15, 16] for example. Simulation of the workings of the internal models may help in understanding what happens in these group of patients. For example when the actual or predicted feedback is not available, the internal models can not learn on the basis of the discrepancy between the actual and the predicted feedback. In the absence of the actual feedback, the models may assume that all the generated motor commands worked as expected which is not necessarily true especially if the intended task is novel. Also the model may assume the opposite (i.e. that the motor command was completely wrong) since comparing the predicted feedback with zero actual feedback will lead to maximum discrepancy. In the other hand, in the absence of the predicted feedback, an internally generated movement may be misinterpreted as externally generated since an external feedback may be anticipated.

These issues in the model due to missing signals/feedbacks may contribute to cortical reorganisation that can be detrimental following an injury to the nervous system.

1.4.3 Attempted and imaginary movement

Attempted movement

For healthy individuals, *attempted movement,(AM)* results in the movement similar if not exact to that desired. This is not necessarily the case in patients who have neurological injuries.

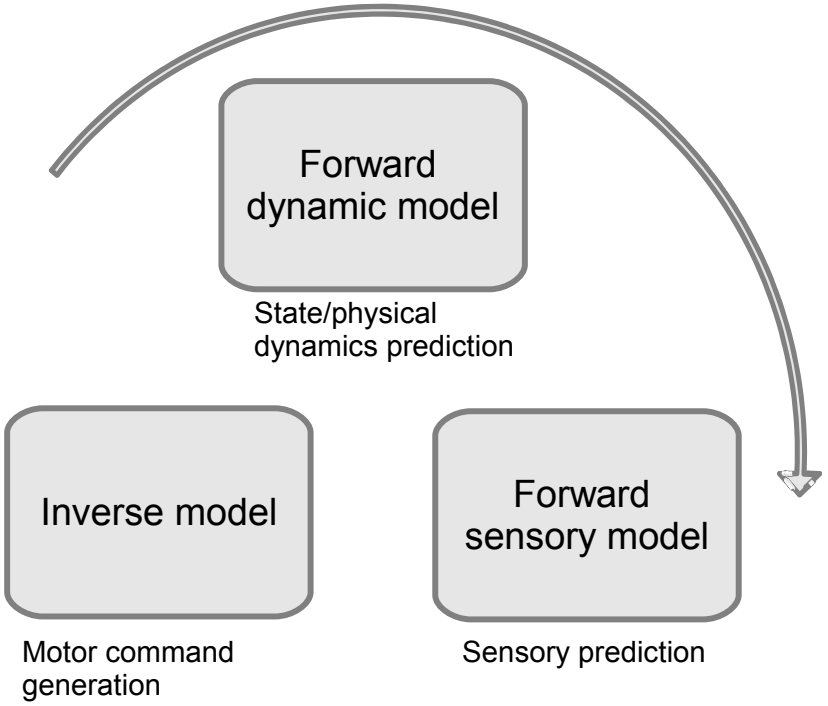

Figure 1.6: The sensorimotor loop showing the internal models [10].

As a result of the injury the desired movement might not be produced when attempted. In some case no movement at all might be observed.

Motor imagery

Motor Imagery (MI) is the mental simulation of an action. It is also called *explicit MI* because it is a conscious process unlike mental rotation discussed below. Motor imagery is similar to physical motor execution except that the movement is not physically performed in the case of MI. The mechanisms of MI is not fully understood but studies have shown that similar areas of the motor cortex activated during actual physical movement are activated during MI of the movement [17, 18].

Unlike a physical movement execution which is an overt process, MI is a covert process [18]. A covert action is not physically executed but it has similar neural characteristics as an executed action [18]. Covert actions also include movement observations [18]. During movement observation of an action, the motor cortex is also activated in a similar manner as during MI [18].

There are two main kinds of MI, namely kinesthetic and third-person MI [19, 20]. The kinesthetic kind involves MI performed in the first person perspective with the performer experiencing the kinesthetic feeling or bodily sensations associated with the action being imagined [21]. On the other hand, the third-person kind is performed in the third person perspective where the performer forms the visual representation of the action or of the scene

of the action [21]. The former is more similar to physical movement than the later because of the nature of their motor cortex activation [17, 18, 19, 21].

Mental rotation of hands

The *mental rotation* of a hand occurs when an internal representation of the hand is rotated. It is an *implicit MI*. This means that it is similar to MI. An example of when mental rotation occurs is when judging the laterality of human hand pictures at various orientations. If a picture of a hand is presented to a subject for laterality judgement, the subject implicitly rotates an internal representation of each of his/her hands in order to determine which hand aligns correctly with the hand picture. The rotation of the internal representation of the hands activate the motor cortex in a similar manner as MI. Mental rotation will be discussed further in Chapter 4.

1.5 Electroencephalogram

Electroencephalogram (EEG) is extracellular electrical field potentials recorded from the scalp. It is a measure of direct neuronal electrical activity. It has milliseconds resolution and can be studied in different frequency bands [22, 23, 24]. Its is recorded by placing electrodes on the scalp.

1.5.1 Electrodes positioning

Recording of EEG is done by placing electrodes on the surface of the scalp. Electrical contact between the electrodes and the scalp can be achieved by application of a conductive gel. The position of the electrode are often determined by the international standard system of electrode placements including the 10/20, 10/10 and 10/5 systems [25]. The 10/10 standard electrode positions and some of their names are shown in Fig. 1.7. The standard electrodes positions are available on commercial EEG caps. The EEG caps come in different sizes to allow for different head sizes based on measurement of head circumference and the distance between the nasion and the inion.

1.5.2 Electrode montage

Different electrode montages are used in EEG recording. The most often used montages can be derived offline or during the online recording of EEG. The montages include the monopolar, bipolar, Laplacian and the *common average reference*.

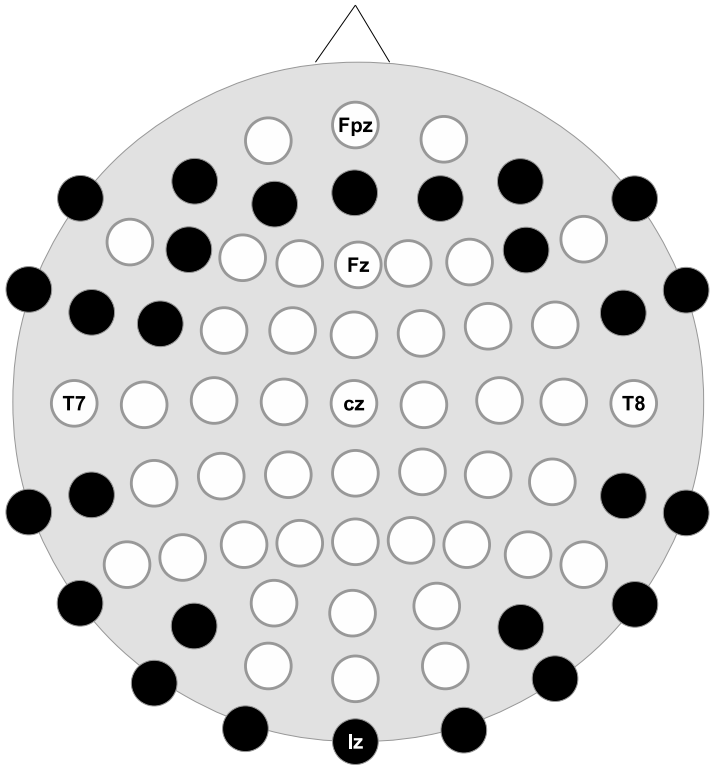

Figure 1.7: The 10/10 standard electrode positions.

The monopolar derivation is the default montage of EEG recording and the other montages mentioned above are derived from monopolar recording. Three electrodes can be used to derive a monopolar signal. The electrodes include an active electrode, a *ground electrode* and a *reference electrode*. Simplifying, the signal is derived as $(active-ground)-(reference-ground)$. The active electrode is placed on the scalp on the location of interest while the choice of the locations for the ground and the reference electrodes can be anywhere else on the scalp, ear lobes or the tip of the nose. The main choice of location for the reference is usually a location lacking in brain activity. The ground electrode provides a connection to the earth.

The bipolar montage is obtained by subtracting two monopolar derivations. Since it gives the difference in voltage between the two monopolar montages, the bipolar montage can help to attenuate noise represented similarly in both monopolar recordings.

The Laplacian montage is derived by approximation of the Laplace filter [26, 27]. To derive the Laplacian signal for a channel, the average of the surrounding channels is subtracted from the channel. The distance of the surrounding channels determines the size of the Laplacian filter. Small Laplacian filters with surrounding channels at 10% distance as defined in the 10/20 standard system is often used. Laplacian signal can greatly enhance local activities by subtracting activities represented similarly in surrounding electrodes.

The common average referencing method reduces the influence of far field sources but may

introduce artefact from one channel into another [27]. It is derived by subtracting the average of all channels from each individual channel.

1.5.3 Frequency bands

The EEG signal is processed in specific frequency bands. Different specific EEG *frequency bands* are associated with various physiological processes. The EEG frequency band used in this thesis ranges from 0.5 to about 30 Hz. This range includes the δ, θ, α, μ and the β frequency bands. The δ-band has frequencies less than 4 Hz. It is found in the frontal areas in adult during sleep and during some continuous attention tasks [24].

The θ-band has a frequency range of 4-8 Hz. The θ-band can occur during action inhibition, drowsiness and it is found in locations that are not associated to a task at hand [24].

The α-band has a frequency range of 8-13 Hz [24]. It is found around the occipital and frontal areas of the head and is associated with process inhibition. The α-band amplitude is enhanced when the eyes are closed or during relaxation [24]. The μ-band often referred as the Rolandic μ rhythm has frequency range of 8-12 Hz which overlaps with that of the α-band [24]. For this reason the two may be confused and the α-band which has a larger amplitude and spatial distribution may overshadow the μ-band. Electrode derivation methods that enhances local activities can be exploited to differentiate between the two. The μ-band is found in the central cortical representation areas that are concerned with sensory input and movement control. Consequently the μ-band is associated with movement related cortical activities. Its amplitude in the contralateral hemisphere is suppressed during movement related cortical processes like movement imagination, execution and observation of a body part [28]. The μ-band has several applications in this thesis.

The β-band has a frequency range of about 12-30 Hz [24]. It can be found in the frontal and the central areas. It is associated with active mental state, focus and alertness. Its activities during motor processes varies. Often the lower frequency band (12-16 and 16-24 Hz) decreases in amplitude during motor processes (in a similar manner as the μ-band) while the the upper band may show increased amplitude in the brain hemisphere contralateral to the one performing the motor processes [28]. The β-band has several application in this thesis.

1.6 Brain computer interface

A *brain computer interface (BCI)* is a system that allows direct communication between the brain and a computer. In a typical BCI system, signal is acquired from the brain and used by the computer to determine the state of the brain. After determining the state of the brain by processing the recorded signal, the computer can translate the state into an action command.

The action command can include moving a computer cursor, control of a computer game or control of external devices like a wheelchair, control of a robotic hand and so on. A diagram showing the basis of a BCI is shown in Fig 1.8.

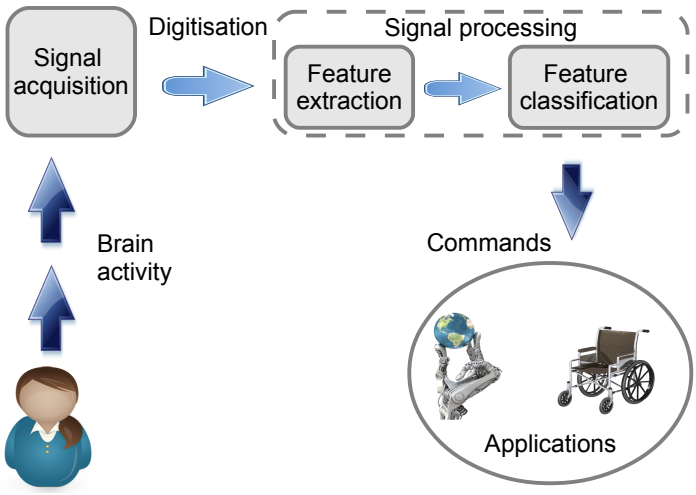

Figure 1.8: The schematic diagram of a BCI system.

Brain computer interface was originally developed for communication purposes. It has only recently been applied to rehabilitation. There are various signals modalities that can be used to build a BCI system used for the purpose of communication. The signal modalities are described in Table 1.2. This thesis focuses on BCIs that can be used for movement rehabilitation following neurological injury. In movement rehabilitation, only EEG from Table 1.2 is widely used. The EEG can be easily recorded and it is portable compared with fMRI for example. It provides a measure of neuronal electrical activity and not hemodynamic response in the case of fMRI, the later having latency between a task and the related brain activity.

Also in BCI for communication, different EEG control signals are used. These are described in Table 1.3. The *Event related desynchronisation (ERD) and event related synchronisation (ERS), ERD/ERS* which can be effectively modulated by users even following many neurological injuries is widely used in movement rehabilitation. These features are easy to compute and require minimum number of EEG electrodes minimizing setup time. This advantage makes the ERD/ERS method suitable especially for therapeutic BCI where setup time must be minimized given that patients are not normally available for experiments for a long period of time. The features are well established and researchers can target physiologically relevant frequency bands when using it as features for therapeutic BCI.

Table 1.2: Signal modalities used in brain computer interface.

	Modality	Description
Non-invasive		
	EEG	EEG (described in Section 1.5) is the extracellular electrical field potential recorded from the scalp with milliseconds temporal but poor spatial resolution [24]. It is a direct measure of neuronal electrical activity recorded by placing electrodes on the scalp [29].
	MEG	Magnetoencephalography (MEG) is the recording of magnetic field arising from neuronal electrical activities. It has similar temporal but higher spatial resolution than EEG [29].
	fMRI	Functional magnetic resonance imaging (fMRI) is a method of measuring brain activity by measuring hemodynamic response during mental activity. It has a lower temporal ($\approx$1 s) but a higher spatial ($\approx$1 mm) resolution compared with EEG. Since it determines brain activity by measuring the associated hemodynamic response, it is an indirect measure [29].
	NIRS	Near infrared spectroscopy (NIRS) can be used to indirectly measure brain activity exploiting hemodynamic response to brain activity in a similar manner as fMRI [29]. Hemodynamic changes are determined from changes in attenuation of light of near infrared wavelength. It has similar temporal but about five times lower spatial resolution than fMR [29].
Semi invasive		
	ECoG	Electrocorticography (ECoG) is a technique that measures direct brain electrical activity through semi invasive electrodes placed on the surface of the cortex. It provides signal of higher amplitude and is not artefact prone compared to EEG [29]. It also has higher spatial resolution than EEG [29].
Invasive		
	IcNR	Intracortical neuron recording (IcNR) is an invasive technique for measuring direct electrical brain activity by placing electrodes inside the gray matter of the brain [29]. It has similar temporal resolution as ECoG but because it can capture spike signal from single or a small pool of neurons it allows for the highest spatial resolution.

Table 1.3: EEG-based control signal used in brain computer interfaces

Feature	Description
P300	A P300 potential occurs at about 300 ms following a visual, auditory and other stimuli. The P300 signal is used in BCI by exploiting the oddball paradigm. In this paradigm, when two stimuli are presented interchangeably at different rate, the infrequent stimulus is associated with a larger potential [29].
VEP	Visual evoked potentials (VEP) are EEG potentials occurring as a result of processes in the visual cortex in response to visual stimuli [30]. It includes steady state visual evoked potential (SSVEP). Following visual stimulation at a specific frequency, SSVEP with fundamental frequency equal to that of the stimuli is generated in EEG [31].
ERD/ERS	Event related desynchronisation (ERD) and event related synchronisation (ERS) [28, 32] refer to decrease and increase respectively of EEG power relative to a baseline period within a narrow frequency band. Movement related cortical processes like those during MI and physical execution can be quantified with ERD across the sensorimotor cortex. ERD/ERS, sometimes referred to as event related spectral perturbation [33], is used as a general term to refer to both ERD and ERS.
MRCP	Movement related cortical potential is a negativity in EEG signal that occurs as a consequence of movement execution or imagination [34].
SCP	Slow cortical potential (SCP) is a slow change in EEG below 1 Hz lasting from one to several seconds [35]. An increase in brain activity is marked by negative SCP while a decrease in brain activity is marked my positive SCP.

1.7 Functional electrical stimulation

A *functional electrical stimulation (FES)* device delivers a small electrical current that activates motor units (consisting of an alpha motor neuron and the muscle fibres it innervates) [36] in such a pattern to allow functional tasks to be carried out. The electrical current induces contraction of muscles and therefore causes movement. The stimulation can be applied noninvasively using bipolar electrodes placed on the neuromuscular junctions of the muscle of interest. It can also be applied by placing an active electrode on the nerves innervating the muscles of interest with the anode placed along the path of the nerve. The former will be used in the experiments described in this thesis.

1.7.1 FES versus voluntary muscle activation

In voluntary muscle activation, motor units fire asynchronously and are recruited in a certain order where low-force and fatigue-resistant motor units are preferentially recruited first (Henneman,1981 as cited in [37]). The results of this method of firing and recruitment are smooth and fairly energy conserving motion. Motor units activation by FES differ from this. In FES, largest axons which innervate large motor units are first recruited before the smaller ones [37] because the large motor units have smaller resistance and conducts current at faster rates [38]. The large motor units have the least fatigue resistance and smallest energy conservation. Therefore these motor units cause fatigue more quickly. Their recruitment means that muscles can contract with non-smooth excessive force that lasts only a short time. For these reasons FES can easily cause muscles fatigue and produces less smooth motion when compared to voluntary muscle activation. Nevertheless, FES can still produce functional movements that mimic voluntary motor activation if the parameters of the stimulation are carefully chosen.

1.7.2 Parameters of FES

Surface FES devices have several parameters, illustrated in Fig. 1.9, that can be varied. The main parameters and their typical settings used in this thesis include the current amplitude typically between 10 to 60 mA, frequency of stimulation typically about 26Hz and the stimulation pulsewidth typically about 200 ms. In Fig. 1.9 the current is ramped while the pulsewith is kept constant but this can be reversed where the current is kept constant and the pulsewidth is ramped. An FES device normally have multiple channels to allow simultaneous and sequential activation of different muscles in order to achieve a more realistic movements. They can interface directly to a computer through the USB bus which

allows easy control of the parameters to achieve a desired quantity of charge and pattern of stimulation.

The charge deposited by an FES device is given by,

$$\begin{aligned} Q &= Ip_w t_s / IPI \\ &= Ip_w t_s v \end{aligned} \tag{1.1}$$

where I is the current, p_w is the pulsewidth, t_s is the total stimulation time, IPI is the inter pulse interval and $v = 1/IPI$ is the frequency. The charge per unit pulse is given by Ip_w. To prevent potential damage to cells, the pulses can be delivered in a biphasic shape as shown in Fig. 1.9. Also as shown in Fig. 1.9 the shape of the overall stimulation is trapezoid in order to allow the receiver to gradually adapt to the stimulation to reduce pain.

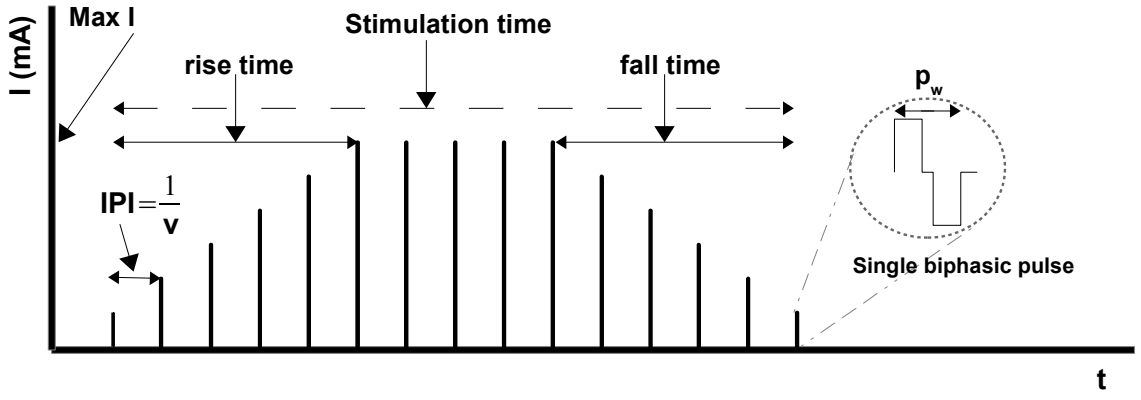

Figure 1.9: A single channel illustration of common FES parameters used in BCI-FES. The inset shows the p_w of a charge balanced single biphasic pulse. IPI, inter pulse interval; I, current; v, frequency; p_w, pulsewidth; t, time.

The FES parameters must be carefully chosen to avoid painful stimulus. This can be achieved by keeping the charge Q as low as possible by adjusting the current, frequency and pulsewidth. The frequency of stimulation require special consideration because low frequencies below 12.5 Hz produces unpleasant non-tetanic contraction [39]. On the other hand, high frequency of about 50 Hz and above will cause fast muscle fatigue. This is because FES will keep recruiting the same group of motor units and at high frequency of stimulation, these motor units are recruited at faster rate accelerating muscle fatigue.

1.8 Spinal cord injury

Spinal cord injury (SCI) is caused by either trauma or disease. It leads to reduced sensory, motor functions and reflex control, control of involuntary functions. The SCI negatively

affects the quality of life making sufferers dependent on others for even basic life needs. Traumatic causes of SCI include accidents, assaults and sports related injuries. Disease related SCI includes multiple sclerosis, ischemia, spinal cord tumour and others [40]. More men suffer SCI than women mainly because most of the injuries are caused by trauma which occurs in activities dominated by men [41].

1.8.1 Categorisation of SCI

Level of injury

The lowest spinal segment below which abnormal motor and sensory functions are present is known as the neurological level of injury. The higher the neurological level of injury, the more the loss of functions. A cervical injury (injury at the cervical segment) results in tetraplegia. Tetraplegia is the loss of upper and lower extremity functions also known as quadriplegia. An injury below the cervical segment results in paraplegia which is a loss of lower extremity functions [41]. Tetraplegia is more serious than paraplegia because it involves more complications and loss of hand functions. The loss of hand functions makes patients more dependent and most patients regard the loss of hand functions as the most devastating consequence of their injury [42].

Completeness of injury

A SCI can be complete or incomplete. According to the American spinal injury association (ASIA) impairment scale, an injury is *incomplete* if the patient has anal sensation, deep anal sensation and sensation at the mucocutanouse junction at spinal segments S4 to S5 [43]. A SCI patient with these sensations is scored/classed in the ASIA impairment scale as having at least ASIA B. But if the patient has preservation of voluntary function of the anal sphincter then the injury is scored as at least ASIA C and the injury is referred to as motor incomplete. A *complete injury* which is scored as ASIA A is an injury where there is no motor and sensory functions in the spinal sacral segments, S4 to S5. The guidelines to assessing the ASIA impairment score is shown in Fig. 1.10[2]. The ASIA impairment scale assessment form is shown in Fig. 1.11[3]. A complete injury is more severe than an incomplete one. Kirshblum and colleagues showed that a patient with initially incomplete injury has a better chance of improvement in the level of injury and motor index score [44].

[2]The guidelines to assessing the ASIA impairment score is available at: `http://www.asia-spinalinjury.org/elearning/isncsci_worksheet_2015_web.pdf`, Accessed: 26/06/2015

[3]The ASIA impairment scale assessment form is is available at: `http://www.asia-spinalinjury.org/elearning/isncsci_worksheet_2015_web.pdf`, Accessed: 26/06/2015

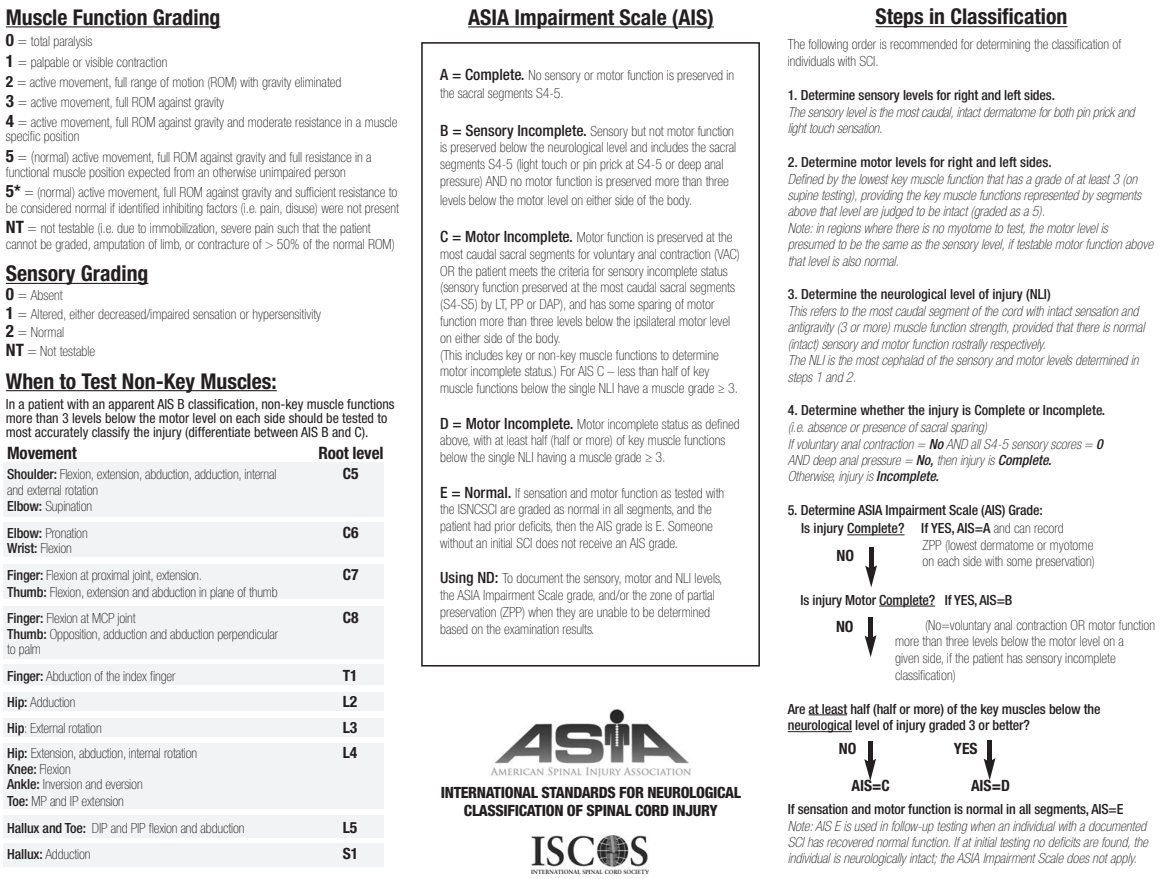

Figure 1.10: The guidelines to assessing the ASIA impairment score.

Acute, sub-cute and chronic SCI

The acute stage begins from the time of injury up till about a few days or weeks[4] [4]. This is the stage when a patient is in a critical condition and in shock due to the injury. From about a few weeks to the first six months, post-SCI, can be regarded as the *sub-acute* stage of the injury [4]. Following the sub-acute stage is the chronic stage. Natural recovery of functions occurs mostly in the sub-acute stage rather than in the chronic state [4, 44].

1.9 Methods of neurorehabilitation of hand functions after spinal cord injury

Different non-invasive neurorehabilitation methods are used in spinal units to help patients to regain their hand functions. These methods are discussed in subsequent paragraphs.

[4]Note that there are no general definition of the acute, sub-acute and the chronic stages in SCI: see `http://sci.rutgers.edu/index.php?page=viewarticle&afile=10_January_2002@AcuteSubChronicSCU.html`, Assessed: 22/07/2015

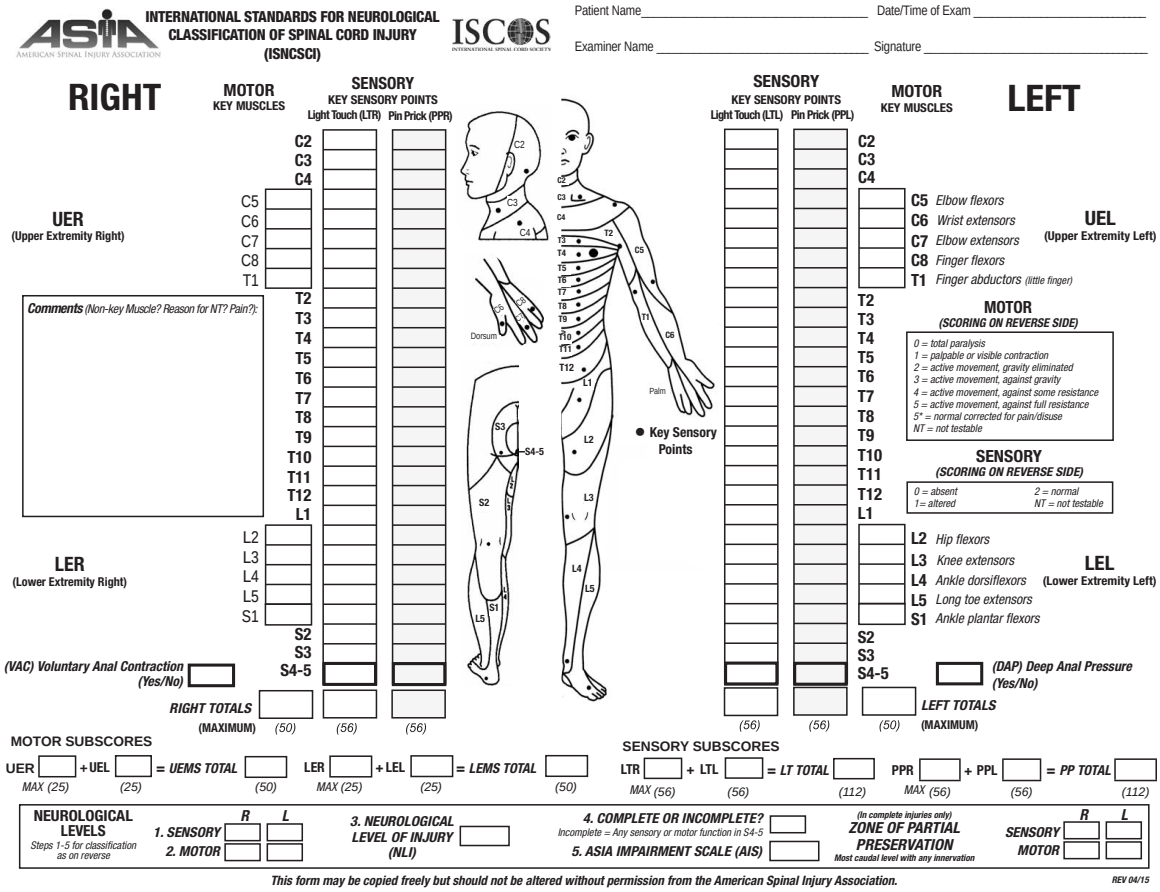

Figure 1.11: The ASIA impairment scale assessment form.

Physical and occupational therapy are major part of the intervention SCI patients receive for neurorehabilitation purposes. For example it is an integral part of the rehabilitation plan at the *Queen Elizabeth National Spinal Injury Unit, Southern General Hospital, Glasgow*. This is the hospital where major part of the work on this thesis was performed. Patients at this hospital normally attend therapy sessions four days in a week from Tuesday to Friday. A session lasts for one hour. During the sessions patients' hands are massaged and stretched to straighten the fingers preventing them from clawing. The patients are then given several physical activities involving functional use of the hands. These activities include grasping objects like spoons, using computer keyboards, gaming with playstation keypads and practicing different kinds of pinch. The activities are normally repetitive and the patients are supported with splints, orthosis and other supporting devices.

Functional electrical stimulation is widely used for functional hand neurorehabilitation [45, 46, 47]. For example, at the Southern General Hospital, FES is used during the hand therapy sessions. It is applied using surface electrode and is primarily used for strengthening muscles. The FES is set to repeatedly and automatically move the patient's hands, i.e without the patients' input. The use of FES in this automatic mode is said to be passive because the FES is not controlled by the patients' actions of the hand being stimulated. The stimulation

normally last about 30 minutes (for every ten seconds at ten seconds interval). The current is ramped and set to visibly contract the muscles with pulsewidth and frequency set to 200 μs and 30 Hz respectively.

Instead of applying the FES completely passively, the patients can be engaged in the rehabilitation process by getting them to control the FES. This method involving the *active participation* of a patient is used in functional electrical therapy [47, 48]. In functional electrical therapy, a patients uses the unimpaired hand and/or residual hand function to control the FES, starting and stopping it using a button. Another method that can be used to engage the patient is the use of EMG to trigger the FES [49]. In this method, a patient uses a residual movement to produce EMG which is detected and used to trigger the FES to assist in completing the movement. These methods require an active participation of a patient in the neurorehabilitation process and may therefore lead to better outcome [50, 51, 52].

Some commercially available products incorporate FES. Examples are the Handmaster [53] and the Bionic glove [54]. The Handmaster has a splint through which FES electrodes are attached to stimulate the flexor digitorum superficialis, extensor digitorum communis, flexor pollicis longus, extensor pollicis brevis and the thenar muscles. With the stimulation of these muscles, the Handmaster can assist in repetitive hand opening and closing allowing object manipulation. The Bionic glove is controlled by a wrist position transducer that works by augmenting wrist extension and flexion tenodesis effects [53]. Tenodesis effect here is the mechanism of a passive hand grasp and release mediated respectively by wrist extension and flexion. The Bionic glove uses three channels of electrical stimulation to activate the finger flexors and extensors and thumb flexors.

The methods incorporating FES especially those requiring active participation of a patient have been hypothesised to be hugely beneficial in neurorehabilitation [55]. However the usual implementation of the methods require a patient to have residual hand or generally upper limb function or be able to produce muscles contraction that can be recorded with an EMG device. During the early sub-acute stage of an injury, patient might not meet these requirements. But it is important that rehabilitation is started as early as possible in order to enhance natural recovery process occurring during the sub-acute stage. For these patient who do not meet the requirement of residual function, alternate rehabilitation techniques supporting physical and occupational therapy are needed in order to start the neurorehabilitation as early as possible. An investigation into an alternative rehabilitation technique forms the main aim of this thesis.

1.10 Aim

The main aim of this thesis is to build a BCI-controlled FES for neurorehabilitation of hand functions. The BCI-controlled FES called BCI-FES would allow a thought-controlled FES. Among other benefits which will be discussed in later chapters, BCI-FES encourages active participation of a patient during rehabilitation and no residual motor function of the hands is required. Because no residual function is required, BCI-FES will allow a patient-controlled FES neurorehabilitation to be started very early in the sub-acute stage of SCI during which a patient might lack residual functions. The BCI-FES system will be tested on sub-acute SCI patients. The aim is divided as follows:

1. Researching of current methods in BCI-FES
2. Development of patient assessment methods and BCI features for BCI-FES therapy
3. Treatment of patients with BCI-FES and results

1.11 Overview

The work carried out in this thesis in order to fulfill the aim are presented in subsequent chapters as follows. In this first chapter, important terms relevant to the thesis were introduced. The work done for the first aim is presented in Chapter 2 and Chapter 3. In Chapter 2 the theoretical framework and the past studies of BCI-FES are reviewed. Chapter 3 formulates the mathematical techniques and methods followed in the thesis. Chapters 4 to 7 are for the second aim. A possible tool, mental rotation of body parts, that can be used in rehabilitation is studied and compared with movement imagination in Chapter 4 and 5. Chapter 6 studies a BCI feature called time domain parameter which was later used in Chapter 8 and Chapter 7 studies a method of outcome assessments also used in Chapter 8. For the third aim, a study which investigates the use of BCI-FES for rehabilitation of hand functions in SCI patients is in the Chapter 8. For the last part, Chapter 9 discuses and summarises the thesis.

Chapter 2

Theoretical framework and literature review

Some say the rich get richer, but I say, the higher you fly the less gravity.

2.1 Abstract

Brain computer interface and functional electrical stimulation systems are either coupled or used individually in neurorehabilitation therapies after stroke or spinal cord injury. The first activates the nervous system in the efferent direction while the second can activate it in both efferent and afferent directions. When both systems are used together, the efferent and the afferent pathways of the nervous system are simultaneously activated with reenforcement by the brain computer interface system. This activation encourages the Hebbian type learning which researchers believe may facilitate recovery after spinal cord injury. In this article, the current state of the art in the brain computer interface coupled functional electrical stimulation technologies are reviewed with respect to neurorehabilitation. The results of past studies from patients using the systems are discussed.

2.2 Introduction

Neurons adjust their activities and/or morphologies in response to changes [56]. This is termed neuroplasticity. Following an injury to the nervous system, neuroplasticity occurs leading to desirable and undesirable effects in the nervous system. The clinical practice that exploits neuroplasticity, encouraging its desirable effects, to restore or improve impaired functions after injury to the nervous system is termed neurorehabilitation [56].

Classically, there are two main approaches used in rehabilitation namely behavioural and restorative approaches [57]. The behavioural approaches are those in which patients are taught strategies that compensate for lost functions. The restorative approaches which is most suited to neurorehabilitation constitutes those that targets the improvement or restoration of the lost function itself. An addition to these two main approaches is the metacognitive approach in which patients are taught techniques that facilitates self monitoring when performing tasks [57].

Researchers are working towards understanding the mechanisms of neuroplasticity in order to achieve better neurorehabilitation. It is now known that existing connections in the nervous system can be altered and new ones can grow [58]. It is also known that following axotomy (axon slicing/severing), axons can regenerate by growing new branches [58]. Such regrowth can lead to good reinnervation when the degenerating synapses are not concentrated in an area but rather distributed among intact synapses [58]. Many injuries in nature lead to distributed degenerating synapses and therefore good reinnervation can occur following axonal regrowth leading to restoration of lost functions [58].

In order to understand neuroplasticity, appreciating the basic neural mechanisms governing memory acquisition and learning is vital [59]. In the early 20th century, Ivan Petrovich Pavlov, described a learning mechanism commonly known as classical conditioning [60]. In classical conditioning, a conditioned stimulus (CS) is paired with an unconditional stimulus (US) which is accompanied by an unconditional response (UR). Following conditioning, involving repetitive pairing of the CS and the US, the CS is accompanied by a conditional response (CR) which is similar to UR. In essence the general idea of this conditioning is that: events become associated with one another in the brain if the events tend to occur together [59].

The Pavlov's theory in 1927 is the basis of a later postulate in the middle of the 20^{th} century by a Psychologist, Donald Olding Hebb. The Hebb's theory on the neural basis of plasticity/learning is commonly known as the Hebbian learning or Hebb's postulate [61]. Hebbs stated that if a repetitive activation of a presynaptic cell causes a repetitive activation of a postsynaptic cell, changes occur in both or one of the cells in order to encourage the activation pattern. This postulates at a cellular level a plausible basic mechanism of neuroplasticity. Several studies have confirmed that paired repetitive activation leads to neuroplasticity in human and animals [62, 63, 64, 65, 66].

One method researchers believe can be used to achieve Hebb's type learning for neurorehabilitation is the use of motor imagery (MI) or attempted movement (AM) based brain computer interfaces (BCI) coupled with neuromuscular electrical stimulation or functional electrical stimulation (FES). This coupling is called BCI-FES and it was first demonstrated non-inversely in human by Pfurtscheller and colleagues [67] in a study that was not directly

targeting functional recovery. Motor imagery which is used in BCI-FES is the mental simulation of a motor action which activates the motor cortex as though the motor action is physically performed (see Section 1.4.3). The FES on the other hand can passively stimulate the muscles to contract them and at the same time activates the nervous system in the afferent direction (somatosensory cortex activation). The role of the BCI is to precisely determine from the activities of the motor cortex when MI is performed. The FES is activated once motor cortex activity is detected. By temporally correlating the repetitive and simultaneous activation of the motor cortex and the somatosensory cortex, the Pavlov/Hebbian learning or neoplastic effect could be achieved [62]. Since this is the case, BCI-FES should benefit patients with neurological injuries.

The aim of this work is to review the rational, methods and the benefits of using BCI-FES in neurorehabilitation of hand after stroke and spinal cord injury. The BCI-FES described is for patients with mild to intermediate motor impairment or in the case of SCI, incomplete injury.

2.3 BCI-FES as a device for inducing neural plasticity

Brain controlled FES is relatively a new and developing technology (see [68] for a review of the technology) with promising clinical application. It has recently been shown that BCI-FES leads to short-term plasticity [69]. This was shown with ten healthy subjects where motor evoked potential (MEP) was enhanced more when the subjects' grasp functions were guided with BCI-FES than when the grasp functions were guided with BCI alone, FES alone or when they were under voluntary control. A similar result has been reported by Niazi and colleagues [34] who also used MEP to quantify neuroplastic effect of applying electrical stimulation following detection of movement related cortical potential (MRCP). The MRCP is a negativity of time domain that relates to movement planning and can be seen on EEG prior to movement onset [70, 71]. The subjects in the study by Niazi and colleagues performed MI of ankle dorsiflexion to generate the MRCP. The MEP was compared between three conditions namely MI with electrical stimulation, MI alone and random electrical stimulation alone. Subjects were assigned to one of the conditions. They found that MEP of the tibialis anterior muscles was significantly more enhanced in the MI with electrical stimulation condition than in the other two. These results on healthy subjects suggest that BCI-FES can induce neural plasticity. The neuroplastic effect of a device like BCI-FES has been explained using Pavlovian and operant/instrumental conditioning and the interested reader should look at a review by Silvoni and colleagues [72]. This section explores the plausible mechanisms by which each of MI/AM based BCI and FES contributes to the possible neuroplastic effect of BCI-FES system.

2.3.1 Role of MI/AM-based BCI

In addition to encouraging active participation, the role of BCI is to detect objectively the cortical activation representing an intention to move. For MI/AM-based BCI the cortical activation is due to performance of MI/AM. So the role of BCI is to detect MI/AM objectively. Therefore an appropriate name for the BCI-FES system in this article would be MI/AM-FES. So in this section, the propagation of efferent signal due to MI/AM activation of the motor cortex and the afferent signal due to FES activation of motor neurons and the sensory cortex will be discussed. Furthermore, the interactions of both signals that possibly lead to neurorehabilitation will be highlighted. For reasons that will be given later, AM rather than MI should be used in neurorehabilitation. But because MI also allows the rehearsal of movement and gives a way for healthy individuals to simulate AM of stroke and SCI patients and therefore enables BCI-FES to be tested, MI will be included in this discussion.

Role of AM

Movement intent resulting from MI/AM activates the motor cortex in a similar manner as actual movement execution [17, 18]. The activation of the motor areas of the cortex is very important for motor neurorehabilitation given that the activation of the contralateral hand area of the motor cortex is a predictor of functional hand rehabilitation in patients with brain lesions [73]. See Soekadat et.al. [74] for AM or motor execution-based BCI rehabilitation following stroke.

Following a neurological injury leading to impaired motor functions, the motor cortex can still be activated albeit with some differences when compared with healthy individuals [75, 76] during action execution. Due to injury, the number of synapses between the upper motor neurons and the α-MN in the anterior horn of the spinal cord can be diminished [77]. Such reduction in the number of synapses might result from upper motor neuron death following their denervation caused by the injury [58]. The remaining synapses might not be enough to transmit the correct signal to allow the intended movement to be carried out. So no physical movement might be observed when a patient with the motor impairment attempt to move and consequently no feedback will be received by the somatosensory cortex and the internal monitoring system. A discrepancy which might be detrimental is created because the monitoring system has no feedback to compare with the efferent copy. Because no feedback is received, the activation of the muscle involved is assumed to have no effect and the brain can assume that the muscle no longer exists leading to detrimental cortical reorganisation [78, 79, 80, 81]. However the activation of the motor cortex and the subsequent activation of the spared upper motor neurons and the α-MN synapses allows for the possibility of rehabilitation to occur as follows. If the intended movement can be externally completed with FES

for example, an approximate feedback can be made available to the somatosensory cortex and the internal monitoring system. In this manner the sensory cortex (including the internal monitoring system) is activated with the already activated motor cortex. Such simultaneous activation of the sensory and motor cortex can lead to rehabilitation according to the Hebb's theory. Also antidromic action potential resulting from FES can interact with the intent related action potential in the spared upper motor neuron in the Hebb's fashion as explained in Section 2.3.2.

Role of MI

For rehabilitation purposes AM might work better than MI since AM, usually preferred, [82] is more closely related to actual movement. Obviously while performing MI, one refrain from executing the imagined action [8]. So it can be argued that MI is not useful for rehabilitation purposes. Nevertheless, since MI activates the same neural pathways as actual movement execution, it can help to rehearse motor schema and therefore offer benefits similar to 'practice effect' of physical practice. Indeed studies have shown that MI is an important tool for motor rehabilitation following stroke [83, 84, 85]. See Soekadat et.al. [74] for MI-based BCI rehabilitation following stroke. In rehabilitation, the kinesthetic MI is preferred to the third-person MI since the kinesthetic kind is more related to real movement as discussed in Section 1.4.3. So the following discussion is about kinesthetic MI.

The reason overt movement is not observed during MI is still under investigation but there are suggestions which includes subliminal motor activation and inhibitory mechanism that would block the motor output [18, 20, 86]. Since the motor cortex remains active during MI, any suggestion of a complete inhibition at the level of the cortex can be dismissed [18]. The MEP studies show that MI effect can be recorded even beyond the spinal level showing also that no complete inhibition exist at the spinal level. MEP has been reported to increase following MI [87] and MI-BCI [88] sessions showing at least short term neuroplastic effects in the pathways from the cortex to a muscle. The increase in MEP is interpreted by researchers as corticospinal excitation thereby assuming that MI has effect at the motor neuron level. There are also evidence of EMG activity during MI [89, 90] showing that MI has effect at the muscular level. Therefore the level at which an inhibition of overt movement might occur during MI is unclear. If no complete inhibition occurs then a plausible explanation to why no overt movement is observed during MI is that motor system activation is subliminal [18]. Such a subliminal motor system activation is enough to cause a neuroplastic effect in the motor pathway but insufficient to trigger large contraction of muscles to allow movement. The neuroplastic effect which can be traced down to the motor neurons suggests that the discussions on AM can be applied to MI. Therefore the role of MI is likely similar to that of AM in rehabilitation.

2.3.2 Role of FES

Functional electrical stimulation can help in strengthening muscles that are under voluntary control [91] and can increase range of motion [92]. It can be used for neurorehabilitation purposes [47]. Functional electrical stimulation devices are widely used clinically because they have been shown to aid rehabilitation/neurorehabilitation after stroke and spinal injuries [45, 47, 93, 94, 95, 96, 97]. Patient-controlled functional electrical therapy in which patients use a switch to control functional stimulation patterns has lead to functional improvement [47, 48]. However the mechanism or mechanisms that lead to the observed rehabilitation/neurorehabilitation after using FES are not well understood [48]. A plausible model was put forward by Rushton [55] as follows. The electrical stimulus delivered by an FES device elicits action potentials in both motor and sensory fibres. The action potentials in the motor fibres travel orthodromically and antidromically. The antidromic action potential reaches the anterior horn where the axons of the upper motor neurons and cell bodies/dendrites of the α-MN make synapses. Assuming that these synapses follow the Hebb's mechanism, they are modified/strengthened when the antidromic action potential correlates with voluntary command in the form of action potential descending down the pyramidal tract. It is this correlation of action potentials that possibly leads to the observed functional improvement.This model which is yet to be thoroughly tested explains that voluntary effort or active participation is necessary in order to make the most of the therapeutic power of FES. Without active participation/voluntary effort, FES may only just strengthen the muscles and increase the range of motion but may not lead to neurorehabilitation [94].

In addition to the above model, the orthodromic action potential, when above motor threshold produces movement which in turn produces sensory feedbacks. These feedbacks are sent to the central nervous system through the sensory fibres and result in activation of the somatosensory cortex [98]. Without going into too many details regarding which synapse is modified, if the activation of the sensory cortex correlates with voluntary effort that activates the corresponding motor cortex area, Hebb's type strengthening can be expected in the synapses along the correlating pathways. Furthermore, of course feedback (consequence/causal relationship) is an important aspect of Pavlovian conditioning which is most likely the basics of associative learning [59]. So such a simultaneous activation resulting from intentional activation followed by re-afferent stimulation would encourage memory encoding and learning.

2.3.3 Role of BCI-FES

Before highlighting the role of BCI-FES it is important to point out that from the preceding section (2.3.2) it is clear that FES can be used independently for neurorehabilitation. But as

discussed in that section, active participation is a requirement when using FES in this way. A BCI based on MI/AM provides an objective method of ensuring/encouraging the active participation. Like the FES, MI/AM can be used independently for rehabilitation [74]. But in a situation where a patient has no residual movement, passive movement synchronised with MI/AM would yield a better result as discussed in Section 2.3.1. FES can provide such a passive movement. Therefore both FES and MI/MA based BCI should be integrated so as to achieve better results in neurorehabilitation.

The role of BCI-FES is that of providing neurofeedback and integration. Firstly, as a neurofeedback tool BCI-FES rewards a user's movement intention with application of FES for example. Such neurofeedback will encourage cortical modification that would benefit functional recovery. Secondly, BCI-FES system is designed to integrate its constituents ensuring synchrony between the onset of cortical motor activity due to performance of MI/MA and the onset of FES. The illustration in Fig. 2.1[1] shows how MI/AM generated activity is integrated with signal arising from FES. The propagation of these signals have already been discussed in the appropriate sections. The following explains how the signals are integrated in a BCI-FES system to achieve Hebbian learning.

Hebbian learning mechanism for BCI-FES

When a stroke or a SCI user of BCI-FES performs MI/AM of e.g. hand movement, the hand area of the motor cortex is activated and commands flow from the brain towards the muscles of the hand through the pyramidal tract in the spinal cord. Due to the depleted number of the upper motor neurons caused by the lesion as shown on Fig. 2.1, the correct movement is not produced. But the BCI system detects the MI/MA process from the activities of the motor cortex and activates the FES attached on the muscles of the hand to mimic the intended movement. The passive movement of the hand by the FES cause feedback/afferent information to be sent to the sensory cortex if the pathway is preserved (and may reduce the discrepancy in the internal monitoring system). So the MI/AM of hand movement causes hand movement associatively activating efferent and afferent neurons. Hebbian learning could be achieved by making this process repetitive. In addition, at the anterior horn of the spinal cord, the antidromic FES action potential is associated with the action potential traveling towards the muscle through the pyramidal tract and Hebb's mechanism is achieved as explained in Section 2.3.2.

[1]The brain image is adapted from: `http://en.wikipedia.org/wiki/Cortical_remapping#/media/File:Cerebrum_lobes.svg` while the lower limb is from: `http://gb.fotolibra.com/images/previews/49908-arm-muscles-illustration.jpeg`, Accessed: 15/05/2015

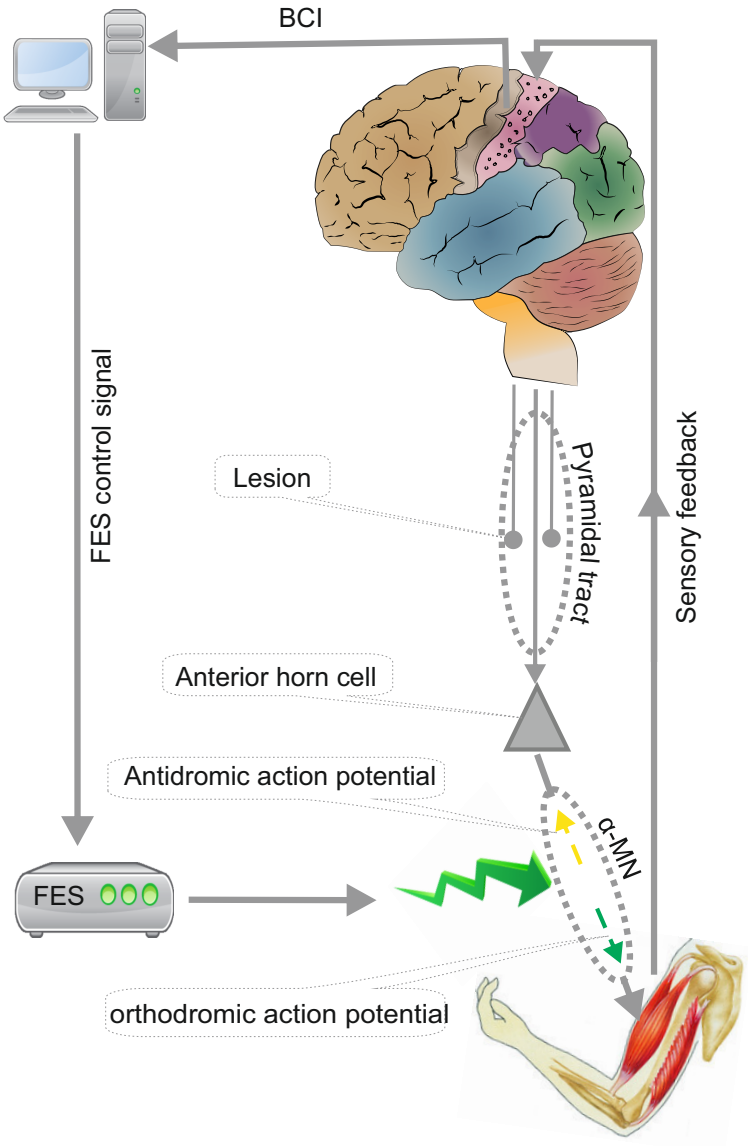

Figure 2.1: The schematic diagram of a plausible mechanism supporting BCI-FES benefits in neurorehabilitation. MN, motor neuron.

2.4 BCI-FES Experimental procedures

Studies of BCI-FES are performed on patients with mild to intermediate motor impairment. Table 2.1 shows several design parameters that have been used in BCI-FES studies for neurorehabilitation. The studies have been mostly done on chronic and acute stroke patients; only two articles [99, 100] reported studies on SCI patient. Only two of the studies [101, 102] are randomised controlled and the rest of them are either pilots, case series or single subject crossover studies. In the randomised controlled studies, the control group do not use the BCI system instead they receive passive FES [102] or no study related therapy at all [101]. The treatment group is normally referred to as the BCI-FES group.

The study sessions are usually grouped into three, namely the initial assessment, therapy

or training or treatment and the final assessment sessions. These sessions are carried out in the order they are listed here. In some cases further assessments are done within the therapy sessions. During the assessment sessions (initial and final) a patient is assessed using various outcome measures shown on Table 2.1. These outcome measures include the manual muscle test (MMT), modified Ashworth scale (MAS) for assessing spasticity, action research arm test (ARAT) for assessing the activities of daily living etc and Fugl-Meyer assessment (FMA) for assessing functional mobility etc. Further information on these measures can be found on the web[2]. Also the range of movement (ROM) and EEG is sometimes recorded in these sessions while the patient is performing functional tasks [101, 103]. The ERD activity computed from the recorded EEG can be compared between the initial and the final assessments to determine any difference.

A therapy session begins with attachment of 2-64 electrodes using gel to make contact with the scalp. Typical number of electrodes are shown on Table 2.1. The number of electrodes depends on the number of targeted muscles and the feature of EEG used to implement the BCI. At least 16 electrodes are placed around the sensorimotor areas when using the CSP method independent of the target muscle and a minimum of two electrodes are used for bipolar recording. For upper limbs rehabilitation employing the bandpower/ERD EEG features, electrodes are usually placed around the hand areas in each hemisphere. In this case as small as four active electrode can be placed when using the bipolar method of electrode derivation (to get 2 channels, one on each hemisphere). The number of active electrodes is at least nine/ten when using the Laplacian method of electrode derivation (to get 2 channels, one on each hemisphere).

After electrode placement, patients are normally asked to perform goal oriented AM/MI of the body part that they cannot move. The brain response to the AM is recorded and used to train a BCI classifier as described in Section 3.1.3. During the online part of the BCI, a patient can be asked to perform the AM repeatedly. The trained BCI classifier outputs the correct control signal to the FES whenever it recorgnises the brain responses. The FES is attached in such a way to activate the muscles that controls the part of the body that the patient is attempting to move. So whenever the brain is activated due to AM, the FES is activated to move the correct muscle which can be in a functional manner in order to assist the patient in completing the task. The precise location of electrode and the number of FES electrodes are not reported.

In a typical therapy session the patient will activate the FES about 50-75 times by performing AM [103, 104]. Most studies have 20 and above (see Table 2.1) therapy sessions and a session typically lasts about 60 minutes [103, 104]. Patients are normally scheduled to attend the therapy sessions three times in a week [101, 103, 104].

[2]Further information on assessment measures can be found at `http://www.rehabmeasures.org/rehabweb/allmeasures.aspx`.

Table 2.1: Demographic information and study design used in BCI-FES for neurorehabilitation

Ref.	Subjects	Injury onset (m)	Age	Gender	Design	#Treat./contr.	# Sessions	Outcome measure
[101]	Stroke	1.6±0.5	66±4.7	F,M	Rand. contr.	5 /3	24	FMA*,EEG*,etc
[103]	Stroke	10	43	F	Case study	1/0	9	ROM*,etc
[105]	Stroke	14	38	M	Crossover	1/ 1	10	LI*,CMC*, etc
[106]	Healthy	na.	35.4±13.0	F,M	Feasibility	5 /0	1	
[107]	Stroke	1.0±0.8	58.2±9.3	F,M	Case series	9 / 0	-	BCI control
[102]	Stroke	2.7±2.0	67.6±5.5	F,M	Rand. contr.	8/7	24	ARAT*,etc
[104]	Stroke	4	48	M	Case study	1/0	13	GS*,SIS*,MAL*, etc
[82]	Stroke	30	55	M	Crossover	1/1	-	EMG*,ROM*
[99]	SCI	3-4	32-45	M	Pilot case	2/0	10	MMT*
[108]	Stroke	25	60	M	Feasibility	1	3	BCI control
[109]	Stroke	9-29	67.3±13.6	-	Case series	3 / 0	3	ROM*
[110]	Stroke	>12	20-70	-	Pilot case	2 / 0	20	MAS, etc
[111]	Stroke	1-2	67.6±3.7	F,M	Pilot case	5/0	24	ERD*, etc
[112]	Healthy	-	26	M	Feasibility	1/0	2	BCI-control
[100]	SCI	2	37.5±22.5	M	Case series	4/0	20	MMT*,ERD*

Note: Ref, Reference; CMC, corticomuscular coherence; GS, Grip strength; SIS, Stroke impact scale; MAL, motor activity log; LI, laterality index; MMT, manual muscle test. For more information on FMA, ARAT, SIS, MAL, MMT and MAS see the web page at `http://www.rehabmeasures.org/rehabweb/allmeasures.aspx`. Outcome with '*' are those recording improvement in the corresponding study.

Table 2.2: Parameters of BCI used in BCI-FES for neurorehabilitation

Ref.	Task classified	# Chan	Band (Hz)	Feature	Classifier	Feedback	Cued	Accuracy (%)
[101]	Left vs Right MI	16	8-45	TNFLD	SVM	visual, audio		70.5± 4.3
[103]	Finger MI/AM vs rest	4	21-24	PSD	Threshold	visual		89.0
[105]	Left AM vs rest	10	α, β	ERD	LDA	-		>90.0
[106]	Active foot vs rest	64	8-50	PSD	LB	-		100.0
[107]	Hand AM/MI vs rest	6	8-12	PSD	-	visual		-
[102]	Hands MI	16	8-30	CSP	SVM	visual, audio	y	77.0
[104]	Hand AM vs rest	5	α, β	ERD	-	visual,TS	y	>70.0
[82]	Ankle AM vs rest	2	24-26	ERD	Threshold	visual	y	100.0
[99]	Hand MI vs rest	4	0.5-30	PSD	Threshold	visual	n	83.8
[108]	Foot AM vs rest	64	15-25	PSD	LB	-		77.0
[109]	Foot AM vs rest	32-63	8-30	PSD	LB	-		-
[110]	Hand MI vs rest	18	8-15	CSP	LDA	visual		>80.0
[111]	Left vs Right MI	16	8-30	CSP	SVM	tactile etc.		62.1±5.6
[112]	Left vs Right vs feet MI	63	8-30	CSP	LDA	visual	y	88.3
[100]	Hand AM vs rest	6	0.5-30	TDP	LDA	visual	y	88.3

Note: Ref, Reference; Band, EEG frequency band; Task, tasks classified; Accuracy, online BCI accuracy; Feedback, feedback provided in addition to FES; #Chan, number of EEG channels; Cued, is the BCI synchroneous; LB, linear Bayesian; TS, tongue stimulation; TDP, time domain parameters [113]; see text for other abbreviations.

The BCI system on Fig. 3.2 consists of parameters of the BCI system typically used for BCI-FES. Table 2.2 shows the choice of BCI parameters that authors have made when building a BCI for BCI-FES. Features of choice include ERD, power spectral density (PSD) and tensor-based nearest feature line distance (TNFLD) algorithm [101]. The classifiers of choice include the use of simple thresholds on ERD [103], LDA, support vector machine (SVM) [114] and the linear Bayesian (LB) classifier [115]. The number of EEG channels used ranges from 2 to 64 while the EEG frequency bands includes the α (8-13 Hz), β (13-30 Hz) and the wide band (8-30 Hz). Authors have mostly, in addition to FES, provided visual feedback [101] with a few providing audio [101], tactile [111] and tongue stimulation [104] feedbacks. In order to achieve better classification result (62.1-100%), authors have mostly used two tasks in which one of the task is to perform MI or AM of a body part and the other is to relax/rest.

For a list of FES parameters used in BCI-FES for neurorehabilitation see Table 2.3.

Table 2.3: Parameters of FES used in BCI-FES for neurorehabilitation

Ref.	**I_{max} (mA)**	**F(Hz)**	**P.w (μ s)**	**Muscle**
[101]	25	60	150	Ext. carpus radialis
[103]	-	83.3	255	Indicis proprius, Ext.digitorum
[105]	15-20	20	100	Left ext.digitorum
[106]	88-100	20-30	120-200	Tibialis anterior
[107]	-	25	250	Wrist/Finger ext.
[102]	20-27	60	150	Ext. carpus radialis
[82]	8	50	1200	Tibialis anterior
[99]	15	30	300	Ext. muscles
[100]	35	26	200	Hand ext., flexor muscles

Note: Ref, Reference; F, frequency; I_{max}, maximum current; P.w, pulsewidth, Ext, extensor

2.5 Results of BCI-FES studies on patients

Fig. 2.2 shows the number of articles on BCI-FES for rehabilitation published per year so far. These articles were obtained by searching Pubmed, Medline and Google Scholar with the phrases: BCI-FES, Brain computer/machine interface controlled functional electrical stimulation and BCI rehabilitation. Conference papers and journal papers are both included. These articles are those listed in Table 2.1. The first article on BCI-FES for neurorehabilitation was published in 2009 by Daly and colleagues [103]. Since then the number of articles published in the field is increasing though rather slowly peaking in the year 2014. The jump

in the number of high impact articles published in 2014 holds promise for BCI-FES for rehabilitation.

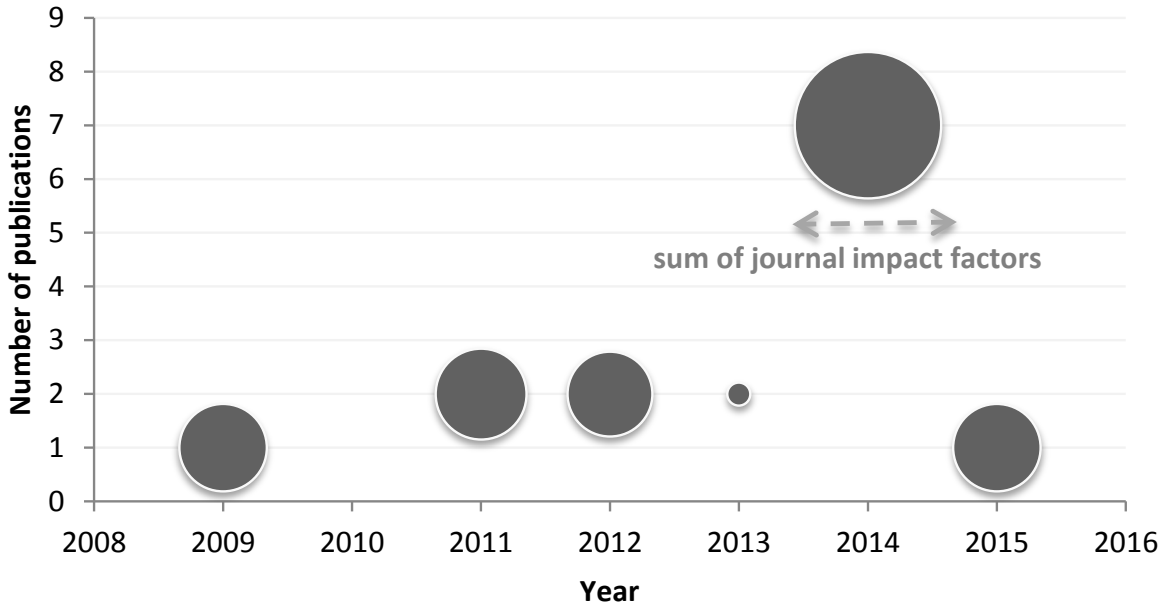

Figure 2.2: The yearly publication of BCI-FES articles for neurorehabilitation. The width of the bubble represents the sum of the impact factors of the corresponding journals (at the time of this writing) where the articles were published. The journal impact factor of conference papers are chosen to be 0.1. New journals without impact factor are set to 0.5.

A number of these articles show positive results on stroke patients. Following only nine sessions of BCI-FES therapy, a 43 years old female stroke patient who had lesion on the left hemisphere gained 26^{o} of volitional index finger extension in an experiment by Daly and colleagues [103]. This improvement was accompanied with better BCI control. These results were remarkable and 'sparked' up research on BCI-FES for neurorehabilitation. See Table 2.1 for studies showing results on BCI-FES studies.

Two crossover studies each featuring one subject reported significant improvements only within the BCI-FES therapy period. Firstly Mukaino and colleagues [105] reported that a 38 years old stroke survivor showed changes in ERD, fMRI images and electromyogram (EMG) signal that suggested functional improvement during the BCI-FES therapy period. This suggestion was supported by improvement observed from FMA and MAS measures. Secondly Tatahashi and colleagues [82] provided BCI-FES therapy for only 20 minutes to a 55 years old stroke patient and found significant changes in EMG and range of movement.

Young and colleagues [104] reported in a study on a 48 years old stroke patient, recruited after months following injury, who also had congenital deafness and a history of depression. They assessed various outcomes on the patient four times (at $\approx$ 3 weeks intervals) within ten weeks prior to the start of the study. Following six weeks of BCI-FES therapy comprising 13 two-hour sessions, the patient made significant clinical improvements that was not seen

in the prior ten weeks. It was not possible to isolate the contribution of BCI-FES therapy to the improvements; given that other factors including natural recovery may have contributed to the observed improvements. But it is important to note that the outcome measures were better following the six weeks of BCI-FES therapy than the prior ten weeks to the start of the study. Furthermore other medications and therapies received by the patient were similar in the six weeks of BCI-FES therapy and in the prior ten weeks.

Up until 2014 BCI-FES studies have been hampered by low number of subjects and lack of control groups. Two articles in 2014 [101, 102] on a combined 23 sub-acute (<=6 months) stroke patients showed results from randomised controlled studies with promising results. In the first study, after two months, patients who received BCI-FES (treatment/BCI-FES group) showed positive changes in EEG pattern within the lesioned hemisphere and also showed better functional improvements (measured with FMA and ARAT) than control patients [101]. The control group in this study received no study related therapy so it can be argued that the improvements in the BCI-FES group is due in part or in full to the FES and goal oriented movement practice. In the second study, following eight weeks of treatment, the BCI-FES group showed significant functional improvement measured with ARAT. Furthermore post treatment ERD was significantly enhanced compared with the pre treatment values in the BCI-FES group alone [102]. In this second study the control group received FES so BCI modulated FES must have had a contribution towards the improvements observed. These two studies highlight the promise of BCI-FES on sub-acute stroke patients.

Also, recently studies by Vuckovic et al. [99] and Osuagwu et al. [100] suggest that SCI patients can also benefit from BCI-FES therapy. These are the first studies of its type in SCI patients. The authors showed using MMT and ERD that the patients had benefited from the therapy functionally. Both of the studies were case series by design and therefore did not include controls. So it was not possible to determine if the observed functional improvement has any contribution from the BCI-FES therapy. However the authors showed that BCI-FES can be successfully carried out in SCI patients for motor rehabilitation in a similar manner as in stroke patients.

2.6 Summary

Neurorehabilitation aims at achieving permanent recovery after an injury to the nervous system. BCI-FES is a promising novel therapy with application in neurorehabilitation. With BCI-FES the nervous system is activated in the efferent and the afferent directions simultaneously. Such pattern of activation can have a learning effect according to the Hebb's learning theory. Research studies mostly done on stroke patients so far have indicated the potential therapeutic effect of using BCI-FES in motor neurorehabilitation. The number

of research studies in the field is increasing indicating interests in the research community. However research in the field is still in its infancy as more studies are required in order to make strong conclusions.

Chapter 3

Methods

"Any method stands and falls according to the assumptions implicit in that method" James V. Stone, [116]

3.1 Brain computer interface technologies

Brain computer interface (BCI) is a technology that allows direct interaction between the brain and a computer [29]. This interaction creates a communication channel with which a BCI user can control external devices and carry out tasks. A BCI system works by analysing signals recorded from the brain to determine the occurrence of already learned brain states. After detecting the learned brain state, the computer carries out an associated task and provides feedback explicitly or implicitly to the user.

In this section the technologies behind BCI are introduced. Also the BCI used in this project will be discussed.

3.1.1 EEG features

The followings are the EEG features for BCI investigated in this project. They include bandpower or event related desynchronisation/synchronisation, time domain parameters, adaptive autoregressive parameters and common spatial patterns.

Bandpower and event related desynchronisation/synchronisation

The power of an EEG signal, bandpower, is one of the most commonly used EEG features in motor imagery-based BCI [117, 118, 119]. The bandpower is usually computed within a narrow frequency band. This allows the selection of specific narrow frequency bands that are

most relevant for a particular BCI subject since the reactive frequency band may vary for each subject in a motor imagery-based BCI [120]. The computation of bandpower is done by first filtering the EEG data in the required frequency band, squaring and smoothing/averaging the resulting signal. This is shown in Equ. 3.1 where $X(t)$ is the narrow bandpass filtered signal and the $\langle . \rangle$ is used to represent smoothing/averaging operator. The smoothing is usually done over a time of one second.

$$Bandpower = \left\langle X(t)^2 \right\rangle . \tag{3.1}$$

Event related desynchronisation/synchronisation: The traditional method of visualising power changes of EEG signal is the event related desynchronisation (ERD) and event related synchronisation (ERS) [32, 121]. The ERD and ERS refer to decrease and increase respectively of EEG power relative to a baseline period within a narrow frequency band. Movement related cortical processes like those during motor imagery and physical execution can be quantified with ERD across the sensorimotor cortex. Brain activities like the processing of a visual or auditory stimuli can be quantified with ERS. The methods are sometimes together referred to as event related desynchronisation/synchronisation (ERD/ERS).

$$\begin{aligned} Ref &= \frac{1}{t_{ref}.L} \sum_{t=t_{ref1}}^{t_{ref2}} \sum_{i=1}^{L} X^i(t)^2 \\ ERD/ERS(t) &= \frac{\sum_{i=1}^{L} X^i(t)^2}{Ref} - 1 \end{aligned} \tag{3.2}$$

The ERD/ERS method was introduced by Pfurtscheller and colleagues [32, 121]. It is computed by subtracting the baseline/reference EEG power from the EEG power in a period containing a response to an event. It is normally averaged over several trials to reduce noise. A formula for computing ERD/ERS is shown in Equ. 3.2 where L is the number of trials, t is the sampling interval, $t_{ref} = t_{ref2} - t_{ref1}$ is the reference period. This equation gives ERD as negative values and ERS as positive values.

Time domain parameter

Time domain parameter (TDP) is similar to bandpower features except that TDP uses broad band filtered instead of narrow band filtered EEG signal [113]. It is less popular in the field of BCI than the bandpower method even though it has been shown to outperform the bandpower [113]. It is typically calculated within the entire active band of EEG during motor imagination which is about 7-30 Hz [113]. The TDP method used in this thesis is given by

Equation 3.3 [113],

$$TDP(t)_j = \left\langle var\left(\frac{dX(t)^j}{dt^j}\right)\right\rangle, j = 0, ...p \tag{3.3}$$

where $X(t)$ is a wide band filtered EEG, t is the current sample, j is the derivative order ($0 \leq p \leq 9$) [113], var is the variance operator and $\langle . \rangle$ is used to represent smoothing/averaging operator. Note that the variance operator in this equation acts like the bandpower operator since the variance of a centered (mean=0) signal is equal to the bandpower [113]. The computation of TDP and its usage in an adaptive BCI system is shown schematically in Fig. 3.1. The squaring and smoothing is part of bandpower calculation while the logarithmic transformation enforces normal distribution of the feature as required by the linear discriminant classifier. The BCI system in Fig. 3.1 is merely used to showcase the TDP method; the details of the entire BCI system will be presented later in this chapter (see 3.1.3).

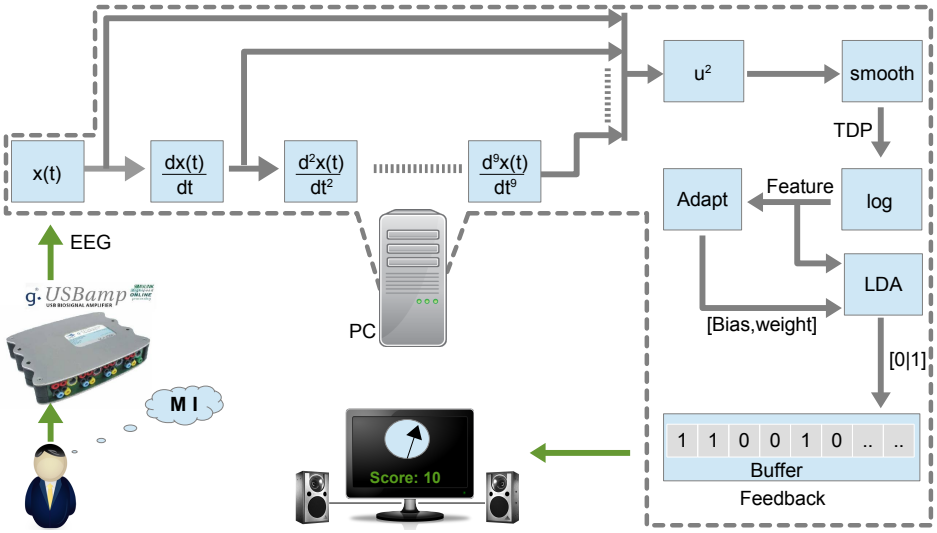

Figure 3.1: BCI setup showing the computation of TDP

Autoregressive parameters

The autoregressive parameters [122] in the adaptive form [123, 124] were one of the method considered in this thesis as EEG features for BCI. This section describes the autoregressive model.

Let $X(N,t) = X(t)$ represents an N-channel EEG signal at time t. The autoregressive model describes the signal $X(t)$ as a sum of its p (order) weighted past values with added white noise $e(t)$ [122]. An equation of the autoregressive model is shown in Equ. 3.4 where $A(j)$ ($j = \{1, 2...p\}$) is a matrix of size $N \times N$ containing the coefficients for weighting the

past values. The noise is described by a Normal distribution, thus: $G\{0, \sigma_e^2\}$.

$$\begin{aligned} X(t) &= \sum_{j=1}^{p} A(j)X(t-j) + e(t) \\ e(t) &= \sum_{j=0}^{p} A(j)X(t-j) \ . \end{aligned} \tag{3.4}$$

In the second line of Equ. 3.4 the sign of A is assumed to be inverted and $A(0)$ is set to the identity matrix. Applying the z-transformation on the second line of Equ. 3.4 gives Equ. 3.5 where v here is the frequency.

$$\begin{aligned} e(f) &= A(v)X(v) \\ X(v) &= A^{-1}(v)e(v) = H(v)e(v) \ . \end{aligned} \tag{3.5}$$

The autoregressive method works well for a stationary signal where the parameters $A(j)$ characterising the model are constants (i.e. they are time invariant). But the EEG signal in BCI is non-stationary. The adaptive autoregressive model is used to describe such a non-stationary signal. Equ. 3.6 describes an adaptive autoregressive model where the noise $e(t)$ is thus: $G\{0, \sigma_e^2(t)\}$. This formula is similar to that of Equ. 3.4 except that the $A(j,t)$ and the variance of $e(t)$ are time-varying.

$$\begin{aligned} X(t) &= \sum_{j=1}^{p} A(j,t)X(t-j) + e(t) \\ e(t) &= \sum_{j=0}^{p} A(j,t)X(t-j) \ . \end{aligned} \tag{3.6}$$

The classical method of dealing with the computation of the time-varying autoregressive parameters is to segment $X(t)$ into short time windows and then compute the parameters individually in each window. Other methods have been used recently. Of these are, the least mean squares approach [124] and the Kalman filtering approach [124, 125]. These methods are capable of estimating the time-varying autoregressive parameters even in real-time. The Biosig and the rtsBCI toolboxes [126] include methods for computing the parameters. Since the parameters are time-varying due to changes in EEG signal, differences between for example the left and right hand motor activities can be coded in the adaptive autoregressive parameters. The estimated parameters serve as features for a classification algorithm like that described in Section 3.1.2. The adaptive autoregressive parameters were investigated in this thesis but other methods were preferred as BCI features.

Common spatial pattern

The method of common spatial pattern (CSP) can be applied to two classes of EEG time series to create a new time series which can have a reduced dimension. The variance of the new time series serves as a feature to a classification algorithm because one of the classes in the new time series has a minimised variance while the other has a maximised variance. The following describes the CSP method.

Let $X_c^i(N,t)$ denotes trial number i of a bandpass filtered EEG of condition/class $c = \{1,2\}$ with N channels and t samples.

The normalised covariance matrix R_c^i for trial i in class c is given by

$$R_c^i = \frac{X_c^i X_c^{iT}}{trace(X_c^i X_c^{iT})} \tag{3.7}$$

where the superscript T denotes the matrix transpose operator. The covariance matrix is then averaged across trials for each class thus:

$$R_c = \sum_{i=1} R_c^i \, . \tag{3.8}$$

Then the composite covariance matrix is given by [127]

$$R = R_1 + R_2 \, . \tag{3.9}$$

The composite matrix can be decomposed to get

$$R = B\lambda B^T \tag{3.10}$$

where B is a matrix eigenvector such that $BB^T = 1_{N\times N}$ and λ is a diagonal matrix of eigenvalues sorted in the descending order of magnitude. Next, applying the whitening transform [128] given by

$$W = \frac{1}{\sqrt{\lambda}} B^T \tag{3.11}$$

makes the variance in the B space a unity [128, 129]. Now filtering R, R_1 and R_2 with W gives Equ. 3.12 [129].

$$WRW^T = 1_{N\times N},\ S_1 = WR_1W^T,\ S_2 = WR_2W^T,\ S_1 + S_2 = 1_{N\times N} \, . \tag{3.12}$$

Therefore the individual eigenfunction decomposition of S_1 and S_2 should give Equ. 3.13

$$\begin{aligned} S_1 &= U\lambda_1 U^T \\ S_2 &= U\lambda_2 U^T \ . \end{aligned} \tag{3.13}$$

So S_1 and S_2 share the same eigenvectors U, but the sum of the corresponding eigenvalues to the eigenvectors sum up to one as shown in Equ. 3.14 where I in this equation is the identity matrix.

$$\lambda_1 + \lambda_2 = I \ . \tag{3.14}$$

The spatial filter required for discriminating the EEG data classes in terms of their variances is obtained by projecting W onto U as in Equ. 3.15.

$$P^T = U^T W \ . \tag{3.15}$$

The new times series $Y(2m, t)$ with a different variance for each of the EEG data class can be created by filtering $X(N, t)$ as in Equ. 3.16 where m specifies the number of first and last spatial filters to be used. So the EEG is filtered with m pairs of spatial filters.

$$Y(2m, t) = P^T X(N, t) \ . \tag{3.16}$$

The variances of the $2m$ dimensional time series $Y(2m, t)$ serve as feature vectors (Equ. 3.17) to a classification algorithm [127, 129].

$$f(M, q) = \frac{var[Y(2m, t^{'})]}{\sum_{k=1}^{2m} var[Y(k, t^{'})]} \qquad M = 2m, q = t^{'} . \tag{3.17}$$

The feature vectors $f(M, q)$ is given by Equ. 3.17 [127] where $M = 2m$ and $q = t^{'}$ is a small sliding window starting from t. In this thesis, the sliding window has no overlap and it has a length of 100 samples at the EEG data recording sample rate of 256 Hz.

3.1.2 Classification

Feature classification is at the root of BCI. It is the part of the interface that attempts to convert the user's intention into action. Before a classifier can make such interpretations, it is first trained with EEG feature so that it can learn to associate certain states of the brain to user's intentions.

Below is the description of the BCI classifier used in this thesis.

Linear discriminant classifier

The linear discriminant analysis (LDA) classifier is one of the most often used classifiers in the BCI field. As a linear classifier, LDA works well when the difference between classes of data to be classified is in the mean rather than in the covariance matrix [128]. The classifier also assumes normality and equality of variance of the data classes. When these assumption are not met which is often the case, the simplicity and robustness of the LDA classifier compensate for its loss in performance [128].

In this thesis, LDA is used for all classification operation. This section describes the LDA method for a 2-class system and shows how its parameters are adapted to account for the variations in baseline EEG.

Let $f_c(M, q)$ denotes an M dimensional feature matrix with q observations of class c where $c = \{1 \rightarrow Class\ 1,\ 2 \rightarrow Class\ 2\}$. An example source of the feature matrix f is Equ. 3.17. The goal here is to project f onto a line that maximizes the separability of the scalars $h(f)$ in Equ. 3.18 where $h(f)$ is the *linear discriminant function* and A is the transformation [128].

$$h(f) = A^T f\ . \tag{3.18}$$

The expected value and a measure of scatter/variance for each class is given by Equ. 3.19 and 3.20 in the projected space (i.e the $h(f)$ space) in terms of the equivalent variables in the original space. The operator E is the expectation value operator and tilde is used to specify that a variable is obtained in the projected space. The term μ_c is the mean of class c and Equ. 3.21 defines the scatter matrix Σ_c of class c in the original data space. The scatter matrix has a dimension of $M \times M$.

$$\tilde{\mu_c} = E[h(f)|_c] = A^T E[f|_c] = A^T \mu_c \tag{3.19}$$

$$\tilde{\Sigma_c} = Var[h(f)|_c] = A^T \Sigma_c A\ . \tag{3.20}$$

$$\Sigma_c = E\left[\sum_{q=1} (f(M,q) - \mu_c(M))(f(M,q) - \mu_c(M))^T|_c\right] \tag{3.21}$$

One of the ways of determining the best line on which to project f is by maximising the *Fisher criterion* [128] given by Equ. 3.22. The numerator in Equ. 3.22 is the *between class scatter* while the denominator is the *within class scatter*.

$$J(A) = \frac{|\tilde{\mu}_1 - \tilde{\mu}_2|^2}{\tilde{\Sigma}_2 + \tilde{\Sigma}_1}\ . \tag{3.22}$$

Equ. 3.23 gives the Fisher criterion in terms of the transformation A where S_b the between

class scatter and S_w the within class scatter are given in the original space by Equ. 3.24 and 3.25 respectively.

$$J(A) = \frac{A^T S_b A}{A^T S_w A} \, . \tag{3.23}$$

$$S_b = (\mu_1 - \mu_2)(\mu_1 - \mu_2)^T \tag{3.24}$$

$$S_w = \Sigma_1 + \Sigma_2 \, . \tag{3.25}$$

Equ 3.26 is obtained by equating the $\frac{d}{dA}J$ of Equ. 3.23 to zero (see Appendix C.1, Table C.1 for the solution). The Equ 3.26 is the generalised eigenvalue problem which can be solved by diagonalizing $S_w^{-1}S_b$ to obtain its eigenvalues and the corresponding eigenvector.

$$S_w^{-1} S_b A = JA \, . \tag{3.26}$$

Since S_b has a rank of one, there is only one non-zero eigenvalue for $S_w^{-1}S_b$ [128]. The eigenvector A corresponding to this one non-zero eigenvalue is that used in Equ. 3.18 to project f. The classifier is completed by choosing a hyperplane normal to A for classifying the values of $h(f)$ into Class 1 or Class 2. On the assumption of equal distribution of the classes, a choice of the position of the hyperplane is given by Equ. 3.27.

$$b = \frac{1}{2}(\mu_1 + \mu_2).A \, . \tag{3.27}$$

Using Equ. 3.28

$$h(f) = A^T f - b \tag{3.28}$$

if $h(f(q)) > 0$ then the observation q is classified as Class 1 otherwise it is classified as Class 2. An example of computing LDA is given in Appendix C.1.2.

Online adaptation: In order to easily adapt the classifier online, it is important to realise that the solution to Equ. 3.23 can also be written as Equ. 3.29. From Equ. 3.28, it can be seen that only A and b require adaptation. As it can be seen from Equ. 3.29 only the individual means (μ_1 and μ_2) and the within class inverse covariance matrix (S_w^{-1}) are required in order to update A. Once A is updated, it can be used in addition to the means to update b. Therefore the adaptation problem is solved by updating the means and the within class inverse covariance matrix.

$$A = (\mu_1 - \mu_2).S_w^{-1} \tag{3.29}$$

The adaptation can be performed in a supervised or unsupervised manner. For the case of a supervised adaptation, the individual mean of each class is separately updated. For the unsupervised case, only overall mean of the classes ($\mu_1 + \mu_2$) are updated. Assuming that the inverse covariance matrices are equal, the pooled covariance matrix can be updated in each

case. Whether the adaptation is supervised or not, Equ. 3.30 shows how a mean value at a time t can be updated in terms of its previous value, the current feature value and the update coefficient UC which determines the adaptation speed [130]. Similarly, the within class inverse covariance matrix is updated using Equ. 3.31 and Equ. 3.32 ensures that the matrix maintains symmetry [130]. Once the mean and the inverse covariance matrix is updated, A can be computed using Equ. 3.33 and b is computed using Equ. 3.27. Note here that A cannot be updated in the unsupervised case.

$$\mu(t) = (1 - UC).\mu(t-1) + UC.f(t) \tag{3.30}$$

$$\Sigma(t)^{-1} = \frac{1}{(1-UC)}.\left(\Sigma(t-1)^{-1} - \frac{1}{\frac{1-UC}{UC} + f(t).v}.v.v^T\right) \tag{3.31}$$
$$where\ v = \Sigma(t-1)^{-1}.f(t)^T$$

$$\Sigma(t)^{-1} = \left(\Sigma(t)^{-1} + \Sigma(t)^{-1,T}\right) \times 0.5 \tag{3.32}$$

$$A = (\mu_1(t) - \mu_2(t)).\Sigma(t)^{-1} \tag{3.33}$$

Dimensionality reduction: A method tried in this thesis was the use of principal component analysis (PCA) for dimensionality reduction of the feature matrix before performing classification of data. The PCA is a linear statistical method that transforms a data set into independent/uncorrelated components [131]. By keeping only few components (those that represents most of the information in the original data) and by working in the component space, the dimension of the data can be reduced. The computation of the PCA of a data set f is straight forward from Equ. 3.21. It is done by finding the eigenvalues and the eigenvector P of Σ in Equ. 3.21. By rejecting the eigenvectors with small eigenvalues and transforming the data as shown in Equ. 3.34,

$$f_{pca} = (P^T f^T)^T. \tag{3.34}$$

a low dimensional data f_{pca} containing most of the information in the feature data f can be obtained. the new series f_{pca} can then be used for classification purposes. In most cases in this thesis, the dimension of f was small enough for the PCA to be ignored.

3.1.3 Brain computer interface setup

There are different mental strategies used in designing BCI [29] but only those based on movement attempt and imagination are relevant in neurorehabilitation of movement. The

type of BCI used for rehabilitation of movement is mostly designed with EEG. During movement imagination of a body part for example, EEG recorded over the sensory and motor representation areas decreases in power. Such a power loss is termed event related desynchronisation (ERD, see Section 3.1.1) [132]. Because of the separate cortical representation of different body parts, ERDs relating to the movement imagination of different body parts differ especially in spatial localisation. This makes it possible to, for example, classify the ERD arising due to movement attempt of the left and that arising due to movement attempt of the right hand.

In order to make such classification, machine learning methods are employed. First, the features of EEG (discussed in Section 3.1.1) during task performances are extracted. The features are transforms of the EEG data such that the differences in the classes of data are enhanced. In a two-class system, the classes might include a left hand motor imagery (MI) as Class 1 and a right hand MI as Class 2. The features are passed on to a classifier to determine if the data represents Class 1 or Class 2. One of the classifiers popularly used in BCI is the linear discriminant analysis (LDA, see Section 3.1.2) [115]. The LDA identifies the class of the input feature data. The output of the classifier serves as the computer's knowledge of the BCI user's intention and therefore can be used by the computer to carry out the users intention.

Offline and Online BCI

A typical BCI system consists of two main parts, the training/offline part and the online part. In the offline part the classifier is trained using multiple trials of the feature data with known class information/label. Normally, a BCI user would perform multiple trials (about 80 trials) of each of the two tasks (Class 1 and Class 2) for the two-class system mentioned earlier. The EEG corresponding to Class 1 and Class 2 are processed to extract features $f1$ and $f2$ respectively. The features, $f1$ and $f2$ are then used to train the classifier which linearly maps the features onto a lower dimensional space in the case of LDA. In this space, $f1$ and $f2$ can be classified. The transformation that maps the features onto the new dimension is transfered for use in the online part.

In the online part, the EEG response of the BCI user's during task performance of Class 1 or Class 2 is transformed unto the feature space and further transformed using the classifier transformation map. The BCI user's intention is then interpreted as either Class 1 or Class 2 by the classifier.

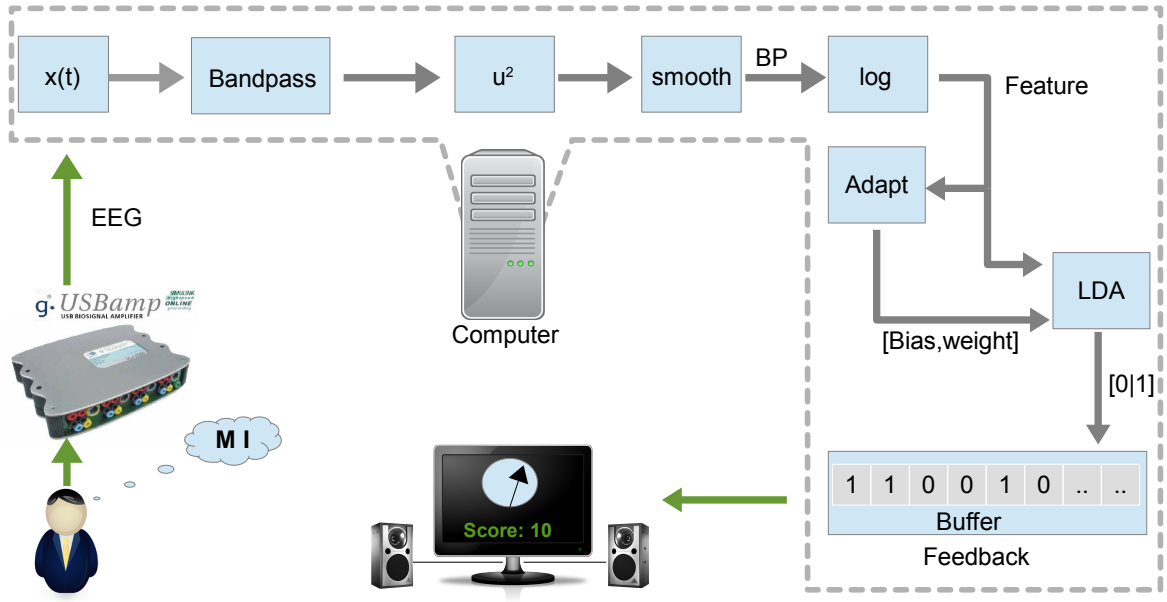

Figure 3.2: The schematic diagram of a basic BCI showing the flow of signal. MI, motor imagery; EEG, electroencephalogram; BP, bandpower; LDA, linear discriminant analysis.

BCI setup

Based on empirical results, only bandpower and TDP features are chosen to implement the online therapeutic BCI in this thesis. A schematic diagram of an EEG-based BCI system is shown in Fig. 3.2. This, Fig. 3.2 is based on bandpower features. For one based on TDP features see Fig 3.1. On these systems the subject performs a set task and the output of an EEG recorder (g.USBamp) is sent to the computer for processing. The signal is bandpass filtered typically between 8-12 Hz (α-band) and 16-24 Hz (β-band) for the bandpower and between 0.5-30 Hz for TDP. The computer calculates the bandpower features (Fig. 3.2) or TDP features (Fig. 3.1) of the signal and forwards the result to a LDA classifier and the adaptation algorithm discussed in Section 3.1.2. The adaptation algorithm can either update the bias, weight or both the bias and the weight of the classifier. The classifier system then uses the updated bias and/or weight to classify the features as either a '0' or a '1' (e.g. 0≡ Class 1, 1≡Class 2). The classification result is buffered for a set amount of time (see BCI-difficulty in Section 3.1.4) and Class 1 or Class 2 is detected when the number of Class 1 or Class 2 in the buffer passes a set threshold. The classification result is used to provide a visual and auditory feedbacks in this case as shown. The feedbacks play an important roll as discussed in Section 1.4.2.

3.1.4 Performance measures in BCI

Classification accuracy which is the probability of performing a correct classification and Cohen's kappa are often used in BCI as measures of performance [133]. Both measures can

be derived from the confusion matrix which is shown in Equ. 3.35

$$Confusion\ matrix = \begin{array}{c} \\ Class\ 1^{act} \\ Class\ 2^{act} \end{array} \begin{array}{c} \begin{array}{cc} Class\ 1^{pred} & Class\ 2^{pred} \end{array} \\ \begin{pmatrix} C_{1,1} & C_{1,2} \\ C_{2,1} & C_{2,2} \end{pmatrix} \end{array} \tag{3.35}$$

for a two-class system of class labels Class 1 and Class 2. The first entry in this confusion matrix, $C_{1,1}$ represents the number of trials of Class 1 correctly classified (true positives) while the entry $C_{1,2}$ give the misclassified (false positives with respect to Class 1) trials of Class 1. Similarly, the entry $C_{2,2}$ represents the number of Class 2 that are correctly classified while the entry $C_{2,1}$ is for the misclassified trials of Class 2; the superscripts $pred$ and act represent the predicted and actual class labels respectively.

The accuracy is the total number of correctly classified trials over the total number of trials as given in Equ. 3.36

$$ACC = \frac{\sum C_{i,j} \,.\, \delta_{i,j}}{\sum C_{i,j}} \tag{3.36}$$

where $C_{i,j}$ are the entries of the confusion matrix and $\delta_{i,j}$ is the Kronecker delta.

The Cohen's kappa is used to assess the agreement between the true class labels and classifier output labels. It is computed using Equ. 3.37 where ACC_0 is the chance level under the assumption that all agreement between the true class label and the classifier output occurred by chance [133]. It can be estimated from the entries of the confusion matrix using Equ. 3.38 where $C_{k,:} = \sum_{j=1} C_{i=k,j}$ and $C_{:,k} = \sum_{i=1} C_{i,j=k}$.

$$kappa = \frac{ACC - ACC_0}{1 - ACC_0} \tag{3.37}$$

$$ACC_0 = \frac{\sum C_{k,:} C_{:,k}}{(\sum C_{i,j})^2} \tag{3.38}$$

BCI activation threshold

The BCI activation threshold is defined here as BCI-difficulty. It is called BCI-difficulty because the parameters of the threshold can be varied to make the activation of the BCI system more or less difficult. A high BCI-difficulty level can be set to reduce false positives. In this thesis a BCI-difficulty is set as follows.

Let the classifier output produced per sample be given by $c = \{Class\ 1, Class\ 2\}$. Let c be buffered for a variable length of time up to a maximum of 3 s or 768 samples (Samplerate is 256 Hz). Let a BCI detection occur when a percentage of a defined sub-length of the buffer is filled with Class 1. This defined sub-length of the buffer is called a sub-buffer. The

length of the sub-buffer, usually 1.5-2 s long, is determined for a subject and optimized to significantly reduce false positives which was reported by the subject. The BCI-difficulty is set using Equ. 3.39

$$d = \frac{bf}{B} \, . \tag{3.39}$$

where d is the BCI-difficulty, b is the sub-buffer length, B is the maximum buffer length (set to 3 s) and f is the percentage filling of the sub-buffer that activates the BCI. For example when $b = 2\ s$, f was set to 75% to get d equal to 50% BCI-difficulty level.

The BCI-difficulty can be set to allow session to session comparison (which was not done in this thesis) as follows. During a session, vary the length of B such that at certain length no false positive is observed with the subject relaxed and at 5% below this length of B, false positive is observed. Now set the desired detection window length b and calculate the BCI-difficulty d as $d = b/B$. A subject's performances in different sessions can be compared with each other by setting d to be the same in the sessions.

3.2 BCI-FES

The BCI-FES system combines the BCI and FES technologies. The components of the BCI-FES system developed in this thesis are shown in Fig. 3.3. In this figure, the EEG corresponding to the attempted right hand movement is recorded by the EEG amplifier and sent to the computer. The computer performs BCI-related analysis and the output is used to drive the FES as shown in the figure. This BCI output signal can either be used to start and stop the FES, modulate the current and/or the stimulation pulsewidth. In this thesis the output of the BCI was simply used to control the starting of the FES. The FES stays active for 10 s each time it is activated. The BCI-FES was implemented using Simulink and the Simulink model is shown in Fig. 3.4.

The EEG recorder used was the g.USBamp as shown in Fig.3.3 which attaches to the computer through a USB port. Six standard EEG recording electrodes were used bipolarly for signal acquisition. The bipolar montage is as follows: Fc3-Cp3, Fcz-Cpz and Fc4-Fc4. The first (Fc3-Cp3) was used to derive the C3 channel and it corresponds to the right hand area of the brain. The second (Fcz-Cpz) was used to derive the Cz channel and it corresponds to the central area of the brain. The third (Fc4-Cp4) was used to derive the C4 channel and it corresponds to the left hand area of the brain.

The FES device used was the Hasomed Rehastim shown in Fig. 3.3. It attaches to the computer through a USB port. It has a Simulink block which allows easy control of the intensity, pulsewith and the frequency of stimulation. The output of the BCI forms the input of the FES simulink block. This device has eight channels but only four of them were used in

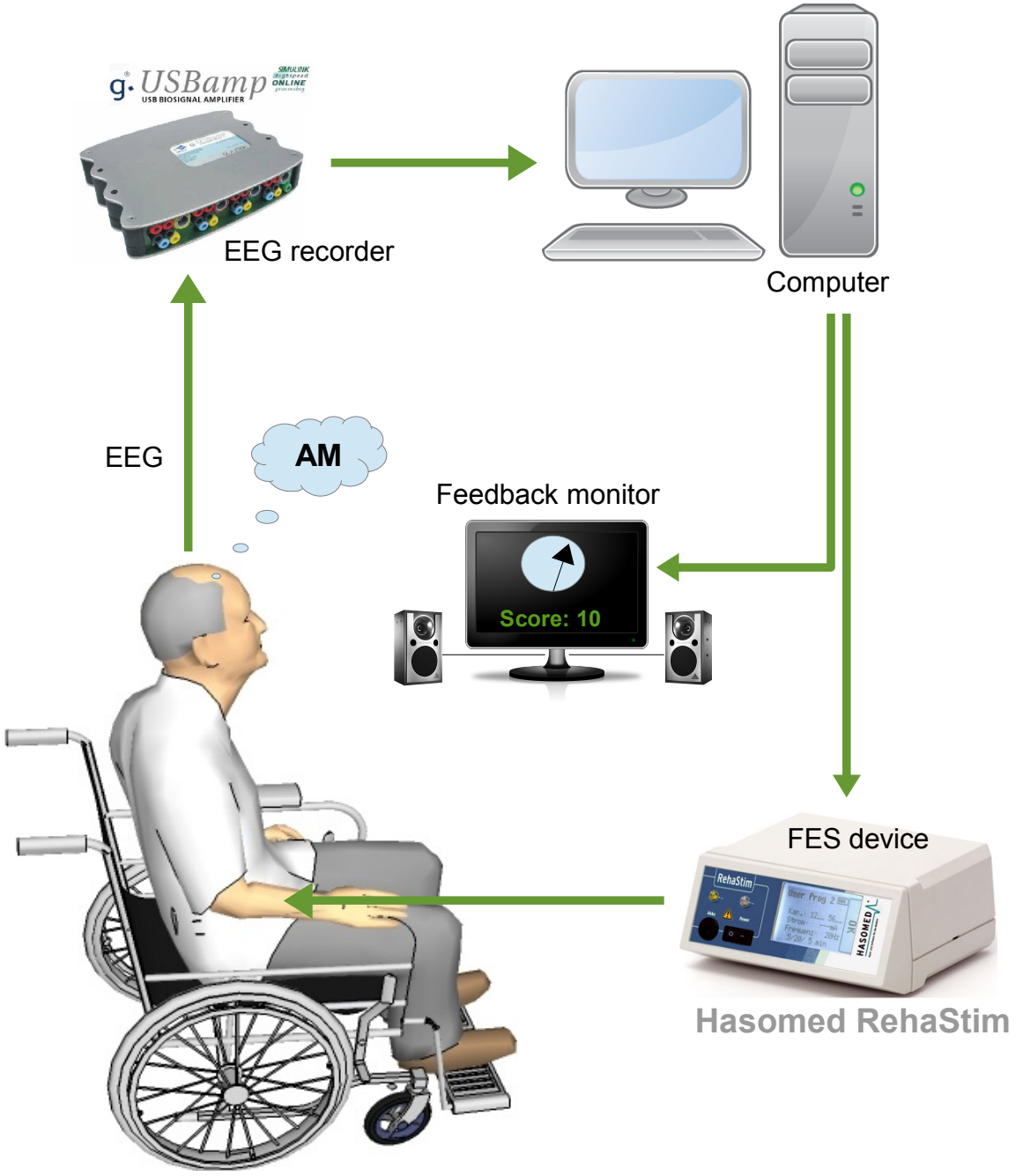

Figure 3.3: The diagram of the BCI-FES system. AM, attempted movement.

this thesis. The four channels were attached to the hand through neurostimulation electrodes of various sizes including 5 by 9 cm and 3.3 by 5.3 cm rectangular electrodes. Two channels were used for hand extension positioned to activate the Extensor digitorum and the extensor pollicis longus as shown in Fig. 3.5 a). Similarly the remaining two channels were used to close the hand and so were positioned to activate the flexor digitorum superficialis and the flexor pollicis brevis muslces as shown on Fig. 3.5 b). The FES frequency was set to 25.6 Hz and the pulsewidth was set to 200 μs. When activated the FES assisted in repetitive hand opening and closing for 10 s with the hand muscles stimulated with similar FES current and

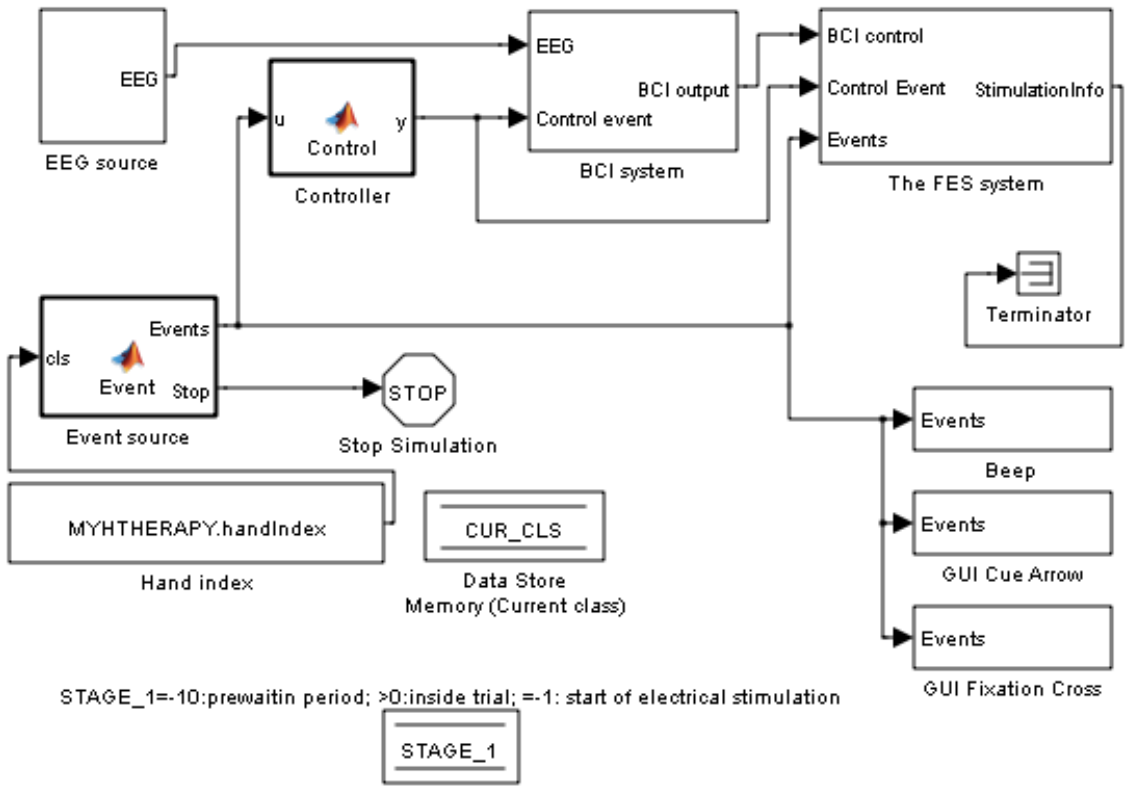

Figure 3.4: Simulink implementation of the BCI-FES.

in the order shown in Fig. 3.6. In addition to the FES, the BCI-FES system provided visual and auditory feedbacks in order to guide task performance.

Visual and auditory feedback were implemented using the Java programming language executed in Simulink through a MATLAB script. The details of the software tools used in this thesis are shown in Appendix A.1. The output of the BCI forms the input of the Java program. The visual feedback included a gauge on the computer screen as shown in Fig. 3.3 which moves to the left when AM of the subject is detected and to the right otherwise. The FES is activated at the same time as when the gauge reaches the extreme left and remained for a set period of time determined by the BCI-difficulty of Section 3.1.4. Another visual feedback is a score displayed on the screen as shown in Fig. 3.3. The score increments whenever the FES is activated and tells the subject how many times the subjects has managed to activate the FES. When the FES is activated, a congratulatory message is displayed on the screen and an acknowledgment sound is played. If the FES was not activated after a set amount of time, a message is printed on the screen and a sound is played to mark a failed attempt. When this happened, the system was manually terminated. For a full description of how to operate the software for the BCI-FES system, see Appendix B.1.

For application in neurorehabilitation, the BCI-FES system must run in a near real-time in order to reduce the time lag between the activation of the motor cortex and the activation of

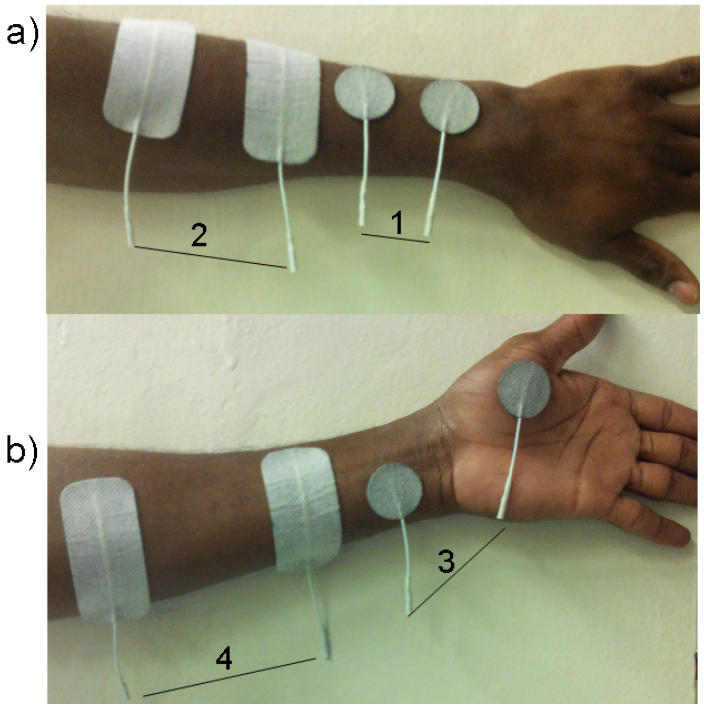

Figure 3.5: An example of a set FES electrode positions used in this thesis. a) Electrodes for opening the hand: 1, Extensor pollicis longus; 2, Extensor digitorum. b) Electrode for closing the hand: 3, Flexor pollicis brevis; 4, Flexor digitorum superficialis.

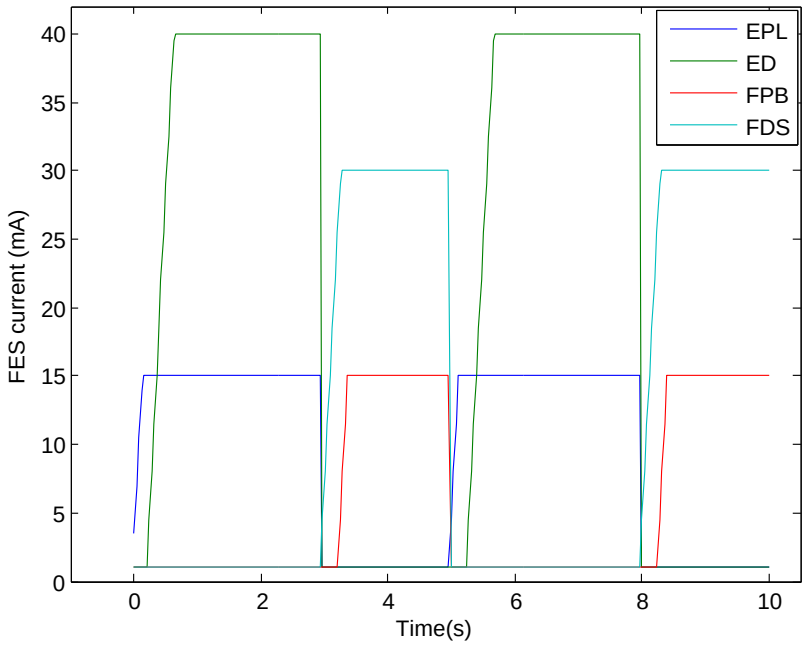

Figure 3.6: Ten seconds of FES to the hand muscles. EPL, Extensor pollicis longus; ED, Extensor digitorum; FPB, Flexor pollicis brevis; FDS, Flexor digitorum superficialis

the FES device so that temporal contiguity exists between the two activations. In order to avoid a large time lag, EEG feature like the bandpower and TDP which are easy to compute are chosen for the BCI. Also the LDA and computational inexpensive classifier adaptation

methods are employed (see Section 3.1.2 for the classifier and the adaptation methods).

3.3 Assessment methods in patients

Several methods were used to assess patients in this thesis. The assessment methods included the somatosensory evoked potential (SSEP, Chapter 7), range of movement (ROM, Section 8.3.4), ERD/ERS (Section 3.1.1) and sLORETA localisation (Appendix A.1.4). Other methods used are discussed below.

3.3.1 Manual muscle testing

The manual muscle testing (MMT) [134] grading system was used in this thesis to assess the strength of the muscles of patients. The grading was performed by a qualified occupational therapist. In order to grade a muscle, the therapist asks the subject to produce a movement typically produced by the muscle. The grades range from 0 to 5 for no observable or palpable muscle contraction and normal muscle function respectively. The guidelines used by the occupational therapist for grading the muscle function is shown in the left side of Fig. 1.10. Each non-zero grade, G is subdivided into three thus: G-, G and G+ where G- is slightly less that G and G+ is slightly better than G but not enough to make the next grade. The muscles of the hand tested included the extensor digitorum (ED), extensor carpi radialis (ECR), extensor pollicis longus (EPL), flexor carpi radialis (FCR), flexor digitorum profundus (FDP), and intrinsic hand muscles (I). In addition to these muscles, the latissimus dorsi, pectoralis major, serratus anterior, deltoid, triceps, biceps, brachioradialis, supinator and the pronator muscles of the upper limbs were also tested.

3.3.2 Laterality index

A brain's hemisphere may dominate a cognitive process. An example is in language processing where the left hemisphere dominates [135]. Also due to contralateral representation of body parts in the brain, motor functions can be dominated by a hemisphere. It is well known that the left hemisphere of the brain controls the right part of the body and the right hemisphere controls the left. The degree of hemispheric dominance is called the laterality index (LI). It can be calculated by taking the ratio of a measure of activities in the brain hemispheres. The measure of activities can be quantified by counting the number of active voxels in an fMRI images. Laterality index is classically computed using Equ. 3.40 [135].

$$LI = \frac{v_l - v_r}{v_l + v_r} \tag{3.40}$$

In Equ. 3.40, v_l, v_r are respectively the number of active voxels in the left and right hemispheres or left and right regions of interests. A negative value of $LI < -0.2$ is interpreted as right hemispheric dominance while $LI > 0.2$ is interpreted as a left hemispheric dominance. A value of $|LI| \leq 0.2$ is interpreted as bilateral dominance.

The classical method of LI computation can be problematic because the absence of voxel weighting allows less statistically significant voxels (due to their relative activation intensity) to equally contribute to LI as more significant ones. The voxels' contributions can be weighted or scaled so that each contribute in accordance with their respective significance [136, 137]. The statistical values of significance can be used as a weight and summed for the voxels in the left and right hemispheres or left and right regions of interests. The index is then computed using Equ. 3.41 [135], where $\sum v_l^w$ and $\sum v_r^w$ are respectively the weighted sum of the voxels in the left and right hemispheres. This weighted index is denoted as wLI.

$$wLI = \frac{\sum v_l^w - \sum v_r^w}{\sum v_l^w + \sum v_r^w} \tag{3.41}$$

Following a neurological injury, the degree of lateralisation as represented by LI/wLI might change. So LI/wLI can be used to assess such an injury and it has been used to assess recovery in stroke patients in BCI [138, 139] and BCI-FES [105] therapy. In SCI, it has been used to assess cortical reorganisation [140].

Weighted laterality index will be used in this thesis to assess the changes in the brain during hand AM before and after therapy. Weighted voxels will be obtained from sLORETA localisation of wholehead EEG. Instead of using activated voxels all over the hemispheres, pairs of regions of interest are created in sLORETA package. The regions of interest have 15 mm radius with centres in MNI coordinate [x,y,z] as follows: [$\pm$56 8 22], [$\pm$26,-12,52] and [$\pm$38, -28 ,46]; where $\pm$ shows that a pair of region of interest (one in a hemisphere) is created by reflecting the x-coordinate. These are locations with maximal activation during hand movement [141]. The closest voxels to these locations in the sLORETA package are the BA 45, BA 6 and BA 40 respectively. In addition to these three locations, another location [$\pm$36,-22,58], which is BA 4 in sLORETA, representing the centre of activity/gravity for the primary motor cortex during hand movement was included [142]. So there are in total 4 pairs of regions of interests with one of each pair in a hemisphere. The regions of interests generated a total of 477 sLORETA voxels.

Chapter 4

Motor Imagery in mental rotation

In order to 'simply' tell the left from the right, the brain runs simulations.

4.1 Summary

Several studies have shown that motor imagery is used implicitly during mental rotation tasks where subjects for example judge whether a picture of a hand is of left or right. Because explicit motor imagery activates the sensorimotor areas of the brain, mental rotation should do similar if it involves a kind of motor imagery. Currently, studies of mental rotation have focused on the use of modalities like fMRI and PET with little attention paid to EEG which offers a high time-frequency resolution. The time-frequency method of EEG analysis is a useful research tool for studying explicit motor imagery. Although hand mental rotation is claimed to involve motor imagery, the time-frequency analysis has never been used to compare motor imagery with mental rotation. In this study, the time-frequency analysis is used to compare motor imagery and mental rotation. Fifteen able-bodied individuals took part in this study. They performed motor imagery of hands in one condition and a mental rotation task inducing implicit imagery in another while EEG was recorded. The time-frequency method and a 3D localisation of the EEG revealed that the activities in the sensorimotor cortex had similar characteristics in explicit motor imagery and implicit motor imagery conditions. Also the sensorimotor activation characteristics were different for the left and for the right hand in both explicit and implicit motor imagery. These suggests that motor imagery is used during mental rotation. This result should encourage the use of mental rotation of body parts in motor rehabilitation programmes in a similar manner as motor imagery is used.

Note that this chapter has now been published.

4.2 Introduction

When attempting to judge the laterality of a picture of a human hand, it is believed that subjects mentally rotate an internal representation of their own hand in order to match it with the presented hand [143]. Such a task is referred to as hand laterality test/judgement task (HLT) [144]. A degree of mental effort applied in this task is proportional to the degree of mental rotation.

This rotation is similar to the mental rotation used for searching the congruency between two 3-D objects [145], in which subjects holistically, mentally rotate one of the 3D objects to match its orientation with that of the other [143]. This holistic mental rotation model is supported by neuroimaging studies of mental rotation consistently finding the activation of the superior parietal lobule (SPL) and the intraparietal sulcus (BA 40) . These are brain areas known for implementation of spatial maps that code the position of body parts in relation to each other [146, 147, 148]. Remarkably, activities in these region is proportional to the degree of mental rotation performed [146, 149, 150].

The hand mental rotation does not violate the bio-mechanical constraints imposed by the joints [151, 152, 153]. As shown by several chronometric studies, the time (reaction time, RT) it takes to mentally rotate the hand is proportional to the angular disparity between the current hand orientation and the new orientation [145, 154]. Most interestingly, this time is also proportional to the time it would take to perform the movement physically [153]. These findings suggest that the neural system of movement is used to mentally rotate the hand in order to make a match with the presented hand picture. Since there is no overt movement, the neural system should resemble that of Motor Imagination/Imagery (MI) which is the mental simulation of motor action [8, 19]. MI is neurally similar to physical execution of the action except that no movement is observed. During the mental rotation tasks, subjects are often unaware of imagination of movement. For this reason the term 'implicit MI' is used to describe the unrequested/unconscious imagination of movement during mental rotation tasks [154, 155]. Explicit MI therefore refers to a conscious motor imagination.

Implicit MI in mental rotation of body parts is an idea supported by many studies [143, 151, 152, 153, 154, 156, 157]. Several brain areas known to be active during explicit MI have been found active during the mental rotation tasks [146, 154, 156]. Parsons and colleagues used mental rotation induced by HLT to show that apart from the primary sensorimotor cortices, all the brain regions known to participate in the planning and execution of movement were activated by mental rotation of hands [154].

So far extensive neuroimaging studies of mental rotation have been done using PET and fMRI which offer a high spatial resolution. EEG is a technology offering a higher temporal and frequency resolution which is useful in studying the dynamic brain processes. Time-

frequency analysis of EEG is a well-established technique used to study MI [158]. Although hand mental rotation is claimed to involve MI, the time-frequency characteristics of mental rotation has never been compared with that of MI. Such an analysis is necessary to establish the relationship between MI and hand mental rotation. Previous 3D objects and alphanumeric based mental rotation studies [159, 160] using EEG did not describe the complete time-frequency characteristics.

In a recent study, Chen and colleague [161] only analysed an early induced EEG activity during hand mental rotation induced by HLT. Their experimental design involved subjects pressing buttons with their hands to indicate their judgements. Since the subjects were believed to be mentally rotating their hands, pressing the button with the same hands could interfere with the results. An important, yet unanswered question that would further confirm similarity between explicit and implicit MI is whether it is possible to discriminate between left and right mental rotation using EEG signal recorded during a hand mental rotation task such as HLT.

The present study has three main objectives. (1) To study the time-frequency dynamics and spatial localisation of sensorimotor activities during mental rotation of hands induced by HLT. (2) To test whether it is possible to discriminate between left and right hand mental rotation using EEG recorded during HLT. (3) To compare time-frequency responses over the sensorimotor cortices between implicit MI (in HLT) and explicit MI. The knowledge gained by studying the above is relevant in understanding the mental rotation process. Furthermore establishing that implicit MI is involved in mental rotation and that it is similar to explicit MI can open new areas of application in which mental rotation induced implicit MI can be used to complement explicit MI used in rehabilitation of movement [162, 163, 164, 165]. Patients who find it difficult to perform explicit MI due to loss of proprioception/sensation for example following incomplete spinal cord injury may use the implicit MI automatically invoked in the brain to activate the motor cortex in a similar manner as explicit MI in rehabilitation. Hand mental rotation induced with HLT is already in use in the treatment of complex regional pain [144, 166, 167] and its use is expected to widen [144].

4.3 Methods

4.3.1 Data collection

Subjects

Fifteen right handed (Edinburgh handedness inventory [168] mean, +76 $\pm$ 19) healthy subjects (mean age 24.9 $\pm$ 5.0, 6 females) volunteered for this study. The subjects gave their informed consents. The study was approved by the University ethics committee.

MI trials

A cue-based paradigm implemented with rtsBCI [169] was used. A trial lasted for 6000 ms. At the beginning of a trial (t=-3000 ms), the user was presented with a blank screen. A warning cue (a cross) appeared on the screen at t = -1000 ms informing the user to get ready. This cross disappeared at the end of the trial (t= 3000 ms). From t=-3000 ms to t=0 ms, the subjects were asked to relax, rest and they were not performing any study related task. At t = 0 ms an execution cue (which is an arrow pointing to either left or right) was presented on the screen and stayed there till t=1250ms. Depending on the cue the subjects had to perform continuous kinesthetic MI of opening and closing (or hand waving) of the left or the right hand. This gave two types of MI condition namely, right hand MI and left hand MI. Subjects were asked to continuously imagine waving their hand from t=0s till t=3000ms. They were allowed to rest from t = 3000 ms for a variable length of time (between 1000 to 3000 ms) before another trial started. This paradigm, often used in brain computer interface experiments [117, 170], is shown on Fig. 4.1 a.

HLT trials

The timing of the HLT paradigm was similar to that of MI. At t = -1000 ms the warning cue appeared accompanied with a beep sound. The beep sound was used as a reference for determining the subjects' response time on an audio recording explained later. At t = 0 ms, an execution cue in form of a hand picture was presented on the screen replacing the cross. The picture disappeared at t = 3000 ms regardless of the subject's response. This paradigm is shown on Fig. 4.1 b. The subjects were asked to verbally express their laterality judgement of the presented hand picture by answering 'left' or 'right'. Using verbal expression avoids hand movement unlike in the case of pushing a button to give an answer. Such a hand movement might interfere with the outcome of the experiment [171]. The hand pictures had plain backgrounds and each contained only one hand performing a gesture. They were processed to the size of 408 by 408 pixels. For each hand gesture there was a left and a right hand picture. Each of the pictures was presented in two orientations, counter-clockwise by 90^{o} (CCW) and clockwise by 90^{o} (CW). This gave four types of HLT condition namely right CCW HLT, left CW HLT, right CW HLT and left CCW HLT. The first two are termed medial orientations because they involve rotations towards the midline of the body while the last two are termed lateral orientations because they involve rotation outside the midline of the body [152]. Examples of the stimuli are shown on Fig. 4.2.

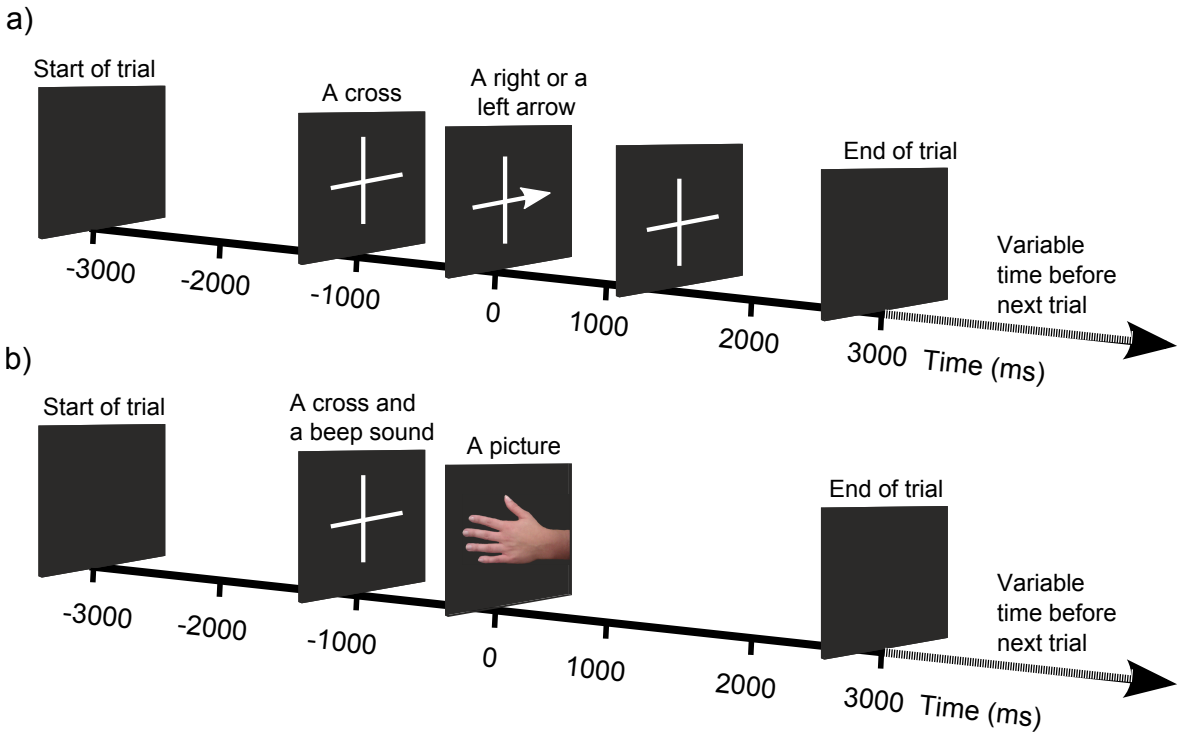

Figure 4.1: The sequence of events for a) MI and b) HLT trials.

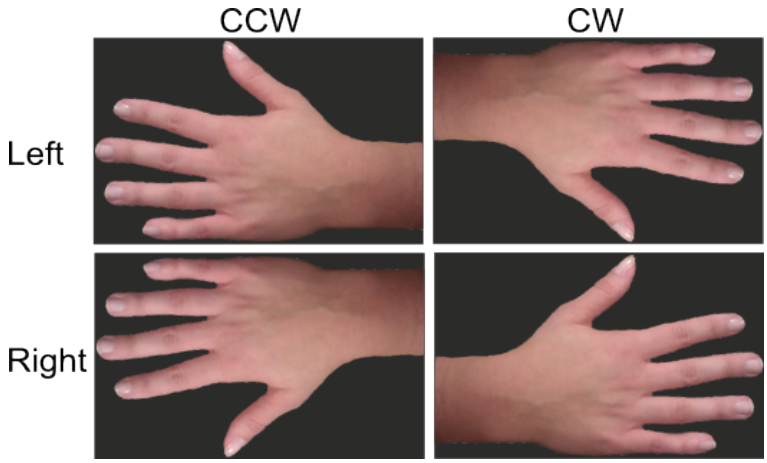

Figure 4.2: The first column shows the images rotated counter-clockwise (CCW) by 90^{o} while the second column shows images rotated clockwise (CW) by 90^{o}. All rotations are relative to the hands at upright position.

Procedure

Subjects sat in an armchair facing a computer screen. Their hands were pronated and placed on a table in front of them. Subjects were instructed to relax and avoid physical movements during the experiment. They were monitored throughout the experimental session to make sure that they followed the instructions and a part of the experiment was restarted if instructions were not followed. The MI trials (which took on average only 20 minutes in total) were followed by HLT trials after the subjects have had about 15 minutes of rest. It was

necessary to separate the MI runs from the HLT runs to avoid possible interference of the techniques the subjects employed [172]. For example the hand pictures might encourage visual MI during the MI trials if the MI trials were shown interchangeably with HLT trials or if the HLT runs were performed first. Also the performance of explicit motor imagery in the MI trials might influence the technique used during the HLT trials if the two conditions were presented interchangeably [172]. A total of 120 trials for MI were obtained (60 trials for each of left and right hand) divided into 4 runs of 30 trials (15 for each hand presented in a random order). A total of 240 trials for HLT were obtained (60 trials for each of right CCW, left CW, right CW and left CCW). This was divided into 6 runs of 40 trials consisting of 10 trials for each of the orientation presented in a random order. The subjects were allowed to rest between the runs. A relatively small number of trials were purposely chosen to reduce the influence of fatigue in both MI and HLT runs.

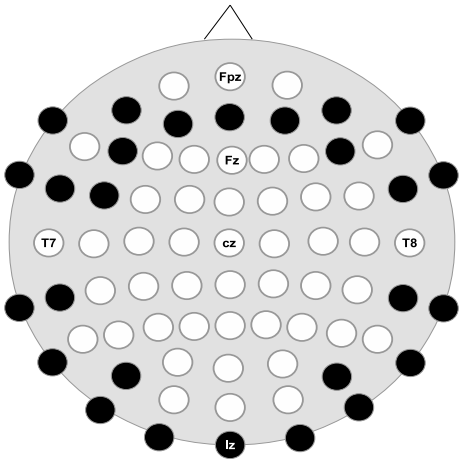

Figure 4.3: The 10/10 international electrode positioning standard used for HLT and MI experiment. The black circles show unused positions.

Data recording

Signal recording was performed under MATLAB and Simulink (MATLAB R2012a, The MathWorks Inc., Natick, MA). Electrodes were placed on 47 different locations on the scalp following the International 10/10 electrode positioning standard as shown on Fig. 4.3. Linked ear reference was used and the ground electrode was placed on location Afz. An electrode was attached to the lateral canthus on the orbicularis oculi of the right eye to record Electrooculogram (EOG) for the purpose of artefact detection. EEG and EOG were recorded at the sample frequency of 256 Hz using three modules of the g.USBAmp (biosignal amplifier, g.tec Medical Engineering GmbH, Austria). The impedance of the electrodes was kept below 5 kΩ. Signal was filtered online between 0.5 and 60 Hz with a notch filter at 50 Hz using the IIR digital Butterworth filters built into the amplifiers. In addition to EEG

and EOG, audio signal was recorded during the HLT trials which enabled a subject to give his/her judgement by verbal response [173].

4.3.2 Data analysis

Behavioural data

The beep sound during the HLT trials was used to retrieve the subjects' RTs from the audio recordings. The RTs for HLT trials were obtained by splitting the recorded audio signal into trials using the beep events. The beep time point (btp) was determined at two standard deviations from the start of the beep sound wave while the subjects' response time point (rtp) was detected at five standard deviations into the subjects' response speech wave. Given that the beep occurred at t=-1000 ms and the stimuli appeared at t=0 ms into the trials, RT = $(rtp - btp) - 1000$ was calculated in milliseconds. The subjects' mean RTs for the correct laterality judgements were submitted to a two-way analysis of variance (ANOVA), with hand pictures (left and right hands) and picture orientations (CW, CCW) as within subjects factors. The error rate was taken as the percentage number of trials with incorrect laterality judgement while the accuracy was calculated as 100 minus the error rate. The error rate was obtained by listening back to the audio trials for the subjects' response for each hand picture.The Wilcoxon rank sum test was used to compare the medians of the accuracies between the hands and orientations. Statistical significance level was to p =0.05.

EEG data pre-processing

The continuous EEG data of MI and HLT were split into trials. HLT trials with incorrect response were eliminated. All data were visually inspected and epochs with artefact like a sudden burst in amplitude over all electrodes were eliminated. For each subject, the MI and HLT trials were concatenated to form a single data set. The data sets were individually decomposed into 48 maximally independent temporal components using the logistic infomax independent component analysis (ICA) algorithm [174, 175] implemented in EEGLAB [176]. The components were visually inspected and components corresponding to ocular artefact were removed [177]. All other artefacts like electrocardiogram and electromyogram (which mostly occurred when subjects gave their answers) were identified and removed by considering their typical morphology, spectrum, topography and temporal characteristics [178]. The remaining components were back projected to EEG channels and then used for group analysis in EEGLAB and sLORETA after separating the data set back to HLT and MI trials and computing common average reference of the EEG channels.

Time-frequency analysis in EEGLAB

Group analysis was performed under EEGLAB to visualize and compare the Event Related Desynchronisation (ERD)[32, 179] and Event Related Synchronisation (ERS) [28, 121] arising from MI and HLT trials. Recall from Section 3.1.1 that ERD and ERS refer to decrease and increase respectively of EEG power relative to a baseline period within a narrow frequency band. Also recall that movement related cortical processes like those during MI and physical execution can be quantified with ERD across the sensorimotor cortex. ERD/ERS, sometimes referred to as event related spectral perturbation [33], will be used in this text as a general term to refer to both ERD and ERS when necessary. ERD/ERS was computed using EEGLAB routines. The Morlet Wavelet transform was used to perform time frequency analysis of the EEG data in the frequency band 3 to 60 Hz with a Hanning-tapered window applied and the number of cycles set to 3. These wavelet parameters allowed low frequencies starting from 3 Hz to be analysed in a one second window [180]. The ERD/ERS was computed as power changes in decibels relative to a baseline period (t=-2000 to -1000 ms). The full description of ERD/ERS method is given in the EEGLAB's methods by Delorme and Makeig [176]. ERD/ERS averaged over trials and subjects per experimental condition type is presented. Also presented are ERD/ERS scalp maps in small time windows of 200ms and in chosen frequency bands. The statistical non-parametric method with Holm's correction for multiple comparison [181] was used to assess the differences in ERD/ERS within and between the conditions at p=0.05.

sLORETA localisation

The trials were split into one second long time windows. Frequency domain sLORETA was computed for each window in the frequency bands including 1-3Hz (δ), 4-7Hz (θ), 8-12Hz (α/μ), 12-16Hz ($\beta 1$), 16-24Hz ($\beta 2$). Baseline was taken from the period before the warning sign (t=-2000 to -1000 ms). Images of sLORETA were computed over one second time windows beginning at t=500 ms post execution cue. Shifting the analysis window in 100 ms time steps over the period of interest and computing sLORETA image at each step yielded a temporal activation pattern of different cortical structures. The extent of activation at each time step was quantified for each brain structure by summing up the number of voxels active for that structure in the corresponding sLORETA image. The rationale for presenting the number of active voxels was to obtain a measure of temporal dynamic activity of each structure. The brain structures of interest included those found active in MI and HLT experiments [17, 156].

To find the predominantly active areas on the cortex for HLT and MI, the sLORETA statistical package was used to perform a paired group analysis (n=15) for HLT and MI trials

where a pair comprises the baseline window and a selected one second window. Paired group analysis was also performed to compare the differences in spatial activation and activation intensity between MI and HLT types. Using sLORETA's log of ratio of averages (r-value) for the first test and t-statistics (t-value) for the second test, 5000 randomization of statistical non-parametric mapping (SnPM) [182] implemented in sLORETA package was used to calculate corrected critical thresholds and p-values. Statistical significant level was set at p=0.05.

4.4 Results

4.4.1 Behavioural data

The mean RTs across all subjects and trials are shown in Fig. 4.4. The mean RT for the right hand CCW was 1427± 493 ms (MEAN ±STD), for the left hand CW it was 1549± 500 ms, for the right hand CW it was 1613± 554 ms and for the left hand CCW it was 1638± 551 ms. The mean RTs together with accuracies are presented in Table 4.1. The two-way ANOVA showed main effects for hand pictures, F(1,14)=6.163, p=0.026 and picture orientations F(1,14)=6.475, p=0.023 and significant interaction of hand pictures × picture orientations, F(1,14)=14.068, p=0.002. The interaction was significant because as shown on Fig. 4.4 the right hand pictures were recognised quicker at CCW orientation than at CW orientation and left hand pictures were recognised quicker at CW orientation than at CCW orientation. These results have shown that the pictures at the medial orientations (right hand

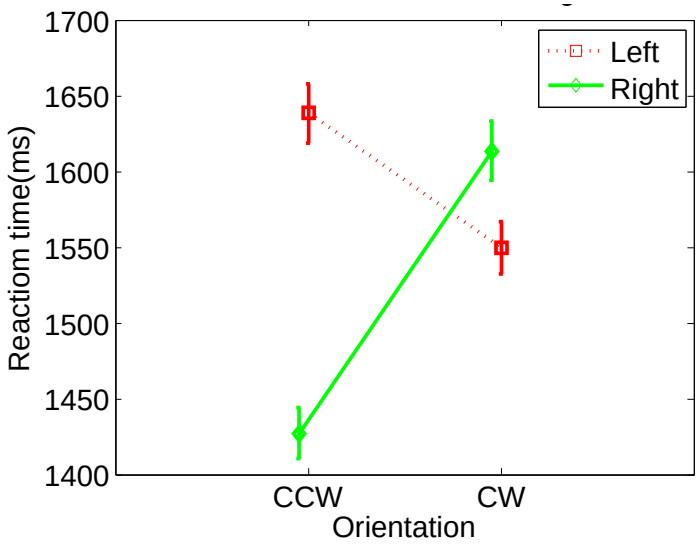

Figure 4.4: The mean reaction time for all subjects.

CCW and left hand CW) had the smallest RTs. The RTs obtained here are similar to those

Table 4.1: Mean RTs and accuracies for each subject and each condition.

Subj.ID	RT (ms)				Accuracy (%)			
	Left CW	Right CCW	Left CCW	Right CW	Left CW	Right CCW	Left CCW	Right CW
1	1833	1647	1881	1879	95	97	97	92
2	1604	1381	1798	1770	92	97	92	90
3	1816	1453	1688	1754	97	98	95	100
4	1415	1099	1527	1441	83	85	85	93
5	1122	953	1253	1212	80	78	75	58
6	1482	1378	1511	1500	98	98	93	100
7	1669	1552	1660	1454	95	98	93	97
8	1515	1672	1761	2023	87	93	88	87
9	1312	1253	1375	1364	98	100	100	100
10	1633	1751	1785	1763	97	92	93	87
11	1799	1732	1850	1909	97	100	92	92
12	1004	933	1100	1038	100	97	100	100
13	1417	1406	1528	1393	100	93	100	95
14	1546	1416	1546	1515	100	100	100	97
15	2346	1820	2918	2540	76	72	62	66

from the published literature [143, 171], although in the referenced studies participants provided their response by pressing buttons rather than by responding verbally. The accuracies (100% - % error rate) had medians of 97, 97 93 and 93% for left CW, right CCW, left CCW and right CW respectively. There were no statistically significant differences in the medians of the accuracies between the hand pictures (z=0.1343, p=0.8931) and picture orientations (z=-0.1418, p=0.8872). There was also no statistically significant difference in the median accuracy between the hand pictures in the lateral (right CW+left CCW) and the hand picture in the medial (right CCW+left CW) orientations (z=-0.8359, p=0.4032).

4.4.2 Time frequency analysis

The RTs differed for medial and lateral orientations but their ERD/ERS maps were not found to be different statistically. For this reason results will be presented only for the medial orientation. The ERD/ERS maps averaged across subjects and trials for two channels C3 and C4 located over the sensorimotor areas are plotted on Fig. 4.5 to show the time-frequency changes. The plot starts from when the execution cue was shown to the subject. The ERD is represented with negative values while ERS is represented with positive values. The last column shows the area of significant differences in ERD/ERS between MI and HLT in frequency and in time. The last row shows the area with statistical significant differences in ERD/ERS between the hands. The plot at the bottom right presents the area with statistical

interactions.

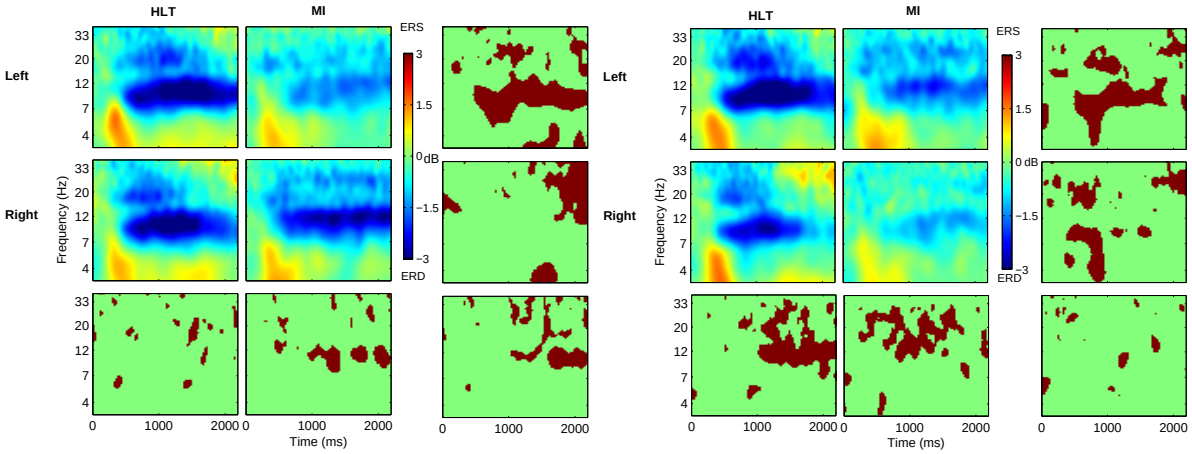

(a) Channel C3 (b) Channel C4

Figure 4.5: ERD/ERS maps of channels (a) C3 and (b) C4 averaged across all subjects and trials for MI (left and right) and HLT (left CW and right CCW). The plot is shown for t=0-2200 ms and frequency 3-40 Hz. The areas of statistical differences between the corresponding two conditions in frequency and time are shown on the last column. On the last row, the area of statistical differences between the right and left hand is presented. The plot shown on the bottom right is for the statistical interactions between the conditions and their types.

The ERS at about 300 ms is related to visual processing possibly of the execution cue. At around 500 ms, ERD is seen for all conditions in the α/μ, $\beta 1$ and $\beta 2$ bands. The intensity of the ERD is generally lateralised with the right hand having more intensity on C3 and the left hand on C4. In the case of MI, the left and right hand ERD differences (shown on the second map on the last row of Fig. 4.5b) is apparent early at about 500 ms and it is more pronounced on channel C4.

For HLT, inspecting the ERD/ERS of the right and the left hand and the corresponding statistical difference maps reveals that the ERD can be divided into an early and a late ERD. The early ERD is the HLT ERD that occur between 500 to approximately 1000 ms. The late ERD starts from about 1000 ms. From the plot of RT on Fig. 4.4, the early ERD can be said to occur long before laterality decisions were reached while the late ERD began just before and after laterality decisions were reached. This late and early ERD phenomenon first described in this study is more pronounced on channel C4. The early ERD is not significantly different between the left and the right hand, as shown by the map on the bottom left of the Fig. 4.5b. However, the late ERD is different between HLT of the left and the right hand, showing that it is hand specific.

The ERD of MI is significantly different between the left and right hand in the whole period and it is hand-specific from the onset of ERD at t=500 ms. The late ERD in HLT is similar to that of MI of the matching hand and this similarity is more pronounced in the $\beta 1$ and $\beta 2$

bands. The ERD for the HLT tends to decrease after verbal response. This may have created the differences between HLT and MI towards the end of the trials because subjects continued MI until the end of the trials. The statistical interactions between the conditions and types are only more profound in the later part at C3 in the α/μ frequency band.

The ERD/ERS distribution on the scalp in α/μ, $\beta 1$ and $\beta 2$ bands are shown on Fig. 4.6. The maps were obtained in the window t=1000-1200 ms which is a window that includes the late ERD. This time-window is prior to the fastest RT (1427 ms) and therefore should have a reduced interference from the verbal response. The last columns highlights recording channels that show statistically significant differences in ERD/ERS between the matching two conditions (left HLT and left MI in the first rows, right HLT and right MI in the second rows for a given frequency band) while the last rows show the statistically significant differences between the right hand and the left hand. The plot on the bottom right presents the statistically significant interactions between HLT, MI, left and right. The Differences between MI and HLT task will be assessed first. At the chosen time window for the scalp map, most of the ERD/ERS differences between the right hand MI and right CCW HLT appear in the posterior parietal and occipital channels. This shows that their ERD/ERS in the sensorimotor areas are similar in the α/μ, $\beta 1$ and $\beta 2$ bands. In the case of the left hand MI and left CW HLT, the difference is widespread including the motor areas in the α/μ band but in the $\beta 1$ and $\beta 2$ bands the differences is concentrated on the parietal and on the occipital areas. The absence of significant differences on the frontal and paracentral areas shows a comparable intensity of activation of the sensorimotor areas during MI and HLT. When ERD scalp maps were compared between the left and right hand significant differences can be seen in all the three frequency bands for MI but predominantly in the $\beta 1$ and $\beta 2$ bands in HLT. For MI, areas of statistical significant difference between left and right hand include dominantly the right parietal and central channels including C4. Because the late ERD in HLT is hand specific and therefore resembles the ERD of MI, areas of statistically significant difference between two hands are similar to those of MI.

4.4.3 sLORETA localisation

Changes in the cortical activation of relevant brain structures over time were expressed as a function of the number of active voxels in different time windows. Different experimental condition showed distinctive temporal variations of the cortical activity. Temporal activation of representative structures are shown on Fig. 4.7. The HLT had larger number of active voxels and larger temporal variation than MI. Selected brain regions reached their maximum activity fastest for the right hand CCW where the activities plateaued at the time window t=700-1700 ms. For left CW the plateau was within the time window t=1000-2000 ms and for both the right CW and left CCW (not shown on the figure) it was within the window

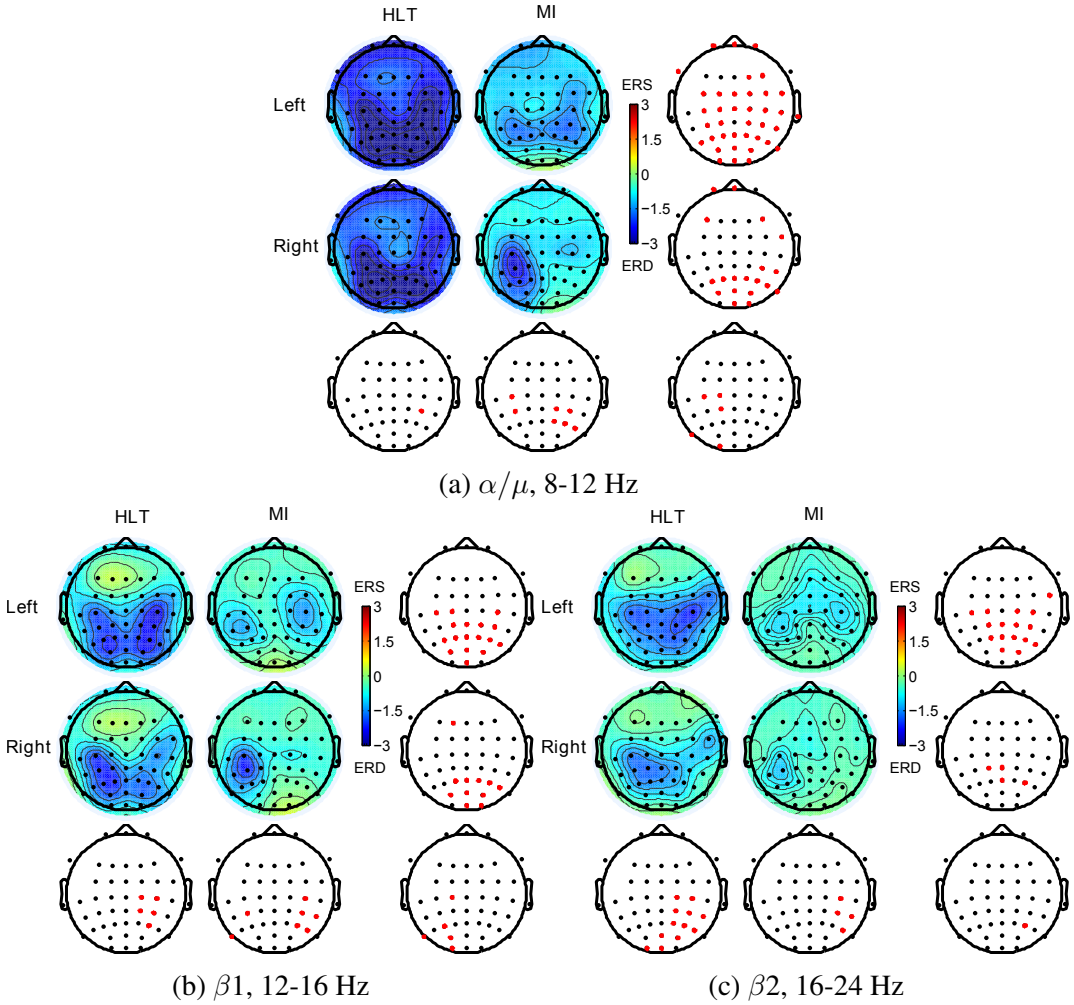

(a) α/μ, 8-12 Hz

(b) β1, 12-16 Hz

(c) β2, 16-24 Hz

Figure 4.6: Scalp maps of ERD/ERS in different frequency bands at 1000-1200 ms post cue for MI (left and right) and HLT (left CW and right CCW). ERD is shown with negative values while ERS is shown with positive values. The last columns highlight channels/electrodes that show statistical difference between the corresponding two conditions (p=0.05 with Holm's correction for multiple comparison) while the last rows show the same for the difference between the right and left hand. The plot on the bottom right represents the statistical interactions between the conditions and their types.

t=1100-2100 ms with temporal distribution similar to that of left CW HLT. The time window used for sLORETA analysis in which plateaus occurred corresponds to the time window as their respective RTs, apart from the plateau for the right CCW which had significantly shorter RT. Compared to HLT the number of voxels during MI was less variable over time (note the different time scales for HLT and MI). In both MI and HLT there are clear activities of the postcentral gyrus and precentral gyrus and the plateaus in the case of HLT are possibly related to the maximum activity occurring during implicit MI. The IPL and the middle frontal gyrus were active for the right hand MI but did not reach the significance level (p=0.05) in the case of the left hand MI. The cingulate gyrus and the paracentral lobule were also activated in HLT.

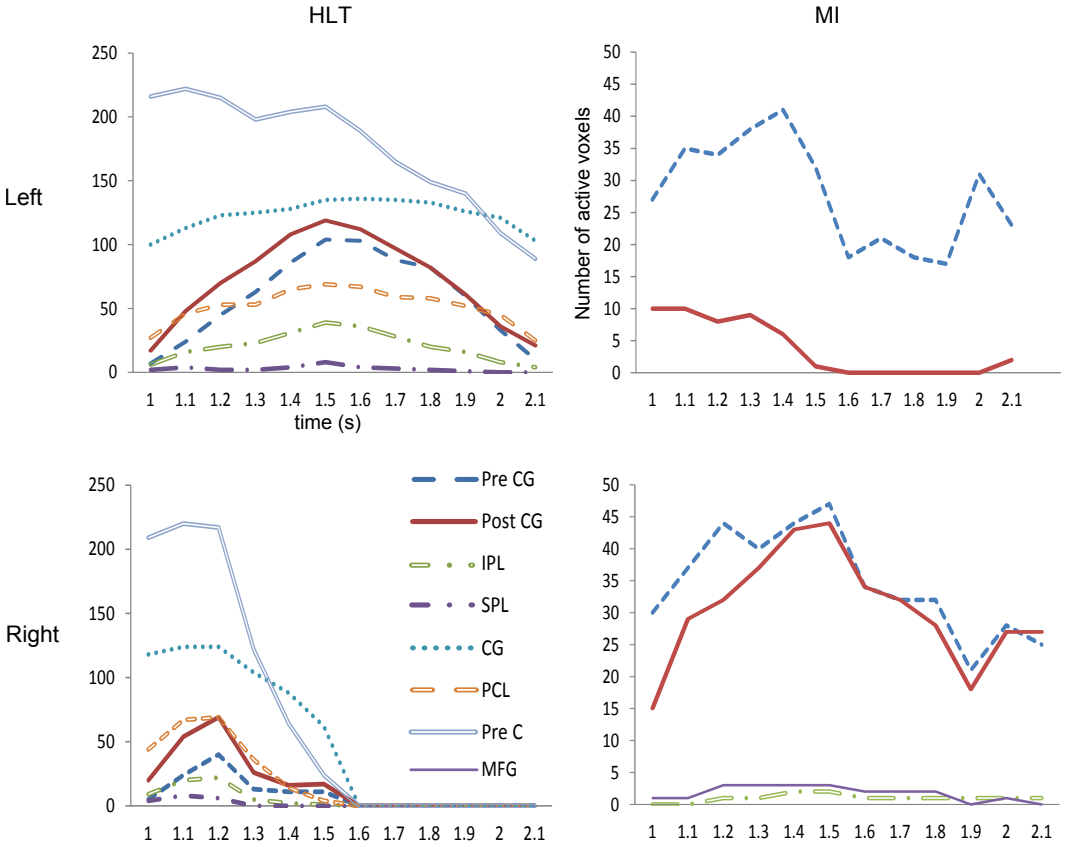

Figure 4.7: Temporal activation pattern of cortical structures (n=15) in the α/μ-band of sLORETA localisation for MI (left and right) and HLT (left CW and right CCW). The number of active voxels was counted for each cortical structure for each sLORETA image computed in a one second sliding window with a step size of tenth of a second. The time axis represents the centres of the one second sliding windows. Pre CG, Precentral gyrus; Post CG, Postcentral gyrus; IPL, Inferior Parietal Lobule; SPL, Superior Parietal Lobule; CG, Cingulate gyrus; PCL, Paracentral lobule; Pre C, Precuneus; MFG, Middle Frontal Gyrus.

The rest of sLORETA results will be presented as follows. sLORETA images and the corresponding tables of activities will be presented for each of the four conditions on Fig. 4.7 (i.e left hand MI, right hand MI, left CW HLT and right CCW HLT) in order to individually describe each condition. Afterwards, an sLORETA image and corresponding table of activities will be presented for the comparison between right hand MI and the right CCW HLT to further show the similarities and differences between MI (explicit MI) and HLT (implicit MI).

In order to present a sLORETA image that best describes each of the conditions' sensorimotor activities, sLORETA images corresponding to a condition's specific plateau time window of the sensorimotor area is presented. Assuming that in the case of MI, the number of active voxels were relatively constant, the time window t=500-1500 ms was chosen to present MI images.

As it can be seen from Figs. 4.8 and 4.9 the right and left hand MI engendered strong

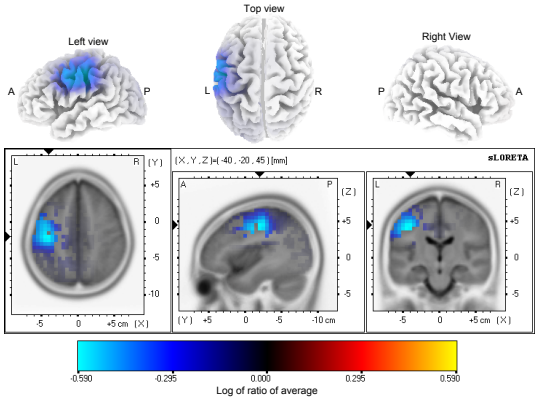

Figure 4.8: sLORETA localisation for MI of right hand compared with the baseline period in the α/μ-band at the time window 500-1500 ms relative to execution cue onset. The first row shows 3D map of the localisation while the second row shows a 3D slice at the displayed location (BA 4). The localisation for the $\beta 1$-band is similar to that of α/μ and therefore it is not shown here.

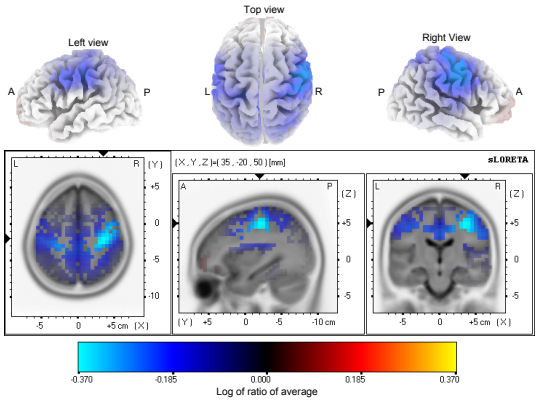

Figure 4.9: sLORETA localisation for MI of left hand compared with the baseline period in the α/μ-band at the time window 500-1500 ms relative to execution cue onset. The first row shows 3D map of the localisation while the second row shows a 3D slice at the displayed location (BA 4). The localisation for the $\beta 1$-band is similar to that of α/μ and therefore it is not shown here.

activation contralaterally. Active regions are summarized in Tables 4.2 and 4.3 for the right and left hand MI respectively. The sLORETA images are presented for the right CCW HLT on Fig. 4.10 and for the left CW HLT on Fig. 4.11. The activities in the α/μ band were significant for both conditions; those in the $\beta 1$ frequency band were significant in the case of MI but not in the case of HLT. The sLORETA localisation for MI in the $\beta 1$ band is similar to that in the α/μ band, therefore unless otherwise specified the α/μ localisation for MI is referred. The activities in the $\beta 2$ frequency band did not reach significance level in any condition. In both MI and HLT the postcentral gyrus, the precentral gyrus and IPL (BA 40) and the middle frontal gyrus were always active. For HLT the activities of these structures were bilateral with the strongest active voxel contralateral to the chosen hand. The medial frontal gyrus active during mental rotation task [149] and the paracentral lobule

Table 4.2: Significantly active structures for right hand MI compared with the baseline period in α/μ-band and $\beta 1$-band obtained at time window 500-1500 ms relative to cue onset.

					Voxel with max. r-value			
F	Structure	BA	H	nv	r-value	x	y	z
α/μ	Postcentral Gyrus	2 ***3***	L	15	-0.59	-45	-18	38
	Precentral Gyrus	**4** *6*	L	30	-0.59	-40	-17	42
	Middle Frontal Gyrus	***6***	L	1	-0.54	-45	2	41
$\beta 1$	Postcentral Gyrus	**3** *2*	L	29	-0.63	-40	-22	43
	Precentral Gyrus	***4*** 6	L	10	-0.62	-40	-17	42
	Inferior Parietal Lobule	***40***	L	1	-0.54	-50	-27	43

Notes: The structures are sorted in the descending absolute values of r-value. F, Frequency band; BA, Brodmann Area; H, Hemisphere; nv, Number of Voxels; r-value, Statistics (log of ratio of averages implemented in sLORETA, read like t-values); xyz, Talairach coordinates; R, Right; L, Left. The BA in bold font is the Brodmann area whose coordinate is displayed. The BA in italics is the Brodmann area contributing most in nv. The H in bold font is the hemisphere that contributes more than 20% of nv.

Table 4.3: Significantly active structures for left hand MI compared with the baseline period in the α/μ-band and $\beta 1$-band at the time window 500-1500 ms relative to cue onset

					Voxel with max. r-value			
F	Structure	BA	H	nv	r-value	x	y	z
α/μ	Precentral Gyrus	***4*** 6	R	27	-0.37	35	-17	47
	Postcentral Gyrus	***3***	R	10	-0.37	35	-22	47
$\beta 1$	Precentral Gyrus	***4*** 6	R	7	-0.35	35	-17	42

Notes: See table 4.2

part of the frontal and the parietal lobe were also active in HLT. Like in other neuroimaging studies on mental rotation [146], SPL and IPL were always active bilaterally for all types of HLT. The cingulate gyrus, posterior cingulate and the precuneus which has been referred metaphorically to as the mind's eye [183] were particularly active. In the occipital cortex, the notable active areas included the cuneus, middle occipital gyrus and the lingual gyrus. The activities found in the auditory cortex namely the superior temporal gyrus and the transverse temporal gyrus might have been due to the beep sound used in the HLT trials although the superior temporal gyrus has been found active in a mental rotation task [149]. There were also activities in the insula and the parahippocampal gyrus. These and other active areas are summarized in Tables 4.4 and 4.5 for the right CCW and the left CW respectively.

The results of comparing cortical activity between MI and HLT are presented for the right hand MI versus right CCW HLT on Fig. 4.12 and in Table 4.6. There were no differences

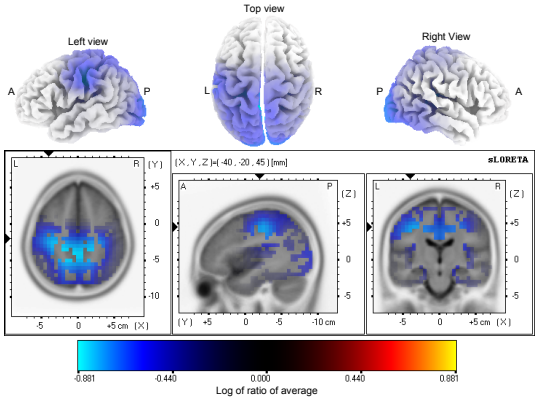

Figure 4.10: sLORETA localisation for right CCW HLT compared with the baseline period in the α/μ-band at the time window 700-1700 ms relative to execution cue onset. The first row shows 3D map of the localisation while the second row shows a 3D slice at the displayed location (BA 4). The localisation for the $\beta 1$-band is similar to that of α/μ but it was not statistically significant.

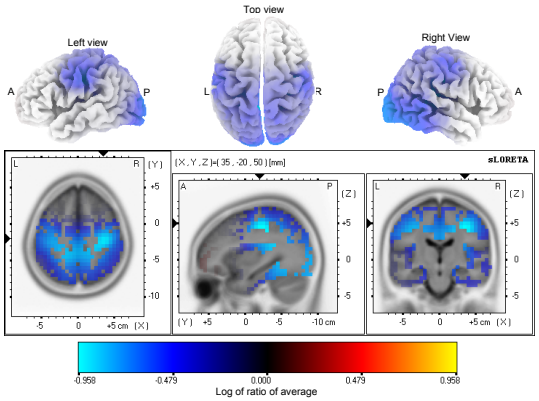

Figure 4.11: sLORETA localisation for left CW HLT compared with the baseline period in the α/μ-band at the time window 1000-2000 ms relative to execution cue onset. The first row shows 3D map of the localisation while the second row shows a 3D slice at the displayed location (BA 4). The localisation for the $\beta 1$-band is similar to that of α/μ but it was not statistically significant.

between the conditions in the hand areas of the precentral gyrus and the postcentral gyrus, indicating similarities in the intensity of activation in these areas in both conditions. As expected there were more activities in the SPL in HLT than in MI. Other areas more active during HLT included the central areas, the precuneus and the sub-gyral. Similar results to those presented was also obtained by comparing left hand MI with left CW HLT, right hand MI with right CW HLT and left hand MI with left CCW HLT.

Table 4.4: Significantly active structures for right CCW HLT compared with the baseline period in α/μ-band at the time window 700-1700 ms relative to cue onset

					Voxel with max. r-value			
F	Structure	BA	H	nv	r-value	x	y	z
α/μ	Cingulate Gyrus	***31***	R L	124	-0.88	-10	-42	34
	Precuneus	**31** *7*	R L	217	-0.88	-5	-47	30
	Posterior Cingulate	***30***	R L	87	-0.87	5	-47	25
	Sub-Gyral	**31** *7*	R **L**	14	-0.86	-20	-47	35
	Cuneus	***18***	R L	237	-0.83	15	-67	17
	Paracentral Lobule	**31** *5*	R L	69	-0.82	0	-32	43
	Postcentral Gyrus	***3***	R **L**	69	-0.81	-30	-22	43
	Lingual Gyrus	***18***	R L	165	-0.81	20	-53	7
	Precentral Gyrus	***4*** 6	R **L**	40	-0.79	-25	-27	47
	Parahippocampal Gyrus	***19***	**R** L	56	-0.79	20	-48	2
	Insula	***13***	**R** L	15	-0.79	30	-33	20
	Inferior Parietal Lobule	***40***	R **L**	22	-0.79	-35	-32	38
	Middle Occipital Gyrus	***18*** 19	**R** L	56	-0.75	-15	-87	14
	Superior Temporal Gyrus	***41***	R	3	-0.74	35	-33	15
	Superior Parietal Lobule	5 ***7***	R **L**	6	-0.73	-25	-51	44
	Medial Frontal Gyrus	***6***	R L	9	-0.72	10	-22	47
	Fusiform Gyrus	***19***	R	35	-0.71	25	-54	-10
	Inferior Occipital Gyrus	***18***	**R** L	11	-0.71	30	-92	-4
	Transverse Temporal Gyrus	***41***	R	2	-0.68	40	-33	11
	Middle Frontal Gyrus	***6***	L	2	-0.67	-35	-8	42

Notes: See table 4.2

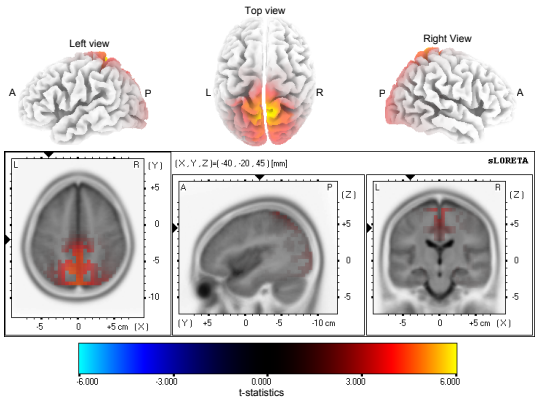

Figure 4.12: sLORETA localisation of the differences between the right hand MI and the right CCW HLT in the α/μ-band at the time window 500-1500 ms. In all the presented areas (red), HLT is more active than MI. The first row shows 3D map of the localisation the second row shows a 3D slice at the displayed location (BA 4). The localisation for the β1-band is similar to that of α/μ but it was not statistically significant.

Table 4.5: Significantly active structures for the left CW HLT compared with the baseline period in the α/μ-band at the time window 1000-2000 ms relative to cue onset.

					Voxel with max. r-value			
F	Structure	BA	H	nv	r-value	x	y	z
α/μ	Postcentral Gyrus	***3***	R L	119	-0.96	35	-22	43
	Precentral Gyrus	***4*** 6	R L	104	-0.96	35	-17	42
	Sub-Gyral	**2** *7*	R **L**	19	-0.93	35	-27	38
	Cingulate Gyrus	***31***	R L	135	-0.93	20	-42	25
	Precuneus	**31** *7*	R L	208	-0.93	20	-42	30
	Posterior Cingulate	**23** *30*	R L	87	-0.92	5	-42	25
	Lingual Gyrus	***18***	R L	180	-0.91	20	-53	7
	Insula	***13***	**R** L	31	-0.89	30	-33	20
	Parahippocampal Gyrus	***19***	**R** L	81	-0.89	20	-48	2
	Cuneus	**30** *18*	R L	250	-0.88	10	-58	8
	Paracentral Lobule	**31** *5*	R L	69	-0.86	0	-32	43
	Inferior Parietal Lobule	***40***	R L	39	-0.85	40	-32	34
	Superior Temporal Gyrus	***41***	R	22	-0.85	35	-33	15
	Fusiform Gyrus	**19** *37*	**R** L	100	-0.83	25	-54	-10
	Middle Frontal Gyrus	***6***	R L	11	-0.83	35	-8	42
	Middle Occipital Gyrus	***18***	**R** L	107	-0.82	30	-92	5
	Inferior Occipital Gyrus	***18***	**R** L	20	-0.81	30	-92	-4
	Transverse Temporal Gyrus	***41***	R	5	-0.81	40	-33	15
	Supramarginal Gyrus	***40***	R	3	-0.79	40	-42	34
	Middle Temporal Gyrus	***37***	R	52	-0.78	45	-58	-1
	Medial Frontal Gyrus	***6***	R L	11	-0.77	10	-22	47
	Inferior Temporal Gyrus	***37***	R	27	-0.76	45	-68	-1
	Superior Occipital Gyrus	***19***	R	2	-0.74	30	-86	23
	Superior Parietal Lobule	5 ***7***	R L	8	-0.74	25	-51	44

Notes: See table 4.2

4.5 Discussions

It is believed that mental rotation of hand involves MI implicitly. Using time-frequency decomposition methods, EEG recorded during mental rotation tasks was studied with three main objectives. First to understand the dynamics of sensorimotor activity during mental rotation induced by HLT. Second, to investigate if it is possible to discriminate between left and right hand mental rotation exploiting the time frequency technique. The third was to compare temporal dynamic activation of the sensorimotor cortex during implicit and explicit MI across different frequency bands.

In the first objective, the time frequency analysis of EEG signal recorded during HLT showed activities in the α/μ frequency band and in the β (β1 and β2) bands. Similar frequency

Table 4.6: Structures with significant differences in activity between right hand MI and right CCW HLT in α/μ-band at time window t=700-1700 ms. In all the presented structures, HLT is more active than MI.

					Voxel with max. t-value			
F	Structure	BA	H	nv	t-value	x	y	z
α/μ	Postcentral Gyrus	***5***	R L	46	5.90	5	-45	67
	Paracentral Lobule	***5***	R L	58	5.61	5	-45	62
	Precuneus	***7*** 19	R L	125	5.48	0	-50	62
	Superior Parietal Lobule	**5** *7*	**R** L	28	4.62	-20	-41	62
	Medial Frontal Gyrus	***6***	R L	8	4.40	0	-26	57
	Precentral Gyrus	***4***	R **L**	3	4.37	-15	-31	66
	Cingulate Gyrus	***31***	**R** L	4	4.35	5	-42	44
	Sub-Gyral	***7***	L	1	4.13	-20	-46	53

Notes: See table 4.2.

bands showed ERD activities in previous mental rotation studies using 3D objects and hands [159, 160, 161]. Activities in these frequency ranges are believed to show spatiotemporal patterns in motor, and cognitive tasks [184, 185, 186] such as HLT. The maximum α/μ ERD in HLT was localized on the sensorimotor, posterior parietal and the occipital areas although this ERD was not spatially specific. The activities in about 8-12 Hz band in the posterior parietal and the occipital areas during mental rotation [187] might have a global effect and therefore contribute to this non-spatial specificity. The 8-12 Hz band activities might influence α/μ activities recorded in the sensorimotor areas although we used the common average method of electrode derivation to enhance local activities. In the case of the β bands in HLT, activity was more transient and spatially specific in accordance with the characteristics of motor related ERD in the β band [186]. These β ERDs were localized over the sensorimotor and posterior parietal areas. Temporally the ERD in all the frequency bands began at approximately t=500 ms and diminished soon after the subjects' verbal responses measured by RT. These results suggest that the sensorimotor activities quantified with ERD during mental rotation of hands can be studied in the chosen frequency bands. sLORETA localisations in the α/μ band confirmed that structures in the sensorimotor areas contributed to the ERD activities. Furthermore the sLORETA localisations showed that the activation of the sensorimotor areas peaked at different times for each hand and picture orientations during the trials. Apart from the right CCW HLT, where the peak activity in sLORETA occurred about 200 ms earlier than RT, the mean RTs closely followed the times of peak sensorimotor activity (because RTs occurred in the same time window as the corresponding sensorimotor peak activity). This means that the time of sensorimotor peak activity corresponds to the RT, being faster for medial than for lateral orientation. According to Parsons [144, 155], when

a person is presented with a HLT, the person makes an initial spontaneous pre-conscious judgement which is subsequently confirmed by an implicit MI of the hand implicated in the pre-conscious judgement. It is possible that the pre-conscious judgement was biased towards the right hand given that the subjects were right-handers. This would imply that the first confirmation process involving implicit MI was biased towards the right hand. So given a right hand image in a medial orientation, this first confirmation process was often successful. This might explain the early peak activity for the right CCW HLT although it does not explain why its mean RT occurred at about 200 ms after the peak activity.

For the second objective, statistical analysis of ERD/ERS showed that there were differences between left and right mental rotation induced by HLT. The differences could only be observed during the late ERD phase in HLT, 1000 ms after the execution cue. Hemispheric differences could be observed with the late ERD but not with the early ERD. This explains why a previous EEG study did not report any hemispheric difference between left and right HLT [161]. In the case of MI the left and right hands' ERD differences started at the onset of ERD (t=500 ms). Discrimination between left and right hand MI has been exploited in brain computer interface [188, 189, 190]. The results of this study suggested that the discrimination can also be achieved with data recorded during HLT. Furthermore, similar electrode locations can be used for this discrimination for both MI and HLT. With regard to sLORETA localisations, there were no quantitative differences between the left and right hand mental rotation although there were stronger activations in the contralateral hemisphere to the presented hand. There was also no difference between left and right hand MI in sLORETA analysis despite differences being present in the channel based time frequency analysis.Vingerhoets and colleagues faced a similar issue in an fMRI study [156] on mental rotation. As suggested in the Vingerhoets' study activities in the ipsilateral hemispheres to each hand were sufficient to neutralise the lateralised activities when both hands data were contrasted.

For the third objective, ERD/ERS was compared between MI (explicit MI) and HLT (implicit MI). There were similarities between the two conditions in the later part of the trials when the late ERD occurred. The similarities were present in the sensorimotor areas. The results also showed that MI and HLT mainly differ in the activation of the posterior parietal and occipital regions where ERD activation intensity was stronger for HLT. The frequency bands that best described the similarities between MI and HLT were the $\beta 1$ and $\beta 2$. The α/μ band in the case of HLT was not spatially specific although its maximum was on the sensorimotor, parietal and occipital areas.

The sLORETA localisation of MI resembles those obtained in a study by Dyson and colleagues [191] who localised cortical activities during explicit MI. All of the structures active during MI were active during HLT. These structures included the precentral gyrus, postcentral gyrus, IPL and the middle frontal gyrus (BA 6). This result supports the propositions

in the literature that MI is used during mental rotation [143, 151, 152, 153, 154, 156, 157] and suggests that implicit MI is similar to explicit MI. In the case of MI the statistically significant active sensorimotor areas were completely lateralised while for the HLT they were bilateral possibly because the late and early ERD both occurred within the long-time window analysed in sLORETA. However, the strongest active voxel in the sensorimotor areas for HLT were always contralateral to the hand chosen by the subjects. The activities in the $\beta 1$ frequency band were found significant for the MI but it did not reach significance level in the HLT condition. This was attributed to the excessive energy in the α/μ band in HLT which dominated the activities in the β bands following the correction for multiple comparisons over all frequency bands. When the α/μ band was excluded from the analysis the β band became significant.

Comparing HLT and MI data in sLORETA did not reveal any statistical significant difference in the sensorimotor cortex of the hand suggesting that these areas were similarly active in both conditions. Instead, as expected the SPL, active in mental rotation tasks [156], and other areas in the parietal cortex were among the areas showing higher activation in HLT than in MI condition. Some previous studies have suggested that the primary sensorimotor cortices are not active during HLT unlike during MI [144, 155]. The absence of any difference in primary sensorimotor activity between the two conditions might be due to the EEG methodology used in this study. Its disadvantage lies in the low spatial resolution in which neighbouring cortical structures may have correlated activity. However, it could be that the EEG method which offers highly resolved time-frequency analysis may be more sensitive to transient changes. This was demonstrated by the temporal dynamics of the activities of cortical structures which peaked at certain times during HLT.

4.5.1 Other Active areas in HLT

A literature review on mental rotation reported that activities were wide spread over several brain areas [146, 160, 192, 193]. The only areas consistently reported in all studies were the SPL and the intraparietal sulcus and similar areas were presented in the current study. The other areas mostly reported in mental rotation or related tasks which were also reproduced by sLORETA in this study included the following. The insula cortex [146, 172], found active during voluntary hand movement [194], was consistently active. The precunues (BA 5 and 7) which has been implicated in self centered mental imagery [195] and other parietal areas were major active areas [146, 192]. In the limbic lobe the cingulate gyrus and the posterior cingulate cortex were prominantly active in all types of HLT conditions [172]. The posterior cingulate cortex has previously been found active in attention requiring tasks [196] and in visual mental imagery [197]. In the temporal lobe, activities were found in the posterior temporal cortex (BA 37 including the fusiform gyrus) [160, 193, 197, 198]

and the parahippocampal gyrus. The parahippocampal gyrus is known to play a part in the memory encoding and retrieval. It has also been implicated in the encoding and recognition of scenes [199]. In the occipital lobe there were activities in the cunues [172], the fusiform gyrus (BA 19) which has overlapping areas that respond to faces [200] and body parts [201]. Other areas included the lingual gyrus, the superior, middle, and the inferior occipital gyri. [149, 150, 156, 193].

4.5.2 Shortcomings

A possible shortcoming of the study is that the results were derived from only 15 young healthy individuals and therefore might not reflect a general case. Also it was not possible to determine whether the HLT and the MI tasks were of equal difficulty. However, the chosen orientation of the pictures especially the medial orientations were relatively natural to the hands so the HLT was not expected to be more difficult than MI of movement in a similar orientation as the medial and lateral orientations.

4.6 Conclusions

During the hand mental rotation task, the recorded brain activity had similar spatial and time-frequency characteristics to those found during explicit motor imagery. The sensorimotor activity is known to be distinctive for left and right hand explicit MI. It was shown here that the sensorimotor activity was also distinctive for the left and right hand mental rotation. These suggest that implicit MI used during the mental rotation of hand in HLT is similar to explicit MI. These results indicate that mental rotation of body parts can be used to complement MI in areas of rehabilitation in which MI is used for therapeutic purposes. Patients who are unable to perform explicit MI could use implicit MI. Patients may more easily understand a laterality judgement task than a task involving movement imagination which is often abstract. Unlike in the case of MI, therapists can easily tell when the patients are correctly performing a judgement task.

Chapter 5

Left-right classification: mental rotation versus motor imagery.

"What is essential is invisible to the eye" The Little Prince, cite in [116]

5.1 Summary

Mental rotation involves motor imagery. It has been shown that differences in sensorimotor activities exist between the left and the right hand mental rotation. This left and right hand differences appear to be similar to the left and right hand differences in motor imagery. In brain computer interface, the left and right hand differences in motor imagery is exploited. In this study, a classification procedure used to implement left-right motor imagery-based brain computer interface was used to assess the left-right differences in mental rotation. The results confirmed that the left-right difference in mental rotation is similar to that in motor imagery. This results suggest that a special kind of brain computer interface for rehabilitation in patients who are unable to perform motor imagery could be constructed using mental rotation.

5.2 Introduction

Hand motor imagery (MI) and mental rotation (MR) in hand laterality test (HLT) share a common characteristic because they both activate similar area of the sensorimotor cortex [151].

For MI, the pattern of activation of the sensorimotor cortex depends on whether the left or the right hand movement imagination is performed. The activation is left-hemispheric

lateralised if the hand is right and right-hemispheric lateralised if the hand is left. This difference makes it possible for a machine learning algorithm to classify between the left and right hand MI [127]. This possibility to classify between the left and the right hand MI has found a great application in brain computer interface (BCI) [127]. Such MI-based BCI is used in movement rehabilitation because MI allows mental rehearsal of movement and the BCI encourages MI through its detection and feedback provision [74].

Since MI and mental rotation in HLT (MR-HLT) similarly activates the sensorimotor cortex, left and right hand differences is expected to exist in MR-HLT in a similar fashion as in MI. Indeed, MI-like left and right hand differences in sensorimotor cortex activation has been recently identified in MR-HLT [202, 203] as presented in Chapter 4. Although the authors showed that differences exist, they did not quantify the degree of discrimination that can be achieved when classifying between the left and right MR-HLT. If a similar accuracy as in MI can be achieved in MR-HLT, then a special BCI channeled for rehabilitation could be constructed. Such a BCI would be relevant because processes in MR-HLT forces mental hand rehearsal by implicitly and automatically activating the sensorimotor cortex of the hand. This automatic activation is unlike in MI where conscious/explicit imagination is needed. Because the activation is automatic/unconscious in MR-HLT, the BCI could still be implemented in patients who are unable to perform MI due to for example loss of proprioception/sensation following spinal cord injury.

This study aims at obtaining the left-right classification accuracy that is possible in MR-HLT. To do this, methods used in assessing classification accuracy in MI are applied to MR-HLT. The term MR-HLT will be referred to simply as HLT for the remainder of this chapter.

5.3 Methods

5.3.1 Data collection

Subjects

Data from fifteen right handed healthy subjects who gave their informed consents were used for this study. The subjects with mean age of 24.9 ± 19 included six females and nine males.

Data recording

Data recording and experimental procedure was performed as in Chapter 4. Since the data used in the current chapter is exactly the same as that used in Chapter 4, the experimental protocol is not repeated here. The paradigm for data collection is shown in Fig. 4.1.

5.3.2 Data analysis

The recorded EEG data (sample rate 256 Hz) was visually inspected and bad epochs were removed. The logistic infomax independent component analysis (ICA) implemented in EEGLAB was used to remove artefacts from the EEG by rejecting affected components. The artefacts included ocular, electrocardiographic and electromyographic artefacts which were identified by their typical morphology, spectrum and temporal characteristics. The remaining artefact free EEG data was bandpass filtered between 8 to 30 Hz using 97-taps Hamming-window based linear-phase finite impulse response filter. The average referencing of the electrodes was performed and the data for each trial (from -3000 to 3000 ms) was split into segments of 100 samples. The resultant data was used in further analysis.

The method of common spatial pattern (CSP) (see Section 3.1.1) was used to design spatial filters applied on pair of classes to be classified. This CSP filtering minimises the variance of one of the classes while maximising that of the other. For the analysis of the CSP, two sets of electrodes were used. The first set, CSP1 consists of 47 electrode (all recording electrodes minus the EOG) and the second set, CSP2 consists of 17 electrodes around the sensorimotor areas as shown in Fig. 5.1.

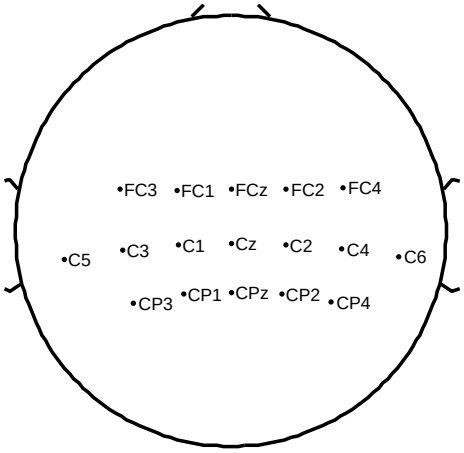

Figure 5.1: The channel locations for CSP2.

The CSP filters were computed using data segments that fall within t=500-2500 ms following the execution or picture presentation (see Fig. 4.1 for the timing of events). Data in these segments should provide the most significant discriminant features for classifying between classes of the data.

The common spatial filters were used to filter all the data segments to obtain a new time series. The variance of this new time series was computed for each of the defined time segment of 100 samples (over the whole 6 s trial). The variance in each time segment formed features for classification purposes. The size of the features depends on the number of CSP

filters[1] used. Since it was difficult to decide on a particular number of CSP filters to be used to build the features, the number of CSP filters was made a variable which ranges from two to the maximum number of CSP filters possible for CSP1 and CSP2.

For classifying the variance of the segmented data, the LDA (see Section 3.1.2) method was used. In order to find the best segment of the data from where to obtain the training set, each of the segments used to obtain the CSP filters was individually used to perform initial classification without cross-validation. The segment with the highest Cohen's kappa (see kappa below) was chosen. Then classification employing the leave-one-out cross-validation followed. This procedure is as follows. At each step of the leave-one-out procedure, the trials belonging to a current training group were identified and the segment in each trial corresponding to the one identified in the initial classification was extracted for each class of data. This extracted data was then used to compute a 2-class LDA classifier. This LDA classifier built with the data from the selected segment of the training set was used to classify all the data *samples* of the testing set as either one class or the other.

The pairs of classes of data classified are, for hand MI, left MI versus right MI; and for the HLT, left CW versus right CCW, left CW versus right CW, left CCW versus right CCW and left CCW versus right CW. In addition to these, further pairs of classes for the HLT was classified. These are classification between the left CCW vs left CW and the right CCW versus right CW. These two pairs of classification was performed in order to find if it is possible to decode the direction of the movement of the same hand in HLT.

The classification was assessed by measuring accuracy and Cohen's kappa as described in Section 3.1.4. For each number of CSP filter, the confusion matrix described in Section 3.1.4 was computed at each time point or segment along the trial. The confusion matrix was then used to compute the accuracy and the Cohen's kappa as functions of time and number of CSP filters. The segment along the trial with the best/maximum classification accuracy was obtained as the one with the highest Cohen's kappa allowing kappa to validate the accuracy. The value of the maximum classification accuracy and the time of the corresponding segment are presented as functions of number of CSP filters.

For each CSP filter, paired sample Wilcoxon signed rank test was performed to compare the maximum classification accuracy between MI and HLT. To correct for the multiple comparison due to testing at each CSP filter (recall that the number of CSP filter is a variable), the test significance level was treated with the Holm-Bonferroni correction. Furthermore, a one-way ANOVA was conducted on averages across CSP filters of the maximum classification accuracy. The time corresponding to the maximum classification accuracy was averaged across CSP filters and compared between MI and HLT using paired t-test. In all the statistical tests,

[1]Note that CSP filters are used in pairs; so m number of CSP filters stands for m first CSP filters and m last CSP filters (=$2m$), with the CSP filter matrix sorted in the descending magnitude of the corresponding eigenvalues.

n=15 and the statistical significance level was set to 0.05.

5.4 Results

The value of kappa as a function of time and the number of CSP filter (for CSP1) is first presented for the left versus right MI in Fig. 5.2 and HLT in Fig. 5.3. For the HLT, the first image represents kappa for the left CW versus right CCW, the image on the top-right represents that of the left CW versus right CW, on the bottom-left is for the left CCW versus right CCW and finally the bottom-right image is for the left CCW versus right CW.

Prior to the presentation of the execution cue in MI and hand picture presentation in HLT (t<0), the values of kappa were low indicating low performance or chance level separability of the classes. Although one of the reasons that kappa has low values in these regions was because data from the regions was not used in the CSP filter computation. However, the data in this region is not expected to show class specific differences. In the case of MI, the values of kappa indicate that the best performance occurs for 6-12 CSP filters at about 500 ms following the execution cue. In the case of the HLT, unlike in the MI condition kappa reach high values after about 1000 ms into task execution. These results supports the findings in Chapter 4 (see Figure 4.5) where differences in the MI and HLT conditions start at about 500ms and 1000ms respectively following cue presentation. The number of CSP corresponding to the high kappa values is similar to that of MI.

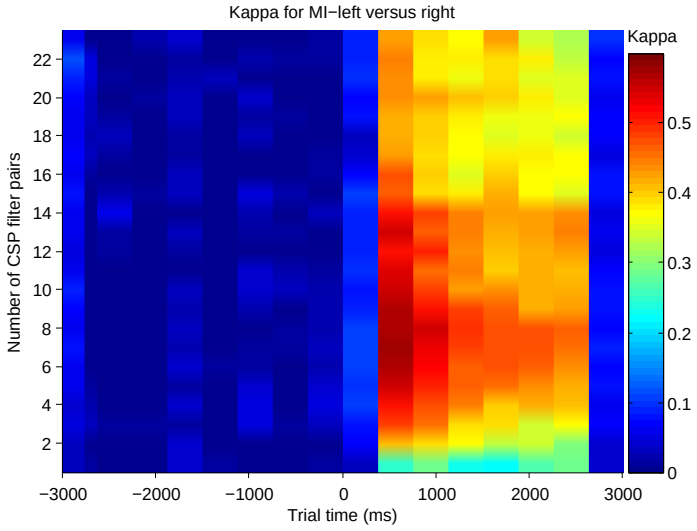

Figure 5.2: The kappa values for the left versus right MI (for CSP1). The colour-coded legend on the right given the values of kappa. Recall that the time t=0 ms is the time when the execution cue was presented.

Since kappa was used to determine the maximum classification accuracy, the accuracy should have high values at the time when kappa has high values in order for kappa to be a good

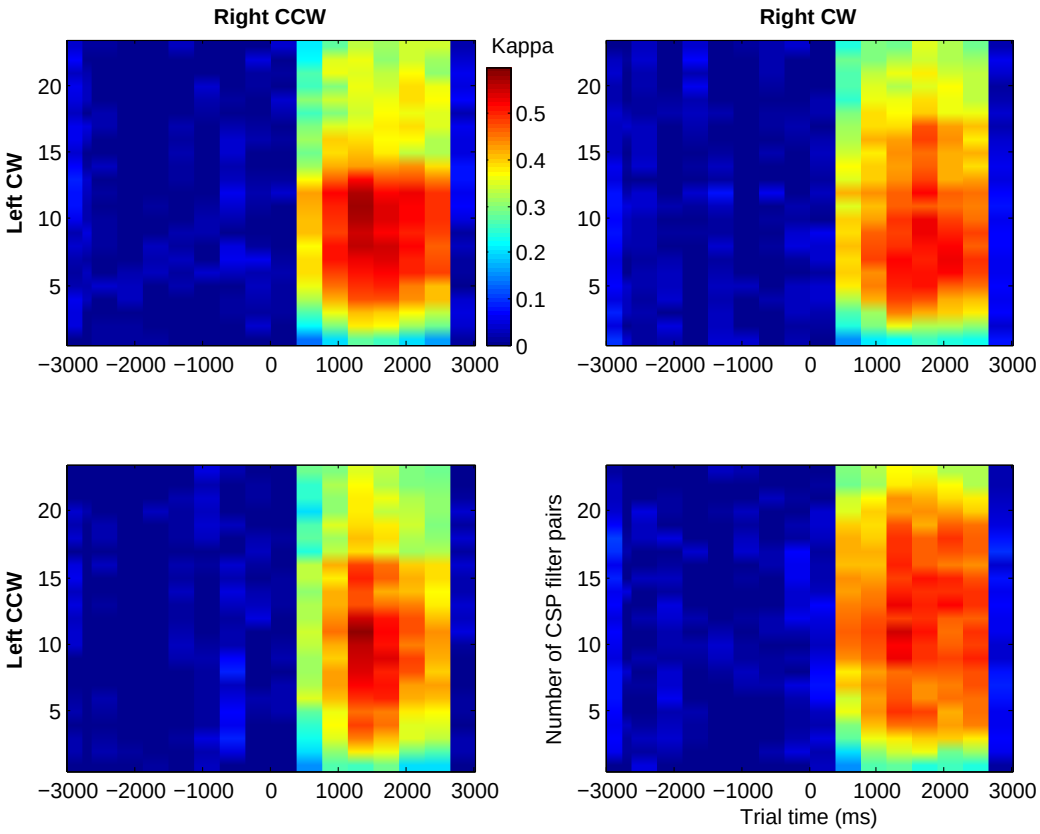

Figure 5.3: The kappa values for the HLT (for CSP1). The first image represents kappa for the left CW versus right CCW, the image on the top-right represents that of the left CW versus right CW, on the bottom-left is for the left CCW versus right CCW and finally the bottom-right image is for the left CCW versus right CW.

determinant. In order to show that this is the case the classification accuracies as a function of time into the trial and the number of CSP filters is presented for the MI and the HLT in Fig. 5.4 and 5.5 respectively. As it can be seen these figures look similar to Fig. 5.2 and 5.3 indicating that accuracies were obtained at the right times.

The maximum classification accuracy as a function of the number CSP filters is shown in Fig. 5.6 for both MI and HLT. In order to easily compare the MI with HLT, the accuracy for MI is repeatedly plotted with each of the HLT combinations.

For both MI and HLT, the maximum classification accuracy is low when the number of CSP filters used was below four. The accuracy peaked when the number of CSP filters was about between 6-12. After about 15 CSP filters classification accuracy decreased. The general relationship observed here where accuracy increases and then decreases with increasing number of CSP filters is reported in another study [204]. At each number of CSP filter, statistical comparison showed no significant difference between the maximum accuracy for the MI and each of the HLT combinations.

In order to perform further analysis, the maximum classification accuracy was averaged be-

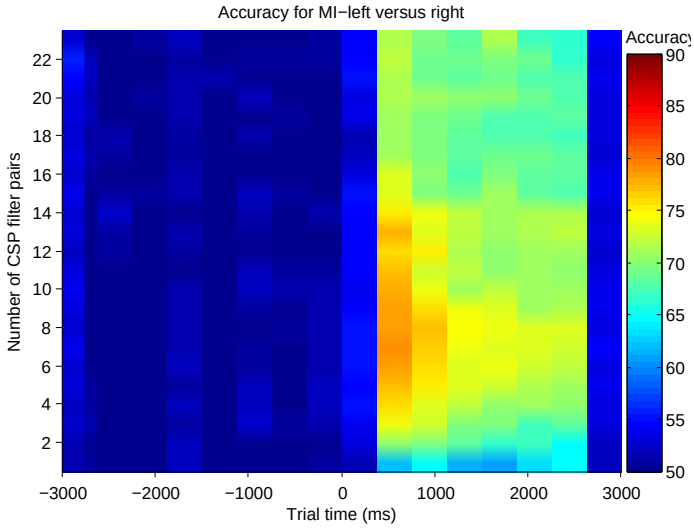

Figure 5.4: The accuracy values as a function of time and number of CSP filters (CSP1) for MI.

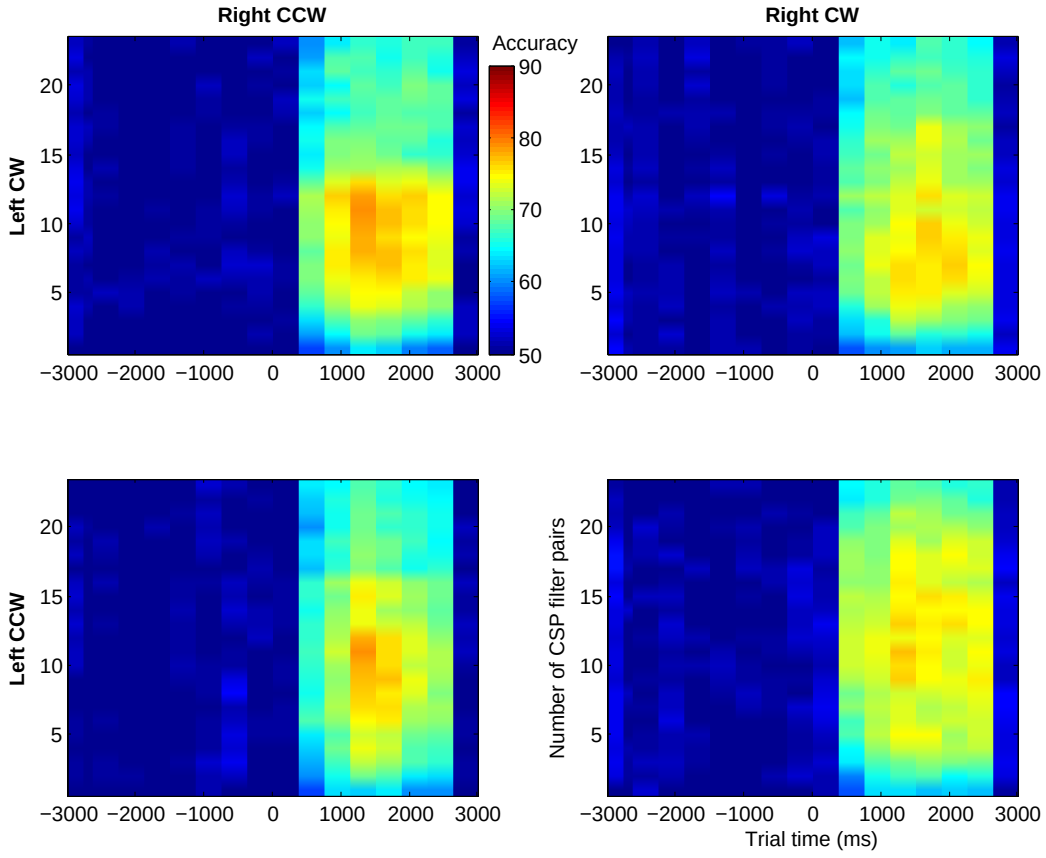

Figure 5.5: The accuracy values as a function of time and number of CSP filters (CSP1) for the HLT.

tween 6-12 CSP filters. All the classifcations between condition pairs are high between these number of CSP filters. The average is shown in Table 5.1. One-way ANOVA of the data in Table 5.1 needed a correction because the Mauchly's Test of Sphericity showed that the as-

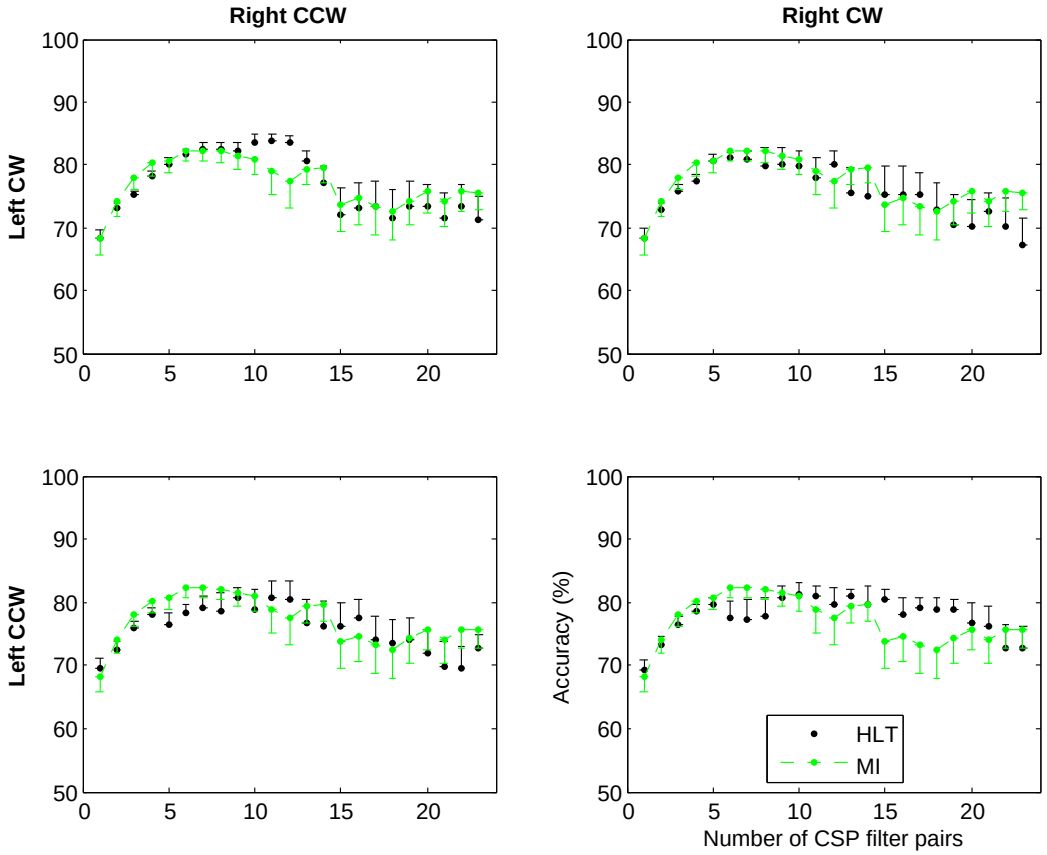

Figure 5.6: Maximum classification accuracy values as a function of the number of CSPs (CSP1) for MI and HLT.)

sumption of sphericity is violated, $\chi^2(9) = 26.717$, p = 0.002. With a Greenhouse-Geisser correction the ANOVA revealed no main effect (F(2.3,32.195)=0.729,p=0.508) suggesting no difference in classification accuracy between MI and HLT or between the pairs (as shown on Table 5.1) of HLT. These results further suggest that MI is highly similar to HLT.

The time along the trial when the maximum difference appear between the classes (i.e the time at which maximum classification was determined) is shown in Fig. 5.7 for both MI and HLT. In accordance with Figs. 5.2, 5.3, 5.4 and 5.5, Fig. 5.7 shows a time difference in when maximum classification was attained between MI and HLT. Statistical comparison performed on the average across CSP filters revealed that the difference in time is significant. the p-values showing that the time is greater for HLT is as follow: left CW versus right CCW, p=0.001; left CW versus right CW, p=0.002; left CCW versus right CCW, p=0.003; and left CCW versus right CW, p=0.001. The reason for this difference is published [202] and it is simply because classification between conditions peaks for the HLT only after a decision on the presented hand was made. This is unlike in the case of MI where no such a decision is required; imagination of movement begins soon after execution cue presentation since the correct hand is immediately identified for MI.

The classification results for MI and HLT are compared and presented once again but this

Table 5.1: The maximum classification accuracy averaged between 6-12 CSP filters (CSP1) for MI and HLT

Subj.ID	MI	HLT			
	Right vs Left	Right CCW vs Left CW	Right CW vs Left CW	Right CCW vs Left CCW	Right CW vs Left CCW
1	82	85	84	83	83
2	84	87	81	84	79
3	76	81	59	83	82
4	80	81	82	83	78
5	83	80	88	78	84
6	85	80	80	80	77
7	87	76	78	79	77
8	70	87	82	49	50
9	96	85	87	84	83
10	79	84	87	83	84
11	89	84	81	86	84
12	81	86	81	84	79
13	77	78	71	78	79
14	79	83	78	77	81
15	64	86	83	84	90

time the electrodes used for the classification are restricted to those closest to the sensorimotor cortex areas (CSP2). Following the reduction in the number of channels the classification accuracy for the HLT dropped with respect to that of MI but this was not statistically significant except for one CSP filter which does not correspond to the maximum classification accuracy as shown in Fig. 5.8. On visual inspection of Fig. 5.8, an interesting result is that the standard errors corresponding to the HLT are smaller than that of MI. This is possibly because the implicit motor imagination in mental rotation is an automatic process.

Further classifications performed (using all 48 EEG channels) in order to see if there is a difference between CW and CCW movement of the same hand is presented in Fig. 5.9 (i.e within hand classification). The trend shown by the accuracy over number of CSP filters in Fig. 5.9 is similar to that already described for between hand classification shown in Fig. 5.6. The classification accuracy reached 81% for the left CCW versus left CW and 78% for the right CCW versus right CW. This is interesting and suggests that the direction of implicitly imagined movement can be predicted.

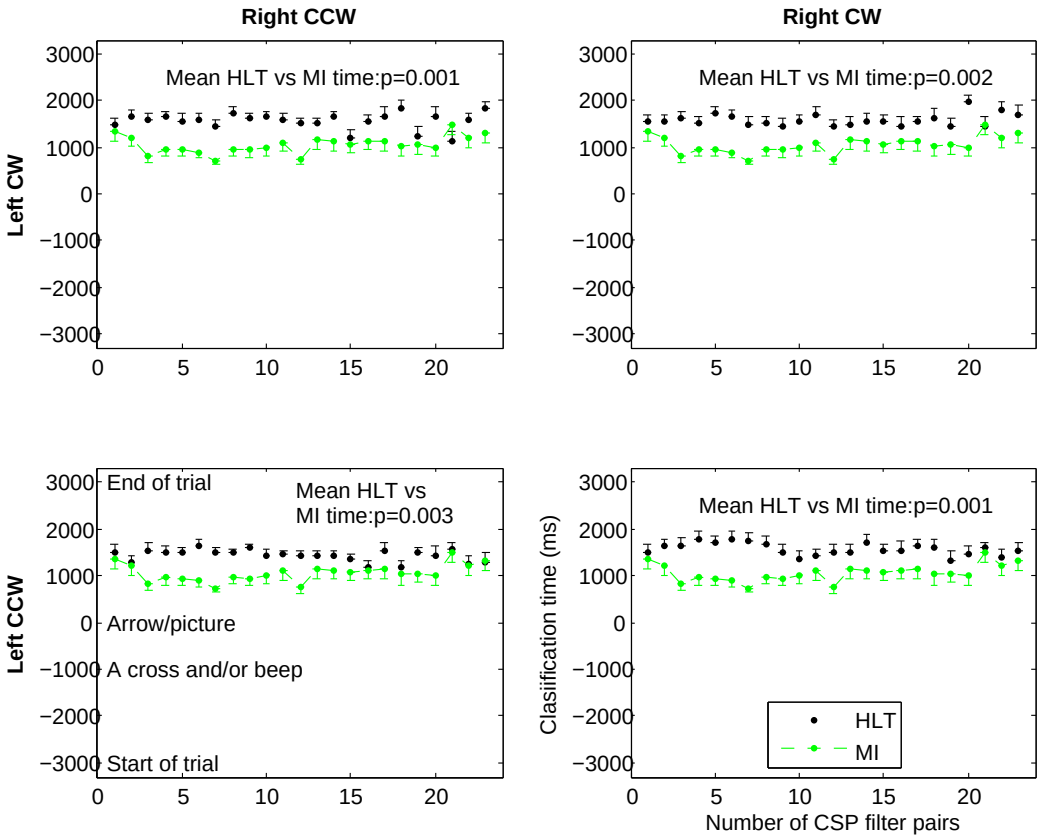

Figure 5.7: The time along the trial at which maximum classification was determined.

5.5 Discussions

This study applied methods used in assessing left-right classification accuracy for MI in HLT. By so doing it was possible to quantify the left-right classification accuracy possible in HLT. The most significant result was that the classification accuracy did not statistically differ between MI and HLT.

Several studies supports the involvement of MI in mental rotation [146, 156, 202]. A previous study also argued that since this is the case, the brain activity associated with the mental rotation of the left hand should be distinctive from that of the right hand [202]. This argument arises since the MI of the left hand is distinctive from that of the right hand. The observable difference in the brain signal between the left and the right hand MI is due mainly to the different somatotopic representation of the left and the right hand in the brain [205]. The main argument of the current study is that similar left-right classification accuracy in MI should be possible in mental rotation. This argument was supported by the results of the study. The results therefore support that MI and mental rotation involve similar phenomena. Therefore similar methods used to detect left-right differences in MI-based BCI can be implemented to construct a mental rotation-based BCI. Such a BCI might not be useful for healthy individual but will be useful as a rehabilitation tool which may be necessary in

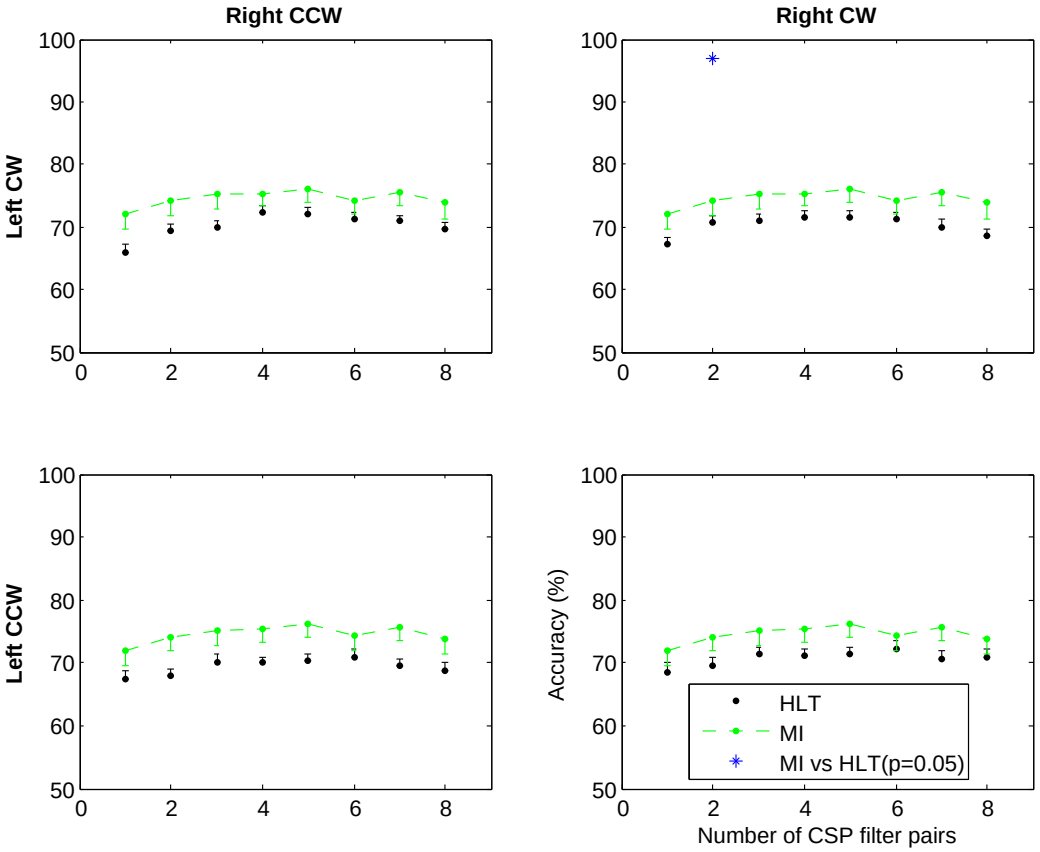

Figure 5.8: Maximum classification accuracy for MI and HLT obtained with electrodes located around the sensorimotor cortex (CSP2).

patients who are unable to perform MI due to for example loss of proprioception/sensation following spinal cord injury. During a HLT, unless told otherwise subjects tend to move their heads and hands physically in attempt to align the hand with a presented hand picture. So not only that the sensorimotor cortex can be implicitly activated, the test enforces physical movement. Furthermore a HLT is game-like and so came be competitive which allows it to support motivation in a movement rehabilitation setting.

When the left-right classification accuracy of the mental rotation was compared, there was no statistical differences among orientations. For example the accuracy for the left CW versus right CCW was not statistically different from that of the left CCW versus right CW. This result suggests that high between-hand classification accuracy can be achieved by placing the hand pictures at various orientations although it should be noted that only two orientations were studied here.

The time along the trial at which maximum classification was reached differed between MI and mental rotation. This result is expected [202]. This is because in the case of MI, subjects began imaginary movement of the hand soon after the execution cue presentation since a hand is explicitly stated. But for the mental rotation, the subjects were not sure which hand was presented at first and therefore had to go through a decision process to identify the

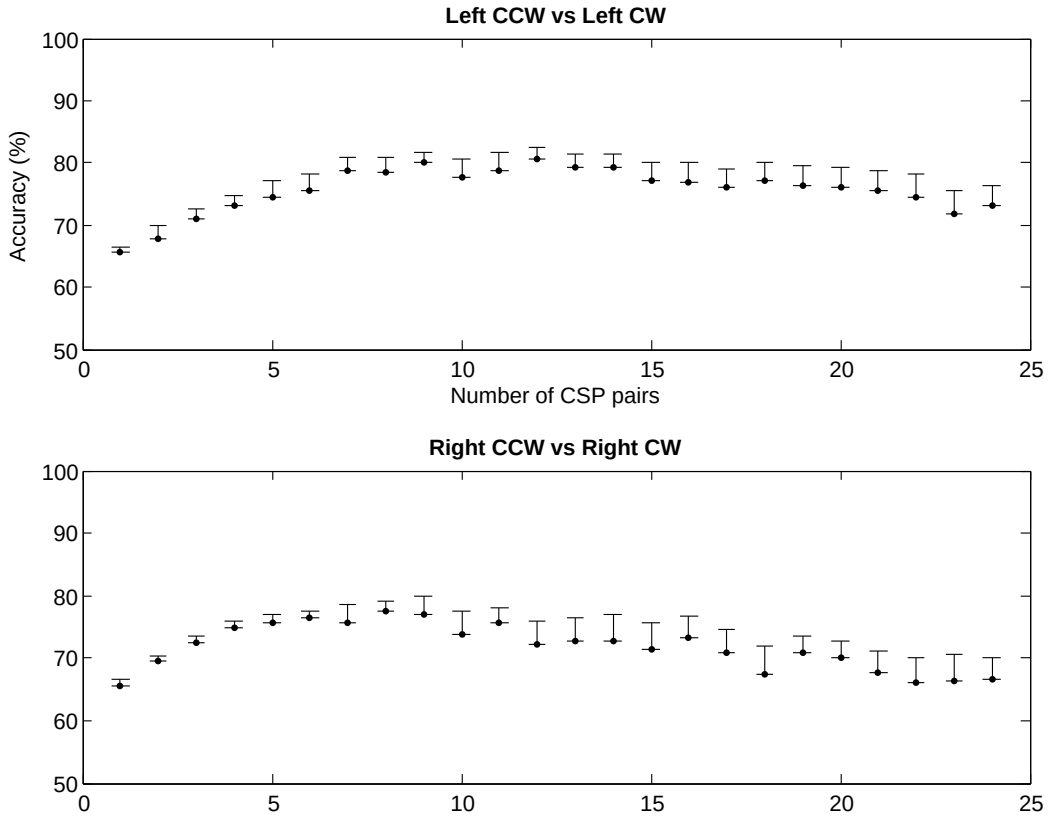

Figure 5.9: Within hand classification results showing that direction of implicitly imagined movement can be decoded.

hand. The decision process takes time and may involve individual comparison of each hand with the presented hand picture [202]. Since this might involve moving from one hand to the other, the EEG immediately following the picture presentation may not show left-right differences. A previous study reported that left-right differences appear earlier in MI than in the HLT [202]. Also the study showed that there was no left-right differences in a HLT until after about 1000 ms following hand picture presentation. That finding is replicated in the current study where the time of maximum left-right classification accuracy was higher for the HLT than for MI and that of the HLT was higher than 1000 ms.

This study further performed within-hand classification to find if there is a difference between CW and CCW implicit imaginary movement of the same hand. Decoding the direction of movement prior to physical movement execution is a research topic which can have application in rehabilitation and neuroprosthesis [206, 207, 208]. The result of the current study is interestingly suggesting that the direction of implicitly imagined movement can also be predicted with a high accuracy. This result is one of the many that suggests the neural pathways similar to that of MI and attempted movement is involved in mental rotation of body parts like the hands.

Future work includes investigation into techniques, methods and choice of number of elec-

trodes and their locations that can improve classification accuracy in mental rotation. Following this would be a mental rotation-based BCI built for rehabilitation purposes. There was not enough time in the current project to implement such a BCI.

It is important to mention that the work done in the present Chapter and Chapter 4 was supposed to be used to develop an assessment tool for patients receiving BCI-FES therapy. However, due to loss of data recorded from the patients, it was not possible to develop the assessment tool.

5.6 Conclusions

This study has shown that similar left-right classification accuracy can be achieved in MI and in mental rotation. The study also showed that it was possible to detect the direction of implicitly imagined movement. These are significant results which go further to support the involvement of MI in mental rotation and suggest that mental rotation can be employed in movement rehabilitation in a similar manner as MI.

Chapter 6

Time domain parameter as a feature of therapeutic BCI

"Scientists have become the bearers of the torch of discovery in our quest for knowledge", Stephen Hawking

6.1 Summary

Feature extraction and selection is a major issue in brain computer interfaces. In an electroencephalogram based brain computer interface, bandpower features are widely used. Time domain parameter (TDP) is another feature which has not been extensively tested in online brain computer interfaces. In this study with eight naive subjects, it is shown that the TDP is a suitable online feature for a motor imagery based therapeutic brain computer interface. ERD/ERS maps were compared between trials selected as motor imagery-active and those rejected when using TDP as a feature. The ERD/ERS maps of the trials selected with the TDP method show ERD mainly in the 8-12 Hz frequency band on the hemisphere corresponding to the hand the subjects were imagining to move. There were significantly stronger ERDs in the trials that were selected than in those rejected.

Note that this chapter has now been published (conference).

6.2 Introduction

In electroencephalogram (EEG) based brain computer interface (BCI), it is important to extract the appropriate feature suitable for classifying EEG arising from different cognitive tasks. Typically the bandpower features (see Section 3.1.1) are extracted from the EEG and

used in the online classification. These features are easy to compute and require minimum number of EEG electrodes minimizing setup time. This advantage makes the bandpower method suitable especially for therapeutic BCI where setup time must be minimized. The bandpower features are well established and researchers can target physiologically relevant frequency bands when using it as features for therapeutic BCI. However the need to select user specific narrow frequency bands can lead to the following two issues. First, the user specific bands are known to vary for the same user making it difficult, for example, to transfer BCI settings from session to session if the specific bands between the sessions changes. Second, due to the uncertainty principle, estimating narrow band spectral powers must be dubious within short time windows.

The time domain parameter (TDP, see Section 3.1.1) [113] is a feature which does not require the selection of narrow frequency bands. In addition TDP targets the most time varying EEG features. The TDP feature has been shown to outperform bandpower [113]. However to be suitable for therapeutic BCI, TDP must be able to select physiologically relevant frequencies despite the use of a wide band filtered signal. Furthermore, the current authors could only find one report [113] on the use of TDP in online BCI; more investigation is required before using TDP on patients.

The aim of this study is to assess the suitability of using TDP for online therapeutic BCI by analysing the time-frequency components of EEG classified into two classes using TDP. It is shown that despite using wide band, TDP targets the relevant frequency band. The TDP method will be used for the BCI-FES in this thesis.

6.3 Methods

Eight BCI naive subjects took part in this study after giving their informed consents. The study was approved by the university ethic committee.

To obtain an initial classifier, a subject performed the motor imagery (MI) of closing and opening of the left and the right hand (20 trials for each hand). During these tasks EEG was recorded, using the g.USBamp (GTEC, Austria) from three pairs of bipolar electrodes, namely Fc3-Cp3, Fcz-Cpz and Fc4-Cp4. The input signal from the amplifier was bandpass filtered (5^{th} order Butterworth) online between 0.5 to 30 Hz. The TDP of the filtered data was computed.

The TDP feature was computed in a similar way as that described by Vidaurre and colleagues [113]. This is shown graphically in Fig. 3.1.

The feature was used to compute initial linear discriminant analysis classifier (described in Section 3.1.2) to discriminate right hand movement MI from resting state. This initial

classifier was saved for online use. These steps were all integrated into a graphical user interface.

In the online classification, TDP feature was estimated using Simulink's difference blocks (see Fig. 3.1). Each sample of the signal in the feature space was binary classified either as an 'Active' or 'Relaxed' state using the initial classifier computed offline. The 'Active' state occurred when the subject performed opening and closing of the right hand MI while the 'Relaxed' state corresponded to a resting period. The BCI-difficulty was set to 50% determined using the Equ. 3.39. The initial classifier was updated online using the fixed rate supervised mean and covariance adaptation methods described in Section 3.1.2.

In the online BCI there were 30 trials in total divided into three runs of 10 trials each. A trial started at t= -3 s with a cross sign on the screen facing the subject. At t=0 s an execution cue in form of an arrow pointing to the right was shown on the screen and the subject was instructed to perform right hand MI until a text and sound feedback were given. The feedback included an acknowledgment text on the screen and a reward sound played to the subject when the 'Active' state was detected. If the 'Active' state was not detected after about 6.5 s following the execution cue onset, a text was shown and a sound was played to reflect the subject's failure for that trial. The subjects were also provided with a continuous feedback in form of a scale that moves counter clockwise when imagery was detected.

Of interest were the time-frequency characteristics of the trials selected as 'Active' state (Detection) and those not selected (No Detection) when using TDP as a BCI feature. Therefore ERD/ERS analysis was carried out by first separating the trials from all subject and all runs into 'Detection' and 'No Detection' groups. The resulting ERD/ERS maps were compared between the two groups of trials using statistical nonparametric method with Holm's correction for multiple comparisons at p=0.05.

6.4 Results and discussions

Table 6.1 shows the initial classifier accuracy, and the detection rate (true positive) per subject. The naive subjects improved the detection rate from run 1 and 2 to run 3 because they got better with experience. No false positive was reported because the subjects were imagining as soon as the execution cue was shown and the false positive was significantly reduced when the BCI-difficulty was set.

Fig. 6.1 shows the ERD/ERS maps of the right hand MI when 'Active' state was detected (first column) and when it was not detected (second column). The third column shows the statistical differences in frequency and time between column one and two for each channel. After the onset of the execution cue, ERD could be seen in all three channels suggesting that the subjects were performing MI. Visually inspecting the ERD/ERS shows that there are

Subjects	Initial classifier (% accuracy)	% rate (run 1 and 2)	% rate (run 3)
1	83	75	100
2	97	0	30
3	78	10	40
4	75	50	100
5	85	40	90
6	83	50	100
7	83	15	50
8	90	61	47

Table 6.1: The initial classifier accuracy and detection rate

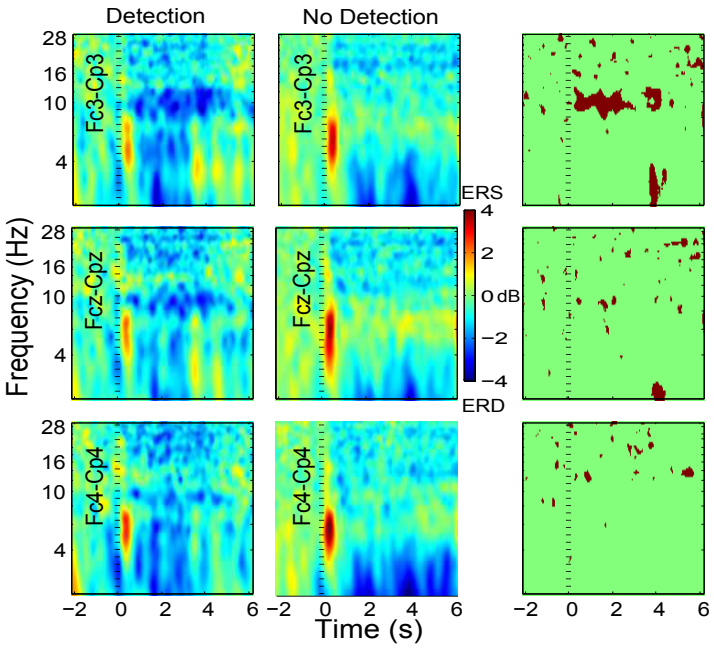

Figure 6.1: ERD/ERS maps of the right hand MI for when 'Active' state was detected (column 1) and when it was not detected (column 2). The column 3 shows the time-frequency statistical differences between column one and two (p=0.05 with Holm's correction). The execution cue was shown at t=0 ms.

more ERD for the Detection group than for No Detection group. However the differences in ERD is only statistically significant in channel location Fc3-Cp3 as shown by the shaded area on the first row, third column in Fig. 6.1. This is a desirable result because this channel is on the left hemisphere which represents the right hand which the subjects were imagining to move. The time-frequency statistical differences appears predominantly within the 8-12 Hz frequency range which is the so called μ-band known to show ERD within the motor areas during MI. There are also small differences in the 12 -30 Hz range. It is an interesting result that the physiologically relevant frequency band is more active in the Detection group despite having not selected narrow frequency bands in this range. Despite the No Detection group showing ERD in the low frequency range they were still not selected. It was possible

that the μ-band has the most time varying activities during the cognitive tasks making it likely to be selected by the TDP. The statistical difference on Fc3-Cp3 at t=4 s is due to the ERD in the low frequencies in the No Detection group.

There were many failed trials because the subjects were naive, no training was given, they had short time to perform the MI and only 20 trials were used to compute the initial classifier although it was updated online to compensate for the low number of trials. However, this is a more realistic BCI as we tend to move it out of the laboratory and also use it in our rehabilitation programmes like the BCI-FES in this thesis.

6.5 Conclusions

The TDP eliminates the requirement to select user specific frequency bands allowing for a more generalised BCI classifier which could be transfered from session to session. It is easy to compute and require minimum EEG electrodes. The current result shows that TDP feature is suitable in online therapeutic BCI because it targets the physiologically relevant frequency band.

Chapter 7

Median and ulnar nerve somatosensory evoked potential in healthy versus SCI patients

"We see in the electroencephalogram a concomitant phenomenon of the continuous nerve processes which take place in the brain, exactly as the electrocardiogram represents a concomitant phenomenon of the contractions of the individual segments of the heart, " Hans Burger

7.1 Summary

Somatosensory evoked potential following electrical stimulation of the median nerve and the ulnar nerve was recorded in 11 healthy volunteers and 11 sub-acute SCI patients. The Somatosensory evoked potential was analysed to detect the latency and the amplitude of the N20 peak that occurs around 20 ms following electrical stimulation. The properties of the N20 peak can be used to assess the integrity of the sensory pathways. A lateralisation index was computed using the N20 peak amplitude. Unlike the healthy volunteers, most of the patients had missing N20 peaks. Furthermore the lateralisation index was found to be significantly lower in patients than in healthy volunteers. The lateralisation index can be used in association with the N20 peak status and latency for assessment of neurological injuries.

7.2 Introduction

Somatosensory evoked potential (SSEP) is a response of the central nervous system to an electrical stimulation [209]. The procedure is used clinically in intraoperative monitoring

[210]. It allows for the testing of the integrity of the afferent/sensory pathways [209, 210]. The SSEP procedure may also infer motor functions on the assumption that an injury severe enough to damage the motor pathways also affects the sensory pathways [209]. Furthermore, since sensory information is an integral ingredient in motor control, a damage to the sensory pathway should affect the motor system [10]. For these reasons, SSEP may give indirect assessment of the integrity of the motor system functions [211].

Although SSEP is used in clinical settings like in intraoperative monitoring [211], its use is scarce in other areas like in SCI assessment [212]. This is despite several research studies reporting potential benefits of using SSEP as an assessment tool in SCI [212, 213, 214, 215, 216, 217]. The median and the ulnar SSEP can be used for the assessment of the level of cervical injury and for the prediction of residual hand function that can help guide a rehabilitation programme [212, 218]. For example SCI patients who have lost both the median and the ulnar nerve SSEP will mostly not regain hand functions. In the other case, patients who show only pathological SSEP are likely to recover passive hand functions. A patient who has normal median and ulnar nerve SSEP is likely able to recover passive hand functions [212, 218].

The first purpose of this study is to define a more suitable SSEP analysis method in SCI. The second purpose is to provide further evidence on the usefulness of SSEP in assessing spinal injuries at early stages by comparing data from patients with that from healthy subjects. The third purpose is to provide information on a lateralisation index that can be used in association and for validation of traditional SSEP peaks and amplitudes. These will guide the use of SSEP as an assessment tool for people receiving BCI-FES therapy in this thesis.

7.3 Methods

7.3.1 Data collection

Subjects

Somatosensory evoked potential data from 11 sub-acute tetraplegic male patients were used. The spinal injuries were caused by trauma. The patients gave their informed consents. Also 11 healthy subjects who gave their informed consents were recruited. Table 7.1 shows the informations of all subjects.

SSEP data recording

Two electrodes for EEG recording were attached at positions Cp3 and Cp4. Two nerves, the median and the ulnar nerves, were stimulated at the wrist in separate runs. Using the Dig-

Table 7.1: The information of the sub-acute patients and the healthy subjects who took part in the study. The patients were recruited seven to eight weeks following injury. The ASIA impairment scale was obtained on admission to the hospital.

Patient					Healthy		
ID	Injury level	ASIA	Age	Gender	ID	Age	Gender
p1	C6	C	70	m	h1	28	m
p2	C4	B	25	m	h2	45	m
p3	C6	B	32	m	h3	27	f
p4	C5	C	36	m	h4	22	f
p5	C5	C	20	m	h5	31	m
p6	C6	C	74	m	h6	21	f
p7	C5	B	51	m	h7	22	m
p8	C6/7	C	53	m	h8	36	m
p9	C5/6	C	61	m	h9	29	f
p10	C4	B	51	m	h10	30	m
p11	C6	C	64	m	h11	25	f

Note: m, male; f, female.

itimer stimulator (Model DS7, Digitimer LTD., England), electrical stimulus was delivered to individually stimulate the nerves. The stimulation intensity was increased until a small twitch could be seen at the thumb for the median nerve and at the little finger (or the thumb at the carpometacarpal joint) for the ulnar nerve. As the stimulation were delivered, the EEG signal from each channel was averaged and the resultant wave form was displayed in real-time at 3 Hz from t= 8.33 to 50 ms following stimulus onset at t=0 ms. After about 250 stimuli, the wave form was collected and stored for further analysis. The EEG was recorded with the g.USBAmp at the sample rate of 4800 Hz with a bandpass filter between 2-2000 Hz and a notch filter at 50 Hz. The electrical stimulus was delivered at 3 Hz. By inspection, if the displayed SSEP looked noisy the recording was repeated two to three times for validation purposes.

Manual muscle testing

In order to check if an SSEP property correlates with another assessment method in SCI, 'manual muscle testing' (MMT) [134] data of the patients were used. An occupational therapist assessed the upper limb functions of the patients using the MMT grading system. This grading system is described in Section 3.3.1. The MMT data used here were those the therapist performed in the initial assessment session of the study presented in Chapter 8. For the present study, the muscles whose MMT scores were considered were those of the forearm and hand; these include EDC, extensor digitorum communis; ECR, extensor carpi radialis;

EPL, extensor pollicis longus; FCR, flexor carpi radialis; FDP, flexor digitorum profundus and the Intrinsic muscles.

7.3.2 Data analysis

7.3.3 Peak and latency of N20 potential

The recorded SSEP was visually inspected for the presence of N20 peak. When present, the latency of the peak was recorded. The latency was taken as the minimum of the N20 wave. When more than one recordings were made, the peak was said to be present if it appear approximately consistently in all the recordings. Also the recording with the minimum latency was chosen.

7.3.4 Lateralisation index

Because in some cases the N20 peak were absent for the patients, there was a need to quantify the potential for the peak to reappear. It is also useful to have a measure that can be used to ascertain the validity of the recorded SSEP especially when it looked abnormal. It has been noted that the ratio of the ipsilateral and the contralateral SSEP signal can be used for its validity [219]. For this reason, a lateralisation index [220] was computed using the Cp4 and Cp3 EEG data. Following the method of assessing the lateralisation of brain functions Equ. 7.1 (see LI in Section 3.3.2) was used where a_l is the peak to peak amplitude of the N20 in the left hemisphere and a_r is the peak to peak amplitude in the right hemisphere.

$$SSEPLI = \frac{a_l - a_r}{a_l + a_r} \tag{7.1}$$

The traditional method of determining the peak to peak amplitude was not used here instead the peak to peak amplitude was estimated. The peak to peak amplitude of the N20 potential was estimated by calculating the range (max-min) of the SSEP potential at each electrode position. The rationale for using estimated amplitude is that it may be subjective to choose the positions from where to obtain the peak to peak amplitude. Furthermore in some patients the N20 peak might be missing making it impossible to measure a peak to peak amplitude. A good example of when the peak is considered missing is shown in Figure 7.2 where no prominent peak is observed on channel C3 (left hemisphere) with the right median nerve stimulated. The time window considered in the range calculation was 15-30 ms post-stimulation and it is shown in Fig. 7.1 and 7.2. Since the N20 peak occurs about 20 ms as shown in Fig. 7.1, this time window is adequate for estimating the peak to peak amplitude by computing the range of the signal in the window. The SSEP laterality index,

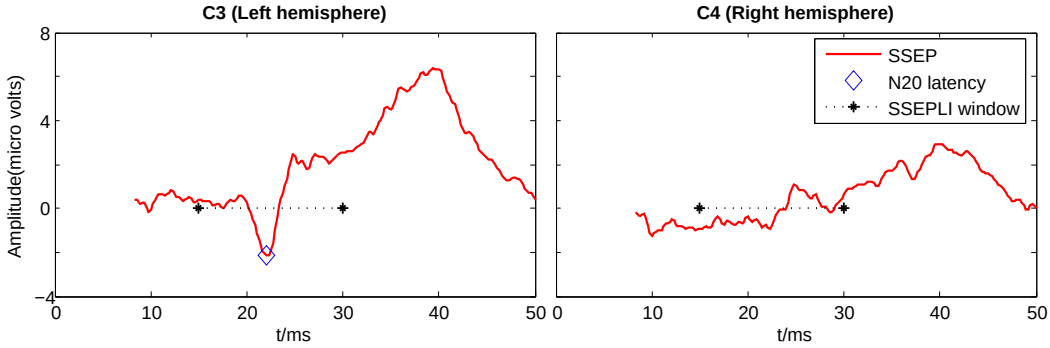

Figure 7.1: The right median nerve SSEP for subject h2 in this study showing the N20 peak and the time window (SSEPLI window) used to estimate the peak to peak amplitude of the N20 wave. Stimulation was applied at t=0 ms. The SSEP potentials that fall within the SSEPLI time windows are the only considered potentials in the amplitude estimation.

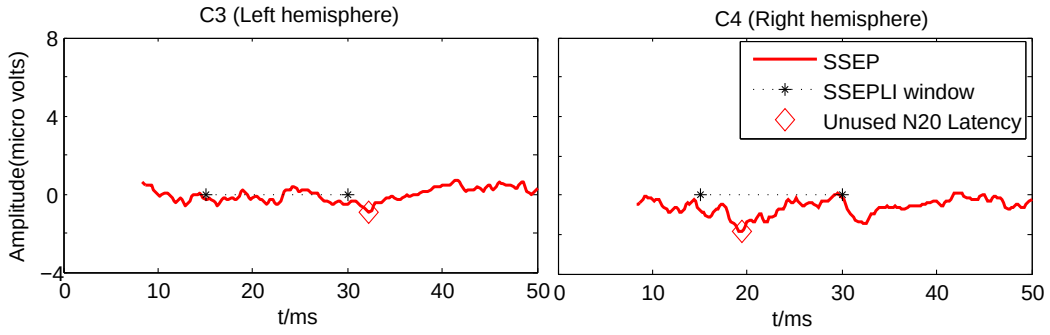

Figure 7.2: The right median nerve SSEP for subject p2 in this study showing the N20 peak and the time window (SSEPLI window) used to estimate the peak to peak amplitude of the N20 wave. Stimulation was applied at t=0 ms. The SSEP potentials that fall within the SSEPLI time windows are the only considered potentials in the amplitude estimation. The SSEP peak was considered to be absent in this case and the peaks (Unused SSEP latency) were those that would be detected as the minimum potentials.

SSEPLI can be computed using equation 7.1, where a_l and a_r are the estimated peak to peak amplitude of N20 for the left (Cp3) and for the right (Cp4) electrode respectively. Following the definition for LI in Section 3.3.2, a negative value of $SSEPLI < -0.2$ is interpreted as right hemispheric amplitude lateralisation while $SSEPLI > 0.2$ is interpreted as a left hemispheric amplitude lateralisation. A value of $|SSEPLI| \leq 0.2$ is interpreted as bilateral amplitude.

Manual muscle testing

In order to allow statistical operation on continuous data, the MMT scores were transformed. The transformation was to eliminate the negative and the positive assignments and replace them with -0.25 and +0.25 respectively. For example, if an MMT score is G = 3-, after the transformation it becomes G = 2.75. In the other case, G = 3+, after the transformation

becomes G=3.25. The results of this transformation is a continuous data of MMT scores on which further analysis was performed.

7.4 Results and discussions

Plots of the SSEPLI is shown on Fig. 7.3 for all nerves and hands. Table 7.2 shows right median nerve N20 peak status, latency and the SSEPLI for both the patient and the healthy subjects. Similar tables are presented for the left median nerve in Table 7.3, the right ulnar nerve in Table 7.4 and the left ulnar in Table 7.5.

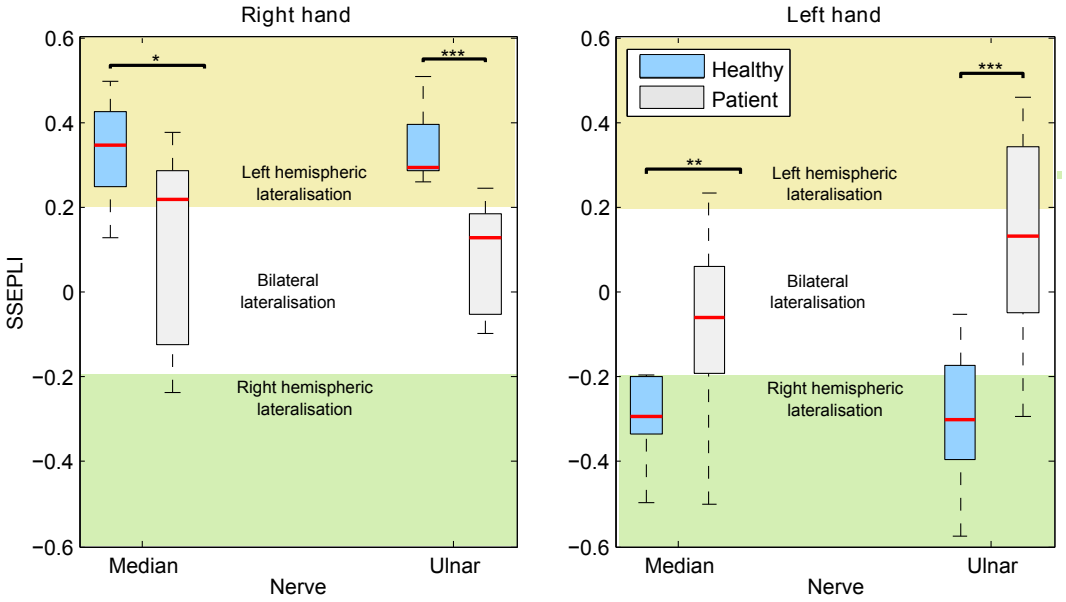

Figure 7.3: The SSEPLI for all nerves, hands and subjects.The red line in the box plots are the medians, the box whiskers are the extreme values that are not considered to be outliers while the bottom and the top edges of the box are the 25^{th} and the 75^{th} percentile respectively. The area of the plots are sub-divided with color coding to show the values that are within define SSEPLI lateralisation values. The statistical significance between the healthy and the patients are shown with asterisk where, *, $p < 0.05$; **, $p < 0.02$; ***, $p < 0.01$.

The N20 peaks were present for the healthy subjects for all nerves. In the case of the patients they were only present in four out of eleven subjects for the right median nerve, one out of nine for the right ulnar nerve, four out of eleven for the left median nerve and one out of eight for the left ulnar nerve.

The average latency of the N20 peak for the patients were higher than that of the healthy subjects. For the right median nerve, the average latency was 19.72 ms (n=11) while it was 24.58 ms (n=4) for the patients. The average latency for the right ulnar nerve was 20.38 (n=11) for the healthy subjects but for the patient only one subject had the N20 peak present at 28.54 ms. For the left median nerve the average latency of the healthy subjects was 19.49

Table 7.2: The status, latency and SSEPLI of the **right median nerve** for all the subjects

Healthy				Patient			
Subj.ID	Status	Latency	SSEPLI	Subj.ID	Status	Latency	SSEPLI
h1	Present	20.21	0.495	p1	Present	27.71	0.314
h2	Present	22.29	0.456	p2	Absent	-	-0.170
h3	Present	18.54	0.409	p3	Absent	-	-0.125
h4	Present	18.75	0.383	p4	Present	23.33	0.218
h5	Present	20.42	0.329	p5	Present	22.71	0.275
h6	Present	18.54	0.129	p6	Absent	-	0.378
h7	Present	20.42	0.313	p7	Absent	-	0.199
h8	Present	19.38	0.228	p8	Absent	-	-0.237
h9	Present	18.33	0.345	p9	Absent	-	-0.118
h10	Present	21.04	0.215	p10	Absent	-	0.291
h11	Present	18.96	0.430	p11	Present	24.58	0.251

ms (n=11) while for the patients it was 24.22 (n=4). In the case of the left ulnar nerve the average latency was 20.44 ms (n=11) for the healthy subjects but for the patient only one subject had the N20 peak present at 23.33 ms. These results of delayed N20 peaks in the SCI patients compared with the healthy subjects are expected and indicate impairment in the somatosensory and possibly motor functions for the patients [213].

Table 7.3: The status, latency and SSEPLI of the **left median nerve** for all the subjects

Healthy				Patient			
Subj.ID	Status	Latency	SSEPLI	Subj.ID	Status	Latency	SSEPLI
h1	Present	20.21	-0.194	p1	Present	28.75	-0.141
h2	Present	21.69	-0.488	p2	Absent	-	0.053
h3	Present	18.13	-0.496	p3	Present	22.50	-0.188
h4	Present	19.17	-0.198	p4	Absent	-	0.202
h5	Present	20.00	-0.335	p5	Present	21.88	-0.195
h6	Present	17.71	-0.297	p6	Absent	-	-0.061
h7	Present	20.21	-0.282	p7	Absent	-	-0.057
h8	Present	19.79	-0.205	p8	Absent	-	-0.192
h9	Present	18.13	-0.292	p9	Absent	-	0.062
h10	Present	20.83	-0.197	p10	Absent	-	0.234
h11	Present	18.56	-0.330	p11	Present	23.75	-0.502

Fig. 7.3 clearly show the difference between the SSEPLI values for the patient and the healthy subjects. Most of the healthy subjects' SSEPLI values were correctly lateralised. This means that the right hand SSEPLI were lateralised to the left hemisphere (+ve SSEPLI) while that of the left hand were lateralised to the right hemisphere (-ve SSEPLI) as shown in Fig. 7.3. This was not the case for the patients whose SSEPLI were mostly bilateral. Statistical analysis shows that for the right median nerve, the SSEPLI for the healthy subjects were

more lateralised to the left hemisphere than that of the patients (p=0.0126). Similarly for the right hand ulnar nerve the healthy subjects show better lateralisation to the left hemisphere ($p<0.001$). For the left hand median nerve, the healthy subjects also show better lateralisation towards the right hemisphere (p=0.0016). Similarly for the left hand ulnar nerve, the healthy subject show better lateralisation to the right hemisphere ($p<0.001$).

Table 7.4: The status, latency and SSEPLI of the **right ulnar nerve** for all the subjects

Healthy				Patient			
Subj.ID	Status	Latency	SSEPLI	Subj.ID	Status	Latency	SSEPLI
h1	Present	21.25	0.412	p1	Present	28.54	0.246
h2	Present	23.13	0.305	p2	Absent	-	-0.047
h3	Present	18.96	0.293	p3	Absent	-	0.094
h4	Present	19.17	0.274	p4	Absent	-	-0.073
h5	Present	21.25	0.428	p5	Absent	-	0.187
h6	Present	18.54	0.293	p6	Absent	-	0.182
h7	Present	20.83	0.340	p7	Absent	-	0.128
h8	Present	20.63	0.261	p8	Absent	-	-0.097
h9	Present	18.75	0.508	p9	Absent	-	0.152
h10	Present	21.67	0.283	p10	-	-	-
h11	Present	20.00	0.293	p11	-	-	-

Note: Data for subjects p10 and p11 were not available.

The absence of the N20 peaks as well as the SSEPLI values obtained for the patients suggest that these subjects have impaired sensory and possibly motor functions [209, 210].

In most of the patients the N20 peaks were missing. Without the SSEPLI, the outcome of the SSEP test for the patients would simply be, 'missing peak' when the N20 peak cannot be clearly identified. An alternative to using the SSEPLI is to use the peak to peak amplitude of the N20 potential. The issue with using the amplitude is that it is only available when the N20 peak is available because it is not possible to certainly measure the peak to peak amplitude of a missing or distorted peak. In patients the N20 peak might be distorted making it difficult to clearly identify the peak to peak amplitude. If the peak cannot be clearly identified it might be recorded as 'missing' even though it might be present but distorted by noise. But with SSEPLI, it is possible to tell the potential for the N20 peak to exist even in the presence of the distortion. This is because if the SSEPLI values show correct lateralisation with a high magnitude, there exist the potential for the peak to be present. Even when the peak has been identified, SSEPLI value can be used for its validity [219, 220].

Research studies have suggested that SSEP can be used for the prediction of functions in SCI patients [212, 213]. It can be used to test for the integrity of the somatosensory functions but can indirectly infer motor functions [209]. It is an objective measure and has similar sensitivity as ASIA scores of the sensory functions [212]. With SSEPLI, an SSEP test becomes

Table 7.5: The status, latency and SSEPLI of the **left ulnar nerve** for all the subjects

Healthy				Patient			
Subj.ID	Status	Latency	SSEPLI	Subj.ID	Status	Latency	SSEPLI
h1	Present	21.25	-0.276	p1	Absent	-	0.069
h2	Present	23.96	-0.465	p2	Absent	-	-0.292
h3	Present	20.00	-0.282	p3	Absent	-	0.192
h4	Present	19.58	-0.073	p4	Absent	-	0.460
h5	Present	21.46	-0.407	p5	Present	23.33	-0.035
h6	Present	17.29	-0.300	p6	Absent	-	0.273
h7	Present	20.83	-0.365	p7	-	-	-
h8	Present	20.42	-0.051	p8	Absent	-	0.413
h9	Present	18.96	-0.574	p9	Absent	-	-0.061
h10	Present	21.04	-0.139	p10	-	-	-
h11	Present	20 .00	-0.344	p11	-	-	-

Note: Data for subjects p7, p10 and p11 were not available.

more than a test for the existence of a peak and the peak's latency; it becomes also a test for lateralisation of amplitude. Since the SSEPLI differ significantly between the patients and the healthy subjects, SSEPLI is suggested as an additional diagnostic criterion to the traditional SSEP criteria.

Instead of measuring the peak to peak amplitude as in the traditional SSEP tests, the amplitude estimation described in the method section can be used to make sure that even in the absence of the peak, the SSEP can still be quantified by computing SSEPLI. The amplitude estimation method avoided the potential problem of obtaining the peak to peak amplitude in the ipsilateral hemisphere which often has low amplitude and unclear N20 peak. The magnitude of the SSEPLI gives both normalised relative hemispheric amplitude and degree of lateralisation while the sign gives the hemispheric lateralisation. If the magnitude of the SSEPLI is small (< 0.2 as defined here) and/or incorrectly lateralised, a recorded N20 peak can be said to be pathological or missing.

There was not enough data to compare between ASIA C and ASIA B patients (see subject information). However, for completeness, a t-test was performed on concatenated data to compare the two group of patients. For the concatenation, the SSPLI data for all nerves and hands were combined for all ASIA C patients and also for all ASIA B patients. This gave n=26 and n=13 for ASIA C and ASIA B, respectively. The sign of the data belonging to the left nerves were again inverted. The mean and standard deviation for ASIA C patients were 0.0533 and 0.2410, and for ASIA B were 0.0329 and 0.1827. Although the ASIA C patients had higher mean SSEPLI, the t-test showed that there was no difference between the ASIA C and ASIA B patients (p=0.79). This result should be treated with care since only small data was available for the ASIA B patients and also because of the manner in which data was

concatenated.

Table 7.6: The MMT results of the patients for right and the left hand.

Subj.ID	EDC	ECR	EPL	FCR	FDP	Intrinsics	TOTAL
			Right hand				
p1	3.75	3.75	2.75	3	3.75	3	20
p2	1	1.25	0	0	0	0	2.25
p3	4	4	0	0	0	0	8
p4	1	0	0	0	0	0	1
p5	0	0	0	0	0	0	0
p6	3	0	0	0	0	0	3
p7	0.75	0.75	0	0.75	0	0	2.25
p8	1	0	1	1.25	1.75	1	6
p9	0	0	0	0	0	0	0
p10	0	0	0	0	0	0	0
p11	3	3	1.25	2	4	3	16.25
			Left hand				
p1	4	4	3.25	4	4	3	22.25
p2	2.25	1	0	0	0	0	3.25
p3	4	4	0	0	0	0	8
p4	0	0	0	0	0	0	0
p5	0	0	0	0	0	0	0
p6	2.75	2.75	0	0	0	0	5.5
p7	0	0	0	0	0	0	0
p8	3.25	2.75	3	1.25	1.25	1.25	12.75
p9	0	0	0	0	0	0	0
p10	0	0	0	0	0	0	0
p11	3	0	1	3	3	1.25	11.25

Note: EDC, extensor digitorum communis; ECR, extensor carpi radialis; EPL, extensor pollicis longus; FCR, flexor carpi radialis; FDP, flexor digitorum profundus and the Intrinsic muscles.

The MMT scores are shown on Table 7.6. Correlation analysis was performed to check if MMT correlates with absolute value of SSEPLI. Given inadequate sample size, data was concatenated for the left and right hand to get n=22 for the MMT versus median nerve and n=17 for the MMT versus ulnar nerve. The MMT values were summed across muscles. The results were weak positive correlation between the MMT and SSEPLI values; 0.22 for the MMT versus median nerve and 0.10 for the MMT versus ulnar nerve. In the context of the current experiment and the available data, this correlation result might be explained as follows. Although it is a sensory test, SSEP properties can infer motor function as suggested earlier. Note that this does not imply that the presence of SSEPs means the presence of motor functions. Indeed, SCI patients might have sensations but no movement during the early acute/sub-acute stage. However the presence of the sensation suggests a possibility of

motor recovery in such patients. Therefore, a sensory test like the SSEP performed during the early acute/sub-acute stage might not correlate with motor functions but gives the likelihood of motor recovery. However, it is still an interesting result that some positive correlation exist between MMT which is a subjective measure and SSEPLI which is an objective measure. The result should be treated with caution for the following reasons. (1) The muscles whose MMT scores were used were not all innervated by the nerves whose SSEPLI values were considered. It might be more appropriate to consider each muscle or group of muscles with only the nerve/nerves supplying them. (2) There were inadequate sample size. (3) It might also be more appropriate to consider each hand at a time instead of the concatenation.

7.5 Conclusions

In this study a suitable method was detailed for the analysis of SSEP in SCI patients. It was shown that SSEP criteria were different between healthy and SCI patients. An SSEP criterion, SSEPLI was shown to be a valuable tool to accompany conventional SSEP criteria. These will guide the use of SSEP as an assessment tool for people receiving BCI-FES therapy in this thesis.

Chapter 8

Functional and neurological outcome in sub-acute tetraplegic patients following BCI-FES hand therapy

Think to move: thought control of movement is not really anymore a fairy tale!

8.1 Summary

This chapter presents a study testing BCI-FES on people with SCI. The test was performed in twelve sub-acute tetraplegic patients; seven of them received BCI-FES therapy while five of them received FES therapy alone for twenty sessions. Neurological assessments, which included AM and SSEP; and functional assessments, which included range of movement and manual muscle testing were used to assess the patients before and after the therapies. The neurological assessments but not the functional assessments showed that BCI-FES may induce desirable neurological changes in sub-acute tetraplegic patients better than FES alone can in a similar amount of time.

8.2 Introduction

Functional electrical stimulation (FES) and Brain computer interface (BCI) are promising technologies with application in neurorehabilitation after neurological injuries. The FES can be used to activate paralysed muscles in individuals with stroke and spinal cord injuries. In these patients FES is known to enhance functional rehabilitation after a period of usage [45, 221, 222]. The rather newer technology, BCI is gradually becoming a tool for functional rehabilitation research, largely used with stroke patients. Such a BCI may be based on motor

imagery (MI) [102, 111] or attempted movement (AM) [105, 109]. In the state of the art, FES and BCI are coupled for function rehabilitation. The technology is referred to as BCI-FES and was firstly used in spinal cord injury (SCI) for movement augmentation [67].

Attempted movement based BCI for BCI-FES enables the simultaneous activation of the motor cortices and the muscles they control [67]. When using the system a subject activates the motor cortex using AM. The BCI system detects the motor cortex activation and activates the FES attached to the muscles actuating the body part the subject is attempting to move. In this way the afferent and the efferent pathways of the nervous system are simultaneously activated. This simultaneous activation encourages Hebbian type learning [61] which could be beneficial in functional rehabilitation after SCI.

The use of FES has gone beyond the research stages and is already in use in several SCI rehabilitation units. It is a major part of the rehabilitation programme at the Queen Elizabeth national spinal injury unit, Southern General Hospital Glasgow where this current study is set [99]. However the coupling of FES with BCI is yet to be thoroughly tested which means that there is currently not enough clinical evidence to support the use of BCI-FES for rehabilitation.

This study aims at providing an assessment of the potential benefit of using BCI-FES in the neurorehabilitation following SCI. Neurological and functional measures were used to assess twelve sub-acute tetraplegic patients who each were either part of a group who got BCI-FES therapy or a group who got FES therapy without the BCI.

8.3 Methods

The experiment was conducted in three stages. (1) In the initial data collection/assessment stage, manual muscle testing (MMT), SSEP, range of movement (ROM) and EEG during AM were used to assess the subjects functionally and neurologically. (2) The subjects received either BCI-FES for a treatment group or FES therapy for a control group for twenty days, Monday-Friday. This is therapy stage. (3) In the final data collection/assessment stage which follows immediately after the therapy stage, the initial assessment was repeated.

8.3.1 Data collection

Subjects

Twelve sub-acute tetraplegic male patients who gave their informed consents were recruited for this study. The patients suffered from traumatic SCI. Seven of the subject were in a treatment group (or BCI-FES group) while five were controls (or FES group or FES-only

group). Attempt was made to match the patients in the two groups according to age, level and severity of injury. Patients were first allocated to the BCI-FES group; a patient was allocated to the FES-only group when the patient matches another patients in the BCI-FES group. It was difficult to carry out the match due to insufficient number of patients. Table 8.1 shows the informations of the patients.

All the patients who took part in this study were also receiving regular physiotherapy at the hospital. The regular therapy involved several activities which were discussed in Section 1.9.

Table 8.1: The information of the sub-acute tetraplegic subjects who took part in the study. All subjects are male. They were recruited between seven to eight weeks following injury. The ASIA impairment scale was obtained on admission to the hospital.

ID	IL	ASIA	Age	Group	Information
ps1	C6	C	70	BCI-FES	Patient was unwell during most of the therapy and so over half of the therapy was done while the patient was in bed.
ps2	C4	B	25	BCI-FES	Therapy was not completed on time because patient was frequently ill. Also the final assessment was not performed on time. Patient's hands was swollen and required up to 50 mA of FES current to produce slight movements. Part of the therapy was done while the patient was in bed.
ps3	C6	B	32	BCI-FES	Patient EEG varied with no ERD making the BCI control impossible sometimes.
ps4	C5	C	36	FES	MMT was done 26 days late on 10/Dec/2013 instead of on 14/Nov/2013.
ps5	C5	C	20	BCI-FES	Completed the therapy as it was designed.
ps6	C6	C	74	BCI-FES	Patient was often unwell leading to postponements of therapy sessions and some therapy was done while patient was in bed.
ps7	C5	B	51	BCI-FES	Patient could not attend therapy sometimes and was, in the first half treated only on the left hand due to fracture on the right. Part of the therapy was done while the patient was in bed due to illness.
ps8	C6/7	C	53	BCI-FES	Completed the therapy as it was designed.
ps9	C5/6	C	61	FES	Patient was not available for the second EEG, SSEP and ROM assessment because the patient left the hospital. All therapy was done while patient was in bed.
ps10	C6	C	78	FES	Did not have SSEP and ROM. Subject had a good recovery and was able to start walking with crutches while in the study. He had central cord syndrome. Some therapy was delivered while patient was in bed.
ps11	C4	B	51	FES	Completed the therapy on time but due to an operation the final EEG and SSEP were obtained a month late. Some therapy was done while patient was in bed.
ps12	C6	C	64	FES	Completed the therapy as it was designed.

Notes: IL, Injury Level.

Manual muscle testing

At the start and at the end of the study, an occupational therapist assessed the upper limb functions of the patients using the manual muscle testing (MMT) [134] grading system (initial and final assessment). This grading system is described in Section 3.3.1.

Somatosensory evoked potential

Somatosensory evoked potential was recorded as part of the initial and final assessments. The recording of SSEP is already described in Section 7.3.1.

Range of movement

The Zebris system (Zebris Medical GmbH, Germany) was used to measure the ROM of the wrist in the initial and final assessments. The measurement procedure is based on the travel time measurement of ultrasonic pulses. The pulses are emitted by three stationary transmitters and are recorded by small *marker*s which are ultrasound microphones. The Zebris system markers were placed on bony landmarks on the subject's hand at the radius (marker 1), carpometacarpal joint (marker 2) and the carpometacarpal bone (of the index finger or the thumb, marker 3) as shown on Fig. 8.1. The subjects who did not have full range of wrist movement of a hand were asked to perform extension and flexion of the wrist while the 3-dimensional position signal from each of the markers were recorded and stored for further analysis.

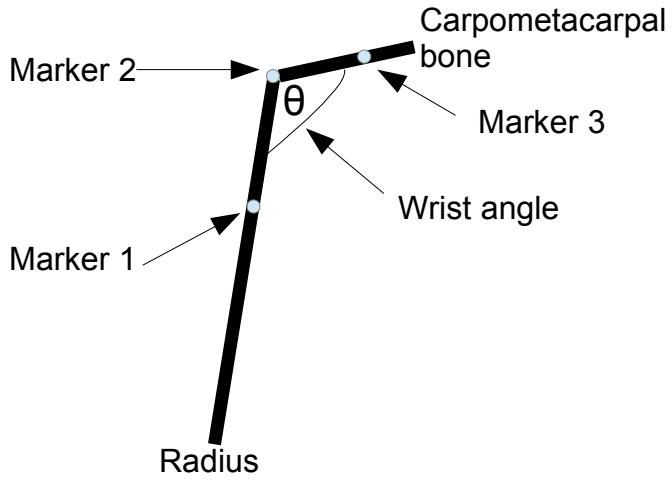

Figure 8.1: Zebris system marker placements on the hand.

Attempted movement

The initial and final assessment also involved measurement of multichannel EEG of the patients with 48 channels while they were performing AM of the left and right hand.

A cue-based paradigm implemented with rtsBCI [223] was used. A trial lasted for 6000 ms. At the beginning of a trial (t=-3000 ms), the user was presented with a blank screen. A warning cue (a cross) appeared on the screen at t = -1000 ms informing the user to get ready. This cross disappeared at the end of the trial (t= 3000 ms). From t=-3000 ms to t=0 ms, the subjects were asked to relax, rest and they were not performing any study related task. At t = 0 ms an execution cue (which is an arrow pointing to either left or right) was presented on the screen and stayed there till t=1250ms. Depending on the cue the subjects had to perform AM of continuous opening and closing of the left or the right hand. This gave two types of AM condition namely, right hand AM and left hand AM. Subjects were asked to continuously attempt the movement from t=0s till t=3000ms. They were allowed to rest from t = 3000 ms for a variable length of time (between 1000 to 3000 ms) before another trial started. This paradigm, often used in brain computer interface experiments [117], is shown on Fig. 8.2.

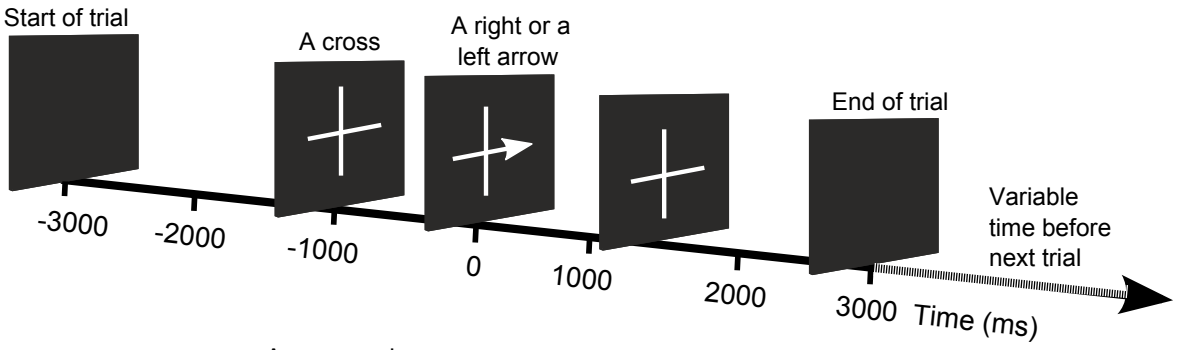

Figure 8.2: The paradigm used for attempted movement.

Subjects sat in an armchair facing a computer screen. Their hands were pronated and placed on a table in front of them as shown in Fig. 8.3. The subjects wore an EEG cap and a conductive gel was used to obtain electrical contact with EEG electrodes and the scalp. Subjects were instructed to relax and avoid physical movements during the experiment. They were monitored throughout the experimental session to make sure that they followed the instructions and a sub-session of the experiment was restarted if instructions were not followed. A total of 120 trials of AM were obtained (60 trials for each of left and right hand) divided into 4 runs of 30 trials (15 for each hand presented in a random order). After each run, the recorded data was inspected for artefacts and more data was collected if the run had many epochs with artefacts.

Signal recording was performed under MATLAB and Simulink (MATLAB R2012a, The MathWorks Inc., Natick, MA). Electrodes were placed on 47 different locations on the scalp

Figure 8.3: Subject's sitting position during data recording

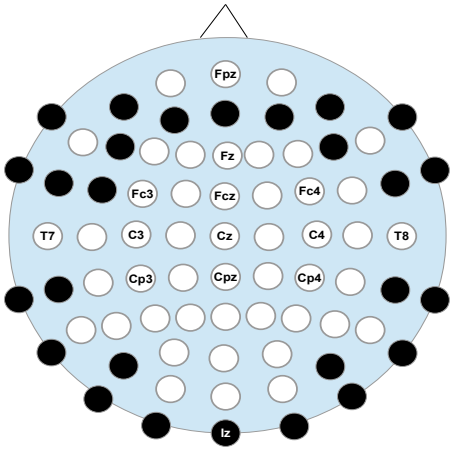

Figure 8.4: The 10/10 international electrode positioning standard used for the wholehead AM experiment. The black circles show unused positions.

following the International 10/10 electrode positioning standard as shown in Fig. 8.4. Linked ear reference was used and the ground electrode was placed on location Afz. An electrode was attached to the lateral canthus on the orbicularis oculi of the right eye to record Electrooculogram (EOG) for the purpose of artefact detection. EEG and EOG were recorded at the sample frequency of 256 Hz using three modules of the g.USBAmp (biosignal amplifier, g.tec Medical Engineering GmbH, Austria). The impedance of the electrodes was kept below 5 kΩ. Signal was filtered online between 0.5 and 60 Hz with a notch filter at 50 Hz using the IIR digital Butterworth filters built into the amplifiers.

8.3.2 BCI-FES therapy sessions

The patients were scheduled to attend therapy sessions between Monday and Friday until they completed twenty sessions. Each session lasted for about an hour.

At the beginning of each therapy session, a BCI classifier was computed to enable the control

of the BCI-FES system. To obtain the classifier, a patient was instructed to attempt closing and opening of the left and the right hand (20 trials for each hand). During this task EEG was recorded from three pairs of bipolar electrodes to derive C3 (Fc3-Cp3), Cz (Fcz-Cpz) and and C4 (Fc4-Cp4). See Fig. 8.4 for the positions of these electrodes. The input signal from the amplifier was bandpass filtered (5^{th} order Butterworth) online between 0.5 to 30 Hz. The time domain parameter (TDP) [113] of the filtered data was computed. The TDP was used to compute linear discriminant analysis (LDA) classifiers to detect when the patient was attempting to move. So when the therapy starts, the patient was instructed to perform AM of the hand receiving the therapy to activate the stimulator. When the classifier detect the AM (or detects the 'Active' state), the FES was activated to continuously open and close the hands. The detail of the BCI-FES system is given in Appendix B.1.

The FES device (Rehastim by Hasomed, Magdeburg) was used to assist the patients to perform grasp functions. Electrodes were attached to sequentially stimulate the extensor digitorum, extensor pollicis longus, flexor digitorum superficialis and the flexor pollicis brevis muscles as shown in Fig. 3.5. These were the main muscles targeted but since the stimulation was transcutaneous the surrounding muscles of the hand will be affected by the stimulation. The stimulation to the extensor digitorum extends the fingers and when the limit of the fingers extension is reached the wrist is forced to extend. The thumb is extended by stimulating the extensor pollicis longus. The stimulation to the flexor digitorum superficialis flexes the fingers and later forces the wrist to flex. The thumb is flexed by stimulating the flexor pollicis brevis.

To open the hand, the extensor pollicis longus was activated and immediately followed by the extensor digitorum. To close the hand, the flexor digitorum superficialis was first activated and immediately followed by the flexor pollicis brevis muscles.

The frequency of stimulation was set to 26 Hz and the pulsewidth was set to 200 μs. The FES current typically 15-35 mA was chosen for each subject to extend and flex the hands or cause visible muscle contraction without discomfort.

The patient was instructed to attempt closing and opening of the hand with the electrodes to activate the FES. A graspable object was sometimes provided so that the patient could perform grasp and release as an object oriented hand opening and closing [117]. Note that this was done on one hand at a time. The FES was activated for a total of 10 s when the active state was detected. During this 10 s period, the FES repeatedly assisted in the opening and closing of the hand in the order shown in Fig. 3.6. Note that when the FES was activated, the patients were instructed to continue to perform AM in synchrony with the FES and only to stop when the FES stopped. This is because the activation of the brain may be stronger if a patient continue to perform AM after FES onset [118]. A therapy session lasted for 60 minutes with 30-40 trials on each hand separately.

8.3.3 FES therapy sessions

The FES group received only FES (i.e without the BCI). The FES was continuously controlled automatically to open and close a subject's hands individually. The FES parameters were similar to those used in the BCI-FES group. On average the amount of stimulation (time and strength) given to the FES group was similar to those received by the BCI-FES group.

8.3.4 Data analysis

Manual muscle testing

In order to allow statistical operation on continuous data, the MMT scores were transformed. The transformation was to eliminate the negative and the positive assignments and replace then with -0.25 and +0.25 respectively. For example, if an MMT score G = 3-, after the transformation it becomes G = 2.75. In the other case, if G = 3+, after the transformation it becomes G=3.25. The results of this transformation is a continuous data of MMT scores on which further analysis was performed.

Range of movement

The ROM of the wrist was obtained for each hand using the 3-dimensional position of the makers placed on the hand. For each marker, the Zebris system returned a 3-D vector at each time point. The angle θ of the wrist at each time point was calculated using equation 8.1, where a represents Zebris system marker 2; b, marker 1; and c, marker 3.

$$\frac{\theta \times \pi}{180} = \arctan \frac{\|(b-a) \times (c-a)\|}{(b-a) \cdot (c-a)} \tag{8.1}$$

Somatosensory evoked potential

The recorded SSEP was visually inspected for the presence of N20 peak. When present, the latency of the the peak was noted. The latency and the SSEPLI were obtained following the description in Section 7.3.4.

Attempted movement

EEG data pre-processing

The continuous EEG data was split into trials. All data were visually inspected and epochs with artefact like a sudden burst in amplitude over all electrodes were eliminated. For each

subject a dataset for initial and final assessment was created. The datasets were individually decomposed into 48 maximally independent temporal components using the logistic infomax independent component analysis (ICA) algorithm [174, 175] implemented in EEGLAB [176]. The components were visually inspected and components corresponding to ocular artefact were removed [177]. All other artefacts like electrocardiogram and electromyogram were identified and removed by considering their typical morphology, spectrum, topography and temporal characteristics [178]. The remaining components were back projected to EEG channels and then used for further analysis in EEGLAB and sLORETA after computing common average reference of the EEG channels.

Event related desynchronisation/synchronisation

Time-frequency analysis was performed under EEGLAB to visualize and compare the Event Related Desynchronisation (ERD)[32, 179] and Event Related Synchronisation (ERS) [28, 121] arising from AM trials. Recall that ERD and ERS refer to decrease and increase respectively of EEG power relative to a baseline period within a narrow frequency band. Also recall that movement related cortical processes like those during physical execution can be quantified with ERD across the sensorimotor cortex. ERD/ERS, sometimes referred to as event related spectral perturbation [33], will be used in this text as a general term to refer to both ERD and ERS when necessary. ERD/ERS was computed using EEGLAB routines. The Morlet Wavelet transform was used to perform time frequency analysis of the EEG data in the frequency band 3 to 60 Hz with a Hanning-tapered window applied and the number of cycles set to 3. These wavelet parameters allowed low frequencies starting from 3 Hz to be analysed in a one second window [180]. The ERD/ERS was computed as power changes in decibels relative to a baseline period (t=-2000 to -1000 ms). The full description of ERD/ERS method which has already been described in this thesis is given in the EEGLAB's methods by Delorme and Makeig [176]. ERD/ERS averaged over trials and subjects per experimental condition type is presented. Also presented are ERD/ERS scalp maps in chosen time windows and in chosen frequency bands. The statistical non-parametric method with Holm's correction for multiple comparison [181] was used to assess the differences in ERD/ERS between subjects in the treatment and control group at p=0.05.

sLORETA localisation

Localisation of the cortical three-dimensional distribution of current density of EEG was done using the Standardized Low Resolution Electromagnetic Tomography (sLORETA) [224]. The method is a linear minimum norm inverse solution to EEG 3D localisation inverse problem. The sLORETA (estimated current density) cortical map/image is computed for 6239 voxel partitions of intracerebral volume at 5 mm spatial resolution. Brodmann ar-

eas are reported using the Montreal Neurological Institute (MNI) space with correction to the Talairach space [225, 226].

The trials were split into one second long time windows. Frequency domain sLORETA was computed for the window at 1000-2000 ms in the frequency bands including 1-3Hz (δ), 4-7Hz (θ), 8-12Hz (α/μ), 12-16Hz ($\beta 1$), 16-24Hz ($\beta 2$). This gave five sLORETA images at each frequency band. Baseline was taken from the period before the warning sign (t=-2000 to -1000 ms).

To find the predominantly active areas on the cortex, the sLORETA statistical package was used to perform a paired group analysis for the AM trials where a pair comprises the baseline window and the selected one second window. Using sLORETA's log of ratio of averages (r-value), 5000 randomization of statistical non-parametric mapping (SnPM) [182] implemented in sLORETA package was used to calculate corrected critical thresholds and p-values. Statistical significance level was set at p=0.05.

Weighted laterality index was computed from sLORETA images to quantify the degree of hemispheric lateralisation of sensorimotor activities during hand AM. A set of ROI for the wLI was defined as in Section 3.3.2. The total number of voxels in the ROI was 477. The wLI was computed at each sLORETA frequency band image and at varying threshold on the voxels. The threshold on the voxels included sLORETA p-values at p=0.1, 0.05 and 0.01. For each dataset (e.g EEG for AM during initial assessment), the corresponding sLORETA images were compared to find the one with the largest wLI. The image with the largest wLI was chosen and its wLI was presented. But to avoid images with too low number of active voxels within the ROI being chosen in place of those with a larger number of active voxels, another selection criterion was introduced. In this criterion, if the image with the largest wLI has less than 10% activated voxels within the ROI, another search was performed for the image with the largest number of active voxels within the ROI.

Presentation of active frequency bands in sLORETA

Images sLORETA will be provided for frequency bands with the most significant activities. Presenting sLORETA images in all frequency bands will make interpretation of results difficult with many irrelevant information considered due to several sLORETA images and table of activities. Since group analysis was not possible (due to small number of subjects) each subject was analysed separately. This resulted to a maximum of 20 sLORETA images and 20 sLORETA tables of activities for each subject (given 5 $\times$ frequency bands, 2 $\times$ sessions-before and after therapy, and 2 $\times$ hands). This clearly makes it difficult to present information in individual frequency bands. So, sLORETA results will be presented in the best frequency bands showing what is expected in healthy individuals. Such frequency bands were those selected during wLI analysis. They are the frequency bands with either maxi-

mum lateralisation or largest number of active voxels within the ROI. So, this is the best performing frequency. The issue here is that it will be hard to assess what changes occur in a particular frequency before and after the therapy. Instead of asking what happens to a particular frequency band, it might be more appropriate to ask of the frequency band with the most activity before and after the therapies. The later is a more appropriate question that can concisely reveal changes in the frequency bands with the maximum activities without overloading the reader with information for each individual frequency band. One effect on EEG following BCI-FES could be a change in the most reactive frequency band. Therefore the sLORETA analysis here is presented in order to show changes in the most reactive frequency bands. Since these are the most significantly active frequency bands, other frequency bands are less important. An indirect information is that when a previously reactive frequency band is deselected following a therapy, then this previously most reactive frequency band has a reduction in reaction relative to the new most reactive frequency band. For a more appropriate analysis with consideration to changes in all major frequency bands before and after the therapies, time-frequency analysis was performed in Section 8.4.5.

8.3.5 Statistics

Statistical analysis for ERD/ERS was performed with non-parametric method implemented in EEGLAB. For the sLORETA localisation, also the non-parametric method implemented in sLORETA was used. The rest of the statistical testing was done using the Wilcoxon signed rank (paired) for within group to compare ‘Before’ and ‘After’ therapies; the Wilcoxon rank sum test for between group differences. For the between group test, a groups data will be obtained by subtracting pre-assessment (‘Before’) from post-assessment data (‘After’). Statistical significant level was set to p=0.05 in all tests.

8.4 Results

8.4.1 Manual muscle test

The MMT scores are shown in Appendix, where the scores for the right hand of the BCI-FES and FES group are in Tables D.1 and D.2 respectively; that of the left hand of the BCI-FES and FES group in Tables D.3 and D.4 respectively.

The p-values obtained by comparing the MMT scores for ‘Before’ and ‘After’ the therapies for each patient group are shown in Table 8.2. For the BCI-FES group, there were statistically significant differences in the MMT scores between ‘Before’ and ‘After’ the therapy. For this group the left hand MMT scores improved significantly in seven muscles following

the therapy as shown in Table 8.2. The BCI-FES group also gained improvement in four muscles of the right hand. These muscles included the extensor digitorum communis and the extensor carpi radialis that extend the hand, the supinator and the pronator which supinates and pronates the hand respectively. In the case of the FES group no statistically significant improvement was found in both the left and the right hand. Statistical comparison between

Table 8.2: P-values of the statistical comparison for the right and left hand MMT scores, 'After' > 'Before' therapies separately for each patient group.

Muscles	Left		Right	
	BCI-FES	FES	BCI-FES	FES
Latissimus dorsi	0.03 *	0.06	0.06	0.13
Pectoralis major	0.03 *	0.06	0.06	0.13
Serratus anterior	0.03 *	0.25	0.06	0.13
Deltoid	0.06	0.13	0.03 *	0.13
Triceps	0.03	0.13	0.25	0.06
Biceps	0.06	0.06	0.13	0.06
Brachioradialis	0.06	0.25	0.13	0.25
Supinator	0.03 *	0.06	0.03	0.06
Pronator	0.02 *	0.25	0.02 *	0.06
EDC	0.03 *	0.13	0.02 *	0.06
ECR	0.03*	0.25	0.03 *	0.25
EPL	0.25	0.06	0.13	0.06
FCR	0.13	0.25	0.13	0.13
FDP	0.06	0.13	0.06	0.06
Intrinsics	0.25	0.13	0.50	0.13

Notes: *, Significantly different at p=0.05 (BCI-FES, n=7; FES, n=5). EDC, extensor digitorum communis; ECR, extensor carpi radialis; EPL, extensor pollicis longus; FCR, flexor carpi radialis; FDP, flexor digitorum profundus.

the BCI-FES group with the FES group shows a difference in one muscle in each hand as shown in Table 8.3. The comparison showed that on the left hand, the extensor pollicis longus improved in the FES group better than in BCI-FES group. On the right hand, the biceps which was not one of the muscles considered/stimulated during the therapies improved better in the FES group than in the BCI-FES group. This is an interesting result given that the pervious analysis showed that the BCI-FES group had better improvements when comparing the 'After' and the 'Before' MMT scores. This highlights the need to cautiously interpret the results of these analyses given the small number of subjects in each of the BCI-FES and the FES groups.

Table 8.3: P-values of the the statistical comparison for the right and left hand MMT scores, 'BCI-FES('After'-'Before') vs FES('Before'- 'After')

Muscles	Left		Right	
	BCI-FES vs FES	P-value	BCI-FES vs FES	P-value
Latissimus dorsi		0.23		0.60
Pectoralis major		0.12		0.22
Serratus anterior		0.94		0.46
Deltoid		0.32		0.86
Triceps		0.62		0.06
Biceps		0.12	BCI-FES $<$ FES	0.02 *
Brachioradialis		0.86		0.67
Supinator		0.20		0.10
Pronator		0.84		0.13
EDC		0.70		0.34
ECR		0.90		0.79
EPL	BCI-FES $<$ FES	0.03 *		0.06
FCR		0.51		0.25
FDP		0.41		0.17
Intrinsics		0.21		0.17

Notes: See Table .8.2.

8.4.2 Range of movement

The results for ROM is shown in Fig. 8.5 for the right wrist and in Fig. 8.6 for the left wrist extension and flexion before and after the therapies. All available ROM are tabulated in Table 8.4. Am example of the trajectory during ROM assessment for one subject is plotted in Fig. 8.7.

All but subject ps11 from the FES group had some improvement in the wrist ROM after the BCI and FES therapies. Subject ps11 had no wrist movement before and after the FES therapy. By visual inspection of Fig. 8.5 and 8.6, there is no clear evidence of BCI-FES group gaining better wrist ROM than the FES group. Since both subject groups are in sub-acute stages, they were expected to gain functions but more subjects are needed to show a difference between the two groups.

Due to missing data and low number of subjects the statistical comparison will be under-powered if performed separately for each movement type (wrist flexion and wrist extension) and hand. In order to increase the number of data points for the statistical testing, data concatenation was performed across hands (left and right) and movement types (flexion and extension). The concatenation increases the number of data points available for the BCI-FES group to n=17 and that of the FES group to n=11. For each of the groups, there is a statistically significant difference between the initial ('Before') and the post-assessment ('After')

Table 8.4: The results of ROM for all subjects. Missing data is shown with '-'

Subject Id	Right wrist ROM (± 0.5, degrees)				Left wrist ROM ((± 0.5, degrees)			
	Extension		Flexion		Extension		Flexion	
	Before	After	Before	After	Before	After	Before	After
				BCF-FES				
ps1	11.5	30.5	10.6	26.1	-	-	-	-
ps2	1.66	19.9	1.3	6.6	2.2	9.8	1.2	3.8
ps3	-	-	-	-	20.1	34.2	-	-
ps5	45.6	52.3	-	-	-	-	2	33.7
ps6	9.1	24.3	3.8	12.7	9.1	29.2	12.9	39.5
ps7	-	-	-	-	4	11.6	6.7	21.5
ps8	16.9	44.8	-	-	18.7	28.4	-	-
				FES				
ps4	22.1	38.8	17.1	36.7	13.2	27.8	31.2	33.8
ps11	0	0	0	0	0	0	0	0
ps12	19.3	23.0	19.5	42.9	-24.4	23.4	34.3	-

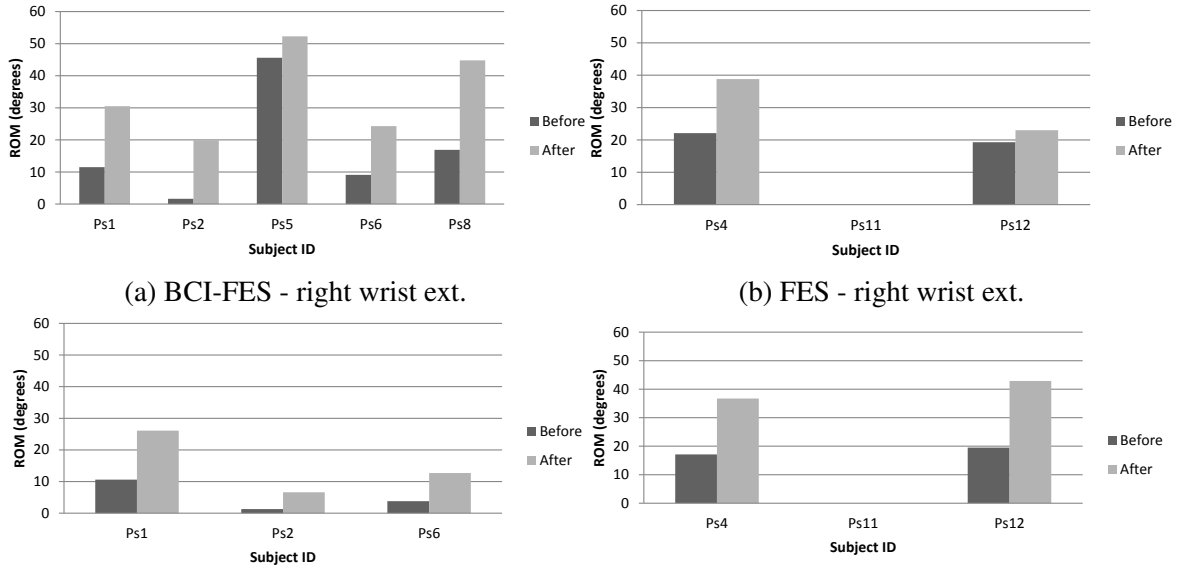

(a) BCI-FES - right wrist ext.

(b) FES - right wrist ext.

(c) BCI-FES - right wrist flex.

(d) FES - right wrist flex.

Figure 8.5: The right wrist ROM before and after the therapies. ext, extension; flex, flexion.

data; $p<0.0005$ for the BCI-FES group and $p=0.0313$ for the FES group. There was no difference between the groups, $p=0.0627$. More subjects are needed because the functional outcome difference between the groups may be small given that the therapy period was only 20 sessions. Neurological measures may better reveal this small difference. The wholehead EEG and SSEP analysis is used for further analysis.

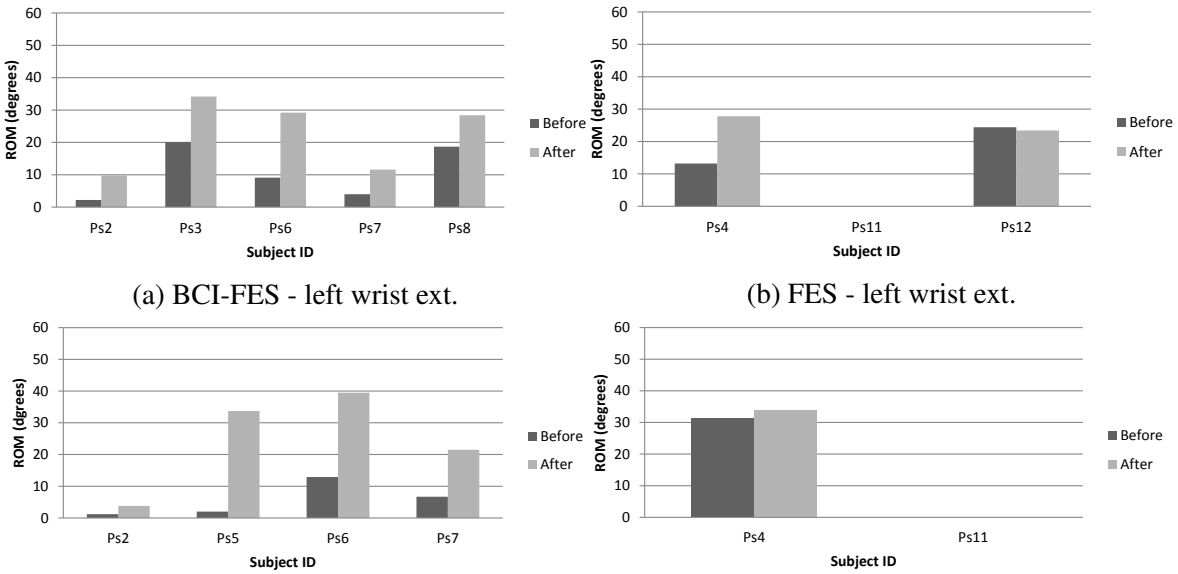

(a) BCI-FES - left wrist ext.

(b) FES - left wrist ext.

(c) BCI-FES - left wrist flex.

(d) FES - left wrist flex.

Figure 8.6: The left wrist ROM before and after the therapies.

8.4.3 Somatosensory evoked potential

Results are provided for patients who were able to perform the SSEP tests. Some patients were not able to complete the test due to illness, injuries that restrict access to a hand and due to being discharged from the hospital. When only part of the subject data is available the missing data is represented as -, not available.

Right Median nerve N20

BCI-FES group

The N20 peak was present in two (ps1 and ps5) out of seven subjects in the treatment group during the pre-assessment. In the post assessment, only one patient (ps2) among those who completed the test still had the N20 peak absent. This means that the peak returned in four of the patients (ps3, ps5, ps6, and ps8) following the therapy. The latencies for the returning N20 peaks are shown in Table 8.5. For the two patients who had the peak present during the pre-assessment, the peak appeared earlier in the post-assessment suggesting improvement of the sensory pathways; for ps1 the peak went from 27.71 to 26.04 ms and for ps5 it went from 22.71 to 22.08 ms.

The SSEPLI values averaged across the subjects increased from 0.091 which is bilateral to 0.279 which is left-lateralised (see Chapter 7 for the meaning of SSEPLI values). This means that on average the SSEP potential went from having approximatley equal amplitude on both hemispheres to being left-lateralised when the right hand was stimulated. This is a good

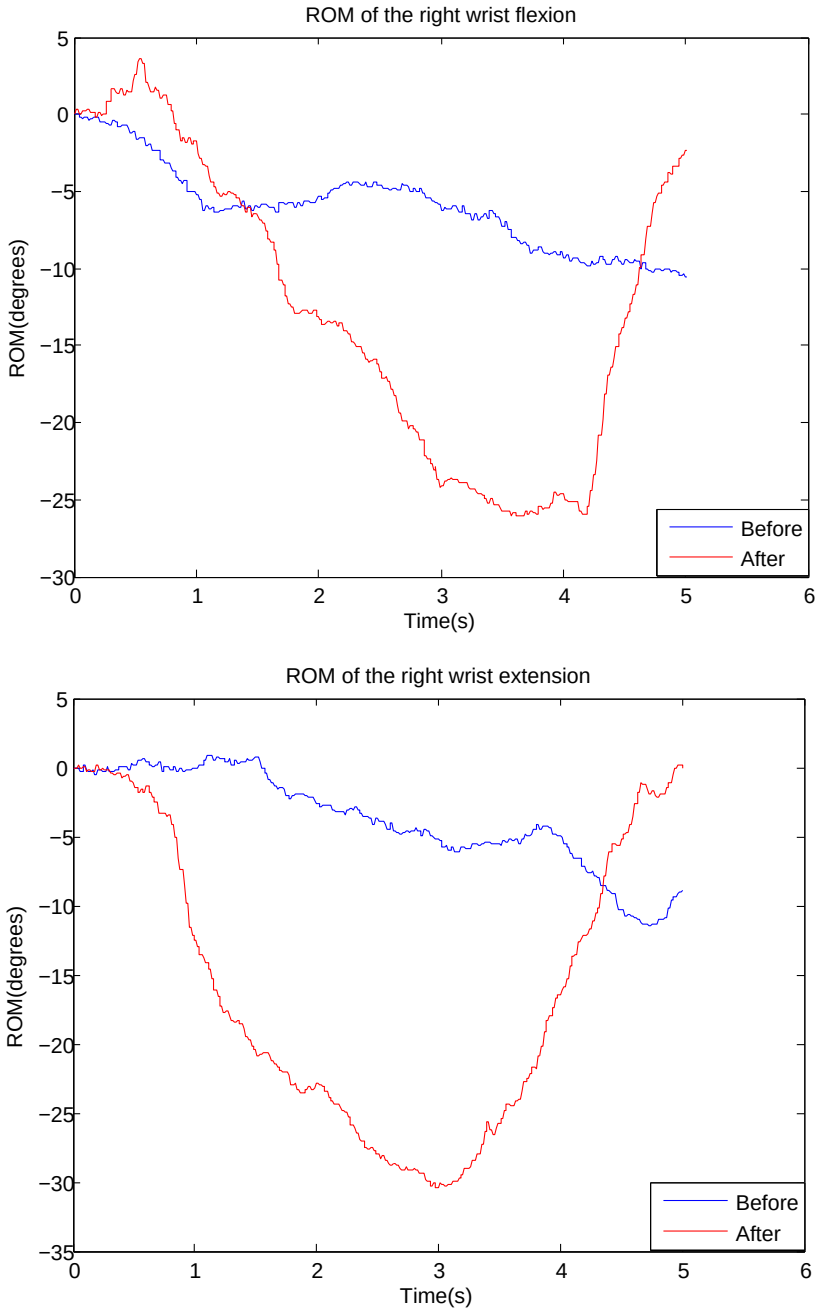

Figure 8.7: The trajectory during ROM assessment for subject ps1. Note that only the range of movement and not the trajectory information was used for assessment purposes. Patients were not advised to produce a quick or a smooth trajectory.

result given that the left hemisphere controls the right hand.

FES group

The N20 peak was present in two (ps4 and ps12) out of 4 subjects in the control group who completed the test during the pre-assessment. In the post assessment, the N20 peak did not return for subject ps9 and SSEPLI remain bilateral. The peak did not also return

Table 8.5: Right median nerve N20 status, peak and latency.

Subject ID	Pre			Post		
	Median EP status	Latency (ms)	SSEPLI	Median EP status	Latency (ms)	SSEPLI
			BCI-FES			
ps1	Present	27.71	0.314	Present	26.04	0.411
ps2	Absent	-	-0.170	Absent	-	-0.085
ps3	Absent	-	-0.125	Present	21.88	0.136
ps5	Present	22.71	0.275	Present	22.08	0.431
ps6	Absent	-	0.378	Present	24.79	0.379
ps7	Absent	-	0.199	Absent	-	0.308
ps8	Absent	-	-0.237	Present	26.67	0.370
			FES			
ps4	Present	23.33	0.218	Present	22.5	0.255
ps9	Absent	-	-0.118	Absent	-	-0.056
ps11	Absent	-	0.291	Absent	-	0.165
ps12	Present	24.58	0.251	Present	25.21	0.457

for subject ps11 whose SSEPLI decreased from 0.291 to 0.165. Both the latency and the SSEPLI improved for subject ps4 (23.33 to 22.5 ms and 0.218 to 0.255 for latency and SSEPLI respectively) but only the SSEPLI improved for subject ps12 (0.251 to 0.457).

Left median nerve N20

BCI-FES group

The left median nerve N20 peak was present in three (ps1 and ps3, ps5) out of seven subjects in the treatment group during the pre-assessment. In the post assessment, only one patient (ps7) among those who completed the test still had the N20 peak absent. This means that the peak returned in three (ps2, ps6, and ps8) of the patients following the therapy. The latencies for the returning N20 peaks are shown on Table 8.6. For the three patients who had the peak present during the pre-assessment, the peak appeared earlier in the post-assessment except for subject ps5 whose N20 peak latency remained unchanged in the two assessment sessions. Note that the latency for patient ps5 was already low. The biggest change in latency was for ps1 where the peak went from 28.75 to 24.58. The SSEPLI only improved for subject ps1, ps5 and ps6 in the post-assessment. The low SSEPLI values obtained for subject ps2 and ps6 casts a doubt into the validity of the N20 peaks. The SSEPLI averaged across the subjects for before and after the therapies were from -0.111 to -0.187.

FES group

Table 8.6: Left median nerve N20 status, peak and latency.

Subject ID	Pre			Post		
	Median EP status	Latency (ms)	SSEPLI	Median EP status	Latency (ms)	SSEPLI
			BCI-FES			
ps1	Present	28.75	-0.141	Present	24.58	-0.426
ps2	Absent	-	0.053	Present	19.58	0.052
ps3	Present	22.5	-0.188	Present	19.58	0.016
ps5	Present	21.88	-0.195	Present	21.88	-0.447
ps6	Absent	-	-0.061	Present	24.79	-0.538
ps7	Absent	-	-0.057	Absent	-	0.007
ps8	Absent	-	-0.192	Present[1]	26.88	0.027
			FES			
ps4	Absent	-	0.202	Present	22.92	-0.143
ps9	Absent	-	0.062	Absent	-	0.145
ps11	Absent	-	0.234	Absent	-	0.252
ps12	Present	23.75	-0.502	Absent	-	-0.012

Note: [1], reduced amplitude.

The left median nerve N20 peak was present in one (ps12) out of 4 subjects in the control group who completed the test during the pre-assessment. In the post-assessment the peak returned for ps4 although the SSEPLI was low with a value of -0.143. The N20 peak did not return for subject ps9 who had SSEPLI values of 0.062 in the pre-assessment and 0.145 in the post assessment. The SSEPLI decreased for subject ps12 going from -0.502 in the pre-assessment to -0.012 in the post-assessment. The decrement of the SSEPLI for this subject is supported by the disappearance of the N20 peak in the post-assessment. For subject ps11, the N20 peak remained missing and the SSEPLI values were similar (0.234 to 0.252) in both assessments.

Right Ulnar nerve N20

BCI-FES group

The right ulnar nerve N20 peak in Table 8.7 was only present in subject ps1 in pre-assessment. In the post assessment, the latency for subject ps1 improved from 28.54 to 27.29ms. This improvement in latency was accompanied with an improved SSEPLI which went from 0.246 in the pre-assessment to 0.405 in the post-assessment. The peak returned for subject ps5 and ps8 as shown in Table 8.7 . Among those who still had the peak absent in the post assessment subject ps7 had improved SSEPLI value 8.7 in the post assessment. In the case of subject ps6 SSEPLI showed that the amplitude of the SSEP was larger in the ipsilateral hemisphere.

This could be an indication of somatotopic changes where the somatotopic map for the right hand may have started moving ipsilaterally (towards the right hemisphere). The SEPLI values averaged across the subjects increased from 0.099 to 0.139.

FES group

Only data for two controls were available for the right ulnar nerve N20 peak. In both subjects the N20 peak was absent in both assessments and the SSEPLI only improved for one of the subjects (ps9) as shown in Table 8.7 .

Table 8.7: Right ulnar nerve N20 status, peak and latency.

Subject ID	Pre			Post		
	Ulnar EP status	Latency (ms)	SSEPLI	Ulnar EP status	Latency (ms)	SSEPLI
			BCI-FES			
ps1	Present	28.54	0.246	Present	27.29	0.405
ps2	Absent	-	-0.047	Absent	-	-0.147
ps3	Absent	-	0.094	Absent	-	0.109
ps5	Absent	-	0.187	Present	23.33	0.256
ps6	Absent	-	0.182	Absent	-	-0.216
ps7	Absent	-	0.128	Absent	-	0.46
ps8	Absent	-	-0.097	Present	27.08	0.108
			FES			
ps4	Absent	-	-0.073	Absent	-	0.099
ps9	Absent	-	0.152	Absent	-	0.337

Left Ulnar nerve N20

BCI-FES group

The left ulnar nerve N20 peak (Table 8.8) was only present in subject ps5 in pre-assessment. In the post assessment, the latency for subject ps5 improved from 23.33 to 22.71 ms. This improvement in latency was accompanied with an improved SSEPLI which went from -0.035 in the pre-assessment to -0.468 in the post-assessment. The peak returned for subject ps1 only as shown in Table 8.8. The SSEPLI values averaged across the subjects improved from 0.103 to -0.147.

FES group

Only data for three subjects was available in the controls for the left ulnar nerve N20 peak. In both subjects the N20 peak was absent in both assessments. The SSEPLI values were low for subject ps9 and ps11 in the post-assessment. The SSEPLI values for subject ps4 indicate lager SSEP in the ipsilateral/left hemisphere suggesting undesirable changes in the CNS.

Table 8.8: Left ulnar nerve N20 status, peak and latency.

Subject ID	Pre			Post		
	Ulnar EP status	Latency (ms)	SSEPLI	Ulnar EP status	Latency (ms)	SSEPLI
			BCI-FES			
ps1	Absent	-	0.069	Present	25.21	-0.202
ps2	Absent	-	-0.292	Absent	-	-0.237
ps3	Absent	-	0.192	Absent	-	-0.056
ps5	Present	23.33	-0.035	Present	22.71	-0.468
ps6	Absent	-	0.273	Absent	-	0.003
ps7	-	-	-	Absent	-	0.187
ps8	Absent	-	0.413	Absent	-	-0.253
			FES			
ps4	Absent	-	0.46	Absent	-	0.197
ps9	Absent	-	-0.061	Absent	-	0.079
ps11	-	-	-	Absent	-	0.012

Summary of N20

The status of N20 peak averaged across nerves, hands and subjects are shown for the BCI-FES group in Fig. 8.8 and the FES group in Fig. 8.9. As shown on Fig. 8.8 and Fig. 8.9, after the therapies the number of N20 peaks present increased only for the BCI-FES group.

The SSEPLI were concatenated across hands and nerves for statistical analysis. The sign of SSEPLI values for the left hand was inverted so that the values become positive when they were correctly lateralised and negative otherwise. This was done to eliminate negation if the lateralisation was correct since this negation only indicated direction of laterality. The concatenation resulted to n=27 for the BCI-FES group and n=12 for the FES group. For the BCI-FES group, there was a statistically significant difference between the initial ('Before') and the post-assessment ('After') data; p=0.003938. In the case of the FES group there was no significant difference; p=0.4238. It could be that the length of the therapy period was short for FES to induce neurological changes in the FES group. But the short therapy was enough for the BCI-FES system to induce changes in the subjects. Given the difference in the number of data points available for each group, it was not adequate to compare both. But for completeness the comparison was performed (BCI-FES('After' - 'Before') versus

FES('After' - 'Before')) to get p=0.2294 which suggest that there was no difference in the SSEPLI values between the groups.

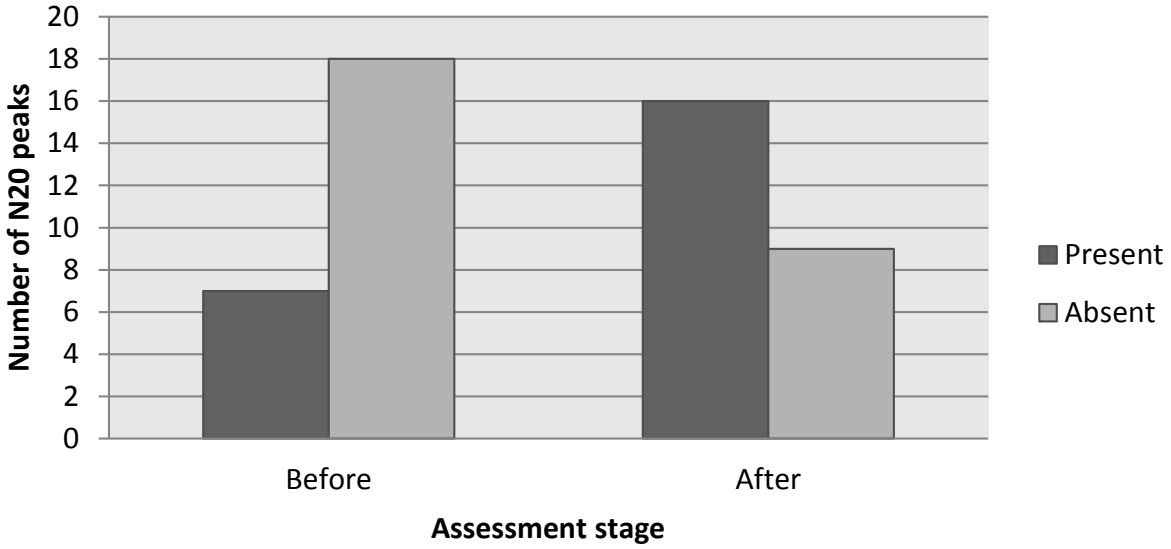

Figure 8.8: The status of N20 before and after the treatment. The result was obtained by summing the number of N20 peaks present and absent across the median and the ulnar nerves, left and right hands and the **BCI-FES** group.

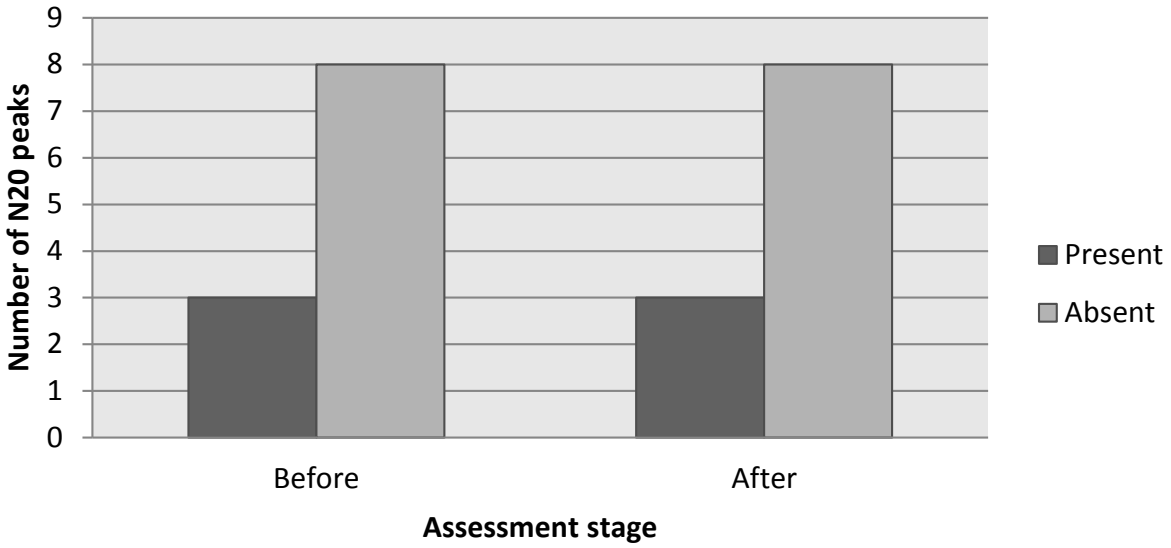

Figure 8.9: The status of N20 before and after. The result was obtained by summing the number of N20 peaks present and absent across the median and the ulnar nerves, left and right hands and the **FES** group.

8.4.4 sLORETA localisation

Laterality index

Given the low resolution of sLORETA, there were not many voxel representing the ROI (477 voxels). Therefore at p=0.01 the number of voxels active within the ROI is highly reduced with zero activity in some subjects leading to undefined value for wLI. It was decided for this reason that the threshold at p=0.01 was not adequate. The trend shown at p=0.1 is similar to that shown at p=0.05. Therefore detailed presentation will only be made for wLI obtained at p=0.05 since this is the chosen p-value in this thesis. Although laterality index is known to depend on the threshold p-value [135], using the same p-value at p=0.05 for analysis before and after the therapies should provide an adequate comparison between the two.

For completeness, plots of wLI at p=0.1 and at p=0.01 are provided with those at p=0.05. The plots of wLI at threshold p=0.1 is shown in Fig.8.10 and at p=0.01 in Fig. 8.11.

Table 8.9 shows the wLI at (p=0.05) for all the subjects before and after the therapies. The data is plotted on Fig. 8.12. The first row in Fig. 8.12 is for the left hand AM while the second row is for the right hand. The first column is for the BCI-FES group while the second column is the for FES group. The wLI is plotted for each subject before and after the therapies.

Left hand AM

For the left hand AM (Fig. 8.12 **'Left'**), all but subjects ps2 and ps3 in the BCI-FES group showed correctly lateralised ('Right dominance', contralateral to the left hand) sensorimotor activities. The wLI also have increased magnitudes in the BCI-FES group following the therapy. Subjects ps1 and ps5 had no significant activity before the therapy but after the therapy correctly lateralised activities emerged. In the FES-only group, subject ps4 showed only a bilateral activity following the therapy during left hand AM. In subjects ps10 and ps12, wLI decreased in magnitude and also incorrectly laid in the ipsilateral hemisphere ('Left' dominance) for subject ps12 after FES therapy. There were no significant activity in subject ps11 after the therapy resulting in wLI having an undefined value. Note that the 'After' data for subject ps9 was note available.

Right hand AM

For the right hand AM, there was no significant activity after the therapy for subjects ps1, ps2 and ps3 in the BCI-FES group. This result was most surprising for subject ps2 because this subject had correctly lateralised activities in the initial assessment. The lack of significant activities for this subject in the sensorimotor areas during the right hand AM suggests a decrement in sensorimotor functions. In the SSEP test, the right hand SSEPLI values for subject ps2 also worsened signaling that this patient might be undergoing undesirable cortical

Table 8.9: The wLI at p=0.05 for all the subjects before and after the therapy.

Hand	Subj.ID	wLI(before)	wLI(after)	F(before)	F(after)	nv(before)	nv(after)
				BCI-FES			
Left	ps1	0.00	-1.00	-	4-7	0	1
	ps2	-0.40	0.00	16-24	-	10	0
	ps3	0.00	0.00	-	-	0	0
	ps5	0.00	-0.62	-	16-24	0	266
	ps6	-0.23	-1.00	12-16	12-16	151	53
	ps7	-0.86	-1.00	12-16	8-12	105	53
	ps8	-0.35	-0.44	8-12	16-24	72	18
				FES			
	ps4	0.00	-0.13	-	16-24	0	67
	ps9	-1.00	na	8-12	na	39	na
	ps10	-0.39	-0.34	12-16	12-16	148	261
	ps11	-0.20	0.00	16-24	-	62	0
	ps12	-0.51	0.30	8-12	12-16	123	25
				BCI-FES			
Right	ps1	0.00	0.00	-	-	0	0
	ps2	0.50	0.00	16-24	-	105	0
	ps3	0.00	0.00	-	-	0	0
	ps5	0.00	0.95	-	8-12	0	104
	ps6	0.17	-1.00	16-24	12-16	151	5
	ps7	-1.00	-0.75	8-12	16-24	68	31
	ps8	0.06	1.00	16-24	12-16	398	1
				FES			
	ps4	0.00	-0.26	-	16-24	0	65
	ps9	0.02	na	8-12	na	126	na
	ps10	0.64	-0.39	16-24	12-16	202	235
	ps11	0.08	0.00	16-24	-	131	0
	ps12	-0.28	-0.13	12-16	8-12	72	21

Notes: Missing data is shown as 'na' while missing frequency band due to zero wLI/zero activity is shown as '-'. Right/left, right/left hand attempted movement; wLI, weighted laterality index; F, frequency band in Hz; nv, number of active voxels within regions of interest; before/after, Before/After the therapies

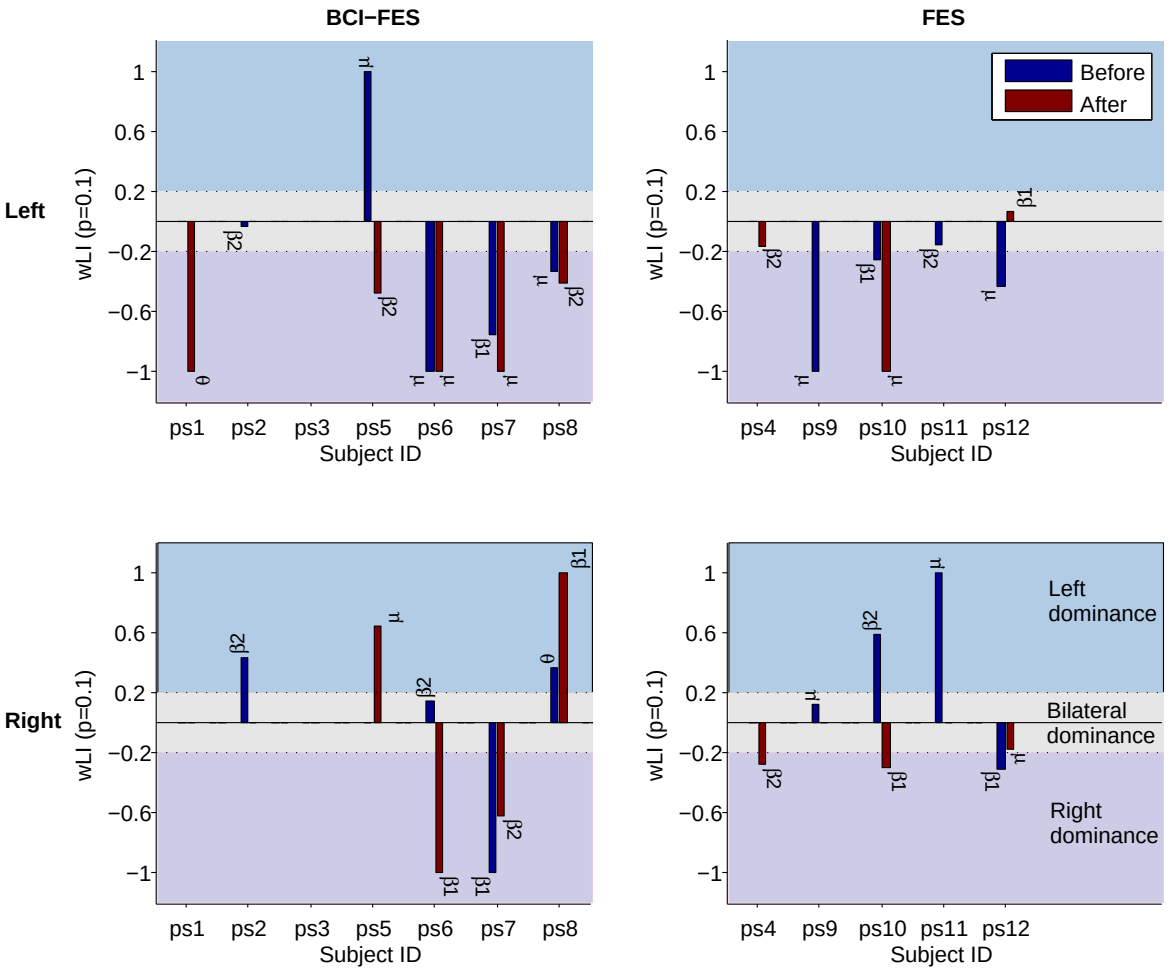

Figure 8.10: Laterality index (p=0.1) for the BCI-FES and the FES group for the left and right hand AM. The frequency bands with the maximum wLIs are shown above the bars; θ, 4-7 Hz; μ, 8-12 Hz; β1, 12-16 Hz; and β2, 16-24 Hz. The plot area is divided into three parts: top, left hemispheric dominance; middle, bilateral dominance; bottom, right hemispheric dominance. Note that the 'After' data for subject ps9 is note available.

reorganisation (see Tables 8.5 and 8.7). It is worth mentioning that this subject has a severe high level injury (level C4, ASIA B). For other subjects, ps5 and ps8 had increased wLI which was also correctly lateralised following therapy. Subjects ps6 also had an increased wLI magnitude but this was wrongly lateralised ipsilaterally. Subject ps7 had ipsilateral lateralisation before and after the therapy. In the FES-only group, all but subject ps4 who had no activity before therapy had reduced magnitude of wLI after the therapy. Subjects ps4 and ps10 had wrong lateralisation, subject ps12 had a bilateral activity and subject ps11 had no significant activity following the therapy.

The frequency bands selected with the wLI analysis did not show any consistent pattern between before and after therapies. The frequency bands are shown in Fig. 8.10, 8.11 and 8.12 for the interested reader.

There was no statistically significant difference between 'Before' and 'After' for each of

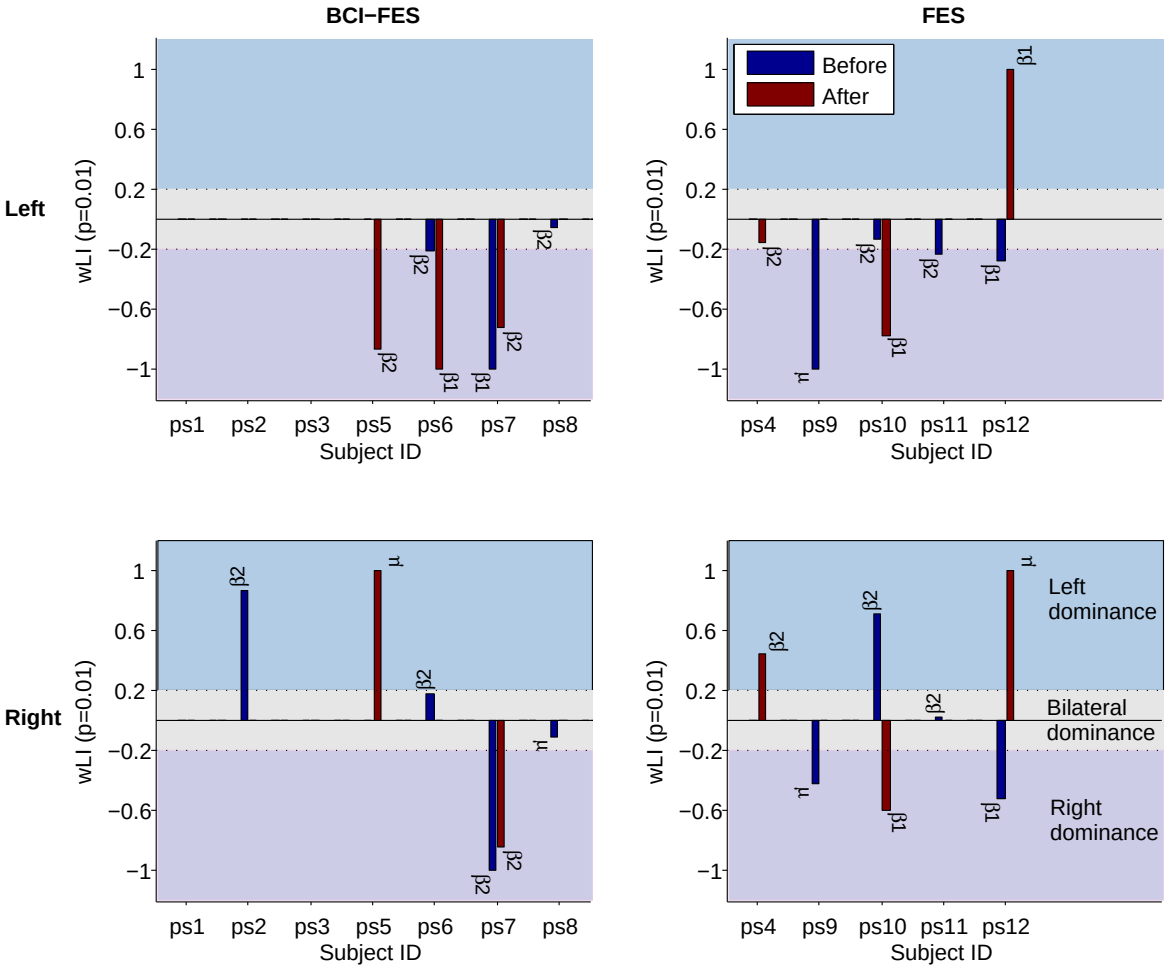

Figure 8.11: Laterality index (p=0.01) for the BCI-FES and the FES group for the left and right hand AM. The frequency bands with the maximum wLIs are shown above the bars; θ, 4-7 Hz; μ, 8-12 Hz; $\beta 1$, 12-16 Hz; and $\beta 2$, 16-24 Hz. The plot area is divided into three parts: top, left hemispheric dominance; middle, bilateral dominance; bottom, right hemispheric dominance. Note that the 'After' data for subject ps9 is note available.

BCI-FES and FES group. This was largely because of the individual differences in the LI values. Also there was no difference between the groups. However, these individual results suggest that the BCI-FES group had an overall better lateralisation of EEG activities after the their therapy. Since a better lateralisation is found in healthy subjects than in patients [140], the improvement in lateralisation obtain here should mean that the BCI-FES group generally benefited from the study. In the following, sLORETA images and table of activities will be presented in the frequency bands selected during wLI analysis in order to visualise the activated areas during hands AM.

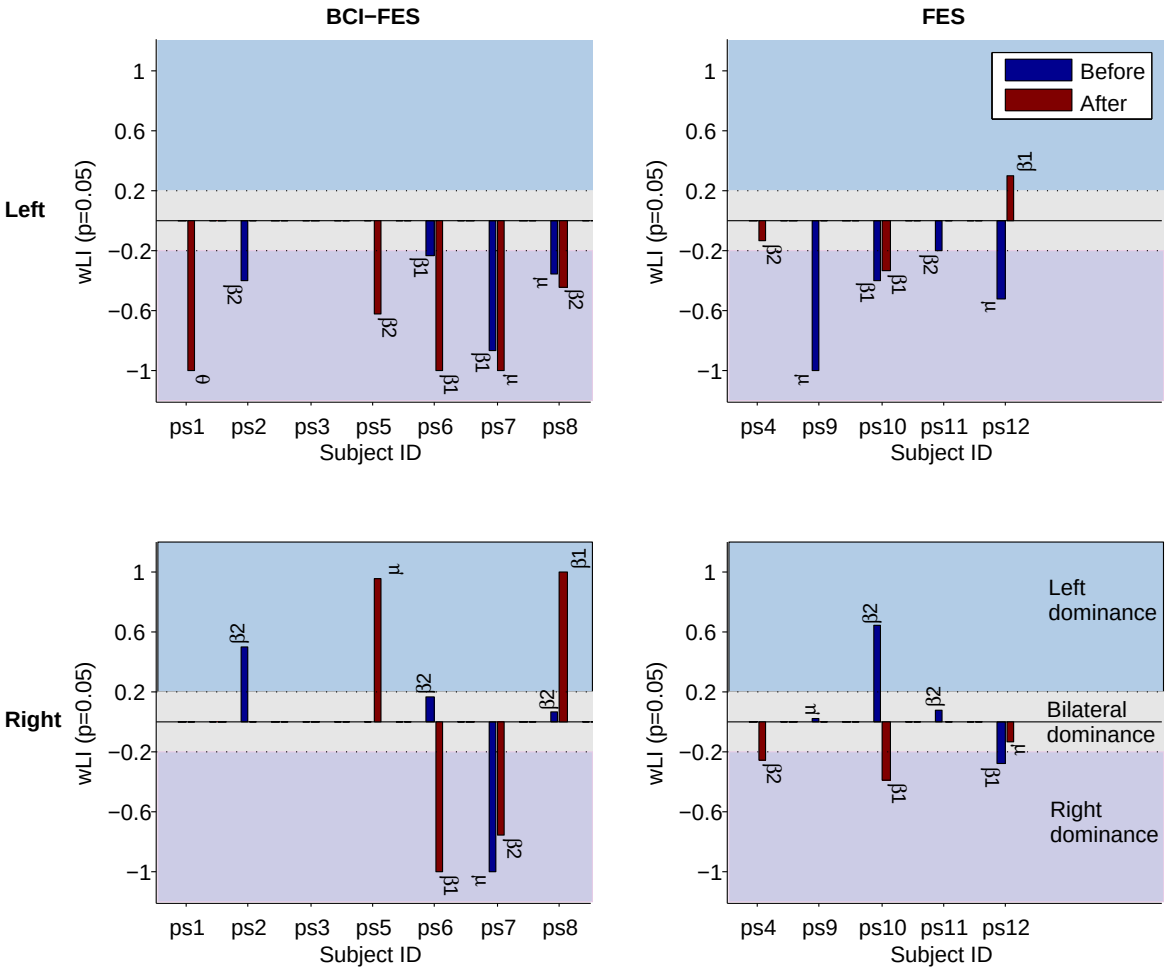

Figure 8.12: Laterality index (p=0.05) for the BCI-FES and the FES-only group for the left and right hand AM. The frequency bands with the maximum wLIs are shown above the bars; θ, 4-7 Hz; μ, 8-12 Hz; $\beta 1$, 12-16 Hz; and $\beta 2$, 16-24 Hz. The plot area is divided into three parts: top, left hemispheric dominance; middle, bilateral dominance; bottom, right hemispheric dominance. Note that the 'After' data for subject ps9 is note available.

sLORETA images and tables of active structures

Images and tables of activities from sLORETA for representative subjects are shown. Subject ps5 and ps10 were selected from the BCI-FES group and the FES-only group respectively. In these two subjects the wLI remained for both hands following the therapies. By observing Fig. 8.12, it can be seen that these subjects are suitable representatives of each group. The most reactive frequency bands as selected by wLI analysis are presented.

As shown on Fig. 8.13, subject ps5 had no significant activity before BCI-FES therapy. Following the therapy, lateralised activities can be seen in the sensorimotor areas. The lateralisation is as expected with more activity on the right hemisphere for the left hand AM and more activity on the right hemisphere for the left hand AM. This clearly has been shown by the wLI analysis where the values obtained for this subject show correct lateralisations. The

most reactive frequency bands were μ band for the left hand AM and the $\beta 2$ band for the right hand AM. The brain structures active in the sLORETA images restricted to the ROI are given in Table E.1. Highest number of active voxels can be seen in the left precentral gyrus (BA 4, 6 and 44) and in the right postcentral gyrus (BA 1, 2, 3 and 44) for the left hand AM. During the right hand AM, the most active voxel changed to the left precentral gyrus (BA 4 and 6) and the left postcentral gyrus ((BA 1, 2, 3 and 40). These results are promising given that similar results are found in healthy individuals [141, 142]. Correct lateralisation and increase in magnitude was also shown for this subject in sensory test using SSEP where the values for the SSEPLI were as expected in healthy subjects (see Fig. 8.5, 8.6, 8.7 and 8.8). So for subject ps5 changes in the sensory test correlated with changes in the sensorimotor test using AM.

In the case of subject ps10 the sLORETA images in Fig. 8.14 show similar activities before and after FES therapy especially for the left hand AM. It can be seen that the most reactive frequency band also remains as $\beta 1$ in before and after the FES therapy for the left hand AM. Furthermore, it seems that following the therapy, the right sensorimotor cortex is activated irrespective of the hand the subject attempted to move. This was shown in the wLI analysis where wLI values were always negative (see subject ps10 in Fig. 8.12); recall that negative wLI means right lateralisation. The active brain structures corresponding to the activities on the images within the ROI are shown in Table E.2 for the right hand and in Table E.3 for the left hand before and after the FES therapy. Similar brain structures as those active for subject ps5 are also active for subject ps10 following therapy. But a major difference between the two subjects is in the lateralisation of the activities. Comparing the result of ps5 (Fig. 8.13, Table E.1) with that of subject ps10 (Fig. 8.14, Table E.2 and Table E.3) shows that subject ps5 has a more lateralised activity concentrating in the sensorimotor areas than subject ps10. These results support a more positive change in the brain for subject ps5 receiving BCI-FES than for the subject ps10 receiving only FES.

In the above sLORETA analysis, results were presented only for the most reactive frequency bands. In order to present results for all the frequency bands, before and after therapies, time-frequency analysis is presented in Section 8.4.5.

8.4.5 Event related desynchronisation/synchronisation

Results of the ERD/ERS analysis are provided for the treatment and the control group. The ERD/ERS for the left hand AM is presented in Fig. 8.15. Due to insufficient number of subjects the scalp maps were plotted over a long period covering 500-2000 ms post execution cue in order to provide a more stable average. This period covers most part of the AM period and should help to avoid any artefact arising due to the mental processing of execution, AM initiation and termination cues. The results are presented in standard frequency bands

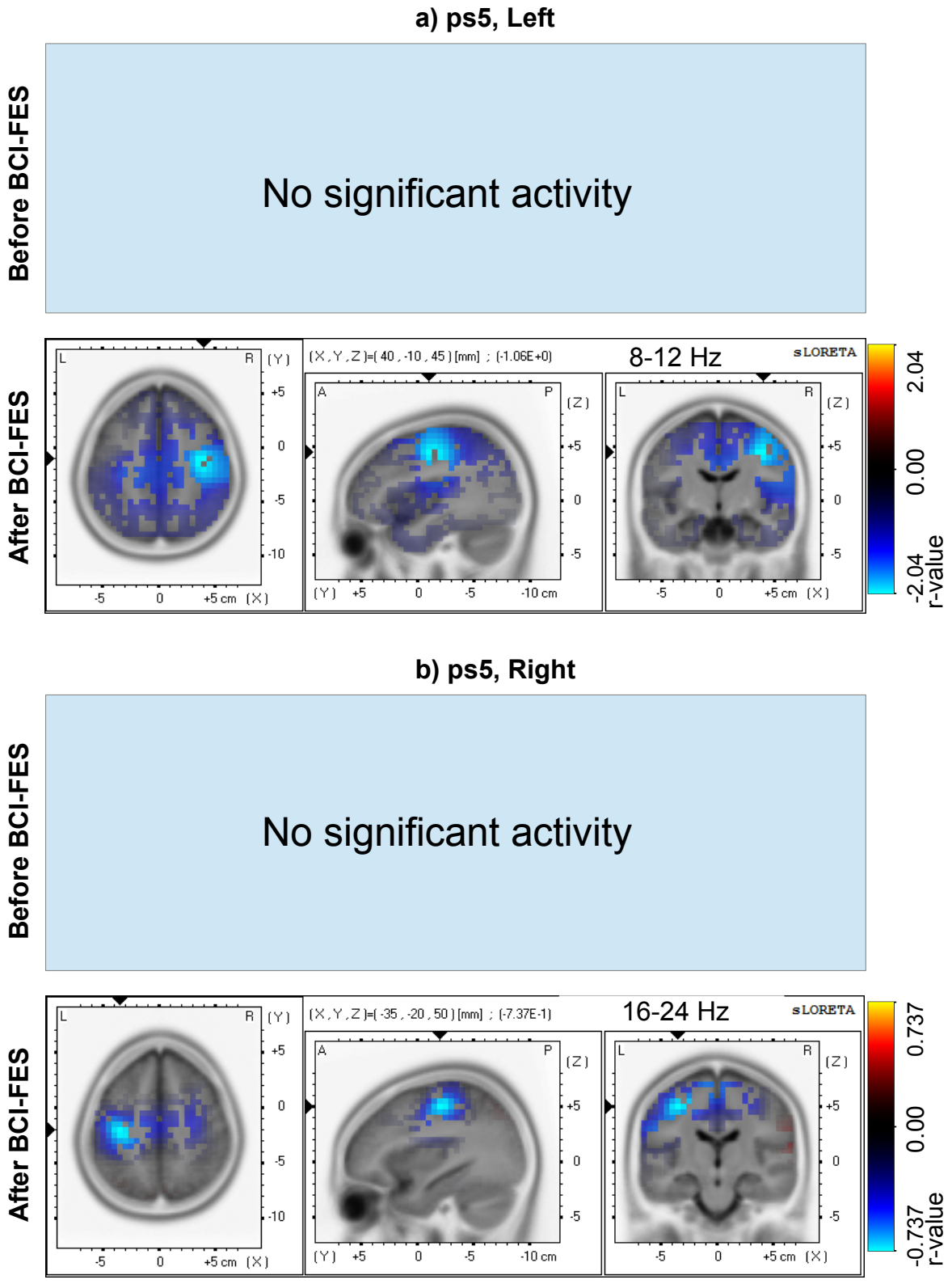

Figure 8.13: sLORETA localisation for subject ps5 for 'Before' and 'After' BCI-FES therapy

including θ, 4-7 Hz; μ, 8-12 Hz; $\beta 1$, 12-16 Hz; and $\beta 2$, 16-24 Hz. The θ band is presented because of the reported slowing of EEG in people with SCI who might develop neuropathic pain [227]. The subject in this study were not tested for neuropathic pain. It was not ad-

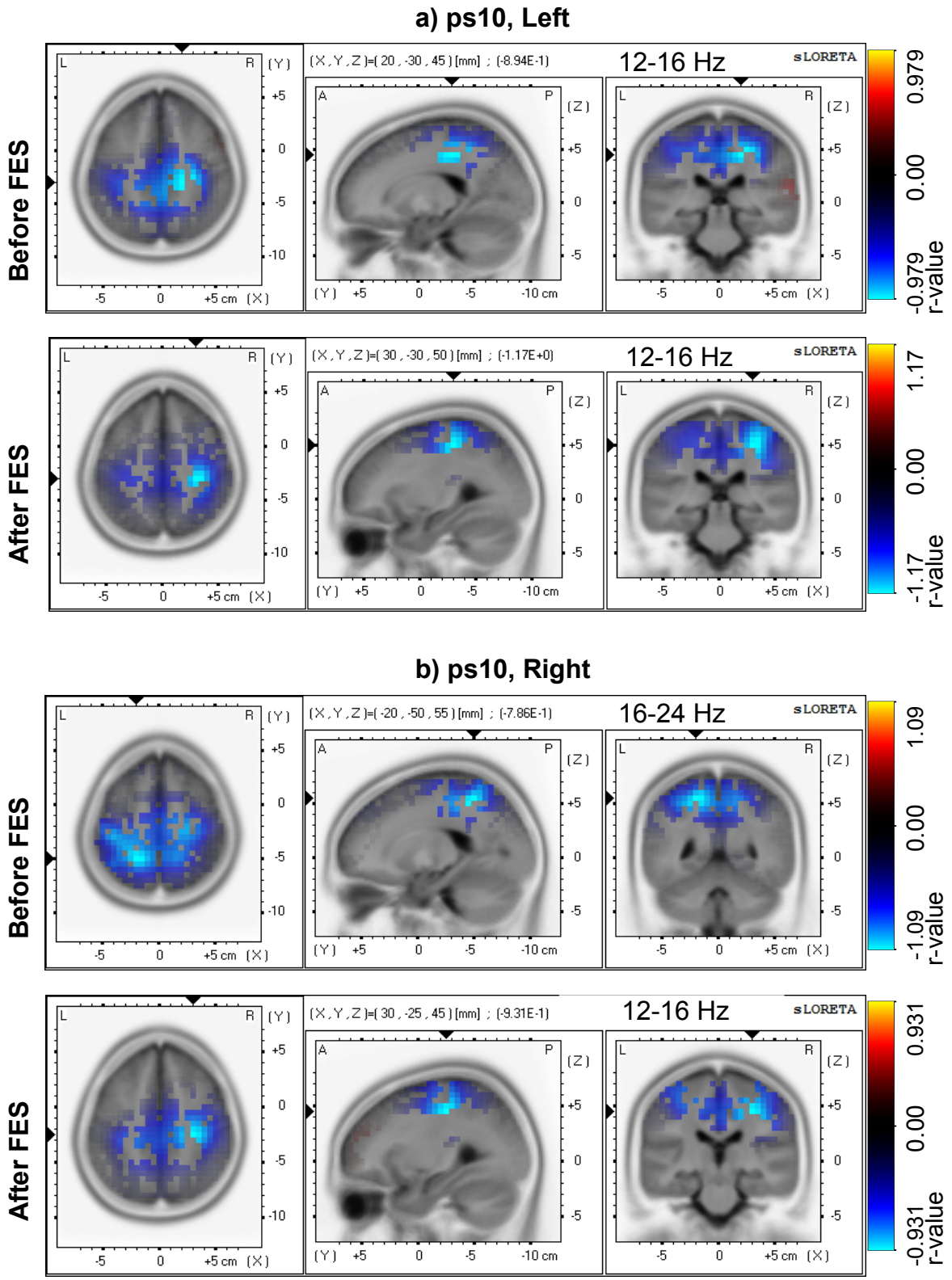

Figure 8.14: sLORETA localisation for subject ps10 for 'Before' and 'After' FES therapy. Motor activities are shown with negative r-values.

equate to perform statistical analysis of comparing ERD/ERS between groups given again insufficient number of subjects especially in the control group.

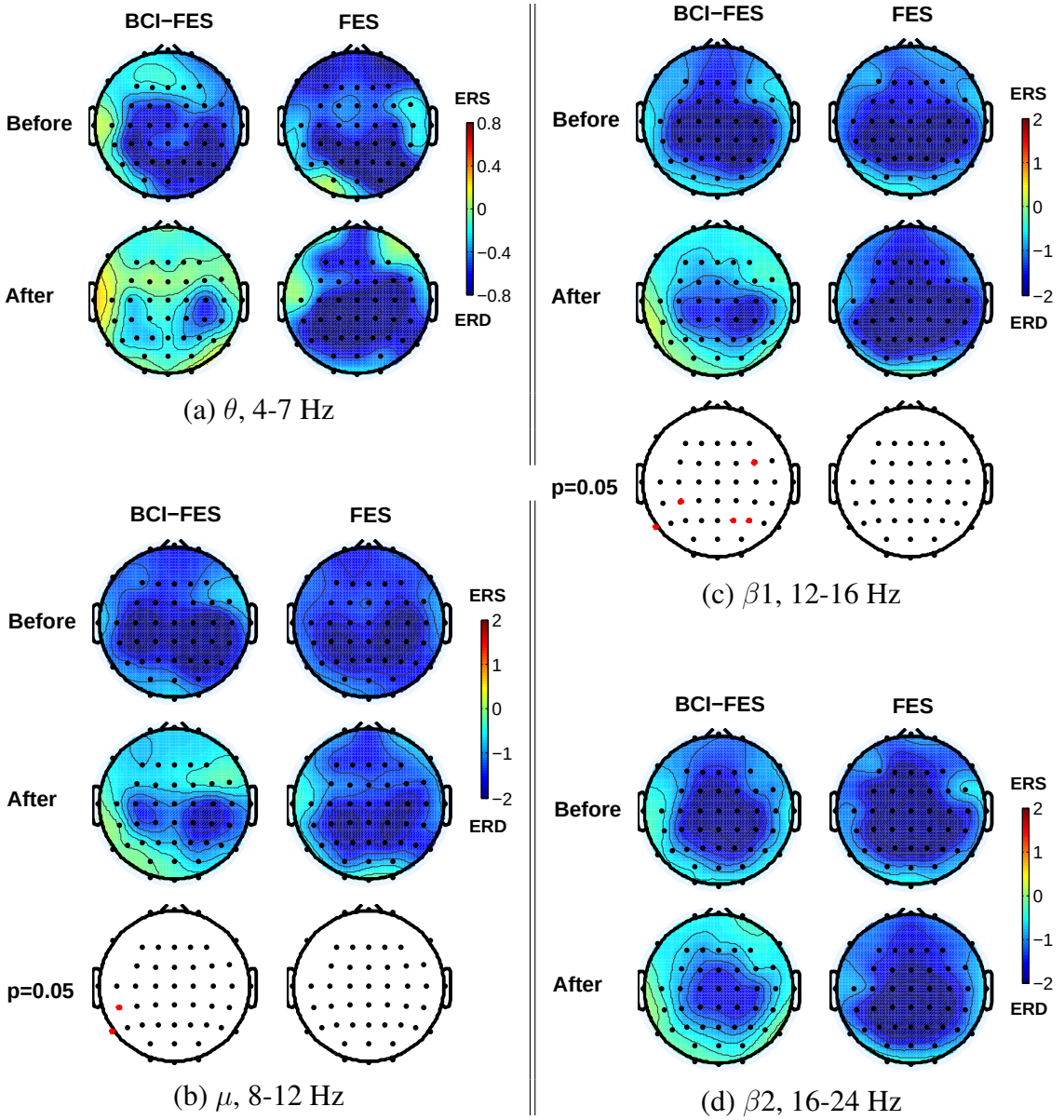

(a) θ, 4-7 Hz

(c) $\beta 1$, 12-16 Hz

(b) μ, 8-12 Hz

(d) $\beta 2$, 16-24 Hz

Figure 8.15: Scalp maps of ERD/ERS in different frequency bands at 500-2000 ms post cue during **left hand AM**. ERD is shown with negative values while ERS is shown with positive values. If present, the third row at each frequency highlights (in red) channels/electrodes that show statistical difference between the corresponding 'Before' and 'After' (p-values with Holm's correction for multiple comparison is indicated where available). The third row is not shown when there is no statistical significance between 'Before' and 'After'.

Starting with the θ band (Fig. 8.15a) ERD activities are strongly bilateral with strong presence in the posterior parietal cortex before ('Before') the therapy in both BCI-FES and FES groups. After the therapy ('After'), the ERD activities in the θ looks similar to how it looked before the therapy for the FES group. But in the case of the BCI-FES group, the activities in the θ band move anteriorly concentrating in the sensorimotor areas with lateralisation towards the right hemisphere after the therapy. This lateralisation is expected recalling that

the right hemisphere controls the left hand. This change in the location of ERD activities is a positive neurophysiolocal change based on what is seen on neurologically intact subjects [202].

The changes seen in the θ for the BCI-FES group look clearer in the μ band (Fig. 8.15b). Statistical comparison between before and after the therapy shows differences in only two electrodes (Cp5 and P7; albeit rather insufficient number of subjects for the statistics) indicating the anterior movement of the ERD activities to the sensorimotor areas. In the $\beta 1$ band (Fig. 8.15c), the ERD activities look similar to those in the μ band with more electrodes including Cp3, P7, P2 and P4, showing significant differences, strongly suggesting anterior movement of the activities for only the BCI-FES group. For the $\beta 2$ band (Fig. 8.15d), ERD activities looks similar before and after therapies in both the BCI-FES and the FES group.

The ERD/ERS scalp map results for the right hand AM is presented in Fig. 8.16 in the same frequency bands and time windows as for the left hand AM. Starting with the θ band (Fig. 8.16a) ERD activities are not strong before ('Before') the therapy in both BCI-FES and FES groups. In the BCI-FES group some ERD activities can be found in the central areas while for the FES group some activities can be seen in the left posterior parietal areas. After the therapy ('After') in the FES group, the ERD activities in the θ band appear towards the sensorimotor motor area ipsilateral to the right hand. This ipsilateral movement is opposite of what is expected because the ERD appears in the contralateral motor areas in neurologically intact subjects [202]. But in the case of the BCI-FES group, the activities in the θ band move to the contralateral hemisphere to the right hand as expected. This lateralisation is expected recalling that the left hemisphere controls the right hand. This change in the location of ERD activities is again a positive neurophysiolocal change based on what is seen on neurologically intact subjects [202].

Similar changes seen in the θ for the BCI-FES group can also be seen in the μ band (Fig. 8.16b). The bilateral ERD activities before the therapy became lateralised towards the contralateral hemisphere to the right hand. In the case of the FES group the ERD activities stay similar before and after the therapy.

In the $\beta 1$ bands (Fig. 8.16c), the statistical difference between ERD before and after the therapy shown in electrodes, P3, P1 ,Pz and POz confirms the anterior movement of ERD activities concentrating on the sensorimotor areas. Similar changes were not seen in the FES group in the $\beta 1$ band. For the $\beta 2$ band (Fig. 8.16d), ERD activities look similar before and after therapies in both the BCI-FES and the FES group.

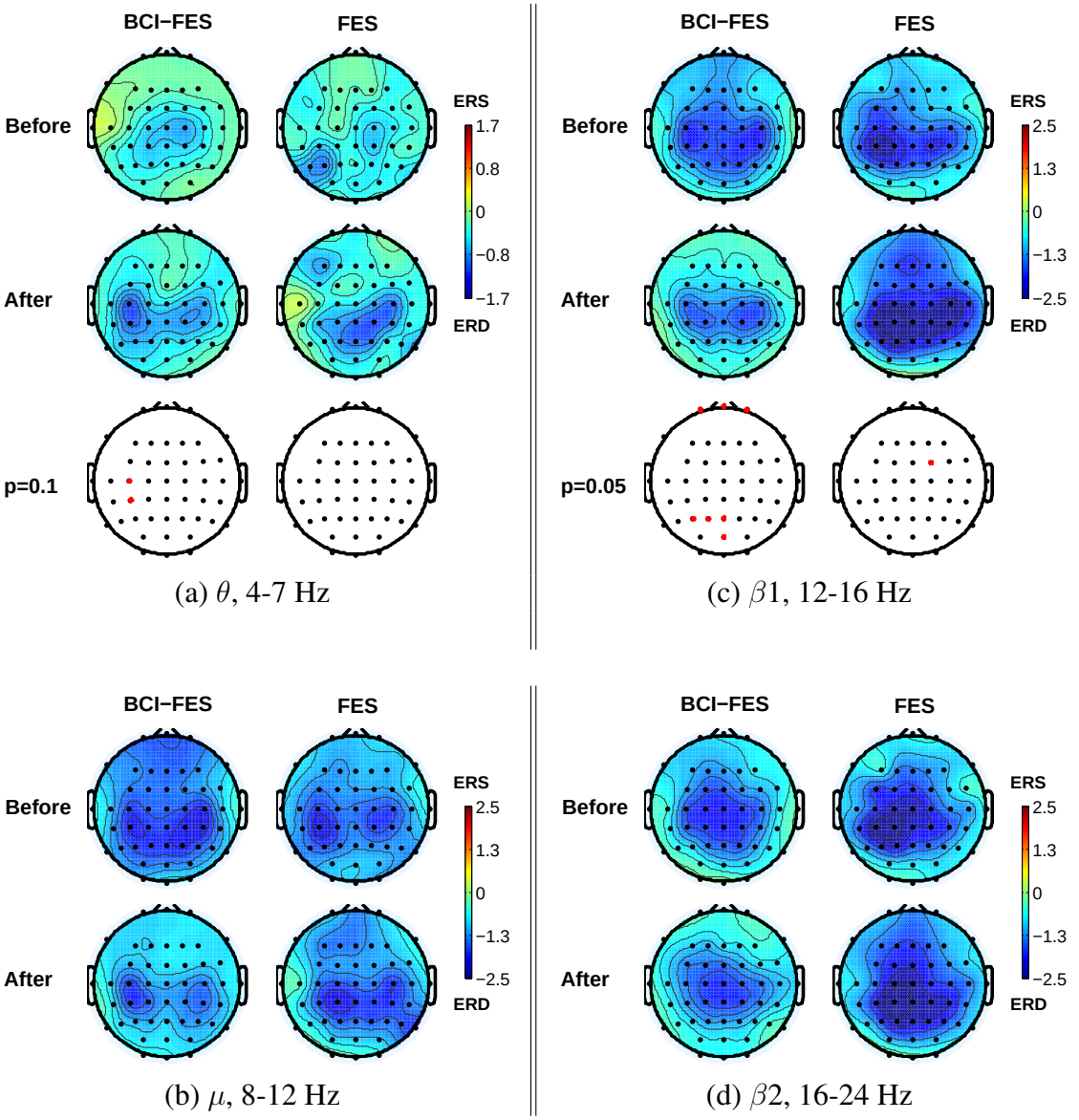

Figure 8.16: Scalp maps of ERD/ERS in different frequency bands at 500-2000 ms post cue during **right hand AM**. ERD is shown with negative values while ERS is shown with positive values. If present, the third row at each frequency highlights (in red) channels/electrodes that show statistical difference between the corresponding 'Before' and 'After' (p-values with Holm's correction for multiple comparison is indicated where available). The third row is not shown when there is no statistical significance between 'Before' and 'After' in order to save space.

8.4.6 Summary of MMT, SSPELI and LI

Table 8.10 provides a summary of the MMT scores, the SSEPLI and LI values. The LI values used were those computed at p=0.05. On the table, the SSEPLI and LI values with correct lateralisation are denoted with ticks while those with incorrect lateralisation are denoted with warning symbols. The SSEPLI and LI values with bilateral lateralisation are denoted with crosses. Note the bilateral lateralisation (crosses) is taken as the most undesirable lateralisa-

Table 8.10: Combined qualitative analysis of MMT, SSEPLI and LI.

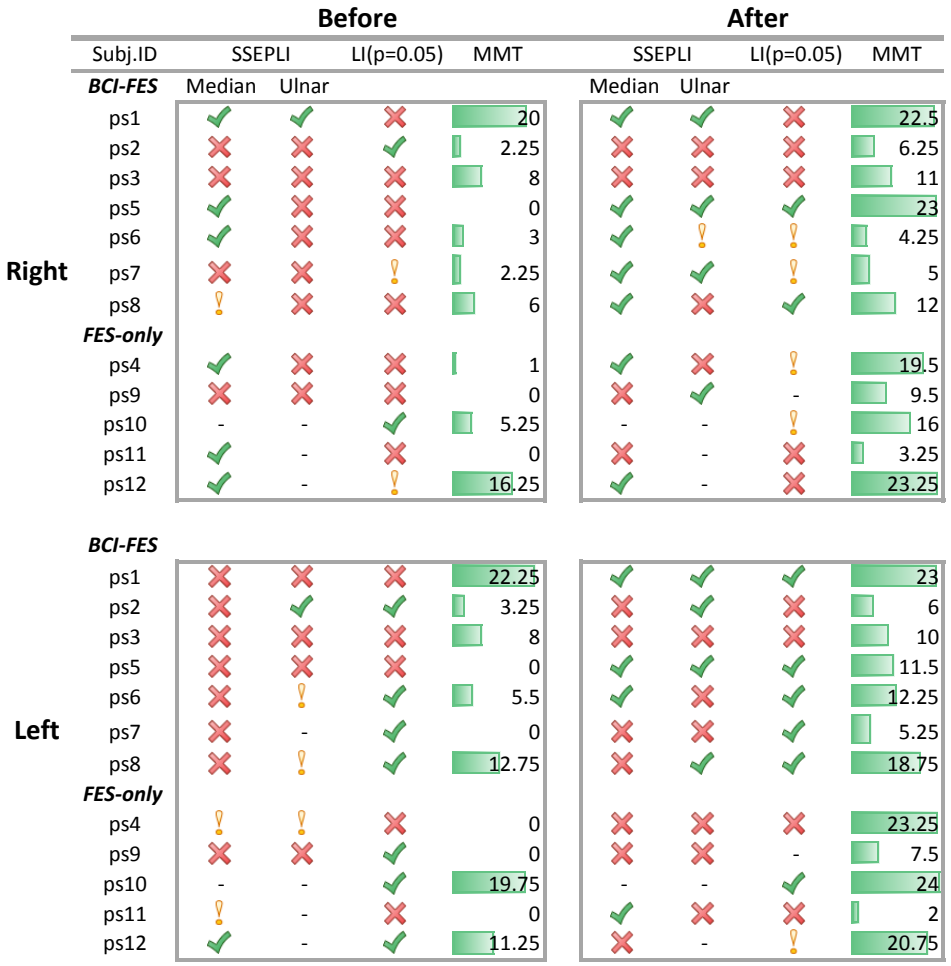

Notes: Please see text for the description of symbols and calculations on this table. Note that the 'After' MMT for patient ps4 was done much later after the neurological tests.

tion followed by the incorrect lateralisation (warning signs). On the table, the MMT values were obtained by summing the MMT scores for the hand and forearm muscles. The muscles included are the EDC, extensor digitorum communis; ECR, extensor carpi radialis; EPL, extensor pollicis longus; FCR, flexor carpi radialis; FDP, flexor digitorum profundus and the Intrinsic muscles. Only these muscles were considered because the median and the ulnar nerves' innervation are found in the hand and forearm and the AM task performed by patients required only hand movement.

Table 8.10 reiterates that in general there are neurological improvements for the BCI-FES but not for the FES group of patients following the therapies (Compare the amount of tick 'Before and 'After'). However the table also reiterates that both patients groups improved with regard to the MMT scores. As shown in earlier analysis, there is no evidence the BCI-FES group benefited more functionally given the MMT and the ROM.

The table shows a mixed result on the relationship between the MMT, SSEPLI and LI making it difficult to draw a conclusion from this small set of data. It is important to note here that

patients ps4 had a late MMT assessment after the therapy (see Table 8.1). So the MMT score for this patient may not correlate with the SSEPLI and LI values since both were not acquired about the same time. For the rest of the patients, there is a slight pattern suggesting a correlation between the MMT, SSEPLI and LI. For example, patients ps1, ps5 and ps8 had good neurological results (judging by the number of ticks) after the therapy which are reflected on their higher MMT scores. Furthermore patients ps2, ps3, ps9 and ps11 had poor neurological results which are also reflected on their low MMT scores. So with the exception of patient ps4, these results seem to suggest that MMT correlates with SSEPLI and LI. However, a numerical analysis on a larger set of data is required.

8.5 Discussion

In this chapter, the effects of BCI-FES and FES alone on functional and neurological outcomes were studied on sub-acute tetraplegic patients. Seven of the patients received BCI-FES therapy while five received FES therapy alone. The neurological outcome measures which included the AM of the left and the right hand and SSEP gave promising results in favour of the patients who used the BCI-FES. In the case of the functional outcome measures which included the ROM of the left and the right wrist and the MMT scores, there was no clear evidence that the patients in the BCI-FES group benefited more than those who use the FES alone. The results of the MMT especially was not conclusive; the BCI-FES group had better improvements on within-group analysis while the FES group performed just better on between-group analysis. It can be speculated that the length of the treatment was not enough for the neurological changes to reach a level that they may begin to effect considerably observable functional changes. Some FES therapy studies ran for longer periods of eight weeks and above [45, 221]. Furthermore the sensitivity of the ROM instruments and the sensitivity and the subjective nature of MMT might have made it impossible for any subtle functional changes to be dictated. However the observed neurological changes hold great promise for the potential of BCI-FES to enforce desirable changes in the CNS. This evidence, albeit rather modest, joins the two previously published studies [99, 100] in suggesting that BCI-FES may lead to a better recovery than FES therapy alone in SCI patients.

8.5.1 Somatosensory evoked potential

In the BCI-FES group, most of the N20 peaks were absent before the treatment but after the treatment most of the peaks returned. However in the FES group there were no changes in the number of N20 peaks before and after. Due to the insufficient number of subjects it was not possible to statistically compare the N20 status between the BCI-FES and the FES groups.

Therefore more subjects are needed in other to conclude on the effect of the treatment on the N20 peaks. However the status of the N20 peaks looks promising in proving that the BCI-FES group had a better return of the N20 peaks especially because the number of peaks did not change at all in the FES group. The returning peaks were overall accompanied by improved values of the SSEPLI showing correct lateralisation and validating the N20 peaks. The returning peaks should mean improved somatosensory functions. This in turn means better communication between the hand peripheral nerves and the central nervous system which should be significant for recovery.

8.5.2 sLORETA localisation

Weighted laterality index computed with sLORETA images shows a more promising result for the subjects who used BCI-FES than those who use FES alone. The wLI revealed that the lateralisation of brain activities during AM of the hands are more after the use of BCI-FES than after using FES alone. The brain areas activated in both the BCI-FES and FES groups are similar in some aspects but those found in the former have locations that are more similar to those in healthy individuals [141, 142].

sLORETA localisation showed that subjects who used the BCI-FES had in general contralateral activation of the brain hemispheres after the therapy. The brain activities concentrated on the precentral and the postcentral gyri with location corresponding to the hand sensorimotor areas that controls the hand [141]. These changes in the brain are in the desired directions especially for the subjects who went from zero significant brain activities to brain activities expected of healthy individuals during hand movement [141, 142].

Three subjects (ps2, ps3 from BCI-FES group and ps11 from FES group), who had severe injuries with ASIA score of B, did not show activities following the therapies. Instead subject ps2 who had correctly lateralised activities prior to the BCI-FES lost the activities after the therapy. It is worth mentioning that this subject did not complete the study in a timely manner and had many issues with his health that set the study back. Subject ps3 however completed the study in a more timely manner but did not show any activity before and after BCI-FES therapy. Another subject who had ASIA score B is subject ps7 whose wLI was similar before and after the BCI-FES therapy. The results obtained for all the subjects with ASIA score of B is consistent with the suggestion that the patients with this score did not benefit from the study. Given the amount of data available in the present study, this is only a mere suggestion.

8.5.3 Event related desynchronisation/synchronisation

The nature of the ERDs shown before and after the therapies by the BCI-FES and the FES-only group suggest strongly that the BCI-FES group benefited at least neurophysiologically

in the study. It is remarkable that the ERD activities in the FES group remain similar before and after the therapy while those of the BCI-FES group move closer to what is seen on healthy subjects. One of the notable changes in ERD activities in the BCI-FES group after the therapy is the contralateral positioning of the activities which is seen on healthy individuals [202]. Another notable change is the movement of the ERD from its posterior location before the therapy to a more anterior location towards the sensorimotor cortex after the therapy.

Posterior positioning of motor potentials has been described in SCI patients as part of cortical sensorimotor reorganisation following the injury [228]. Therefore changes to motor activities from posterior to a more anterior position should be beneficial. In Green et al. [228], a subject who made an excellent recovery from SCI had motor potential for the finger and toe movement relocate from posterior to more anterior locations. Such a change might mean that the sensorimotor cortext is once again reorganising in response to therapy. So the BCI-FES group benefited from this study given the anterior relocation of the ERD activities in this group.

8.6 Conclusions

The results obtained from this study have shown that BCI-FES may induce cortical changes in the desired direction at least quicker than FES alone can. The results back other studies that have shown the potential of BCI-FES in rehabilitation following neurological injuries that lead to movement impairment. Although the results are promising, further studies are necessary due to small number of subjects in the current study.

Chapter 9

Discussions, future work and conclusions

"As far as the laws of mathematics refer to reality, they are not certain, and as far as they are certain, they do not refer to reality.", Albert Einstein

9.1 BCI-FES on SCI patients

9.1.1 Results

The main results as presented in Chapter 8 were the outcomes on SCI patients using the BCI-FES system. The result of these patients were compared with the results of the patients using FES without the BCI. Comparing the two sets of results showed that the patients who used the BCI-FES system had better improvements. These improvements were found with outcome measures assessing neurological changes. The neurological changes following the use of the BCI-FES showed that during movement attempt, the activation of the motor cortex areas of the SCI patients became closer to the activation found in healthy individuals. The intensity of the activation and its spatial localisation both improved signaling desirable cortical reorganisation. Furthermore, the responses of the somatosensory cortex during SSEP were of clear evidence of better improvement in patients who used the BCI-FES. Missing SSEP peaks returned more for the BCI-FES group while there was no overall change in the group who did not use the BCI.

However, with the observed neurological changes there were no counterpart functional changes that suggested that those patients who used the BCI-FES were advantageous. Without functional changes, the neurological changes might be of no relevance to the patients since they have not got better hand functions. However, the neurological measures showing changes

from what is considered undesirable to desirable characteristics is definitely a result of neurorehabilitation. Most of the BCI-FES studies reviewed in Chapter 2 only use neurological measures for assessments making it difficult to compare results of functional outcomes. Possible explanations of equal functional change in both patients groups include short duration of the study and are discussed below as limitations of the study.

9.1.2 Limitations

Study duration

Patients were scheduled to attend only 20 sessions for the BCI-FES study described in this thesis. This short duration of the study might have contributed to the reason that the patients who used the BCI-FES did not show better functional improvement. It is possible that longer period like in some FES studies [45, 221] is required in order for the neurological changes in the patients to be reflected in the functional changes.

Number of subjects

The BCI-FES study in the current thesis provides the first controlled study on SCI patients. The study however is hampered by a low number of subjects which is also the case with many past studies of BCI-FES. Larger controlled trials are required to average out the different recovery rate patients may experience where two patient with similar level of injuries may show different recovery rate. Larger controlled trials are needed not just in studies on stroke patients but also on chronic and sub-acute SCI patients who have received less attention in the studies so far. Patients with SCI should have intact brain functions since the injury is in the spinal cord and therefore should be able to control a BCI. Results from SCI patients will give new insight from a different perspective on the benefit of using BCI-FES after neurological injuries.

Suitability of patients

Some of the patients who took part in the BCI-FES therapy had high level injuries and these patients had the least or no improvement. One important question then is who is suitable for a BCI-FES study. Patients who do not have at least preserved proprioception/sensation (required for proper movement [229]) following injuries are not expected to control the BCI [229, 230] due to disrupted cortical motor processes when imagining movements. Another issue is that patients who do not have preserved proprioception/sensation in the limbs for example normally have severe injuries [231]. In the case of SCI these patient might have

complete injuries where recovery is less likely [232]. Such patients with complete injuries might not be suitable candidates at this experimental stage of BCI-FES due to their low probability to recover in general. In this early stages, attention should be focused on patients who have mild/incomplete injuries so that an establishment can be made on the therapeutic benefit of BCI-FES. The recovery probability of the targeted patient groups worths consideration in new BCI-FES studies.

One of the difficulties experienced during the study in this thesis included the uncertain health of the patients. Some of the patients took ill and some suffered from bed sores and other illnesses associated with SCI during the study. This caused discontinuities in the delivery of the therapies since the patient could not receive the therapy when feeling unwell. In some cases the final assessment therapies were delayed and this may have affected some of the results obtained here. The most notable of this was a patient, among those who did not use the BCI, whose manual muscle testing was done considerably late after the therapy. This is important because this patient may have had functional changes that would be different if the assessments were done at the correct time following the therapy when other subjects were assessed.

9.2 Other results

9.2.1 Motor imagery in mental rotation

In Chapter 4, an experiment to confirm that a form of movement imagination is involved in mental rotation of body parts was an important result of this thesis. The similarity of the two has long been debated and there have been some evidence as highlighted in Chapter 4 to suggest that a form of movement imagination is involved in mental rotation of body parts. This experiment made a direct comparison which was missing in the literature, of data from movement imagination and mental rotation to find that both have similar characteristic. The characteristic is the nature of the activation of the sensorimotor cortex. Given the similarities of the two, Chapter 4 suggested that mental rotation should be used in rehabilitation of movement in a similar manner as movement imagination.

9.2.2 Index of lateralisation

Laterality index discussed in Section 3.3 is an assessment measure usually performed with fMRI data. This thesis showed how the index can be computed using EEG localised in the cortex with sLORETA tool. Using EEG for the computation makes the LI a more interesting measure. This is because the LI can be studied at high temporal resolution and also very

interestingly, it can be studied at different frequencies. Although it might be more difficult to make sense of the LI due to its various time-frequency values, the increased dimension when using cortically localised EEG may lead to a more precise interpretation of results.

Another index of lateralisation, SSEPLI, was studied in Chapter 7. The method of computing the lateralisation index of SSEP is not well-established even though it is perhaps not surprising that SSEP amplitude is lateralised in healthy individuals. Following a more established method for LI computation, a method of computing an index of lateralisation of SSEP called SSEPLI was defined. The robustness of the method was showcased in Chapter 7 and as claimed in the chapter, SSEPLI is a good measure which can validate and predict the existence of SSEP peaks.

9.3 A look at current methods of BCI-FES system design

Since the publication of the first studies of BCI-FES [67, 103], several designs of the system have been used in rehabilitation. Due to the differences in these designs it can be difficult to compare or merge results in order to determine if BCI-FES significantly contributes to positive rehabilitation outcome. Some studies might have obtained positive results with BCI-FES simply because it contributes to positive rehabilitation outcome as expected. Some other studies might find benefits of using BCI-FES in rehabilitation because of other factors that played parts during the therapy period. Such factors that could play parts include natural recovery, conventional treatment, FES and BCI individually. Any of these could confound the effect of BCI-FES although recent cross-over and controlled studies [82, 101, 102, 105] including the present thesis attempting to isolate BCI-FES rehabilitation effects have got positive results. Although promising results have been obtained, an improved design of the BCI-FES system might further improve the results. It is important to note that there are not many published rehabilitative BCI-FES studies since the first study in 2009; possibly because only the few published studies got positive results. Speculating, the negative results might be due to improper designs but it could also be due to ineffectiveness of BCI-FES therapy. Some studies may not find that BCI-FES significantly contributes to rehabilitation outcome simply because the design and delivery of the therapy was inadequate. More importantly a negative result could be obtained because of the nature of the injuries sustained by the chosen subjects; if the injury is severe a patient will be normally unlikely to recover and therefore might not respond to BCI-FES therapy positively as discussed in Section 9.1.2. There is a need for a well designed BCI-FES system that can be similarly adopted by all researchers. This will ensure that BCI-FES is properly tested for its therapeutic benefits and also researchers can easily compare their results.

9.3.1 BCI design and protocols

Mental strategy

It is well known that MI activates similar brain regions as physical motor actions. Several studies have shown that MI has therapeutic effect in motor rehabilitation [83, 84, 85]. But the claimed therapeutic effect of MI has been challenged [233]. As discussed earlier in Section 2.3.1, one refrain from performing an action if one is truly only imagining the action. For motor rehabilitation it would be better if a patient practises the motor action as close as possible to normal practice. Refraining from performing the action would not correspond to normal physical practice. In addition, patient might have reduced imagery ability [230, 234, 235]. Therefore it would be better if patients instead use AM. With AM, patients can more easily mimic the actual action. They can also easily understand the paradigm than when asked to imagine abstractly.

Signal source

Usually a BCI classifier is computed for a patient using BCI for rehabilitation in a similar manner as healthy individuals. In the case of the patients, the signal used to compute the classifier may have been affected by the injury. For example, due to reorganisations in the brain and other factors the EEG corresponding to the left hand movement attempt may differ from that prior to SCI. Using such a 'malformed' signal for rehabilitation of the hand may not give the best results. The aim of rehabilitation of the left hand will be to bring the functioning of the hand as close as possible to what it was prior to the injury. In order to achieve the best results, it is theoretically advisable to use a signal obtained during the normal workings of the hand which can be obtained prior to the injury. Since this optimal signal is often not available the next option will be to approximate it. The approximated signal is hopefully better than a malformed version. The issue then is how to approximate the signal. A starting point is to use signals recorded from healthy individuals. Such signals averaged from a large number of individuals provide data representing the signal in humans. Since the averaged signal may not be specific to an individual, experienced persons can add modifications after studying a patients own 'malformed' signal. Using ERD phenomenon in EEG during hand movement as an example, it may not be necessary to modify the averaged signal given that the individual differences occur majorly at different frequency bands which usually overlap and are within only two distinct physiological bands namely the α and the β-bands defined within 7-30 Hz. So a patient's optimal EEG signal for rehabilitation would not be vastly different from that obtained from a cohort of healthy individuals.

EEG feature

One of the most important aspect that should be considered when choosing parameters is the setup time. When a long setup time is required in rehabilitation application, patient might be left tired or even asleep before the setup is completed. In addition, hospitalised patients may only have limited allowed time for each therapy session and it will be unhelpful to spend most of the available time setting up the system. Long setup times can be caused mainly by (1) the use of large number of electrodes (e.g $>$16) and (2) the need to record large amount of classifier training dataset. The second will be discussed later. The first can be avoided by choosing EEG features that do not require large number of electrodes for classification. Example of such features includes the TDP or bandpower methods and the CSP method based on about sixteen channels. An advantage of the CSP method is that it offers good classification accuracy. The TDP and the bandpower methods however allow the use of fewer electrodes placed in desired physiological locations and the bandpower method has been used in BCI-FES more than the other features as can be seen from Table 2.2.

The TDP method was used in this thesis, instead of the bandpower method, where it was shown to be a good feature for a therapeutic BCI. It mainly deviate from the classical bandpower method because it does not require narrow band filtered signal. A possible drawback of the classical bandpower method is this requirement to select subject specific narrow frequency bands. This is unlike in the CSP methods where a classical frequency band of 8-30 Hz incorporating the so called α (8-12 Hz) and β (13-30 Hz) bands is used. Using a single wider frequency band in the range of 8-30 Hz for bandpower will contribute in three main ways. (1) Power calculation can be more accurately performed in shorter time windows. (2) The use of a single frequency band leads to a reduced feature dimensionality which should favour a classifier like LDA that works by reducing the dimension of the features. (3) A more general classifier can be obtained since all relevant frequency band is included. The TDP method used in this thesis gives these three benefits. Despite using wide band filtered signal, narrow bandpower changes in the α and β bands can still be targeted [236] with TDP. This is because during AM for example, bandpower changes should only occur dominantly in narrow α and β bands so the other frequencies would be redundant in the decision of a classifier. A large band of 8-30 Hz can even perform better than narrow frequency bands [129, 237].

Traditional BCI has relied on features that are directly dependent on EEG power. In the bid to move BCI research forward, there is the need for future investigations to look at other methods. For example, using connectivity between EEG sources [238] or the connectivity between EEG channels [239] should be further investigated. Such methods might offer improvements in BCI [239].

Feature classifier

The LDA classifier has been shown to be a good classifier in BCI. From Table 2.2, it has been often used in BCI-FES. One advantage of the LDA classifier is that it is relatively straight forward to update online as shown in Section 3.1.2. The classifier weight and bias can be updated online depending on the deviation of the values of the feature matrix [130]. Updating the classifier online has two main advantages. (1) A previous classifier can be reused by updating it online and changes in the feature characteristic during a BCI session can be accommodated. (2) There is no need to record large amount of training dataset since a small training dataset can be used to compute an initial classifier which can be updated online. This reduces setup time significantly.

In order to achieve the uttermost classification accuracy, classification should be performed on one AM against the resting/relaxed state. Most researchers as shown in Table 2.2 have chosen this scheme. This means that during a rehabilitation session, the restoration of one movement is targeted at a time. The benefit is that the reduced number of false positives that may arise when classifying between two active tasks may result in better rehabilitation outcome.

Performance feedback

Since feedback plays an important role in BCI and in rehabilitation, the provision of timely and accurate feedback is necessary. From the past BCI-FES studies shown in Table 2.2, the authors have used visual, audio, tongue stimulation and tactile feedbacks. Some authors use a combination of visual and audio feedbacks.

The feedbacks should be continuous rather than binary based since a continuous feedback is more natural like the normal continuous visual input to the brain. Possibly the best feedback would constitute a visual feedback in which the patient watches his/her own body physically moved (by FES) continuously to complete the movement the patient initiated. This would feel more realistic and could better encourage rehabilitation.

It is useful for the patient user to be given a score of their ability to control the BCI system. Such a score can motivate the patients and help in their active participation. The score can also give a meaningful measure of a patient's progress on the use of the BCI system. In order to compute a meaningful score across sessions, there might be a need to obtain a method of comparing different BCI sessions. This is because due to variations in settings and setup in different sessions, a user might have a different control level at each session. This can be dealt with by setting a difficulty level and keeping it the same in each session. A method of setting the difficulty level is described in Section 3.1.4.

9.3.2 Timing and intensity modulation of FES

Contingency of events is a key factor in the Hebbian or associative learning mechanism [240]. Another factor, contiguity, the temporal association/correlation between the events also plays an important role [59, 62]. Mrachacz-Kersting and colleagues [62] using EEG recently demonstrated that precise temporal association between events produces a larger effect. They assessed cortical excitability changes following repetitive voluntary activation of the motor cortex (using MI) associated with artificially generated sensory stimulation. They found that the cortical excitability changes were strongly dependent on the temporal association between the motor cortex activation and the sensory stimulation. Only when the temporal association was precise were the cortical excitability changes significant. Mrachacz-Kersting's experiment stresses the need to ensure timely association between movement initiation and FES onset. Having a large time lag between them might not lead to the desired effect as the association between them might be lost. The question here is how long is too large? An experiment on monkeys showed that a time less that 50 ms is adequate [63]. However, it is important to note here again that although contiguity is necessary, contingency is the key requirement for associative learning [59, 240] . For this reason, attention should be paid to a more accurate BCI and performing many repetitions. This is not to say that temporal association (time lag) should be ignored. The time lag should be kept reasonably short. This time lag between movement initiation and FES onset is not normally reported in BCI-FES studies. A study with such a report was that by Do and colleagues [108] who showed that the time lag was 1.83 s in their experiment. The time window used for BCI analysis significantly contributes to the time lag. By reducing the time window, the time lag can be reduced although the accuracy of the BCI might be compromised. So the time lag should be chosen without compromising the accuracy of the BCI and without losing the temporal association. Using event related potentials as BCI features [241] might help to reduce the time lag. This is because event related potentials can have clear and sharp peaks and usually occur within milliseconds of the eliciting cortical event. The peaks which can be precisely detected should help to significantly reduce the time lag as in [62].

All the articles referenced in Table 2.2 have used a binary control of FES. This means that FES is either activated or not activated. The intensity of the FES was not modulated. Some authors (e.g see [82]) ramped the FES intensity such that the FES intensity slowly increment when activated and slowly decrement when deactivated. But in motor rehabilitation for example, it might be more adequate to modulate the intensity of the FES based on some measure of voluntary motor initiation attempt. Such modulation of FES will further act as a more natural feedback correlating the attempt level to FES intensity and therefore the degree of movement caused by the FES. This will also help to engage a patient who would want to increase the intensity of the FES in order to complete a movement. A patient would clearly

know when he/she is doing below what is expected because they can feel the intensity of the FES.

One measure that could be used to modulate the FES intensity is the degree of desynchronisation of EEG signal recorded over the motor cortex during a motor attempt. This can be done by introducing a threshold of ERD that activates the FES. Above this threshold, the values of the ERD can proportionally determine the intensity of FES. The intensity of FES can be modulated accordingly by either varying the current or the pulsewidth.

9.3.3 Recommendation

In BCI-FES, a subject voluntarily activates FES usually with MI/AM of a body part. The subject is instructed to perform the action to activate the FES but without any clear instruction of what the subject should do following the activation/onset of the FES. Subjects should be instructed to continue the performance of the MI/AM even after the onset of the FES. This is because a recent study [118] has shown that the activation of the motor cortex is reduced if MI/AM is halted following the onset of FES. However continuing the MI/AM following the FES onset results in better activation of the motor cortex.

As it has been stressed throughout this thesis, new large controlled studies of BCI-FES are required. The new studies should use well designed and practical BCI-FES systems.They should employ more natural continuous feedbacks including the continuous modulation of FES intensity which could have positive effect on the outcome of a study. Also using accurate and timely feedbacks and presenting the system in form of a computer game could encourage active participation of patients.

Effort should be made to reduce the time lag between action initiation and FES onset. This is to increase temporal correlation between the two events in order to encourage Hebbian learning. As regards to therapy delivery, parameters of consideration include the number and frequency of sessions and the length of each session or the number of trials per session. A guide to these and the suitable sensitive outcome measures can be emulated from previous studies listed on Table 2.1 who had positive results. With a careful selection of BCI-FES system and therapy delivery parameters it will be possible to conclusively determine the fate of BCI-FES as a tool for inducing neural plasticity.

9.4 Conclusions

This thesis mainly studied the use of BCI-FES for neurorehabilitation of hand functions in SCI patients. The thesis further studied the possibility of using mental rotation in neurorehabilitation and also investigated assessment tools and BCI-FES configurations that are

suitable for patient's therapy. A BCI-FES system was developed and used to deliver neurorehabilitation hand therapy on patients with SCI. After the BCI-FES therapies, neurological assessment measures revealed that the patients had had desirable cortical reorganisations. This shows that brain computer interface-controlled therapy has a potential in neurorehabilitation.

Appendix A

Supplementary materials

A.1 Software tools

A.1.1 MATLAB

Unless otherwise stated, analyses in this thesis were conducted under MATLAB and Simulink (MATLAB R2012a, The MathWorks Inc., Natick, MA) environments under Windows operating system. The MATLAB and Simulink environments allowed the execution of JAVA, C and C++ codes which were used in this thesis.

A.1.2 BIOSIG and rtsBCI

The BIOSIG and rtsBCI toolboxes [169] were predominantly used in this thesis for EEG data classification and construction of BCI paradigms respectively. The rtsBCI is a Simulink library which requires BIOSIG to work. The GDF file format recorded with the paradigms built with the rtsBCI can be imported directly into EEGLAB for further analysis.

A.1.3 EEGLAB

EEGLAB is a well known tool used predominantly for EEG data processing [176]. It is an MATLAB toolbox with numerous tool-sets for EEG signal analysis. In this thesis, analysis of EEG signal which included format conversion, segmentation, concatenation, artefact removal, ERD/ERS analysis and visualisation were performed with EEGLAB. The toolbox implements tools such as the independent component analysis (ICA). This ICA decomposes EEG signal into maximally independent temporal components using the logistic infomax algorithm [174, 175]. The ICA was used in this thesis for artefact removal.

EEGLAB implements methods for group analysis of EEG data. The group analysis which was heavily used in this thesis includes advanced statistical methods making it possible for an EEG analysis to be started and completed without the need to leave EEGLAB for statistical analysis in other software. The version of EEGLAB used in this thesis is the 12.0.2.5b.

A.1.4 sLORETA

Localisation of the cortical three-dimensional distribution of current density of EEG in this thesis was done using the Standardized Low Resolution Electromagnetic Tomography (sLORETA) [224]. The method is a linear minimum norm inverse solution to EEG 3D localisation inverse problem. The sLORETA (estimated current density) cortical map/image is computed for 6239 voxel partitions of intracerebral volume at 5 mm spatial resolution. Brodmann areas are reported using the Montreal Neurological Institute (MNI) space with correction to the Talairach space [225, 226].

EEG and sLORETA

While being spatially less accurate than fMRI and PET, EEG is suitable for analysing extracellular electrical field potentials recorded from the scalp with milliseconds resolution in different frequencies which is important in studying dynamic processes in the brain [23]. It is a measure of neuronal electrical activity and not haemodynamic response, the later having latency between a task and the related brain activity. The ERD/ERS method can reveal time-frequency characteristics of cortical processes but it cannot ascertain precise location of that activity; furthermore it can provide spatially averaged activity over the surface of the cortex only. Multiple EEG sources can be simultaneously localised using source localisation tool such as sLORETA at the expense of low spatial resolution. Given this sharp resolution, neighbouring neuronal sources in the sLORETA localisations will be highly correlated but fMRI and PET studies have produced similar localisations as those presented in this thesis. It is important to point out that sLORETA has been extensively validated and found to have no localisation bias [242, 243, 244]. A previous version [245] has already been validated with fMRI [23, 246], structural MRI [247], and PET [248, 249, 250].

Appendix B

Supplemental materials on BCI-FES system

This section presents the operations of the BCI-FES system. It shows how the BCI-FES software created in this thesis works.

B.1 Running the BCI-FES system

The BCI-FES system is accompanied by a graphic user interface. The main user interface is shown in Fig. B.1. The following are the required steps for running the BCI-FES system designed for use with patients.

1. *Setup:* At the start of a session, the subject wears an EEG cap with three sets of bipolar electrodes at locations Fc3, Cp3; Fcz, Cpz; and Fc4, Cp4. The g.tec bioamplifier is set to record EEG at 256 Hz with bandpass filter set to 0.5-30 Hz.

2. *Initial classifier computation:* Next, an initial classifier is computed. The data for the classifier is obtained using a cue based paradigm similar to that described in Section 4.3 and Fig. 4.1a. In the paradigm, the subject is presented with execution cues that alternate randomly. When the cue is an arrow pointing to the left, the subject performs an AM of the left hand. When the arrow points to the right, a right hand AM is required. The hand movement is the opening and closing of the hands. A trial which consist of one hand AM lasts for 6000 ms. The subjects relaxes from t=-3000 to t=0 ms. The execution cue is shown at the time t=0 ms. The subject performs the AM from the time t=0 to t=3000 ms. See Section 4.3 and Fig. 4.1a for the full details of the paradigm. The data recording using this paradigm is started by clicking on

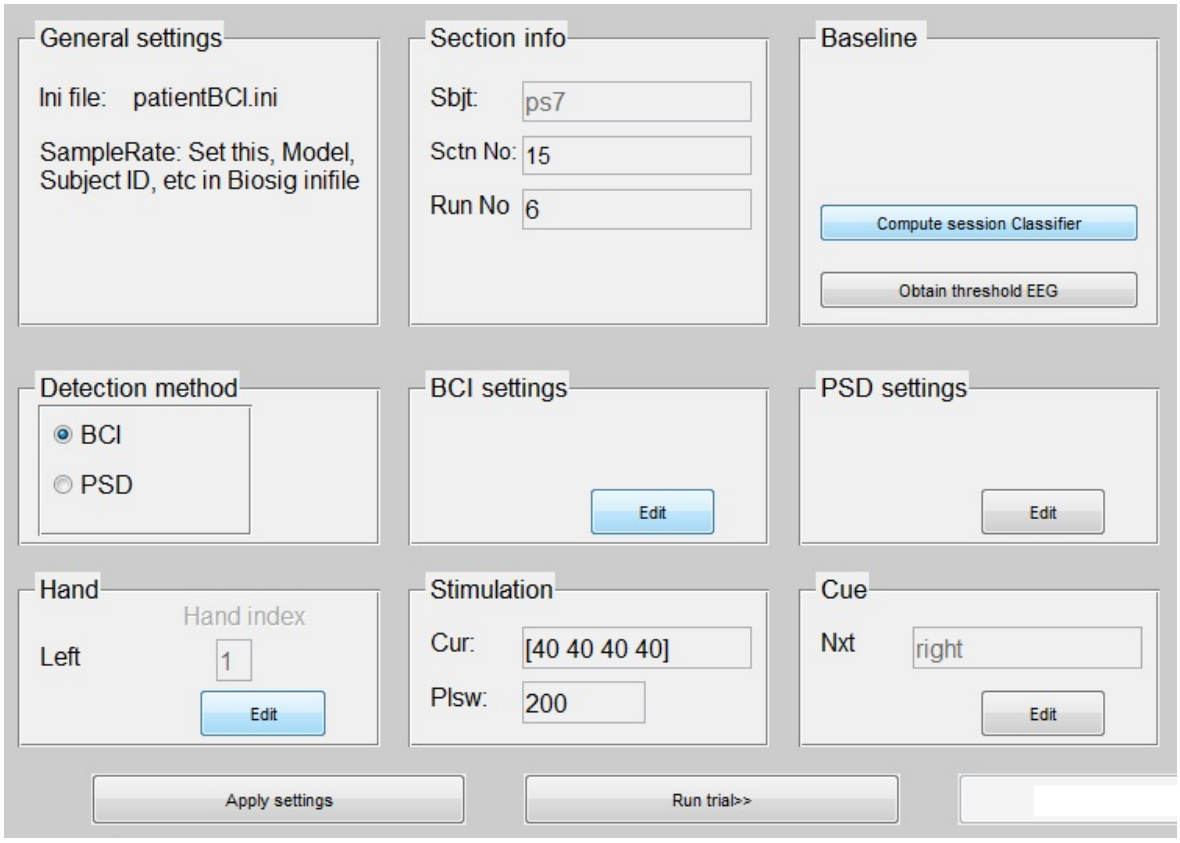

Figure B.1: The main graphic user interface for the BCI-FES system. Cur, Current; Plsw, Pulsewidth; Sbjt, Subject; Sctn No, Section number.

the button,'Record classifier data' in Fig. B.2. At default settings, about 20 AMs are recorded of each hand.

After recording, the data is visually inspected using the ERD/ERS maps by clicking on the button, 'View ERDS' in Fig. B.2. By observing the ERD/ERS maps, two most active bands are entered in the text boxes as shown in Fig. B.2. These bands are only needed for computing bandpower-based classifiers. For patients, TDP features are used instead of bandpower features.

The classifier is obtained by clicking on the button, 'Compute classifiers' in Fig. B.2. Classifiers are created and stored for the classification of the left hand AM versus relaxation and for the right hand AM versus relaxation. Relaxation corresponds to periods prior to execution cue presentation.

3. *Classifier loading and settings:* The next step is to load one of the classifiers computed in the previous step and set classification parameters. The user interface providing these functions is shown in Fig. B.3. Loading a classifier is done by clicking on the button, 'Load classifier'. Then a method of classifier adaptation is selected (see Section 3.1.2 for classifier adaptation). The method chosen for patients is the supervised mean and covariance adaptation. The adaptation periods in samples within a trial and the

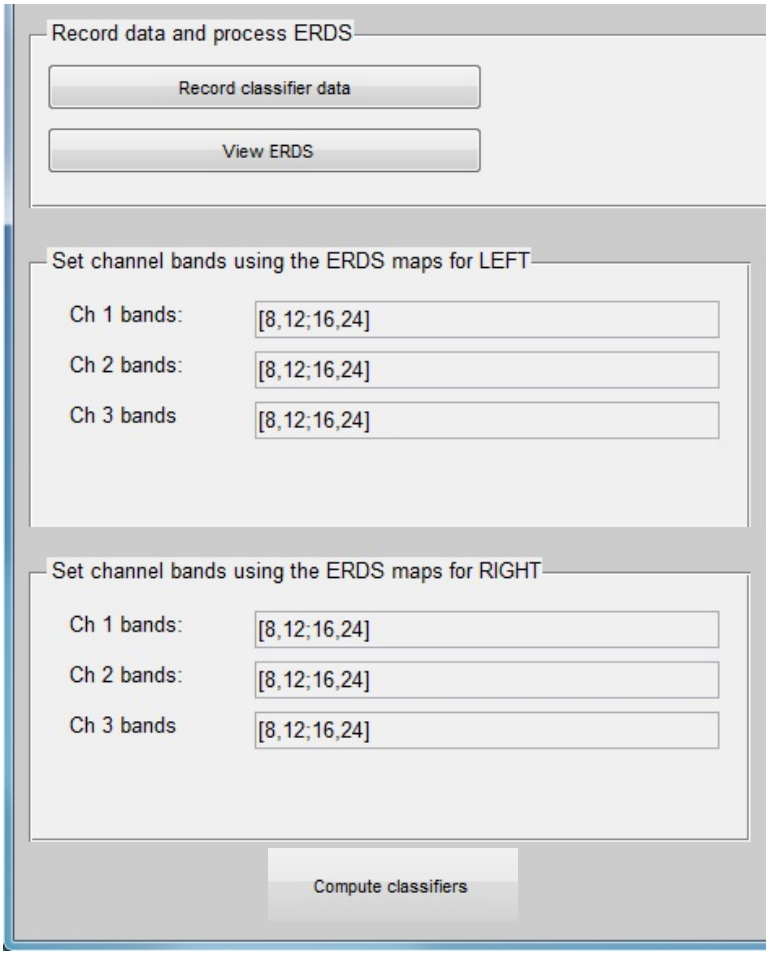

Figure B.2: User interface for classifier computation.

update coefficient, UC are as shown in Fig. B.3.

4. *BCI-difficulty:* After loading the classifier, the BCI is run to determine settings that reduce false positive activation. This is done by setting the BCI-difficulty discussed earlier in Section 3.1.4. Depending on the ability of a subject to activate the system, the BCI-difficulty was varied during the session.

5. *FES settings:* The FES settings are done in the main user interface window in Fig. B.3. The system provides four FES channels. The desired current for each channel is set and universal stimulation pulsewidth is also set as shown in the figure.

6. *Run:* The system is started from the main window shown in Fig. B.1 by clicking on the button, 'Run trial'. At the beginning of a trial, the subject is told to relax with a message on a screen. During this time the classifier adaptation is performed in the period corresponding to the samples 125-507 (relaxation period) as set in Fig. B.3. Recall that the EEG recorder samplerate is set to 256 Hz. The relaxation period ends at sample 768 or t=3000 ms and at this time the subject receives a cue to begin AM. The classifier is updated again in the period corresponding to the samples 894-1276.

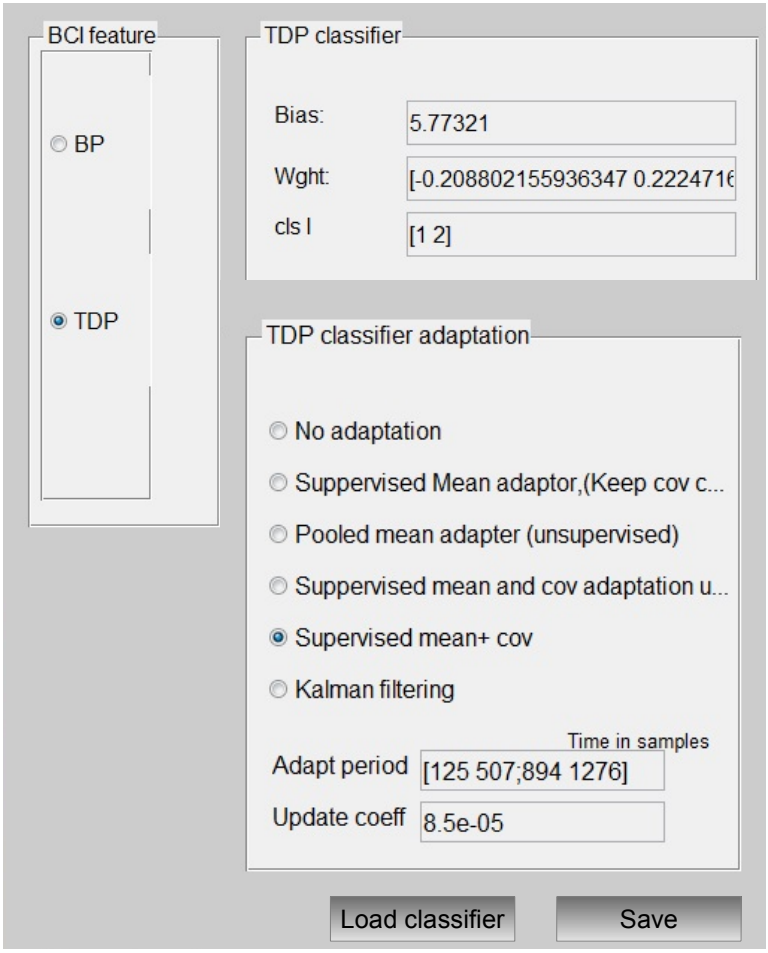

Figure B.3: Graphic user interface for classifier loading settings. Wght, Weight; cls l, Class label; BP, Bandpower; Update coeff, Update coefficient. Note that 'TDP classifier' refers to LDA classifier computed with TDP features.

The trial ends when the subject activates the FES and the stimulation has lasted for 10 s. This procedure is repeated about 20 times before the subject is allowed to rest.

Appendix C

Supplemental materials on LDA

This section provides the mathematical derivation of the Fisher's criterion. It also presents an example of LDA implementation in MATLAB.

C.1 LDA

C.1.1 Derivative of the Fisher's criterion

Table C.1: Taking the $\frac{d}{dA}J$ of Equ. 3.23 and equating it to zero.

The $\frac{d}{dA}J$ can be obtained using the Quotient Rule:

$$\begin{aligned} \frac{d}{dA}J = \frac{(A^T S_w A)\frac{d(A^T S_b A)}{dA} - (A^T S_b A)\frac{d(A^T S_w A)}{dA}}{(A^T S_w A)^2} &= 0 \\ (A^T S_w A)\frac{d(A^T S_b A)}{dA} &= (A^T S_b A)\frac{d(A^T S_w A)}{dA} \\ (A^T S_w A)2S_b A &= (A^T S_b A)2S_w A \end{aligned} \tag{C.1}$$

Dividing both side by $A^T S_w A$ yields:

$$(\frac{A^T S_w A}{A^T S_w A})2S_b A = (\frac{A^T S_b A}{A^T S_w A})2S_w A \tag{C.2}$$

using Equ. 3.23 and rearranging gives:

$$S_w^{-1} S_b A = JA \tag{C.3}$$

which is equal to Equ. 3.26.

C.1.2 An example of LDA

For an example, let f be given by Equ. C.4 where $M = 2$; the first 6 rows of f belong to $c = 1$ and rows 7-12 belong to $c = 2$; and $q = 6/class$. A simple MATLAB code showing the computation of $A = \left(\begin{smallmatrix} 0.9955 \\ 0.0951 \end{smallmatrix}\right)$ for this example is shown in Table C.2. A plot of the solution is shown in Fig. C.1.

$$f = \begin{bmatrix} 1 & 4 & 1 & 2 & 3 & 3 & 10 & 8 & 9 & 8 & 11 & 7 \\ 3 & 2 & 4 & 5 & 6 & 4 & 7 & 6 & 5 & 7 & 9 & 6 \end{bmatrix}^T \tag{C.4}$$

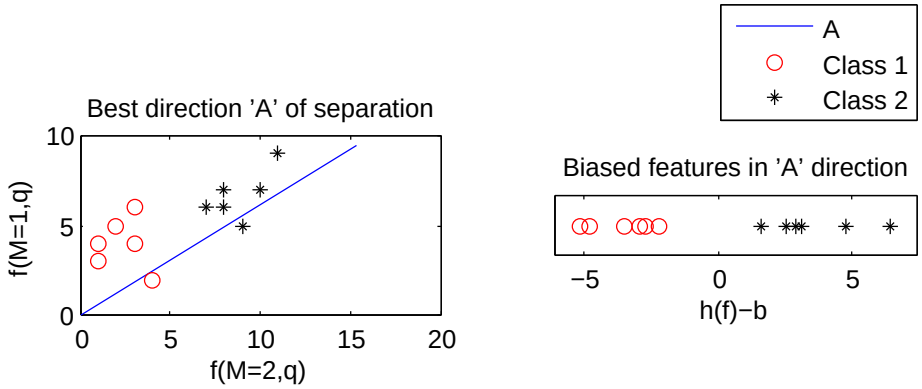

Figure C.1: The plot of the example computation of A. The hyperplane is biased to zero by subtracting the b in Equ. 3.27. In this case when $h(f) - b > 0$ an observation of f is classified as Class 2 otherwise the observation is classified as Class 1.

Table C.2: An example MATLAB code for computing 'A'

```
%Computes the LDA transformation matrix 'A'.
%Note that this code is note optimixed for speed.

%Feature vector of dimension=M=2
f=[1,3;4,2;1,4;2,5;3,6;3,4;10,7;8,6;9,5;8,7;11,9;7,6];

%Assuming that the first 6 values is for class 1 and the rest for Class 2
%then for convinience we write:
f1=f(1:6,:);%so q=6 per class
f2=f(7:12,:);

%% Between scatter
Sb=(mean(f1)-mean(f2))'*(mean(f1)-mean(f2));

%% Within scatter covariance matrix
Sw1=zeros(size(f1,2));
for q=1:size(f2,1)
    temp=(f1(q,:)-(mean(f1)))'*(f1(q,:)-(mean(f1)));
    Sw1=Sw1+temp;
end
% Expecation value
Sw1=Sw1/size(f1,1);

Sw2=zeros(size(f2,2));
for q=1:5
    temp=(f2(q,:)-(mean(f2)))'*(f2(q,:)-(mean(f2)));
    Sw2=Sw2+temp;
end
% Expecation value
Sw2=Sw2/size(f2,1);

%Within Scatter
Sw=Sw1+Sw2;

%% Solve generalised eigenvalue problem
[A,J]=eig(Sw\Sb);
[~,idx]=max(diag(J));
A=A(:,1);
% OR solve directly
%A=inv(Sw1)*(mean(f2)-mean(f1))'; A=A/norm(A);

% Bias
 b=-dot(A,0.5*(mean(f1)+mean(f2)));

%% Output:  Plot the line of the A vector
figure,subplot(1,2,1);
fmax=max(f(:));
plot([0;A(1)*(fmax+fmax/2)],[0;A(2)*fmax+fmax/2])
set(gca,'DataAspectRatio',[1 1 1]),ylabel('f(M=1,q)'),xlabel('f(M=2,q)')
title('Best direction ''A'' of separation')

% Plot Class 1 and Class 2
hold on,
plot(f1(:,1),f1(:,2),'ro'), plot(f2(:,1),f2(:,2),'k*')
legend({'A','Class 1','Class 2'})

% Plot the transformed features with bias
Af=A'*f';
subplot(1,2,2);
plot(b+(A'*f1'),0,'ro'),
title('Biased features in ''A'' direction');xlabel('h(f)-b');
hold on, plot(b+(A'*f2'),0,'k*')
xlim([min(Af)-1+b,max(Af)+1+b]); ylim([-1.1,1.1])
set(gca,'DataAspectRatio',[1 1 1]),set(gca,'box','on','ytick',[])
```

Appendix D

Supplemental materials for MMT in Chapter 8

This section presents the supplemental tables of MMT scores for patients in Chapter 8. The MMT scores (for before and after therapies) are presented separately for each of BCI-FES group and FES/FES-only group. In each group, the MMT scores for each hand are presented separately.

Table D.1: Right hand MMT scores for the BCI-FES group.

	ps1		**ps2**		**ps3**		**ps5**		**ps6**		**ps7**		**ps8**	
Muscles	b	a	b	a	b	a	b	a	b	a	b	a	b	a
Latissimus dorsi	4	4	3	4	5	5	3+	4+	3	4+	3	4	4	4+
Pectoralis major	4	4	3	4	5	5	3+	4+	3+	4	4	4+	4	4+
Serratus anterior	4	4	3	3+	5	5	3+	4+	3	4+	2	2+	3-	4
Deltoid	2	2+	3	4	5	5	3	4+	3+	4+	1	1+	4	4+
Triceps	-	-	1	1	5	5	3	4+	1	1	1+	2	3+	4
Biceps	4	4	4	5	5	5	4	4+	4	5	3+	3+	4	4+
Brachioradialis	4	4	3	5	5	5	4	4+	4	5	3	3	4	4+
Supinator	4	4	3	3+	4+	5	3	4	3+	4	1+	2	4-	4
Pronator	4	5	3	3+	4+	5	3	4	3	4	3	3+	3+	4
EDC	4-	4+	1	3	4	5	0	4+	3	4+	1-	1	1	2
ECR	4-	4+	1+	3+	4	5	0	4+	0	0	1-	1	0	2-
EPL	3-	3	0	0	0	0	0	3+	0	0	0	1	1	2
FCR	3	4	0	0	0	0	0	4	0	0	1-	1	1+	2+
FDP	4-	4	0	0	0	1	0	4	0	0	0	1	2-	2
Intrinsics	3	3	0	0	0	0	0	3+	0	0	0	0	1	2

Notes: The first header row depicts Subject IDs. Missing data is shown as '-'. b, before therapy; a, after therapy.

Table D.2: Right hand MMT scores for the FES group.

	ps4		**ps9**		**ps10**		**ps11**		**ps12**	
Muscles	b	a	b	a	b	a	b	a	b	a
Latissimus dorsi	3	4+	0	3	2+	2+	1+	2+	3	3+
Pectoralis major	3	4+	0	2+	0	0	1+	2	3	4
Serratus anterior	2	4+	1	2	0	3	1+	1	2+	3
Deltoid	2	4+	1	1+	1+	1+	1+	2+	1+	2
Triceps	1	4	0	2	0	2	1	1+	1+	2-
Biceps	3	4	0	1+	1+	3-	3+	4	1+	4
Brachioradialis	3+	4	0	0	0	3	0	0	1+	2+
Supinator	3+	4	0	2-	1+	4	3-	3+	3	4
Pronator	3	4	0	3	1	4	2-	2+	3	4
EDC	1	4	0	1+	1+	4	0	1	3	4+
ECR	0	3	0	2-	0	0	0	0	3	4+
EPL	0	2+	0	1+	2	3	0	1+	1+	3+
FCR	0	4	0	2	1	2	0	0	2	3+
FDP	0	4	0	2	1	4	0	1	4	4+
Intrinsics	0	2+	0	1+	0	3	0	0	3	4

Notes: The first header row depicts Subject IDs. Missing data is shown as '-'. b, before therapy; a, after therapy.

Table D.3: Left hand MMT scores for the BCI-FES group.

	ps1		**ps2**		**ps3**		**ps5**		**ps6**		**ps7**		**ps8**	
Muscles	b	a	b	a	b	a	b	a	b	a	b	a	b	a
Latissimus dorsi	4+	5	3	4	5	5	2+	4	4	5	2+	3	4+	5
Pectoralis major	4+	5	3-	4	5	5	2+	4	4	5	2+	3	4+	5
Serratus anterior	4+	5	3	4	5	5	3	4	4	5	2+	3	4+	5
Deltoid	4-	4-	2	3	5	5	2+	4	4	5	1+	2	4+	5
Triceps	3+	4	1	2-	3	3+	1	3+	3-	5	2+	2+	4+	5
Biceps	4+	4+	4	5	5	5	3	4+	4+	5	3	3+	4+	5
Brachioradialis	4	4	3+	5	5	5	3+	4+	4+	5	0	1+	4+	5
Supinator	4	4	3+	4	4	5	3	4	3+	4+	3	3+	3+	4
Pronator	3+	4	0	3	3	5	2	3	3+	4+	3	3+	3+	4
EDC	4	4	2+	3	4	5	0	1	3-	5	0	1+	3+	4+
ECR	4	4	1	3	4	5	0	4	3-	4+	0	1	3-	4
EPL	3+	3+	0	0	0	0	0	1	0	0	0	1	3	4
FCR	4	4+	0	0	0	0	0	1+	0	0	0	1	1+	2+
FDP	4	4+	0	0	0	0	0	1+	0	3	0	1	1+	2
Intrinsics	3	3+	0	0	0	0	0	3	0	0	0	0	1+	2+

Notes: The first header row depicts Subject IDs. Missing data is shown as '-'. b, before therapy; a, after therapy.

Table D.4: Left hand MMT scores for the FES group.

	ps4		**ps9**		**ps10**		**ps11**		**ps12**	
Muslces	b	a	b	a	b	a	b	a	b	a
Latissimus dorsi	2+	4+	0	1	4	4+	2-	3	2-	3
Pectoralis major	2-	4+	0	1	3+	4+	1	3	3	4
Serratus anterior	2-	4+	0	0	3+	4+	1+	1	3	4
Deltoid	2-	4+	1	1	1+	4+	1	2+	1+	2
Triceps	1	4+	0	2	3	4+	0	0	1	2-
Biceps	2+	4+	0	1	2+	3+	2-	2	1+	4
Brachioradialis	3	4+	0	0	2+	4+	0	0	1+	2+
Supinator	3	4	0	1	3+	4	1+	2+	1+	3
Pronator	2+	4	0	1+	4	4	1+	1+	1+	4
EDC	0	4	0	1+	3+	4	0	0	3	4+
ECR	0	3+	0	0	2	4	0	0	0	3
EPL	0	4	0	1+	3+	4	0	1	1	2+
FCR	0	4	0	2	4	4	0	0	3	4
FDP	0	4	0	2	4	4	0	1	3	4
Intrinsics	0	4	0	1	3+	4	0	0	1+	3+

Notes: The first header row depicts Subject IDs. Missing data is shown as '-'. b, before therapy; a, after therapy.

Appendix E

Supplemental materials for sLORETA in Chapter 8

This section presents the supplemental sLORETA tables of activities for patients in Chapter 8. The sLORETA tables are those of patients ps5 and ps10 presented for each of the patients and each of the hands. The sLORETA tables show activities before and after therapies.

Table E.1: Significantly active brain structures within the ROI for left and right hand hand AM at 1000-2000 ms after BCI-FES therapy for subject ps5. Frequency bands are limited to those showing the best lateralisation which were selected during wLI analysis (p=0.05).

					Voxel with max. r-value			
F	Structure	BA	H	nV	r-value	x	y	z
		Left						
$\beta 2$	Middle Frontal Gyrus	6	L	3	-0.68	-25	-8	42
	Middle Frontal Gyrus	6	R	23	-1.06	35	-8	42
	Precentral Gyrus	4 6	L	22	-0.80	-30	-17	42
	Precentral Gyrus	4 6 44	R	81	-1.05	35	-12	42
	Sub-Gyral	2	L	1	-0.79	-35	-27	38
	Sub-Gyral	2 6	R	6	-1.01	35	-3	42
	Postcentral Gyrus	2 3 40	L	16	-0.81	-30	-22	43
	Postcentral Gyrus	1 2 3 40	R	57	-1.00	45	-18	38
	Inferior Parietal Lobule	40	L	9	-0.74	-35	-32	38
	Inferior Parietal Lobule	40	R	15	-0.90	50	-27	47
	Cingulate Gyrus	24	L	4	-0.80	-20	-17	42
	Cingulate Gyrus	24	R	5	-0.79	20	-17	42
	Inferior Frontal Gyrus	9 44 45	R	15	-0.77	59	6	18
	Medial Frontal Gyrus	6	L	4	-0.74	-15	-12	47
	Medial Frontal Gyrus	6	R	5	-0.73	15	-12	47
		Right						
μ	Precentral Gyrus	4 6	L	41	-0.74	-35	-17	47
	Precentral Gyrus	6	R	1	-0.49	25	-17	52
	Postcentral Gyrus	1 2 3 40	L	41	-0.73	-35	-22	47
	Middle Frontal Gyrus	6	L	7	-0.61	-35	-8	42
	Medial Frontal Gyrus	6	L	4	-0.58	-15	-12	56
	Medial Frontal Gyrus	6	R	2	-0.52	15	-12	56
	Inferior Parietal Lobule	40	L	4	-0.56	-40	-32	48
	Cingulate Gyrus	24	L	2	-0.56	-20	-17	42
	Sub-Gyral	2 6	L	2	-0.53	-35	-27	38

Notes: The structures are sorted in the descending absolute values of r-value. F, Frequency band in Hz; BA, Brodmann Area; H, Hemisphere; nv, Number of Voxels; r-value, Statistics (log of ratio of averages implemented in sLORETA, read like t-values); xyz, Talairach coordinates; R, Right; L, Left.

Table E.2: Significantly active structures for **right hand AM** at 1000-2000 ms for subject ps10 before and after FES therapy (p=0.05).

					Voxel with max. S			
F	Structure	BA	H	nV	S	x	y	z
		Right- Before						
β2	Precentral Gyrus	4 6	L	54	-1.05	-25	-27	47
	Precentral Gyrus	4 6	R	17	-0.76	20	-22	52
	Postcentral Gyrus	1 2 3 40	L	57	-1.02	-30	-32	48
	Postcentral Gyrus	2 3	R	7	-0.64	30	-32	48
	Inferior Parietal Lobule	40	L	20	-0.97	-35	-32	43
	Cingulate Gyrus	24	L	4	-0.92	-20	-17	42
	Cingulate Gyrus	24	R	5	-0.78	20	-17	42
	Sub-Gyral	2 6	L	4	-0.91	-35	-27	38
	Sub-Gyral	2 6	R	2	-0.57	20	-7	56
	Medial Frontal Gyrus	6	L	4	-0.85	-15	-12	47
	Medial Frontal Gyrus	6	R	5	-0.74	15	-12	47
	Middle Frontal Gyrus	6	L	17	-0.74	-20	-12	60
	Middle Frontal Gyrus	6	R	6	-0.61	25	-8	42
		Right- After						
β1	Postcentral Gyrus	1 2 3 40	L	33	-0.79	-30	-31	52
	Postcentral Gyrus	1 2 3 40	R	56	-0.93	30	-22	43
	Precentral Gyrus	4 6	L	30	-0.82	-25	-27	52
	Precentral Gyrus	4 6	R	55	-0.90	30	-17	42
	Sub-Gyral	2	L	1	-0.60	-35	-27	38
	Sub-Gyral	2 6	R	5	-0.87	35	-27	38
	Cingulate Gyrus	24	L	1	-0.65	-20	-17	42
	Cingulate Gyrus	24	R	5	-0.83	20	-17	42
	Middle Frontal Gyrus	6	L	2	-0.58	-25	-12	60
	Middle Frontal Gyrus	6	R	22	-0.76	30	-8	42
	Inferior Parietal Lobule	40	L	5	-0.65	-35	-32	43
	Inferior Parietal Lobule	40	R	12	-0.73	40	-32	38
	Medial Frontal Gyrus	6	L	3	-0.60	-15	-12	47
	Medial Frontal Gyrus	6	R	5	-0.70	15	-12	47

Notes: see Table E.1

Table E.3: Significantly active structures for **left hand AM** at 1000-2000 ms for subject ps10 before and after FES therapy (p=0.05).

					Voxel with max. S			
F	Structure	BA	H	nV	S	x	y	z
		Left- Before						
β1	Precentral Gyrus	4	L	7	-0.67	-25	-27	47
	Precentral Gyrus	4 6 44	R	47	-0.89	25	-27	47
	Postcentral Gyrus	1 2 3 40	L	29	-0.68	-30	-32	48
	Postcentral Gyrus	2 3 40	R	22	-0.87	30	-22	43
	Cingulate Gyrus	24	L	1	-0.56	-20	-17	42
	Cingulate Gyrus	24	R	5	-0.85	20	-17	42
	Sub-Gyral	2	L	1	-0.61	-35	-27	38
	Sub-Gyral	2	R	1	-0.77	35	-27	38
	Medial Frontal Gyrus	6	R	4	-0.74	15	-12	47
	Middle Frontal Gyrus	6	R	8	-0.73	25	-8	42
	Inferior Parietal Lobule	40	L	10	-0.67	-35	-32	43
	Inferior Parietal Lobule	40	R	6	-0.65	40	-32	43
	Inferior Frontal Gyrus	9 44 45	R	7	0.63	59	6	18
		Left- After						
β1	Precentral Gyrus	4 6	L	40	-0.82	-25	-27	52
	Precentral Gyrus	4 6	R	56	-1.17	30	-27	47
	Postcentral Gyrus	1 2 3 40	L	45	-0.79	-30	-22	47
	Postcentral Gyrus	1 2 3 40	R	57	-1.16	35	-27	47
	Sub-Gyral	2 6	L	2	-0.68	-35	-27	38
	Sub-Gyral	2 6	R	4	-1.07	35	-27	38
	Inferior Parietal Lobule	40	L	5	-0.69	-35	-32	43
	Inferior Parietal Lobule	40	R	15	-0.97	40	-32	43
	Cingulate Gyrus	24	L	2	-0.71	-20	-17	42
	Cingulate Gyrus	24	R	4	-0.87	20	-17	42
	Middle Frontal Gyrus	6	L	4	-0.62	-25	-12	60
	Middle Frontal Gyrus	6	R	21	-0.78	30	-8	42
	Medial Frontal Gyrus	6	L	3	-0.65	-15	-12	47
	Medial Frontal Gyrus	6	R	3	-0.69	15	-12	47

Notes: see Table E.1

Bibliography

[1] M. Bear, B. Connors, and M. Paradiso, *Neuroscience: Exploring the brain*. Neuroscience: Exploring the Brain, Baltimore, MD: Lippincott Williams & Wilkins, 3 ed., 2007.

[2] M. Loukas, C. Pennell, C. Groat, R. S. Tubbs, and A. A. Cohen-Gadol, "Korbinian brodmann (1868-1918) and his contributions to mapping the cerebral cortex," *Neurosurgery*, vol. 68, no. 1, pp. 6–11, 2011.

[3] A. Afifi and R. Bergman, *Functional neuroanatomy: Text and atlas*. USA: McGraw-Hill, 2005.

[4] E. C. Field-Fote, *Spinal cord injury rehabilitation*. 2009.

[5] R. Porter and R. Lemon, *Corticospinal function and voluntary movement*. New york: Oxford University Press Inc., 1993.

[6] N. Palastanga, D. Field, and R. Soames, *Anatomy and Human Movement: Structure and Function*. Oxford: Butterworth-Heinemann, 2 ed., 1994.

[7] R. M. Enoka, *Neuromechanics of human movement*. US: Human Kinetics, 4 ed., 2008.

[8] M. Jeannerod, *Motor Cognition: What actions tell the self*. No. 42, Oxford: Oxford University Press, 2006.

[9] J. S. Sabari, "Motor learning concepts applied to activity-based intervention with adults with hemiplegia.," *American Journal of Occupational Therapy*, vol. 45, no. 6, pp. 523–530, 1991.

[10] D. M. Wolpert and Z. Ghahramani, "Computational principles of movement neuroscience.," *Nature Neuroscience*, vol. 3 Suppl, pp. 1212–1217, 2000.

[11] D. M. Wolpert, Z. Ghahramani, and M. I. Jordan, "An internal model for sensorimotor integration.," *Science*, vol. 269, no. 5232, pp. 1880–1882, 1995.

[12] S.-J. Blakemore and A. Sirigu, "Action prediction in the cerebellum and in the parietal lobe.," *Experimental Brain Research*, vol. 153, pp. 239–245, Nov 2003.

[13] J. R. Flanagan and A. M. Wing, "The role of internal models in motion planning and control: evidence from grip force adjustments during movements of hand-held loads," *The Journal of Neuroscience*, vol. 17, no. 4, pp. 1519–1528, 1997.

[14] S. Choudhury, T. Charman, V. Bird, and S.-J. Blakemore, "Development of action representation during adolescence," *Neuropsychologia*, vol. 45, no. 2, pp. 255 – 262, 2007.

[15] L. J. Buxbaum, S. H. Johnson-Frey, and M. Bartlett-Williams, "Deficient internal models for planning hand-object interactions in apraxia," *Neuropsychologia*, vol. 43, no. 6, pp. 917 – 929, 2005.

[16] S. Choudhury, T. Charman, V. Bird, and S.-J. Blakemore, "Development of action representation during adolescence," *Neuropsychologia*, vol. 45, no. 2, pp. 255 – 262, 2007.

[17] J. Decety, D. Perani, M. Jeannerod, V. Bettinardi, B. Tadary, R. Woods, J. C. Mazziotta, and F. Fazio, "Mapping motor representations with positron emission tomography.," *Nature*, vol. 371, no. 6498, pp. 600–602, 1994.

[18] M. Jeannerod, "Neural simulation of action: A unifying mechanism for motor cognition.," *Neuroimage*, vol. 14, no. 1, pp. S103–S109, 2001.

[19] M. Lotze and U. Halsband, "Motor imagery.," *Journal of Physiology-Paris*, vol. 99, no. 4, pp. 386–395, 2006.

[20] J. Decety, "The neurophysiological basis of motor imagery.," *Behavioural Brain Research*, vol. 77, no. 1-2, pp. 45–52, 1996.

[21] M. Jeannerod, "The representing brain: Neural correlates of motor intention and imagery," *Behavioral and Brain Sciences*, vol. 17, pp. 187–245, 1994.

[22] E.-J. Speckmann and C. E. Elger, *Electroencephalography: basic principles, clinical applications, and related fields*, ch. Introduction to the Neurophysiological Basis of the EEG and DC Potentials, pp. 18–31. Lippincott Williams & Wilkins, 5 ed., 2005.

[23] C. Mulert, L. Jäger, R. Schmitt, P. Bussfeld, O. Pogarell, H.-J. Möller, G. Juckel, and U. Hegerl, "Integration of fMRI and simultaneous EEG: towards a comprehensive understanding of localization and time-course of brain activity in target detection," *Neuroimage*, vol. 22, no. 1, pp. 83–94, 2004.

[24] E. Niedermeyer and F. L. da Silva, eds., *Electroencephalography: basic principles, clinical applications, and related fields*. Philadelphia: Lippincott Williams & Wilkins, 5 ed., 2005.

[25] V. Jurcak, D. Tsuzuki, and I. Dan, "10/20, 10/10, and 10/5 systems revisited: Their validity as relative head-surface-based positioning systems," *NeuroImage*, vol. 34, no. 4, pp. 1600 – 1611, 2007.

[26] B. Hjorth, "An on-line transformation of EEG scalp potentials into orthogonal source derivations," *Electroencephalography and clinical neurophysiology*, vol. 39, no. 5, pp. 526–530, 1975.

[27] G. Dornhege, M. Krauledat, K.-R. M´uller, and B. Blankertz, *Toward Brain-Computer Interfacing*, ch. General Signal Processing and Machine Learning Tools for BCI Analysis, pp. 207–233. Cambridge: The MIT Press, 2007.

[28] G. Pfurtscheller and F. H. Lopes da Silva, "Event-related EEG/MEG synchronization and desynchronization: Basic principles.," *Clinical Neurophysiology*, vol. 110, no. 11, pp. 1842–1857, 1999.

[29] L. F. Nicolas-Alonso and J. Gomez-Gil, "Brain computer interfaces, a review.," *Sensors (Basel)*, vol. 12, no. 2, pp. 1211–1279, 2012.

[30] D. Regan, *Evoked Potentials and Evoked Magnetic Fields in Science and Medicine*. New York, NY, USA: Elsevier, 1989.

[31] J. Ding, G. Sperling, and R. Srinivasan, "Attentional modulation of SSVEP power depends on the network tagged by the flicker frequency," *Cerebral cortex*, vol. 16, no. 7, pp. 1016–1029, 2006.

[32] G. Pfurtscheller and A. Aranibar, "Event-related cortical desynchronization detected by power measurements of scalp EEG.," *Electroencephalography and Clinical Neurophysiology*, vol. 42, no. 6, pp. 817–826, 1977.

[33] S. Makeig, "Auditory event-related dynamics of the EEG spectrum and effects of exposure to tones.," *Electroencephalography and Clinical Neurophysiology*, vol. 86, no. 4, pp. 283–293, 1993.

[34] I. K. Niazi, N. Mrachacz-Kersting, N. Jiang, K. Dremstrup, and D. Farina, "Peripheral electrical stimulation triggered by self-paced detection of motor intention enhances motor evoked potentials.," *Neural System Rehabilitation and Engineering, IEEE Transactions on*, vol. 20, no. 4, pp. 595–604, 2012.

[35] N. Birbaumer, T. Elbert, A. G. Canavan, and B. Rockstroh, "Slow potentials of the cerebral cortex and behavior.," *Physiological Reviews*, vol. 70, no. 1, pp. 1–41, 1990.

[36] D. R. Gater, Jr, D. Dolbow, B. Tsui, and A. S. Gorgey, "Functional electrical stimulation therapies after spinal cord injury.," *NeuroRehabilitation*, vol. 28, no. 3, pp. 231–248, 2011.

[37] D. N. Rushton, "Functional electrical stimulation.," *Physiological Measurement*, vol. 18, no. 4, pp. 241–275, 1997.

[38] C. M. Gregory and C. S. Bickel, "Recruitment patterns in human skeletal muscle during electrical stimulation," *Physical therapy*, vol. 85, no. 4, pp. 358–364, 2005.

[39] L. R. Sheffler and J. Chae, "Neuromuscular electrical stimulation in neurorehabilitation.," *Muscle and Nerve*, vol. 35, no. 5, pp. 562–590, 2007.

[40] S. Palmer, K. H. Kriegsman, and J. B. Palmer, *Spinal cord injury: A guide for living*. Baltimore, Maryland: The johns Hopkins University press, 2000.

[41] National Spinal Cord Injury Statistical Center, Birmingham, Alabama, "Spinal cord injury facts and figures at a glance," *Journal of Spinal Cord Medicine*, vol. 34, pp. 620–621, 2011.

[42] C. Ethier, E. R. Oby, M. J. Bauman, and L. E. Miller, "Restoration of grasp following paralysis through brain-controlled stimulation of muscles.," *Nature*, vol. 485, no. 7398, pp. 368–371, 2012.

[43] J. Allibone, B. Taylor, and F. Middleton, *Handbook of neurological rehabilitation*, ch. Spinal injury. New York: Psychology Press, 2003.

[44] S. Kirshblum, S. Millis, W. McKinley, and D. Tulsky, "Late neurologic recovery after traumatic spinal cord injury," *Archives of physical medicine and rehabilitation*, vol. 85, no. 11, pp. 1811–1817, 2004.

[45] M. R. Popovic, N. Kapadia, V. Zivanovic, J. C. Furlan, B. C. Craven, and C. McGillivray, "Functional electrical stimulation therapy of voluntary grasping versus only conventional rehabilitation for patients with subacute incomplete tetraplegia: a randomized clinical trial.," *Neurorehabilitation and Neural Repair*, vol. 25, no. 5, pp. 433–442, 2011.

[46] N. M. Kapadia, V. Zivanovic, J. Furlan, B. C. Craven, C. McGillivray, and M. R. Popovic, "Functional electrical stimulation therapy for grasping in traumatic incomplete spinal cord injury: randomized control trial," *Artificial organs*, vol. 35, no. 3, pp. 212–216, 2011.

[47] M. R. Popovic, T. A. Thrasher, M. E. Adams, V. Takes, V. Zivanovic, and M. I. Tonack, "Functional electrical therapy: retraining grasping in spinal cord injury.," *Spinal Cord*, vol. 44, no. 3, pp. 143–151, 2006.

[48] M. B. Popovic, D. B. Popovic, T. Sinkjaer, A. Stefanovic, and L. Schwirtlich, "Restitution of reaching and grasping promoted by functional electrical therapy.," *Artificial Organs*, vol. 26, no. 3, pp. 271–275, 2002.

[49] G. Francisco, J. Chae, H. Chawla, S. Kirshblum, R. Zorowitz, G. Lewis, and S. Pang, "Electromyogram-triggered neuromuscular stimulation for improving the arm function of acute stroke survivors: a randomized pilot study," *Archives of physical medicine and rehabilitation*, vol. 79, no. 5, pp. 570–575, 1998.

[50] J. J. Daly and R. Sitaran, *Brain-computer interfaces: Principles and practice*, ch. BCI therapeutic application for improving brain function, pp. 351–362. USA: Oxford University Press Inc, 2 ed., 2012.

[51] J. J. Daly and J. R. Wolpaw, "Brain-computer interfaces in neurological rehabilitation.," *Lancet Neurology*, vol. 7, no. 11, pp. 1032–1043, 2008.

[52] M. Grosse-Wentrup, D. Mattia, and K. Oweiss, "Using brain-computer interfaces to induce neural plasticity and restore function.," *Journal of Neural Engineering*, vol. 8, no. 2, pp. 025004–025004, 2011.

[53] M. IJzerman, T. Stoffers, F. in 't Groen, M. Klatte, G. Snoek, J. Vorsteveld, R. Nathan, and H. Hermens, "The ness handmaster othosis: Restoration of hand function in c5 and stroke patients by means of electrical stimulation," *Journal of Rehabilitation Sciences*, vol. 9, no. 3, pp. 86–89, 1996.

[54] D. Popović, A. Stojanović, A. Pjanović, S. Radosavljević, M. Popović, S. Jović, and D. Vulović, "Clinical evaluation of the bionic glove," *Archives of physical medicine and rehabilitation*, vol. 80, no. 3, pp. 299–304, 1999.

[55] D. N. Rushton, "Functional electrical stimulation and rehabilitation–an hypothesis.," *Medical Engineering & Physics*, vol. 25, no. 1, pp. 75–78, 2003.

[56] M. E. Selzer, S. Clarke, L. G. Cohen, P. W. Duncan, and F. H. Gage, *Textbook of neural repair and rehabilitation: neural repair and plasticity*, vol. 1, ch. Neural repair and rehabilitation: an introduction, pp. xxvii–xxxv. New York: Cambridge University Press, 2006.

[57] S. A. Raskin, *Neuroplasticity and Rehabilitation*, ch. Current approaches to rehabilitation, pp. 1–9. London: The Guilford Press, 2011.

[58] O. Steward, *Textbook of neural repair and rehabilitation: neural repair and plasticity*, vol. 1, ch. Anatomical and biochemical plasticity of neurons: regenerative growth of axons, sprouting, pruning, and denervation supersensitivity, pp. 5–25. New York: Cambridge University Press, 2006.

[59] K. M. Christian, A. M. Poulos, and R. F. Thompson, *Textbook of neural repair and rehabilitation: neural repair and plasticity*, vol. 1, ch. Learning and memory: basic principles and model systems, pp. 5–25. New York: Cambridge University Press, 2006.

[60] I. P. Pavlov, *Conditioned Reflexes: An Investigation of the Physiological Activity of the Cerebral Cortex*. London: Oxford University Press, 1927.

[61] D. Hebb, *The Organization of Behavior: A Neuropsychological Theory*. New york: John Wiley & Sons, 1949.

[62] N. Mrachacz-Kersting, S. R. Kristensen, I. K. Niazi, and D. Farina, "Precise temporal association between cortical potentials evoked by motor imagination and afference induces cortical plasticity.," *The Journal of Physiology*, vol. 590, no. Pt 7, pp. 1669–1682, 2012.

[63] A. Jackson, J. Mavoori, and E. E. Fetz, "Long-term motor cortex plasticity induced by an electronic neural implant.," *Nature*, vol. 444, no. 7115, pp. 56–60, 2006.

[64] A. Baranyi and O. Fehér, "Synaptic facilitation requires paired activation of convergent pathways in the neocortex.," *Nature*, vol. 290, no. 5805, pp. 413–415, 1981.

[65] A. Iriki, C. Pavlides, A. Keller, and H. Asanuma, "Long-term potentiation in the motor cortex.," *Science*, vol. 245, pp. 1385–1387, Sep 1989.

[66] A. Iriki, C. Pavlides, A. Keller, and H. Asanuma, "Long-term potentiation of thalamic input to the motor cortex induced by coactivation of thalamocortical and corticocortical afferents.," *Journal of Neurophysiology*, vol. 65, pp. 1435–1441, Jun 1991.

[67] G. Pfurtscheller, G. R. Müller, J. Pfurtscheller, H. J. Gerner, and R. Rupp, "'Thought' - control of functional electrical stimulation to restore hand grasp in a patient with tetraplegia," *Neuroscience Letters*, vol. 351, no. 1, pp. 33 – 36, 2003.

[68] C. Ethier and L. E. Miller, "Brain-controlled muscle stimulation for the restoration of motor function," *Neurobiology of Disease*, 2014.

[69] S. C. McGie, J. Zariffa, M. R. Popovic, and M. K. Nagai, "Short-term neuroplastic effects of brain-controlled and muscle-controlled electrical stimulation," *Neuromodulation: Technology at the Neural Interface*, vol. n/a, no. n/a, pp. n/a–n/a, 2014.

[70] H. H. Kornhuber and L. Deecke, "Changes in the brain potential in voluntary movements and passive movements in man: Readiness potential and reafferent potentials," *Pflügers Archiv für die gesamte Physiologie des Menschen und der Tiere.*, vol. 284, no. 1, pp. 1–17, 1965.

[71] A. Castro, F. Díaz, and G. J. van Boxtel, "What happens to the readiness potential when the movement is not executed?," *Neuroreport*, vol. 16, no. 15, pp. 1609–1613, 2005.

[72] S. Silvoni, A. Ramos-Murguialday, M. Cavinato, C. Volpato, G. Cisotto, A. Turolla, F. Piccione, and N. Birbaumer, "Brain-computer interface in stroke: a review of progress," *Clinical EEG and Neuroscience*, vol. 42, no. 4, pp. 245–252, 2011.

[73] J. Munzert, B. Lorey, and K. Zentgraf, "Cognitive motor processes: The role of motor imagery in the study of motor representations," *Brain Research Reviews*, vol. 60, no. 2, pp. 306 – 326, 2009.

[74] S. R. Soekadar, N. Birbaumer, M. W. Slutzky, and L. G. Cohen, "Brain-machine interfaces in neurorehabilitation of stroke.," *Neurobiology of Disease*, 2014.

[75] K. J. Kokotilo, J. J. Eng, and A. Curt, "Reorganization and preservation of motor control of the brain in spinal cord injury: a systematic review.," *Journal of Neurotrauma*, vol. 26, no. 11, pp. 2113–2126, 2009.

[76] K. K. Ang, C. Guan, K. S. G. Chua, B. T. Ang, C. W. K. Kuah, C. Wang, K. S. Phua, Z. Y. Chin, and H. Zhang, "A large clinical study on the ability of stroke patients to use an EEG-based motor imagery brain-computer interface.," *Clinical EEG and Neuroscience*, vol. 42, pp. 253–258, Oct 2011.

[77] M. L. Latash, *Neurophysiological basis of movement*. US: Human Kinetics, 2 ed., 2008.

[78] R. Chen, L. G. Cohen, and M. Hallett, "Nervous system reorganization following injury.," *Neuroscience*, vol. 111, no. 4, pp. 761–773, 2002.

[79] R. Nardone, Y. Höller, F. Brigo, M. Seidl, M. Christova, J. Bergmann, S. Golaszewski, and E. Trinka, "Functional brain reorganization after spinal cord injury: systematic review of animal and human studies.," *Brain Research*, vol. 1504, pp. 58–73, 2013.

[80] P. Freund, N. Weiskopf, N. S. Ward, C. Hutton, A. Gall, O. Ciccarelli, M. Craggs, K. Friston, and A. J. Thompson, "Disability, atrophy and cortical reorganization following spinal cord injury," *Brain*, vol. 134, no. 6, pp. 1610–1622, 2011.

[81] R. Traversa, P. Cicinelli, A. Bassi, P. M. Rossini, and G. Bernardi, "Mapping of motor cortical reorganization after stroke a brain stimulation study with focal magnetic pulses," *Stroke*, vol. 28, no. 1, pp. 110–117, 1997.

[82] M. Takahashi, K. Takeda, Y. Otaka, R. Osu, T. Hanakawa, M. Gouko, and K. Ito, "Event related desynchronization-modulated functional electrical stimulation system for stroke rehabilitation: a feasibility study.," *Journal of NeuroEngineering and Rehabilitation*, vol. 9, p. 56, 2012.

[83] S. J. Page, P. Levine, S. Sisto, and M. V. Johnston, "A randomized efficacy and feasibility study of imagery in acute stroke.," *Clinical Rehabilitation*, vol. 15, no. 3, pp. 233–240, 2001.

[84] S. J. Page, P. Levine, and A. Leonard, "Mental practice in chronic stroke: results of a randomized, placebo-controlled trial.," *Stroke*, vol. 38, no. 4, pp. 1293–1297, 2007.

[85] S. J. Page, J. P. Szaflarski, J. C. Eliassen, H. Pan, and S. C. Cramer, "Cortical plasticity following motor skill learning during mental practice in stroke.," *Neurorehabilitation and Neural Repair*, vol. 23, no. 4, pp. 382–388, 2009.

[86] Y. Prut and E. E. Fetz, "Primate spinal interneurons show pre-movement instructed delay activity.," *Nature*, vol. 401, no. 6753, pp. 590–594, 1999.

[87] L. Fadiga, G. Buccino, L. Craighero, L. Fogassi, V. Gallese, and G. Pavesi, "Corticospinal excitability is specifically modulated by motor imagery: a magnetic stimulation study.," *Neuropsychologia*, vol. 37, no. 2, pp. 147–158, 1999.

[88] F. Pichiorri, F. D. V. Fallani, F. Cincotti, F. Babiloni, M. Molinari, S. C. Kleih, C. Neuper, A. Kbler, and D. Mattia, "Sensorimotor rhythm-based brain-computer interface training: the impact on motor cortical responsiveness.," *Journal of Neural Engineering*, vol. 8, no. 2, p. 025020, 2011.

[89] F. C. Bakker and M. S. Boschker, "Changes in muscular activity while imagining weight lifting using stimulus or response propositions," *Journal of Sport & Exercise Psychology*, vol. 18, no. 3, pp. 313–324, 1996.

[90] J. R. Livesay and M. R. Samaras, "Covert neuromuscular activity of the dominant forearm during visualization of a motor task.," *Perceptual and motor skills*, vol. 86, no. 2, pp. 371–374, 1998.

[91] J. Powell, A. D. Pandyan, M. Granat, M. Cameron, and D. J. Stott, "Electrical stimulation of wrist extensors in poststroke hemiplegia.," *Stroke*, vol. 30, no. 7, pp. 1384–1389, 1999.

[92] A. D. Pandyan, M. H. Granat, and D. J. Stott, "Effects of electrical stimulation on flexion contractures in the hemiplegic wrist.," *Clinical Rehabilitation*, vol. 11, no. 2, pp. 123–130, 1997.

[93] R. Merletti, R. Acimovic, S. Grobelnik, and G. Cvilak, "Electrophysiological orthosis for the upper extremity in hemiplegia: feasibility study.," *Archives of Physical Medicine and Rehabilitation*, vol. 56, no. 12, pp. 507–513, 1975.

[94] G. H. Kraft, S. S. Fitts, and M. C. Hammond, "Techniques to improve function of the arm and hand in chronic hemiplegia.," *Archives of Physical Medicine and Rehabilitation*, vol. 73, no. 3, pp. 220–227, 1992.

[95] H. M. Feys, W. J. De Weerdt, B. E. Selz, G. A. Cox Steck, R. Spichiger, L. E. Vereeck, K. D. Putman, and G. A. Van Hoydonck, "Effect of a therapeutic intervention for the hemiplegic upper limb in the acute phase after stroke: a single-blind, randomized, controlled multicenter trial.," *Stroke*, vol. 29, no. 4, pp. 785–792, 1998.

[96] J. Chae, F. Bethoux, T. Bohine, L. Dobos, T. Davis, and A. Friedl, "Neuromuscular stimulation for upper extremity motor and functional recovery in acute hemiplegia.," *Stroke*, vol. 29, no. 5, pp. 975–979, 1998.

[97] D. B. P. Popovic and T. Sinkjaer, *Control of movement for the physically disabled*. Belgrade: Academic mind, 2003.

[98] F. Quandt and F. Hummel, "The influence of functional electrical stimulation on hand motor recovery in stroke patients: a review.," *Experimental & translational stroke medicine*, vol. 6, pp. 9–9, 2014.

[99] A. Vuckovic, L. Wallace, and D. B. Allan, "Hybrid brain computer interface and functional electrical stimulation for sensorimotor training of sub-acute tetraplegic particpants: A case series," *Journal of Neurologic Physical Therapy*, vol. accepted for publication, expected 2015.

[100] B. A. Osuagwu, A. Vuckovic, M. Fraser, L. Wallace, and B. D. Allan, "BCI-FES hand therapy for patients with sub-acute tetraplegia," in *Proceedings of the 6th International Brain-Computer Interface Conference*, (Graz, Austria), 2014.

[101] Y. Liu, M. Li, H. Zhang, H. Wang, J. Li, J. Jia, Y. Wu, and L. Zhang, "A tensor-based scheme for stroke patients' motor imagery EEG analysis in BCI-FES rehabilitation training.," *Journal of Neuroscience Methods*, vol. 222, no. 0, pp. 238–249, 2014.

[102] M. Li, Y. Liu, Y. Wu, S. Liu, J. Jia, and L. Zhang, "Neurophysiological substrates of stroke patients with motor imagery-based brain-computer interface training.," *International Journal of Neuroscience*, vol. 124, no. 6, pp. 403–415, 2014.

[103] J. J. Daly, R. Cheng, J. Rogers, K. Litinas, K. Hrovat, and M. Dohring, "Feasibility of a new application of noninvasive brain computer interface (BCI): a case study of training for recovery of volitional motor control after stroke.," *Journal of Neurologic Physical Therapy*, vol. 33, no. 4, pp. 203–211, 2009.

[104] B. M. Young, Z. Nigogosyan, V. A. Nair, L. M. Walton, J. Song, M. E. Tyler, D. F. Edwards, K. Caldera, J. A. Sattin, J. C. Williams, *et al.*, "Case report: post-stroke interventional BCI rehabilitation in an individual with preexisting sensorineural disability," *Frontiers in Neuroengineering*, vol. 7, p. 18, 2014.

[105] M. Mukaino, T. Ono, K. Shindo, T. Fujiwara, T. Ota, A. Kimura, M. Liu, and J. Ushiba, "Efficacy of brain-computer interface-driven neuromuscular electrical stimulation for chronic paresis after stroke.," *Journal of Rehabilitation Medicine*, vol. 46, no. 4, pp. 378–382, 2014.

[106] A. H. Do, P. T. Wang, C. E. King, A. Abiri, and Z. Nenadic, "Brain-computer interface controlled functional electrical stimulation system for ankle movement.," *Journal of NeuroEngineering and Rehabilitation*, vol. 8, p. 49, 2011.

[107] H. G. Tan, C. Y. Shee, K. H. Kong, C. Guan, and W. T. Ang, "EEG controlled neuromuscular electrical stimulation of the upper limb for stroke patients," *Frontiers of Mechanical Engineering*, vol. 6, no. 1, pp. 71–81, 2011.

[108] A. H. Do, P. T. Wang, C. E. King, A. Schombs, S. C. Cramer, and Z. Nenadic, "Brain-computer interface controlled functional electrical stimulation device for foot drop due to stroke.," *In proceedings of the 34th Annual international conference of the IEEE Engineering in Medicine and Biology Society*, vol. 2012, pp. 6414–6417, 2012.

[109] C. McCrimmon, C. King, P. Wang, S. Cramer, Z. Nenadic, and A. Do, "Brain-controlled functional electrical stimulation for lower-limb motor recovery in stroke survivors," *In proceedings of the 36th Annual international conference of the IEEE Engineering in Medicine and Biology Society*, vol. 2014, 2014.

[110] F. Meng, K. yu Tong, S. tak Chan, W. wa Wong, K. him Lui, K. wing Tang, X. Gao, and S. Gao, "BCI-FES training system design and implementation for rehabilitation of stroke patients," in *Neural Networks, 2008. IJCNN 2008. (IEEE World Congress on Computational Intelligence). IEEE International Joint Conference on*, pp. 4103–4106, 2008.

[111] Y. Liu, H. Zhang, H. Wang, J. Li, and L. Zhang, "BCI-FES rehabilitation training platform integrated with active training mechanism," in *Workshop proceedings of the international joint conference on artificial intelligence (IJCAI 2013)* (Z. Shi, P. S. Rosenbloom, and U. Ernst, eds.), (Beijing), pp. 58–63, 2013.

[112] D. Irimia, M. Poboroniuc, and R. Ortner, "Improved method to perform fes amp;bci based rehabilitation," in *E-Health and Bioengineering Conference (EHB), 2013*, pp. 1–4, 2013.

[113] C. Vidaurre, N. Krämer, B. Blankertz, and A. Schlögl, "Time domain parameters as a feature for EEG-based brain-computer interfaces.," *Neural Networks*, vol. 22, no. 9, pp. 1313–1319, 2009.

[114] C.-C. Chang and C.-J. Lin, "LIBSVM: A library for support vector machines," *ACM Transactions on Intelligent Systems and Technology*, vol. 2, pp. 27:1–27:27, 2011. Software available at http://www.csie.ntu.edu.tw/ cjlin/libsvm.

[115] R. Duda, P. E. Hart, and D. G. Stork, *Pattern Classification*. Wiley, 2000.

[116] J. Stone, *Independent Component Analysis: A Tutorial Introduction*. A Bradford book, MIT Press, 2004.

[117] A. Vuckovic and B. A. Osuagwu, "Using a motor imagery questionnaire to estimate the performance of a brain-computer interface based on object oriented motor imagery.," *Clinical Neurophysiology*, vol. 124, no. 8, pp. 1586–1595, 2013.

[118] C. Reynolds, B. A. Osuagwu, and A. Vuckovic, "Influence of motor imagination on cortical activation during functional electrical stimulation," *Clinical Neurophysiology*, 2014.

[119] G. Pfurtscheller, C. Neuper, C. Guger, W. Harkam, H. Ramoser, A. Schlogl, B. Obermaier, M. Pregenzer, *et al.*, "Current trends in graz brain-computer interface (BCI) research," *IEEE Transactions on Rehabilitation Engineering*, vol. 8, no. 2, pp. 216–219, 2000.

[120] M. Pregenzer and G. Pfurtscheller, "Frequency component selection for an eeg-based brain to computer interface," *Rehabilitation Engineering, IEEE Transactions on*, vol. 7, pp. 413–419, Dec 1999.

[121] G. Pfürtscheller, "Event-related synchronization (ERS): An electrophysiological correlate of cortical areas at rest.," *Electroencephalography and Clinical Neurophysiology*, vol. 83, no. 1, pp. 62–69, 1992.

[122] B. Schelter, M. Winterhalder, and J. Timmer, *Handbook of time series analysis: recent theoretical developments and applications*. John Wiley & Sons, 2006.

[123] A. Schlögl, D. Flotzinger, and G. Pfurtscheller, "Adaptive autoregressive modeling used for single-trial eeg classification," *Biomedizinische Technik/Biomedical Engineering*, vol. 42, no. 6, pp. 162–167, 1997.

[124] A. Schlögl, *The Electroencephalogram and the Adaptive Autoregressive Model: Theory and Applications*. PhD thesis, Aachen, Germany, 2000.

[125] A. Schlögl, F. Lee, H. Bischof, and G. Pfurtscheller, "Characterization of four-class motor imagery eeg data for the bci-competition 2005," *Journal of neural engineering*, vol. 2, no. 4, p. L14, 2005.

[126] A. Schlögl and C. Brunner, "BioSig: A Free and Open Source Software Library for BCI Research," *Computer*, vol. 41, no. 10, pp. 44–50, 2008.

[127] H. Ramoser, J. Muller-Gerking, and G. Pfurtscheller, "Optimal spatial filtering of single trial eeg during imagined hand movement," *Rehabilitation Engineering, IEEE Transactions on*, vol. 8, no. 4, pp. 441–446, 2000.

[128] K. Fukunaga, *Introduction to statistical pattern recognition*. London: Academic Press, 2 ed., 1990.

[129] J. Müller-Gerking, G. Pfurtscheller, and H. Flyvbjerg, "Designing optimal spatial filters for single-trial EEG classification in a movement task," *Clinical Neurophysiology*, vol. 110, no. 5, pp. 787–798, 1999.

[130] A. Schlögl, C. Vidaurre, and K.-R. Muller, *Brain-Computer Interfaces: Revolutionizing Human-Computer Interaction*, ch. Adaptive Methods in BCI Research An Introductory Tutorial, pp. 131–356. Springer, 2010.

[131] G. Dunteman, *Principal Components Analysis*. No. no. 69 in A Sage Publications, SAGE Publications, 1989.

[132] G. Pfürtscheller, "Mapping of event-related desynchronization and type of derivation.," *Electroencephalography and Clinical Neurophysiology*, vol. 70, no. 2, pp. 190–193, 1988.

[133] B. Z. Allison, S. Dunne, R. Leeb, J. D. R. Millán, and A. Nijholt, *Towards practical brain-computer interfaces: bridging the gap from research to real-world applications*. Springer Science & Business Media, 2012.

[134] S. C. Cuthbert and G. J. Goodheart, "On the reliability and validity of manual muscle testing: a literature review," *Chiropractic & Manual Therapies*, vol. 15, no. 1, p. 4, 2007.

[135] M. L. Seghier, "Laterality index in functional mri: methodological issues," *Magnetic resonance imaging*, vol. 26, no. 5, pp. 594–601, 2008.

[136] A. Jansen, R. Menke, J. Sommer, A. Förster, S. Bruchmann, J. Hempleman, B. Weber, and S. Knecht, "The assessment of hemispheric lateralization in functional mrirobustness and reproducibility," *Neuroimage*, vol. 33, no. 1, pp. 204–217, 2006.

[137] G. Harrington, M. Buonocore, and S. T. Farias, "Intrasubject reproducibility of functional mr imaging activation in language tasks," *American Journal of Neuroradiology*, vol. 27, no. 4, pp. 938–944, 2006.

[138] B. M. Young, Z. Nigogosyan, L. M. Walton, J. Song, V. A. Nair, S. W. Grogan, M. E. Tyler, D. F. Edwards, K. Caldera, J. A. Sattin, *et al.*, "Changes in functional brain organization and behavioral correlations after rehabilitative therapy using a brain-computer interface," *Frontiers in neuroengineering*, vol. 7, p. 26, 2014.

[139] A. Caria, C. Weber, D. Brötz, A. Ramos, L. F. Ticini, A. Gharabaghi, C. Braun, and N. Birbaumer, "Chronic stroke recovery after combined bci training and physiotherapy: a case report," *Psychophysiology*, vol. 48, no. 4, pp. 578–582, 2011.

[140] L. Sabre, T. Tomberg, J. Kõrv, J. Kepler, K. Kepler, Ü. Linnamägi, and T. Asser, "Brain activation in the acute phase of traumatic spinal cord injury," *Spinal cord*, vol. 51, no. 8, pp. 623–629, 2013.

[141] M. G. Lacourse, E. L. R. Orr, S. C. Cramer, and M. J. Cohen, "Brain activation during execution and motor imagery of novel and skilled sequential hand movements.," *Neuroimage*, vol. 27, no. 3, pp. 505–519, 2005.

[142] H. Alkadhi, G. R. Crelier, S. H. Boendermaker, X. Golay, M.-C. Hepp-Reymond, and S. S. Kollias, "Reproducibility of primary motor cortex somatotopy under controlled conditions.," *AJNR: American Journal of Neuroradiology*, vol. 23, no. 9, pp. 1524–1532, 2002.

[143] L. A. Cooper and R. N. Shepard, "Mental transformations in the identification of left and right hands.," *Journal of experimental psychology. Human perception and performance*, vol. 104, no. 1, pp. 48–56, 1975.

[144] G. L. Moseley, D. S. Butler, T. B. Beames, and T. J. Giles, *The graded motor imagery handbook*. Adelaide, Australia: Noigroup Publications, 2012.

[145] R. Shepard and J. Metzler, "Mental rotation of three-dimensional objects," *Science*, vol. 171, no. 3972, pp. 701–703, 1971.

[146] J. M. Zacks, "Neuroimaging studies of mental rotation: a meta-analysis and review," *Journal of Cognitive Neuroscience*, vol. 20, no. 1, pp. 1–19, 2008.

[147] H. Sakata, Y. Takaoka, A. Kawarasaki, and H. Shibutani, "Somatosensory properties of neurons in the superior parietal cortex (area 5) of the rhesus monkey," *Brain Research*, vol. 64, no. 0, pp. 85 – 102, 1973.

[148] E. Bonda, M. Petrides, S. Frey, and A. Evans, "Neural correlates of mental transformations of the body-in-space.," *Proceedings of the National Academy of Sciences United States America*, vol. 92, no. 24, pp. 11180–11184, 1995.

[149] A. Gogos, M. Gavrilescu, S. Davison, K. Searle, J. Adams, S. L. Rossell, R. Bell, S. R. Davis, and G. F. Egan, "Greater superior than inferior parietal lobule activation with increasing rotation angle during mental rotation: An fMRI study," *Neuropsychologia*, vol. 48, no. 2, pp. 529 – 535, 2010.

[150] M. M. Weiss, T. Wolbers, M. Peller, K. Witt, L. Marshall, C. Buchel, and H. R. Siebner, "Rotated alphanumeric characters do not automatically activate frontoparietal areas subserving mental rotation," *NeuroImage*, vol. 44, no. 3, pp. 1063 – 1073, 2009.

[151] L. M. Parsons, "Imagined spatial transformations of one's hands and feet.," *Cognitive psychology*, vol. 19, no. 2, pp. 178–241, 1987.

[152] L. M. Parsons, "Imagined spatial transformation of one's body.," *Journal of Experimental Psychology: General*, vol. 116, no. 2, p. 172, 1987.

[153] L. M. Parsons, "Temporal and kinematic properties of motor behavior reflected in mentally simulated action.," *Journal of Experimental Psychology: Human Perception and Performance*, vol. 20, no. 4, p. 709, 1994.

[154] L. M. Parsons, P. T. Fox, J. H. Downs, T. Glass, T. B. Hirsch, C. C. Martin, P. A. Jerabek, and J. L. Lancaster, "Use of implicit motor imagery for visual shape discrimination as revealed by PET.," *Nature*, vol. 375, no. 6526, pp. 54–58, 1995.

[155] L. M. Parsons, "Integrating cognitive psychology, neurology and neuroimaging," *Acta psychologica*, vol. 107, no. 1, pp. 155–181, 2001.

[156] G. Vingerhoets, F. P. de Lange, P. Vandemaele, K. Deblaere, and E. Achten, "Motor imagery in mental rotation: An fMRI study.," *Neuroimage*, vol. 17, no. 3, pp. 1623–1633, 2002.

[157] M. Wexler, S. M. Kosslyn, and A. Berthoz, "Motor processes in mental rotation," *Cognition*, vol. 68, no. 1, pp. 77 – 94, 1998.

[158] G. Pfurtscheller, R. Scherer, G. R. Müller-Putz, and F. H. Lopes da Silva, "Short-lived brain state after cued motor imagery in naive subjects," *European Journal of Neuroscience*, vol. 28, no. 7, pp. 1419–1426, 2008.

[159] I. Riečanskỳ and S. Katina, "Induced EEG alpha oscillations are related to mental rotation ability: The evidence for neural efficiency and serial processing.," *Neuroscience Letters*, vol. 482, no. 2, pp. 133–136, 2010.

[160] H. S. Gill, M. W. O'Boyle, and J. Hathaway, "Cortical distribution of EEG activity for component processes during mental rotation," *Cortex*, vol. 34, no. 5, pp. 707–718, 1998.

[161] X. Chen, G. Bin, I. Daly, and X. Gao, "Event-related desynchronization (ERD) in the alpha band during a hand mental rotation task," *Neuroscience Letters*, vol. 541, pp. 238–242, 2013.

[162] S. C. Cramer, E. L. Orr, M. J. Cohen, and M. G. Lacourse, "Effects of motor imagery training after chronic, complete spinal cord injury," *Experimental Brain Research*, vol. 177, no. 2, pp. 233–242, 2007.

[163] H. C. Dijkerman, M. Ietswaart, M. Johnston, and R. S. MacWalter, "Does motor imagery training improve hand function in chronic stroke patients? A pilot study," *Clinical Rehabilitation*, vol. 18, no. 5, pp. 538–549, 2004.

[164] J. E. Driskell, C. Copper, and A. Moran, "Does mental practice enhance performance?," *Journal of Applied Psychology*, vol. 79, no. 4, pp. 481–491, 1994.

[165] M. Grangeon, P. Revol, A. Guillot, G. Rode, and C. Collet, "Could motor imagery be effective in upper limb rehabilitation of individuals with spinal cord injury? A case study.," *Spinal Cord*, vol. 50, no. 10, pp. 766–771, 2012.

[166] A. D. Walz, T. Usichenko, G. L. Moseley, and M. Lotze, "Graded motor imagery and the impact on pain processing in a case of CRPS," *The Clinical Journal of Pain*, vol. 29, no. 3, pp. 276–279, 2013.

[167] K. J. Bowering, N. E. O'Connell, A. Tabor, M. J. Catley, H. B. Leake, G. L. Moseley, and T. R. Stanton, "The effects of graded motor imagery and its components on chronic pain: A systematic review and meta-analysis," *The Journal of Pain*, vol. 14, no. 1, pp. 3 – 13, 2013.

[168] R. C. Oldfield, "The assessment and analysis of handedness: The Edinburgh inventory.," *Neuropsychologia*, vol. 9, no. 1, pp. 97–113, 1971.

[169] C. Vidaurre, T. H. Sander, and A. Schlögl, "Biosig: the free and open source software library for biomedical signal processing," *Computational intelligence and neuroscience*, vol. 2011, 2011.

[170] I. Daly, S. J. Nasuto, and K. Warwick, "Single tap identification for fast bci control," *Cognitive neurodynamics*, vol. 5, no. 1, pp. 21–30, 2011.

[171] K. Takeda, N. Shimoda, Y. Sato, M. Ogano, and H. Kato, "Reaction time differences between left- and right-handers during mental rotation of hand pictures.," *Laterality*, vol. 15, no. 4, pp. 415–425, 2010.

[172] M. Wraga, W. L. Thompson, N. M. Alpert, and S. M. Kosslyn, "Implicit transfer of motor strategies in mental rotation," *Brain and Cognition*, vol. 52, no. 2, pp. 135–143, 2003.

[173] S. Ionta, A. D. Fourkas, M. Fiorio, and S. M. Aglioti, "The influence of hands posture on mental rotation of hands and feet.," *Experimental Brain Research*, vol. 183, no. 1, pp. 1–7, 2007.

[174] A. Hyvärinen and E. Oja, "Independent component analysis: algorithms and applications," *Neural Networks*, vol. 13, no. 4, pp. 411 – 430, 2000.

[175] P. Comon, "Independent component analysis, a new concept?," *Signal Processing*, vol. 36, no. 3, pp. 287 – 314, 1994.

[176] A. Delorme and S. Makeig, "EEGLAB: An open source toolbox for analysis of single-trial EEG dynamics including independent component analysis," *Journal of Neuroscience Methods*, vol. 134, no. 1, pp. 9 – 21, 2004.

[177] S. Hoffmann and M. Falkenstein, "The correction of eye blink artefacts in the EEG: A comparison of two prominent methods," *PLoS One*, vol. 3, no. 8, pp. e3004–e3004, 2008.

[178] J. Iriarte, E. Urrestarazu, M. Valencia, M. Alegre, A. Malanda, C. Viteri, and J. Artieda, "Independent component analysis as a tool to eliminate artifacts in EEG: A quantitative study.," *Journal of Clinical Neurophysiology*, vol. 20, no. 4, pp. 249–257, 2003.

[179] G. Pfurtscheller and A. Berghold, "Patterns of cortical activation during planning of voluntary movement.," *Electroencephalography and Clinical Neurophysiology*, vol. 72, no. 3, pp. 250–258, 1989.

[180] R. K. Young, *Wavelet theory and its applications*, vol. 189. Springer, 1993.

[181] S. Holm, "A simple sequentially rejective multiple test procedure," *Scandinavian journal of statistics*, vol. 6, no. 2, pp. 65–70, 1979.

[182] T. E. Nichols and A. P. Holmes, "Nonparametric permutation tests for functional neuroimaging: a primer with examples," *Human brain mapping*, vol. 15, no. 1, pp. 1–25, 2002.

[183] P. Fletcher, C. Frith, S. Baker, T. Shallice, R. Frackowiak, and R. Dolan, "The mind's eye–precuneus activation in memory-related imagery," *NeuroImage*, vol. 2, no. 3, pp. 195 – 200, 1995.

[184] C. Neuper and G. Pfurtscheller, "Event-related dynamics of cortical rhythms: Frequency-specific features and functional correlates," *International Journal of Psychophysiology*, vol. 43, no. 1, pp. 41 – 58, 2001.

[185] C. Neuper, M. Wörtz, and G. Pfürtscheller, "ERD/ERS patterns reflecting sensorimotor activation and deactivation," in *Event-related dynamics of Brain Oscillations* (C. Neuper and W. Klimesch, eds.), vol. 159 of *Progress in Brain Research*, pp. 211 – 222, Elsevier, 2006.

[186] N. E. Crone, D. L. Miglioretti, B. Gordon, J. M. Sieracki, M. T. Wilson, S. Uematsu, and R. P. Lesser, "Functional mapping of human sensorimotor cortex with electrocorticographic spectral analysis. i. alpha and beta event-related desynchronization.," *Brain*, vol. 121, no. 12, pp. 2271–2299, 1998.

[187] C. M. Michel, L. Kaufman, and S. J. Williamson, "Duration of eeg and meg α suppression increases with angle in a mental rotation task," *Journal of cognitive neuroscience*, vol. 6, no. 2, pp. 139–150, 1994.

[188] G. Pfurtscheller, R. Leeb, C. Keinrath, D. Friedman, C. Neuper, C. Guger, and M. Slater, "Walking from thought," *Brain Research*, vol. 1071, no. 1, pp. 145 – 152, 2006.

[189] C. Enzinger, S. Ropele, F. Fazekas, M. Loitfelder, F. Gorani, T. Seifert, G. Reiter, C. Neuper, G. Pfurtscheller, and G. Müller-Putz, "Brain motor system function in a patient with complete spinal cord injury following extensive brain-computer interface training," *Experimental Brain Research*, vol. 190, no. 2, pp. 215–223, 2008.

[190] J. R. Wolpaw, N. Birbaumer, D. J. McFarland, G. Pfurtscheller, and T. M. Vaughan, "Brain-computer interfaces for communication and control," *Clinical Neurophysiology*, vol. 113, no. 6, pp. 767 – 791, 2002.

[191] M. Dyson, F. Sepulveda, and J. Gan, "Localisation of cognitive tasks used in EEG-based BCIs," *Clinical Neurophysiology*, vol. 121, no. 9, pp. 1481 – 1493, 2010.

[192] M. S. Cohen, S. M. Kosslyn, H. C. Breiter, G. J. DiGirolamo, W. L. Thompson, A. Anderson, S. Bookheimer, B. R. Rosen, and J. Belliveau, "Changes in cortical activity during mental rotation a mapping study using functional MRI," *Brain*, vol. 119, no. 1, pp. 89–100, 1996.

[193] K. Jordan, H. Heinze, K. Lutz, M. Kanowski, and L. Jäncke, "Cortical activations during the mental rotation of different visual objects," *Neuroimage*, vol. 13, no. 1, pp. 143–152, 2001.

[194] G. R. Fink, R. S. J. Frackowiak, U. Pietrzyk, and R. E. Passingham, "Multiple nonprimary motor areas in the human cortex," *Journal of Neurophysiology*, vol. 77, no. 4, pp. 2164–2174, 1997.

[195] A. E. Cavanna and M. R. Trimble, "The precuneus: a review of its functional anatomy and behavioural correlates," *Brain*, vol. 129, no. 3, pp. 564–583, 2006.

[196] R. Leech, R. Braga, and D. J. Sharp, "Echoes of the brain within the posterior cingulate cortex," *The Journal of Neuroscience*, vol. 32, no. 1, pp. 215–222, 2012.

[197] S. M. Kosslyn, N. M. Alpert, W. L. Thompson, V. Maljkovic, S. B. Weise, C. F. Chabris, S. E. Hamilton, S. L. Rauch, and F. S. Buonanno, "Visual mental imagery activates topographically organized visual cortex: PET investigations," *Journal of Cognitive Neuroscience*, vol. 5, no. 3, pp. 263–287, 1993.

[198] B. Alivisatos and M. Petrides, "Functional activation of the human brain during mental rotation," *Neuropsychologia*, vol. 35, no. 2, pp. 111 – 118, 1996.

[199] R. Epstein and N. Kanwisher, "A cortical representation of the local visual environment," *Nature*, vol. 392, no. 6676, pp. 598–601, 1998.

[200] N. Kanwisher, J. McDermott, and M. M. Chun, "The fusiform face area: A module in human extrastriate cortex specialized for face perception," *The Journal of Neuroscience*, vol. 17, no. 11, pp. 4302–4311, 1997.

[201] R. F. Schwarzlose, C. I. Baker, and N. Kanwisher, "Separate face and body selectivity on the fusiform gyrus," *The Journal of Neuroscience*, vol. 25, no. 47, pp. 11055–11059, 2005.

[202] B. A. Osuagwu and A. Vuckovic, "Similarities between explicit and implicit motor imagery in mental rotation of hands: an EEG study.," *Neuropsychologia*, vol. 65, pp. 197–210, 2014.

[203] B. A. Osuagwu and A. Vuckovic, "Time-frequency activity of electroencephalogram is different for left and right hand mental rotation," in *Proceedings of the 8th IEEE EMBS UK & Republic of Ireland Postgraduate Conference on Biomedical Engineering and Medical Physics*, (Warwick, UK), 2014.

[204] A. Vuckovic, M. Hasan, B. Osuagwu, M. Fraser, D. Allan, B. Conway, and B. Nasseroleslami, "The influence of central neuropathic pain in paraplegic patients on performance of a motor imagery based brain computer interface," *Clinical Neurophysiology*, 2015.

[205] S. Waldert, T. Pistohl, C. Braun, T. Ball, A. Aertsen, and C. Mehring, "A review on directional information in neural signals for brain-machine interfaces," *Journal of Physiology-Paris*, vol. 103, no. 3, pp. 244–254, 2009.

[206] Y. Wang and S. Makeig, "Predicting intended movement direction using EEG from human posterior parietal cortex," in *Foundations of Augmented Cognition. Neuroergonomics and Operational Neuroscience*, pp. 437–446, Springer, 2009.

[207] E. Y. Lew, R. Chavarriaga, S. Silvoni, and J. d. R. Millán, "Single trial prediction of self-paced reaching directions from eeg signals," *Frontiers in neuroscience*, vol. 8, 2014.

[208] C. A. Loza, G. R. Philips, M. K. Hazrati, J. J. Daly, and J. C. Principe, "Classification of hand movement direction based on eeg high-gamma activity," in *Engineering in Medicine and Biology Society (EMBC), 2014 36th Annual International Conference of the IEEE*, pp. 6509–6512, IEEE, 2014.

[209] V. Gugino and R. J. Chabot, "Somatosensory evoked potentials.," *International anesthesiology clinics*, vol. 28, no. 3, pp. 154–164, 1990.

[210] R. P. Lesser, P. Raudzens, H. Lders, M. R. Nuwer, W. D. Goldie, H. H. Morris, D. S. Dinner, G. Klem, J. F. Hahn, A. G. Shetter, H. H. Ginsburg, and A. R. Gurd, "Postoperative neurological deficits may occur despite unchanged intraoperative somatosensory evoked potentials," *Annals of Neurology*, vol. 19, no. 1, pp. 22–25, 1986.

[211] J. R. Toleikis, "Intraoperative monitoring using somatosensory evoked potentials," *Journal of clinical monitoring and computing*, vol. 19, no. 3, pp. 241–258, 2005.

[212] A. Curt and V. Dietz, "Electrophysiological recordings in patients with spinal cord injury: significance for predicting outcome.," *Spinal Cord*, vol. 37, no. 3, pp. 157–165, 1999.

[213] F. Kuhn, P. Halder, M. R. Spiess, M. Schubert, and E. M.-S. C. I. S. G. , "One-year evolution of ulnar somatosensory potentials after trauma in 365 tetraplegic patients: early prediction of potential upper limb function.," *Journal of Neurotrauma*, vol. 29, no. 10, pp. 1829–1837, 2012.

[214] A. Curt, "Neurological diagnosis and prognosis: significance of neurophysiological findings in traumatic spinal cord lesions.," *Schweizerische Medizinische Wochenschrift*, vol. 130, no. 22, pp. 801–810, 2000.

[215] A. Curt and V. Dietz, "Prognosis of traumatic spinal cord lesions. significance of clinical and electrophysiological findings.," *Nervenarzt*, vol. 68, no. 6, pp. 485–495, 1997.

[216] A. Curt and V. Dietz, "Ambulatory capacity in spinal cord injury: significance of somatosensory evoked potentials and asia protocol in predicting outcome.," *Archives of Physical Medicine and Rehabilitation*, vol. 78, no. 1, pp. 39–43, 1997.

[217] A. Curt, B. Rodic, B. Schurch, and V. Dietz, "Recovery of bladder function in patients with acute spinal cord injury: significance of asia scores and somatosensory evoked potentials.," *Spinal Cord*, vol. 35, no. 6, pp. 368–373, 1997.

[218] A. Curt and V. Dietz, "Traumatic cervical spinal cord injury: relation between somatosensory evoked potentials, neurological deficit, and hand function," *Archives of physical medicine and rehabilitation*, vol. 77, no. 1, pp. 48–53, 1996.

[219] G. Cruccu, M. Aminoff, G. Curio, J. Guerit, R. Kakigi, F. Mauguiere, P. Rossini, R.-D. Treede, and L. Garcia-Larrea, "Recommendations for the clinical use of somatosensory-evoked potentials," *Clinical neurophysiology*, vol. 119, no. 8, pp. 1705–1719, 2008.

[220] P. Furlong, P. Barczak, G. Hayes, and G. Harding, "Somatosensory evoked potentials in schizophrenia. a lateralisation study.," *British Journal of Psychiatry*, vol. 157, pp. 881–887, 1990.

[221] G. Alon, A. F. Levitt, and P. A. McCarthy, "Functional electrical stimulation enhancement of upper extremity functional recovery during stroke rehabilitation: a pilot study," *Neurorehabilitation and neural repair*, vol. 21, no. 3, pp. 207–215, 2007.

[222] N. M. Gharib, A. M. Aboumousa, A. A. Elowishy, S. S. Rezk-Allah, and F. S. Yousef, "Efficacy of electrical stimulation as an adjunct to repetitive task practice therapy on skilled hand performance in hemiparetic stroke patients: a randomized controlled trial.," *Clinical Rehabilitation*, Aug 2014.

[223] R. Scherer, "rtsBCI: A collection of methods and functions for real-time data acquisition, storage, signal processing and visualization based on matlab/simulink."

[224] R. Pascual-Marqui, "Standardized low-resolution brain electromagnetic tomography (sLORETA): technical details," *Methods and Findings in Experimental and Clinical Pharmacology*, vol. 24, no. Suppl. D, pp. 5–12, 2002.

[225] J. Talairach and P. Tournoux, *Co-planar stereotaxic atlas of the human brain: 3-dimensional proportional system: An approach to cerebral imaging*. Thieme, 1988.

[226] M. Brett, I. S. Johnsrude, and A. M. Owen, "The problem of functional localization in the human brain.," *Nature Reviews Neuroscience*, vol. 3, no. 3, pp. 243–249, 2002.

[227] P. Boord, P. Siddall, Y. Tran, D. Herbert, J. Middleton, and A. Craig, "Electroencephalographic slowing and reduced reactivity in neuropathic pain following spinal cord injury," *Spinal cord*, vol. 46, no. 2, pp. 118–123, 2008.

[228] J. Green, E. Sora, Y. Bialy, A. Ricamato, and R. Thatcher, "Cortical sensorimotor reorganization after spinal cord injury an electroencephalographic study," *Neurology*, vol. 50, no. 4, pp. 1115–1121, 1998.

[229] C. D. Frith, S. J. Blakemore, and D. M. Wolpert, "Abnormalities in the awareness and control of action.," *Philosophical Transactions of the Royal Society of London. Series B, Biological Sciences*, vol. 355, no. 1404, pp. 1771–1788, 2000.

[230] M. G. Lacourse, M. J. Cohen, K. E. Lawrence, and D. H. Romero, "Cortical potentials during imagined movements in individuals with chronic spinal cord injuries.," *Behavioural Brain Research*, vol. 104, no. 1-2, pp. 73–88, 1999.

[231] S. C. Kirshblum, S. P. Burns, F. Biering-Sorensen, W. Donovan, D. E. Graves, A. Jha, M. Johansen, L. Jones, A. Krassioukov, M. J. Mulcahey, M. Schmidt-Read, and W. Waring, "International standards for neurological classification of spinal cord injury (revised 2011).," *Journal of Spinal Cord Medicine*, vol. 34, pp. 535–546, Nov 2011.

[232] A. S. Burns, R. J. Marino, A. E. Flanders, and H. Flett, "Chapter 3 - clinical diagnosis and prognosis following spinal cord injury," in *Spinal Cord Injury* (J. Verhaagen and J. W. McDonald, eds.), vol. 109 of *Handbook of Clinical Neurology*, pp. 47 – 62, Elsevier, 2012.

[233] M. Ietswaart, M. Johnston, H. C. Dijkerman, S. Joice, C. L. Scott, R. S. MacWalter, and S. J. C. Hamilton, "Mental practice with motor imagery in stroke recovery: randomized controlled trial of efficacy.," *Brain*, vol. 134, pp. 1373–1386, May 2011.

[234] F. Malouin, C. L. Richards, A. Durand, and J. Doyon, "Clinical assessment of motor imagery after stroke.," *Neurorehabilitation and Neural Repair*, vol. 22, no. 4, pp. 330–340, 2008.

[235] F. Fiori, A. Sedda, E. R. Ferrì, A. Toraldo, M. Querzola, F. Pasotti, D. Ovadia, C. Piroddi, R. Dell'Aquila, T. Redaelli, and G. Bottini, "Motor imagery in spinal cord injury patients: Moving makes the difference.," *Journal of Neuropsychology*, vol. 8, no. 2, pp. 199–215, 2014.

[236] B. A. Osuagwu and A. Vuckovic, "Feasibility of using time doman parameters as online therapeutic BCI features," in *Proceedings of the 6th International Brain-Computer Interface Conference*, (Graz, Austria), 2014.

[237] W. Hsu and Y. Sun, "EEG-based motor imagery analysis using weighted wavelet transform features," *Journal of Neuroscience Methods*, vol. 176, no. 2, pp. 310–318, 2009.

[238] M. Hassan, O. Dufor, I. Merlet, C. Berrou, and F. Wendling, "EEG source connectivity analysis: From dense array recordings to brain networks," *PLoS ONE*, vol. 9, no. 8, p. e105041, 2014.

[239] I. Daly, S. J. Nasuto, and K. Warwick, "Brain computer interface control via functional connectivity dynamics," *Pattern recognition*, vol. 45, no. 6, pp. 2123–2136, 2012.

[240] R. A. Rescorla, "Pavlovian conditioning: It's not what you think it is.," *American Psychologist*, vol. 43, no. 3, pp. 151–160, 1988.

[241] N. Nicolaou, S. J. Nasuto, J. Georgiou, *et al.*, "Single trial event related potential analysis for brain computer interfaces," in *AISB 2008 Convention Communication, Interaction and Social Intelligence*, vol. 1, p. 13, 2008.

[242] R. D. Pascual-Marqui, "Discrete, 3D distributed, linear imaging methods of electric neuronal activity. part 1: Exact, zero error localization," *arXiv preprint arXiv:0710.3341*, 2007.

[243] K. Sekihara, M. Sahani, and S. S. Nagarajan, "Localization bias and spatial resolution of adaptive and non-adaptive spatial filters for MEG source reconstruction," *Neuroimage*, vol. 25, no. 4, pp. 1056–1067, 2005.

[244] R. E. Greenblatt, A. Ossadtchi, and M. E. Pflieger, "Local linear estimators for the bioelectromagnetic inverse problem," *Signal Processing, IEEE Transactions on*, vol. 53, no. 9, pp. 3403–3412, 2005.

[245] R. D. Pascual-Marqui, C. M. Michel, and D. Lehmann, "Low resolution electromagnetic tomography: A new method for localizing electrical activity in the brain," *International Journal of psychophysiology*, vol. 18, no. 1, pp. 49–65, 1994.

[246] D. Vitacco, D. Brandeis, R. Pascual-Marqui, and E. Martin, "Correspondence of event-related potential tomography and functional magnetic resonance imaging during language processing," *Human brain mapping*, vol. 17, no. 1, pp. 4–12, 2002.

[247] G. A. Worrell, T. D. Lagerlund, F. W. Sharbrough, B. H. Brinkmann, N. E. Busacker, K. M. Cicora, and T. J. O'Brien, "Localization of the epileptic focus by low-resolution electromagnetic tomography in patients with a lesion demonstrated by MRI," *Brain Topography*, vol. 12, no. 4, pp. 273–282, 2000.

[248] T. Dierks, V. Jelic, R. D. Pascual-Marqui, L.-O. Wahlund, P. Julin, D. E. Linden, K. Maurer, B. Winblad, and A. Nordberg, "Spatial pattern of cerebral glucose metabolism (PET) correlates with localization of intracerebral EEG-generators in Alzheimer's disease," *Clinical Neurophysiology*, vol. 111, no. 10, pp. 1817–1824, 2000.

[249] D. Pizzagalli, T. Oakes, A. Fox, M. Chung, C. Larson, H. Abercrombie, S. Schaefer, R. Benca, and R. Davidson, "Functional but not structural subgenual prefrontal cortex abnormalities in melancholia," *Molecular psychiatry*, vol. 9, no. 4, pp. 393–405, 2003.

[250] D. Zumsteg, R. A. Wennberg, V. Treyer, A. Buck, and H. G. Wieser, "H215O or 13NH3 PET and electromagnetic tomography (LORETA) during partial status epilepticus," *Neurology*, vol. 65, no. 10, pp. 1657–1660, 2005.